WASTE GLASS POWDER AS A BINDER IN LOW CARBON CEMENT-BASED MATERIALS

Mirabel De Gabriele

Dissertation submitted to the Faculty for the Built Environment, University of Malta in part fulfilment of the requirements for the attainment of the degree of **Master of Engineering (Structural Engineering)**

July 2025

DECLARATION OF AUTHENTICITY

L-Università ta' Malta

FACULTY/INSTITUTE/CENTRE/SCHOOL Faculty for the Built Environment

DECLARATIONS BY POSTGRADUATE STUDENTS

(a) Authenticity of Dissertation

I hereby declare that I am the legitimate author of this Dissertation and that it is my original work.

No portion of this work has been submitted in support of an application for another degree or qualification of this or any other university or institution of higher education.

I hold the University of Malta harmless against any third party claims with regard to copyright violation, breach of confidentiality, defamation and any other third party right infringement.

(b) Research Code of Practice and Ethics Review Procedures

I declare that I have abided by the University's Research Ethics Review Procedures. Research Ethics & Data Protection form code BEN-2024-00107.

As a Master's student, as per Regulation 77 of the General Regulations for University Postgraduate Awards 2021, I accept that should my dissertation be awarded a Grade A, it will be made publicly available on the University of Malta Institutional Repository.

02.2023

ACKNOWLEDGEMENTS

Firstly, I would like to thank my supervisor Prof. Ruben Paul Borg for his help and guidance throughout this journey. Thanks also go to Prof. Thirumalini Selvaraj, Dr. Deepankar Ashish, Dr. Himanshu Sharma, Dr. Muhammad Ali, Mr. Loai Al Mawed and Mr. Igor Semenov for their expert guidance, invaluable insights and consistent support.

I would also like to thank the multiple experts whose insights on the local and global scene, through interviews and other correspondences, helped me to formulate this research project. Specifically, I would like to thank the following individuals that were the professionals in their respective roles at the time the interviews took place: Ing. Jason Vella - CEO at CE Malta, Mr. Matthew Dimech – COO at BCRS Ltd., Mr. Chris Bonello - Business Development Manager at MStream Ltd., Perit Janice Borg – COO at Infrastructure Malta, Mr. Richard Bilocca - CEO at WasteServ Malta Ltd., Mr. Daniel Tabone - Chief Officer Circular Economy at WasteServ Malta Ltd. and Ing. Dylan Debono - Managing Professional at WasteServ Malta Ltd.

I would like to thank the laboratories and the staff at the University of Malta namely the Faculty for the Built Environment, the Department of Chemistry and the Department of Metallurgy and Materials Engineering.

I would also like to acknowledge the project: “Setting up of transdisciplinary research and knowledge exchange (TRAKE) complex at the University of Malta (ERDF.01.124)” which is being co-financed through the European Union through the European Regional Development Fund 2014 – 2020". Special thanks go to CrEMa Laboratories, Prof. Ulrich Baisch and Dr. Marie Christine Scicluna.

I would also like to thank Diagnostic Science Laboratories at Heritage Malta Services Ltd. for their services.

Moreover, I would like to thank my family for their unwavering support and encouragement throughout my studies. No words can express my gratitude towards my parents and Daniel.

ABSTRACT

The construction sector contributes to the significant consumption of natural resources, the production of large quantities of waste materials. It is a major contributor to greenhouse gases, leading to global warming and climate change mostly due to the production of cement. Globally, waste glass is generated in large quantities but offers opportunities for recycling. In the local scene, it was revealed that the management of glass waste is a continuous challenge. It is often a loss-leader due to the absence of a glass waste recycling plant in Malta which leads to its transportation overseas for its management and recycling to avoid dumping in landfills. Moreover, recycling of glass waste generates a significant carbon footprint due to the high melting point of glass. Furthermore, recycling coloured glass is challenging due to the colour specificity.

The aim of this dissertation is to propose solutions to the glass waste problem by studying different types of glass waste present in the local scenario. Their effective utilisation by transforming the waste glass into a powder to be used as a binder in low carbon cement-based materials was investigated. The effects of contamination, colour and heat treatment of the waste glass were addressed in this research. This repurposing of glass waste can potentially reduce the strain of glass waste on local institutions involved in waste management.

The various samples of waste glass powder were used as partial cement replacements in paste and mortar. Characterisation testing was conducted on the waste glass powders to determine their properties. The testing of the fresh and hardened properties of paste and mortar samples was carried out in aim of gaining knowledge on the materials' behaviour. Noticeable trends appeared which showed that waste glass powder, even with contamination, has great potential to be used as a supplementary cementitious material that, in the long run, outperforms the traditional cement construction products, especially when heat treatment at effective temperatures is carried out.

TABLE OF CONTENTS

TABLE OF FIGURES

LIST OF TABLES

GLOSSARY

Abbreviation	Meaning
AMBT	Accelerated Mortar Bar Test
ASR	Alkali-Silica Reaction
BCRS	Beverage Container Refund Scheme
CE	Circular Economy
CEO	Chief Executive Officer
CSP	Ceramics, Stones and Porcelain
DRS	Deposit Return Scheme
EDS	Energy Dispersive X-Ray Spectroscopy
EDX	Energy Dispersive X-Ray
EHT	Extra High Tension
Eng.	Engineer
EU	European Union
FSEM	Field Scanning Electron Microscope
FTIR	Fourier Transform Infrared Spectroscopy
OPC	Ordinary Portland Cement
PPWD	Packaging and Packaging Waste Directive
PPWR	Packaging and Packaging Waste Regulation
PSD	Particle Size Distribution
rpm	Revolutions per minute
RVM	Reverse Vending Machine
SAWTP	Sant' Antnin Waste Treatment Plant
SCM	Supplementary Cementitious Material
SDG	Sustainable Development Goal
SEM	Scanning Electron Microscopy
UHPC	Ultra-High-Performance Concrete
UPV	Ultrasonic Pulse Velocity
U-WGP	Unwashed Waste Glass Powder
WGP	Waste Glass Powder
WSML	WasteServ Malta Ltd.
W-WGP	Washed Waste Glass Powder
XRD	X-Ray Diffraction
XRF	X-Ray Fluorescence

SYMBOLS USED

Symbol	Meaning
Al_2O_3	Alumina
$C_3S_2H_3$ aka C-S-H	Calcium silicate hydrate
$CaCO_3$	Calcium carbonate
$Ca_3Na_2Si_6O_{16}$	Devitrite
CaO	Calcium oxide
$3CaO.Al_2O_3$ aka C_3A	Tricalcium aluminate
$4CaO.Al_2O_3.Fe_2O_3$ aka C_4AF	Tetracalcium aluminoferrite
$2CaO.SiO_2$ aka C_2S	Dicalcium silicate
$3CaO.SiO_2$ aka C_3S	Tricalcium silicate or Alite
$Ca(OH)_2$	Calcium hydroxide or Portlandite
CO_2	Carbon dioxide
CO_3^{2-}	Carbonate or Calcite
Fe_2O_3	Iron oxide
H_2O	Water
KBr	Potassium bromide
kN	Kilo Newtons
MPa	Mega Pascals
Na_2O	Sodium oxide
Na_2O_3	Soda
NaOH	Sodium hydroxide
SiO_2	Silica
µm	Micrometre

CODE NAMES OF THE DIFFERENT SAMPLES UNDER TEST

Symbol	Meaning
Cem Con	Cement control
Cl	Clear glass acquired from WSML
Co	Uncontaminated coloured glass acquired from WSML
Cl + Co W	Uncontaminated clear and coloured glass acquired from WSML
Cl + Co B	Contaminated clear and coloured glass acquired from BCRS Ltd.
Gl + Ce	A reject containing glass fines that include ceramic and other contaminants obtained from the glass cleaning and sorting process in WSML
Cl + Co W Ca 600	Uncontaminated clear and coloured glass acquired from WSML which is then calcined at 600^oC in the laboratory at the University of Malta
Cl + Co W Ca 850	Uncontaminated clear and coloured glass acquired from WSML which is then calcined at 850^oC in the laboratory at the University of Malta

CHAPTER 1 – INTRODUCTION

1.1 BACKGROUND

Global warming and climate change are prominent challenges in our society. Carbon dioxide (CO_2) emissions from the construction industry contribute to 34% of the world's CO_2 emissions (UN Environment Programme, 2025). Cement production consumes a lot of energy and releases large amounts of CO_2, reaching around 8% of global CO_2 emissions (Purton, 2024). To mitigate this, attempts are being made to replace cement in concrete with alternative materials.

Globally, waste glass is generated in large quantities. The core principles of sustainable waste management – reduce, reuse, recycle – aim to combat this. Although glass offers opportunities for recycling, reuse of glass would be more beneficial than recycling since the recycling process process is still energy intensive. A lot of energy is required to melt the recycled glass, releasing a significant amount of CO_2 into the atmosphere. In countries like Malta, the absence of a glass recycling plant augments the production of emissions since increased vehicle and sea vessel transportation must be used to export waste glass for recycling, further increasing the carbon footprint (Kumari et al., 2022) (Hassani et al., 2023).

Multiple goals can be addressed with the same initiative. The use of glass waste powder in concrete can be used to reduce emissions and repurpose waste. This research aims to gain further knowledge on the utilisation of waste glass as a partial substitute of cement by studying the potential and effectivity of different conditions of glass waste powder as a binder in the production of low-carbon concrete. This would reduce the use of cement in the concrete production, reduce the carbon footprint of construction products and improve waste management in Malta. Moreover, the valorisation of waste glass will present itself as an economic opportunity.

1.2 GOALS AND OBJECTIVES

The major goal of this dissertation is to mitigate the environmental impact of CO_2 emissions generated by cement usage in concrete. This would be done by partially replacing cement with glass waste powder. The research would also look into the optimisation of the performance of different modalities of this type of low-carbon concrete when compared to conventional cement-based concrete. In this way, the environment would benefit from a reduction in greenhouse gases, lessening the acceleration of climate change and global warming. Moreover, glass waste would be reused instead of being recycled which would be more environmentally and economically viable. In the local scenario, this would consequently reduce and potentially eliminate the need for glass waste exportation, further resulting in the reduction of carbon emissions from diesel-powered transportation means.

1.3 RESEARCH QUESTIONS

- What are the effects of contaminants in glass waste when it is used as a supplementary cementitious material in low-carbon concrete?
- Can the reject of the glass sorting process, carried out at a glass waste processing plant (like WasteServ Malta Ltd.) be used as a supplementary cementitious material in low-carbon concrete to improve waste management?
- Are the properties of the low-carbon concrete under test improved when the glass powder is heat treated?
- Does the colour of the waste glass used as a supplementary cementitious material affect the properties of the low-carbon concrete under test?

1.4 RESEARCH METHODOLOGY

The research shall be conducted in stages:

Phase 1: Literature Review

The first phase includes a review of literature on using glass waste in concrete and understanding scientific principles on this. The focus is on using glass waste powder as a binder for low-carbon concrete.

Phase 2: An Analysis of the Local Scenario

This phase, fed by the literature review, involves qualitative research of the glass waste situation in Malta, carried out through interviews with agencies, companies and businesses which are directly involved in glass waste management in Malta. This was done to obtain a deep understanding of the scenario, processes and challenges involved. The data gathered from this phase motivates the research questions posed.

Phase 3: Experimental Programme on Paste and Mortar

This phase of the research refers to an experimental investigation, conducted by laboratory testing, on the utilisation of waste glass as an alternative binder for low-carbon concrete. The research is based on the assessment of different types of glass waste, the effectiveness of heat treatment on a particular type of glass waste, and their effects in paste and mortar. Characterisation testing of the glass powder is carried out along with testing of the fresh and hardened properties of paste and mortar. Both chemical and mechanical analysis is undertaken.

Phase 4: Critical Assessment of Results

The statistical analysis of the data gathered in phase 3 is done by means of graphs, tables and charts to obtain conclusions.

1.5 STRUCTURE OF DISSERTATION

Chapter 2 – Setting the Scene

Chapter 3 – Literature Review

Chapter 4 – Methodology

Chapter 5 – Results and Analysis

Chapter 6 – Conclusion

CHAPTER 2 – SETTING THE SCENE

2.1 THE GLOBAL SCENE

Globally, the building and construction sector contributes to 21% of global greenhouse gas emissions, leaving a significant impact on climate change (UN Environment programme, 2024). Cement, the main constituent of concrete, has a substantial carbon footprint (Khaiyum et al, 2023). During the manufacturing of one tonne of Ordinary Portland Cement (OPC), about 0.73 to 0.99 tonnes of carbon dioxide (CO_2) are expelled. This leads to a contribution of between 5% and 7% of the total carbon footprint (Nasir et al, 2024). With the expansion of the building industry, the rise in demand for cement and the predictions of increase in CO_2 emissions, it is crucial to address this concern.

Another area of global concern is glass waste. Millions of tonnes of non-biodegradable waste glass are generated every year. Besides polluting the environment with contaminants, glass waste disposal into landfills uses up valuable land that could be put to better use (Mohajerani, 2017). However, recycling of glass is not a complete solution to this as the recycling process is very energy intensive (Hamada et al, 2022). The problem is exacerbated when countries, like Malta, do not have a glass waste recycling plant and must export glass waste to deal with the problems it presents.

With such a dire need for more sustainable and environmentally conscientious building practices, as well as the great necessity to reuse glass waste rather than recycling it, sustainable solutions that aim to combat these problems have been considered. Sustainability can be introduced into the construction sector by incorporating waste materials into construction materials. For instance, studies have been undertaken where glass waste has been considered as an aggregate or as a cement replacement in concrete. The two replacement modalities being present at the same time in concrete have also been studied. (Hamada et al, 2022) (Bouchikhi et al, 2023).

2.2 THE LOCAL SCENE

To gather a deep understanding of the current scenario regarding glass waste management in Malta, semi-structured interviews were held with agencies, companies and businesses that deal with cycle economy and glass waste, namely Circular Economy (CE) Malta, Beverage Container Refund Scheme (BCRS) Ltd., MStream Ltd. and WasteServ Malta Ltd.

CE Malta is a Maltese government agency that aims to promote circular economy. Its aim is to reduce the amount of waste disposed in landfills resulting in consequent benefit for the environment. Through monitoring, auditing and enforcement, the agency regulates the BCRS Scheme. BCRS Ltd. is a private non-profit company licensed by CE Malta to collect returns of all single-use beverage containers from individual consumers and businesses throughout Malta and Gozo utilising monetary incentives. It has the responsibility of achieving national single-use beverage container collection goals stipulated by the Beverage Containers Recycling Regulations 2020. In an interview with Eng. Jason Vella, Chief Executive Officer (CEO) at CE Malta (*see Appendix 1.1*), it was gathered that, in 2023, almost 6,500 tonnes of glass waste were collected in the Maltese Islands by BCRS Ltd. and WasteServ Malta Ltd. Due to space limitations, Malta does not have a glass waste recycling plant and storage of the glass waste collected is limited. Therefore, glass waste is exported. However, the cost of transportation for export is remarkably high and, in fact, waste glass collection is not financially feasible. Thus, the incentive for glass waste collection in Malta is environmental protection and lack of storage space. CE Malta is eager to adopt solutions to deal with the management of glass waste and the proposed idea of using glass waste as a supplementary cementitious material in projects in the Maltese Islands has been pleasantly welcomed during the named interview conducted.

The Deposit Return Scheme (DRS) was introduced in Malta in November 2022. Malta was the first country in the Mediterranean to adopt such a scheme following the European Parliament and Council Directive 94/62/EC of 20th December 1994 on Packaging and Packaging Waste (PPWD) (Directive - 94/62 - EN - EUR-Lex, 2018). Since then, in December 2024, this directive has been changed to European Union (EU) law, the Packaging and Packaging Waste Regulation (PPWR) (Regulation - EU - 2025/40 - EN - EUR-Lex, 2025), whereby member countries of the European Union are obliged to adopt this scheme if a minimum 80% collection

rate of plastic bottles has not been achieved through another scheme. This EU law stipulates that, by 1st January 2029, plastic bottles and cans of three (3) litres capacity or less would be collected at a rate of 90%. During the interview with Mr. Matthew Dimech, Chief Operations Officer BCRS Ltd. (*see Appendix 1.2*), it was established that, till the date of the interview, the collection and recycling targets have always been exceeded, making the adoption of this scheme a success. In 2024, the annual return rate of glass beverage containers through the BCRS scheme was 82%. Glass bottles make up 9% of an estimated annual three hundred (300) million glass and plastic bottles and cans utilised for consumption of water, energy drinks, beer, squashes and soft drinks in the Maltese Islands. By weight, twenty-seven (27) million glass bottles are equivalent to 50% of the exported tonnage. These statistics exclude wine and spirit bottles as these are not part of the scheme.

Collection, transportation to the BCRS Ltd. facility in Ħal Far and the actual exportation of glass waste are all paid for by BCRS Ltd., making glass a liability from the start. Currently, excluding management fees, BCRS Ltd. is making a loss of one (1) Euro per tonne on shipping. Glass is collected from two sources - the glass-only reverse vending machines (RVMs) and door-to-door collections from bars, restaurants, and small grocery shops.

Single-use glass containers deposited into RVMs contribute to 90% of the glass waste collected by BCRS Ltd. which would otherwise be thrown away in the Magħtab landfill. Once deposited here, glass containers are instantly crushed in the RVM itself to save space and avoid reclaiming on the same container. However, this leads to contamination of the crushed glass with labels and cap materials. Contaminated glass sells at a lower price than clean glass and therefore, this process negatively impacts the monetary value of the glass waste. This mixed crushed glass is collected by vehicles dedicated solely to glass and transported to the BCRS Ltd. Ħal Far facility where each vehicle is weighed. The glass waste is then deposited in a designated garage nearby. Glass from RVMs is not processed in the facility since the shards of glass would damage the machinery, resulting in more financial losses than are presently incurred. RVMs collect data about the glass bottles collected and thus, no further processing of the glass waste is needed.

80% of the combined waste (glass, metal and plastic containers) collected via door-to-door pickup is glass waste. The combined waste is placed inside provided bags that are tagged to identify the retail outlet from where the waste originated so that refunds can be affected. The bags are transported to the BCRS Ltd clearing and sorting plant in the Ħal Far facility where

the label barcode is scanned. The waste is sorted, and glass is crushed. Glass rejects, most often wine and spirit bottles and other glass containers contaminated with food sources deposited in the collection bags by restaurant and bar owners, are still crushed. In 2023, BCRS Ltd. produced thirty (30) twenty-foot containers filled with these rejects that still need to be exported. This is significant. However, no other option is feasible to avoid its deposition at the Magħtab Landfill. It is also not economically feasible to transfer these rejects to WasteServ Ltd. where glass is separated. All these processes yield glass that is cutlet-sized mixed (transparent and coloured) contaminated glass and thus, its quality is considerably poor. BCRS Ltd. has not opted to purify the glass waste since, according to Mr. Dimech, a study conducted by the company has shown that it would not be economically viable to invest in a separation process and, moreover, foreign recyclers have found no objection to receiving mixed glass waste. Although the glass is not separated, BCRS Ltd. have extensive technological systems that give out valuable data. Every glass bottle deposited in the RVM is logged and through the barcode on the bottle, data is gathered on the clear and coloured glass collected. For instance, in 2023, 1,910.32 tonnes of clear-glass bottles and 1,141.31 tonnes of coloured bottles were collected. Via the bar-code reading, no brown bottles are accepted by the RVMs. Brown bottles that accidentally arrive at BCRS Ltd. through the door-to-door waste stream are handed over to the producer of the beverage to be refilled, promoting reuse instead of recycling.

Although efforts have been made to try and have a green transportation system for waste collected through DRS, the process still causes an environmental impact. Trucks collect returned containers from RVMs all around Malta, seven (7) days a week. A dump truck goes over to Gozo once a month. BCRS Ltd. has nine (9) trucks that collect glass – five (5) of them are electric and four (4) of them are fuelled by unleaded petrol. At the beginning of the scheme, it was not expected that manual collection would pick up so quickly. Even though the company was obliged to buy four (4) electric trucks, it still bought five (5) electric trucks in view of its green perspective. However, to keep up with the fast pickup of the scheme, four (4) other vans had to be bought urgently, and since electric ones were not available, unleaded petrol trucks were bought instead. If this had not happened, the collection process would have completely been by electric vehicles.

MStream Ltd. is the company that handles BCRS Ltd. glass waste export. An interview with Mr Chris Bonello, Business Development Manager at MStream Ltd. *(see Appendix 1.3)*,

yielded the information that around 5,000 to 5,400 tonnes of untreated (washed or cleared of labels and caps) mixed glass cutlets are estimated to have been exported in 2024. Twelve (12) twenty-foot containers, each carrying about 25 tonnes of glass, are loaded every two weeks at the Ħal Far facility and transferred to the Freeport for shipment to Turkey in bulk. The trucks that transport the containers and the ships are diesel operated. On average, eighteen (18) vehicles per month are required for this operation and one (1) ship a week makes the journey from Malta to Turkey. The cost of shipping is over 1,000 Euro per container and so, the expense is quite considerable.

WasteServ Malta Ltd. (WSML) is a government entity that works towards a circular economy to protect the environment. It is responsible for waste management, waste reduction and recycling promotion. WSML receives glass waste from kerbside collection, its own civic amenity sites, bring-in sites operated by GreenMT, iBiNs operated and managed by GreenPak Coop and Roadshow trucks that visit different localities to facilitate waste collection and waste separation (Ħġieġ Nadif Ħġieġ Riċiklabbli | WasteServ Malta, 2021).

National door-to-door collection of glass waste, separate from mixed recycling, commenced in 2023. 3,427.68 tonnes of glass waste were collected in 2023 followed by 3,726.24 tonnes in 2024 (Waste Collection | WasteServ Malta, 2017). Since June 2024, WSML has introduced an electric automated glass sorting line at the Sant' Antnin Waste Treatment Plant (SAWTP) in Marsascala. This has increased the efficiency of glass waste processing as the sorting line can process approximately 10 tonnes of glass waste per hour (Automated Glass Sorting Line | WasteServ Malta, 2020). Moreover, the quality of glass waste has been improved. As per WasteServ statistics of sales opportunities for glass, glass has often yielded financial losses (Sales | WasteServ Malta, 2025). Between June and October 2024, 4000 tonnes of glass processed through this new sorting line have been placed on the market for sale and its monetary value is expected to increase as stated during interviews held with Mr Richard Bilocca, CEO and Mr Daniel Tabone, Chief Officer Circular Economy at WSML (*see Appendix 1.4*).

The process of glass management was also observed during a site visit with Eng. Dylan Debono, Managing Professional of SAWTP & Fleet Departments of WSML. At the Sant' Antnin Plant, glass is separated into 2 different streams - flat glass and bottled glass. The percentage of collected flat glass is very small compared to the other type of glass collected.

Figure A

Figure B

Figure C

Figure D

Figure E

Figure F

Figure G

Figure H

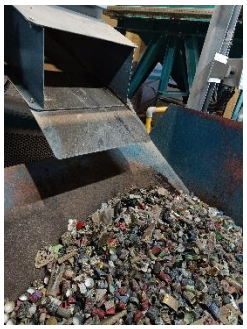

Figure I

Figure J

Figure K

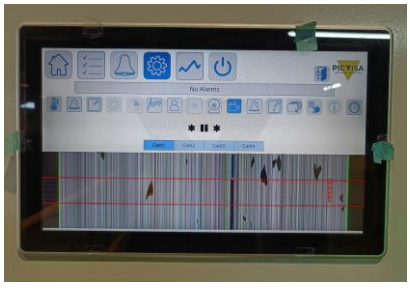

Figure L

Figure 2.1 – Automated Glass Sorting Line at Sant' Antnin Waste Treatment Plant of WSML in Marsascala

At WSML, glass waste is processed to obtain non-contaminated glass. At first, all glass is placed on the ground and big contaminants, like solar panels and metal pipes, are removed manually with hand pickers (*Figure A*). Large pieces of glass are also removed and after this, the glass is transferred into a hopper that directs the falling of glass onto a conveyor (*Figure B*). During the first loop, contaminants are removed from the mixed glass. A magnet is utilised to draw out any metal contaminants from the glass and the metal is collected in large bins (*Figure C & D*. The process of removing metal creates glass fines which are less than 8mm. A vibrating sieve separates the glass waste by size (*Figure E*). The waste fines, which contain contaminants such as ceramic, are collected in large containers. These fines are considered as a reject of the process. Glass pieces which are larger than 60mm are directed to a sorting room where persistent contaminants are removed manually and the glass is inserted manually into a crusher (*Figure F*). All glass crushing is a dry process as glass is not washed at any point. The product is then directed back to the sieve to undergo further separation. This process continues looping until the glass reaches the right size – 8mm to 60mm. Until this point of the process, ceramic contaminants have not yet been separated from the glass waste. Glass of size 8mm to 60mm enters a densimetric table. A large fan generates an extraction system whereby remaining light contaminants such as paper labels are picked up by vacuum and extracted as reject (*Figure G & H*). Glass falls into containers. A ferrous and non-ferrous separator present here serves as a double control measure for the removal of metal. Eddy currents generated here extract metal caps (*Figure I*).

Glass then feeds into the optical sorter which separates glass from ceramics, stones mirrors, porcelain and china (CSP) (*Figure J*). This process is very important as contaminants, particularly ceramic, damage the furnace used for glass recycling. The process of removing CSP from glass waste is necessary since, at source, ceramic waste is discarded along with glass waste. Unfortunately, this arises from the misconception that ceramic and glass can be disposed of together due to lack of education of the general public. CSP and glass are collected in two separate containers (*Figure K*). The glass cullet, now furnace ready, is in high demand as it consists of non-contaminated mixed glass. Most of the time, the loop stops here. When the clear glass needs to be separated from the coloured glass, the glass collected in the initial loop is passed through the entire process once again. Here, the optical sorter utilises lights of different brightness (*Figure L*). Light does not pass through coloured glass, and this is rejected by an air jet that effectively would be separating the coloured from the clear glass. The machinery is also capable of separating the coloured glass according to colour using light with

different wavelengths. Currently, this is not done as it is not required by the current buyers of glass waste.

Therefore, by considering the information presented in this section, it may be concluded that Malta would benefit greatly from repurposing glass locally rather than collecting and exporting it. Utilising this glass waste as a part-replacement of cement used in concrete formation would contribute to the reduction of CO_2 emissions from transportation and reduce economic losses. Moreover, the environment would considerably benefit from the decreased use of cement since CO_2 emissions would be reduced. To get an idea on the amount of cement used in projects of considerable size in Malta, where concrete is majorly used, an interview was held with the Chief Operations Officer at Infrastructure Malta, Perit Janice Borg (*see Appendix 1.5*). Infrastructure Malta is a governmental agency that manages major national developments and public infrastructure in Malta. Data on the type and amount of cement used in the projects listed below was provided by the agency:

- Phase 1 of the project that supplies shore-to-ship electricity to cruise liners berthed in the Grand Harbour, Valletta (Shore-To-Ship | Infrastructure Malta, 2024)
- The merging of Pinto 4 and 5 Quays and Lascaris Wharf in the Grand Harbour, Valletta (Progress on the Extension of Two Quays at the Grand Harbour | Infrastructure Malta, 2024)
- Buġibba Ferry Landing (Buġibba Breakwater Project is 70% complete Infrastructure Malta | Times of Malta, 2024)
- Cargo Facility at Ras Ħanzir between Laboratory and Fuel Wharves in Corradino, Grand Harbour (CTP Consulting Engineers, 2025)

Considering solely these projects, a total of 11,945 tonnes of CEM I, 46,680 tonnes of CEM II/A-L and 23,493 tonnes of CEM IV were used. The major constituent of cement that generates 90% of overall CO_2 emissions from cement is clinker (Purton, 2024). According to BS EN 197-1:2011 Table 1, the minimum amount of clinker used for each type of cement can be determined. At least, 95% of CEM I is clinker. This percentage changes with different types of cement. Clinker in CEM II/A-L constitutes 80% of the product whereas in CEM IV the proportion is 45%. Thus, in the above-mentioned projects by Infrastructure Malta, at least 59,000 tonnes of clinker would be present in the cement used. Based on the fact that approximately 0.541 tonnes of CO_2 are emitted per tonne of clinker (Gartner & Sui, 2018), it follows that at least 32,000 tonnes of CO_2 would have been produced due to these projects.

It can therefore be said that the local scene could benefit greatly from the partial replacement of cement with glass waste powder due to the improvements in glass waste management and environmental sustainability.

CHAPTER 3 – LITERATURE REVIEW

3.1 CONSTITUENTS OF CONCRETE

Concrete consists of a mixture of cement, water, fine aggregate, coarse aggregate and often, admixtures. The concrete mixture varies depending on the required properties and applications. When a binder, like cement, and water are mixed together, a paste forms. The addition of sand, also known as fine aggregate, to the mixture of cement and water results in the formation of mortar. For concrete to be produced, coarse aggregate must then be added to this mortar (Neville & Brooks, 1987).

3.2 BACKGROUND ON CEMENT

Cement is a chemically active constituent which has cohesive and adhesive properties that bind, bond and compact fragments into a whole. Table 1 of BS EN 197-1:2011 lists the different types of cement - CEM I, CEM II, CEM III, CEM IV and CEM V. Each type contains different proportions of the constituents that make up the binder.

The raw materials needed for cement production are calcareous rocks and argillaceous rocks. Calcareous rocks like limestone contain calcium carbonate ($CaCO_3$) whereas argillaceous rocks like clay contain silica (SiO_2), alumina (Al_2O_3) and iron oxide (Fe_2O_3). These rocks are ground, mixed and then burned at about 1450^oC (Nehdi & Yassine, 2020) to produce clinker which is ground again into a powder (Jackson & Dhir, 1996). $CaCO_3$ from the calcareous rocks is broken down by the heating process in the furnace and yields calcium oxide (CaO), otherwise known as lime, and CO_2. This reaction is referred to as the calcination of limestone. During the burning process, the CaO produced reacts with the SiO_2, Al_2O_3 and Fe_2O_3 from the argillaceous rocks to create tricalcium silicate ($3CaO.SiO_2$ noted as C_3S), dicalcium silicate ($2CaO.SiO_2$ noted as C_2S), tricalcium aluminate ($3CaO.Al_2O_3$ noted as C_3A) and tetracalcium aluminoferrite ($4CaO.Al_2O_3.Fe_2O_3$ noted as C_4AF) (Neville & Brooks, 1987). The sources of CO_2 emissions during the production process of cement are the following:

- Transportation of raw materials
- Electricity used in the grinding process and in the cement production facility
- Fossil fuel burning in the furnace to generate the high temperature
- The calcination reaction of calcium carbonate

About 55% of all the CO_2 emissions released in the cement production process result from the calcination of $CaCO_3$ whereas approximately 35% are released from the non-renewable energy sources that fuel the furnace and transportation means. The remaining 10% of emissions are derived from electricity-related activities (Khaiyum et al., 2023)

Cement becomes reactive when it is mixed with water (H_2O). Cement hydration is an exothermic reaction, and heat is released in the process. This is divided into the following stages:

- Initial dissolution phase where the two calcium silicates C_2S and C_3S present in cement combine with water forming ettringite. Heat is released and this is referred to as the initial peak of the heat flow.
- Induction phase that is characterised by a low cement hydration rate. Heat release is low at this stage, and, in graphs of isothermal calorimetry, this is represented by a semi-horizontal line in first hours of hydration.
- Acceleration period that is characterised by an increase of heat flow values. Here, the peak of hydration is achieved, and this releases heat from the breakdown of alite to produce calcium silicate hydrates ($C_3S_2H_3$ noted as C-S-H) that form a gel and calcium hydroxide ($Ca(OH)_2$ noted as CH), also known as portlandite (Neville & Brooks, 1987).
- Deceleration phase in which a low cement hydration rate is present characterised by a decrease in the heat flow values.
- Stable period where the reaction comes to a stop (Jochem et al., 2021)

This hydration chemical reaction leads to the formation of the cement hydration matrix. Together with the metal oxides present in the cement, $Ca(OH)_2$ contributes to the alkaline environment in the concrete which usually has a pH of 12 to 13.8 (Sumra et al., 2020). The C-S-H gel acts as a strong binding medium for the aggregate particles used in the formation of concrete (Neville, 2011) (Jackson & Dhir, 1996). Aggregate does not play a part in chemical reactions as it is solely a filler material that improves the durability of concrete (Jackson & Dhir, 1996).

3.3 BACKGROUND ON GLASS

The major constituent material of glass is SiO_2 which is most often derived from sand (Saud, 2024). There are many different types of glass such as soda-lime glass, borosilicate glass, aluminosilicate glass and lead silicate glass among others. 82% of all glass waste is soda-lime glass that is used to make glass bottles (Zafar, M.J. et al., 2024). Soda-lime glass is amorphous. This means that the glass atoms and molecules are not organized in a definite crystalline lattice but are arranged in a random order (Xiao et al., 2020). Moreover, besides silica, it also contains calcium oxide (CaO) and sodium oxide (Na_2O) interspersed between the silica molecules. These further weaken the bonds between the SiO_2 molecules.

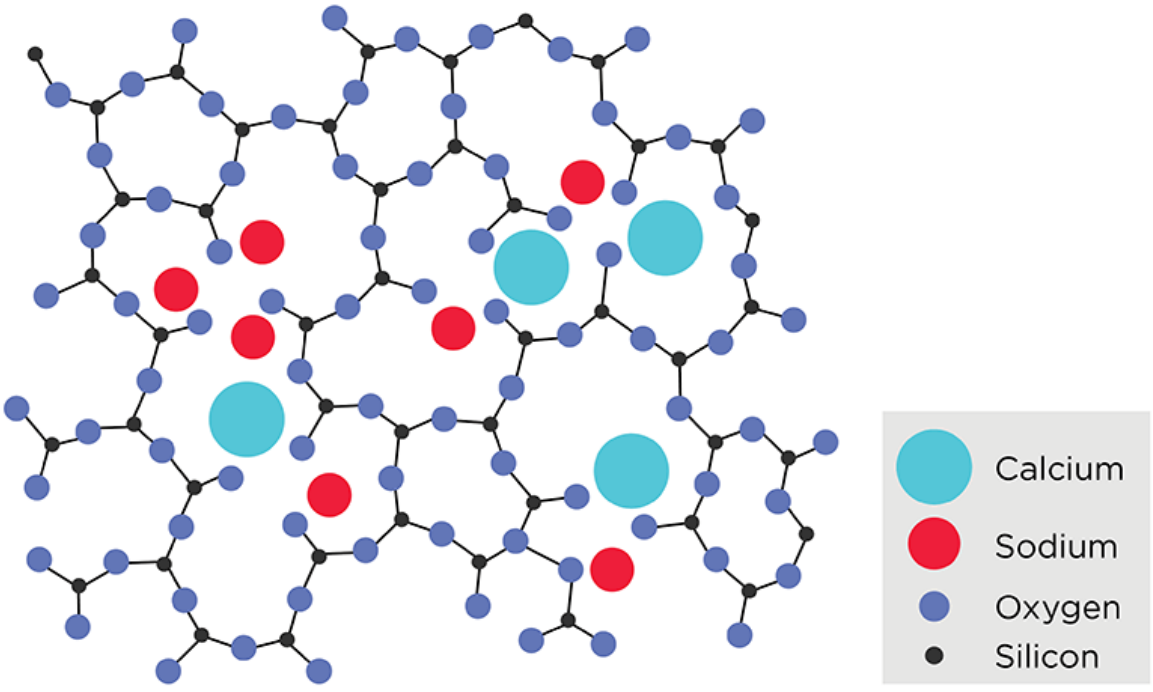

Figure 3.1 – Molecular Composition of Glass with Constituent Elements (Kopp Glass, Inc., 2015)

Several studies have been carried out where glass has been used as a replacement for aggregate as well as a supplementary cementitious material (SCM). Depending on the particle size of glass and the percentage replacement of cement, different outcomes have been observed on the following properties:

- Strength
- Durability
- Susceptibility to the alkali-silica reaction (ASR)
- Chemical resistance
- Permeability
- Workability

3.4 POZZOLANIC REACTIVITY AND PARTICLE SIZE

The presence of a high amount of amorphous silica in glass contributes to the pozzolanic activity of glass. Pozzolanic reactivity refers to the potential that a silica-based material, like glass, possesses to react with the excess $CaOH_2$ produced by the hydration reaction to form additional C-S-H gel. The production of additional C-S-H gel enhances the density, compactness and durability of concrete. However, this is highly dependent on particle size.

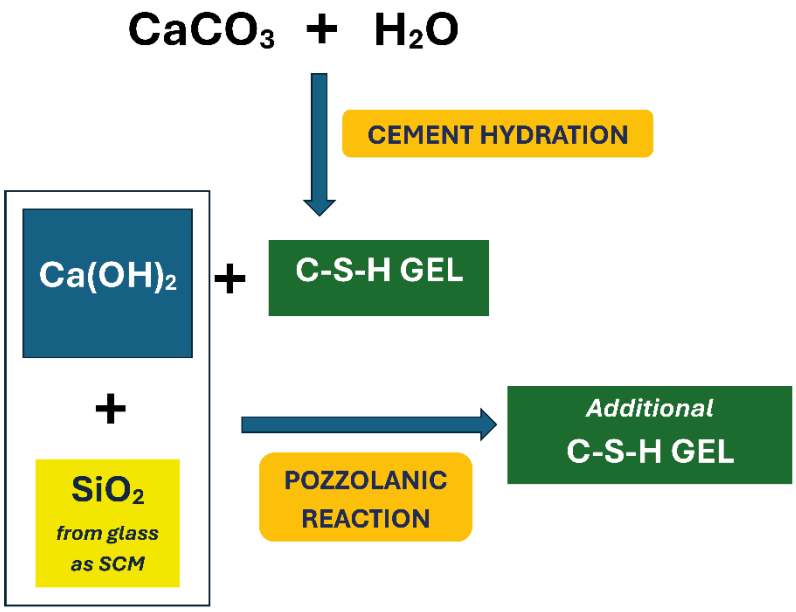

Figure 3.2 – Diagrammatic Representation of the Pozzolanic Reaction

Waste soda lime glass, being rich in silica in an amorphous state, has a high potential for pozzolanic reactivity (Singh, 2023). However, the glass must be highly ground to meet the criteria to be classified as a pozzolan as specified in ASTM C 618 since glass itself has negligible cementitious value (Dong et al., 2021). Waste glass powders have a pozzolanic reactivity of about 70 to 110% at 28 days and so meets the criteria established by ASTM C 618 (Siddika et al., 2021). This is because particle size highly influences this pozzolanic reaction. When glass is ground to a very fine powder, it is transformed from a non-reactive aggregate into a reactive pozzolanic material. In powder form, glass has a larger surface area where the pozzolanic reaction can take place (Taha & Nounu, 2008).

Many studies have been conducted that discuss the effect of glass particle size on the pozzolanic reaction. The pozzolanic activity index (PAI) measured by the mechanical method is also known as strength activity index (SAI) where the compressive strength of concrete is utilised to measure the effects of pozzolan addition to the concrete mix (Siddique & Paulo Cachim, 2018). According to Siddika et al., glass powder, that replaces 30% of the cement in concrete, must have a particle size of 75µm or lower for it to exhibit pozzolanic reactivity (Siddika et al., 2021). The more finely ground the glass waste is, the better the pozzolanic activity. Small particle sizes have a larger surface area bringing about a more extensive and rapid reaction. Pozzolanic activity comes into effect when the particles are smaller than 300 µm (Federico & Chidiac, 2009).

In a study conducted by Khmiri et al., the effects of different sizes of glass particles on the compressive strength of concrete were compared. A mixture of 20% cement replacement with glass waste was used. Four different particle ranges were studied – 80–100µm, 40–80µm, <40µm and <20µm. It was found that the waste glass used exhibited pozzolanic behaviour when it was ground to particle size of less than 20µm. Moreover, it was also established that the compressive strength of concrete increases with finer particle sizes at 7, 28 and 90 days. At 7 and 28 days, the strength of the 20µm concrete was lower than the control sample but at 90 days, this was reversed with the 20µm concrete possessing a higher compressive strength (Khmiri et al., 2013).

Similar studies were carried out by Shao et al. Concrete mixtures with 30% cement replacement by glass particles of sizes 38µm, 75µm and 150µm were studied. Compressive strength was exhibited with smaller particle sizes at 3, 7, 28 and 90 days. Yet again, concrete

utilising the finest glass particle size as a SCM was found to have a larger compressive strength only after curing for 90 days and not before (Shao et al., 2000).

To further corroborate this, when waste glass had a particle size of about 850µm, it could only be used as an aggregate and no longer as a SCM (Hassani et al., 2023). Furthermore, states that waste glass of particle sizes above 600µm are not considered as SCM (Siddika et al, 2021).

Fine glass particles also improve the packing of the concrete mixture as the glass powder fills the internal pores present, making concrete denser and less porous (Singh, 2023) (Hassani et al., 2023). This portrays the great importance of particle size of glass waste powder when used as a SCM, partially replacing cement in concrete. The decrease in porosity leads to less water absorption and consequent decrease in sorptivity of the concrete. The density, porosity and sorptivity of the concrete are all parameters which relate to one another (Dong et al., 2021).

3.5 CURING AGE

When waste glass powder is used as an SCM, the strength and durability of concrete are positively affected. However, this depends on the curing age of the concrete mix.

Most often, early-age concrete with glass powder has a lower compressive strength when compared to the cement control. The strength increases over time as the concrete cures. This is due to the pozzolanic activity offered by the glass powder. Shao et al. (Shao et al., 2000), Pavoine et al. (Pavoine et al., 2014) and Sharifi et al. (Sharifi et al., 2016) have all observed increasing compressive strength with increasing curing age in concrete where glass powder had been used as an SCM. Moreover, the strength of this concrete was higher than that of the control at 90 days (Khan et al., 2020). The pozzolanic properties of glass activate themselves slowly initially. However, as time passes the amorphous silica in glass continues to react, producing more C-S-H gel and refining the pore structure of the concrete. This results in increased strength (Hassani et al., 2023).

3.6 PERCENTAGE REPLACEMENT

Although studies have been carried out using different percentages of waste glass replacement, the ideal percentage of replacing cement with glass powder remains equivocal. Studies have found that the optimal range of percentage replacement for waste glass powder as an SCM is 20 to 30% as improvements in the properties of concrete can be seen in this range (Siddika et al., 2021). When 38µm glass powder replaced 30% of the cement in the mix, after 90 days, the compressive strength of this concrete was larger than that of the control and that of 30% fly ash. However, it was lower than concrete with 30% replacement with silica fume (Shao et al., 2000) (Mohajerani et al., 2017). It was also observed that the particle size of the glass powder affected the optimum percentage replacement of cement by glass. Particle sizes of less than 45µm yielded a significant increase in compressive strength when 30% cement replacement was used (Khan et al., 2020). In another study, it was found that compressive strength continues to increase for up to 25% cement replacement, but the peak of this increase results from 20% replacement. The particles used in this study were of a size of 600µm (Baikerikar et al., 2023). It is important that the percentage of glass is not too high because if so, not enough CaO from the cement would be available to react with the pozzolan to produce additional C-S-H gel (Siddika et al., 2021).

3.7 ALKALI-SILICA REACTION (ASR)

The Alkali-Silica Reaction (ASR) is a chemical reaction that causes crack formation in concrete. When cement is hydrated yielding $Ca(OH)_2$, the alkali cations derived from metal oxides present, such as Na_2O, will react with the hydroxyl (OH^-) ions and the SiO_2 in the aggregate forming a sodium silicate gel. Since this is hygroscopic, the formed gel will absorb water present in the pores within the microstructure of concrete, causing the gel to expand. This creates an internal pressure within the concrete, resulting in crack formation that decreases the strength and durability of the concrete.

When a pozzolan is added to the concrete mix, this reacts with the free $Ca(OH)_2$ present, preventing the above-mentioned reaction with metal oxides and silica in the aggregate. Thus, the ASR is mitigated. Instead, the pozzolanic reaction produces additional C-S-H gel that increases the density of the previously formed C-S-H gel by the hydration reaction

of cement. The increased density will prevent the water in the mixture from reaching the aggregate, thus preventing the ASR (Wang et al., 2021).

Glass waste has been studied as an SCM and as an aggregate. Like cement, glass contains alkali metal oxides, such as Na_2O and CaO, that can potentially induce the ASR. However, this is highly dependent on particle size.

When the particle size of glass powder is 75µm or lower, the glass acts as a pozzolan reacting with the $Ca(OH)_2$ and consumes it. Thus, little to no $Ca(OH)_2$ is left available for the ASR to occur (Siddika et al., 2021). Rajabipour et al. explained that the small-sized particles of glass powder fill up the microcracks in the concrete microstructure, resulting in increased concrete density and stronger non-expansive C-S-H gel (Rajabipour et al., 2010). Thus, when glass powder is used as an SCM, it produces an expansion less than 0.1% which is the acceptable limit stated by ASTM C1260 (Mohajerani et al., 2017). Different studies have shown that the reduction in the presence of the ASR increases with increasing percentage replacement of the cement with glass powder. A 40% decrease in expansion (when compared to the control mortar) occurred when 30% glass powder with particle size of 38µm was added (Pereira-de-Oliveira et al., 2012). On the other hand, when glass powder with 21% of particles had a size smaller than 45µm replaced 40% of the cement in the mixture, expansion was reduced by more than 90% when compared to the control (Dyer and Dhir, 2001).

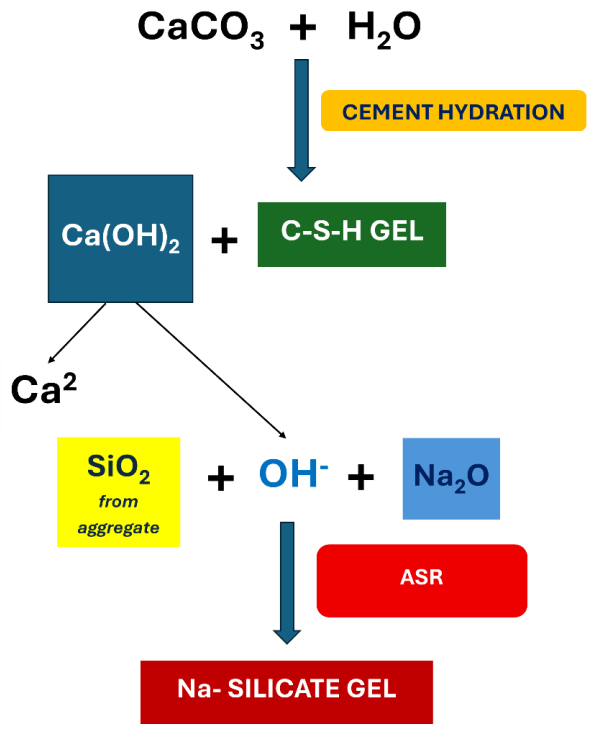

Figure 3.3 – The Alkali-Silica Reaction

3.8 IMPURITIES, CONTAMINANTS & CERAMIC INCLUSIONS

The effect that contaminants have on glass waste as an SCM is understudied. One study by Zhao et al. investigated how impurities in glass waste affect the properties of ultra-high-performance concrete (UHPC) by comparing washed with unwashed glass waste. The unwashed waste glass contained paper, plastic, aluminium and organic impurities. The glass together with the contaminants were crushed and ground to powder as was the washed glass waste. The following observations were made:

- The flowability of washed waste glass powder (W-WGP) increased when compared to the control. That of unwashed waste glass powder (U-WGP) decreased since the impurities absorbed water, reducing water in the mix.
- The compressive strength of W-WGP decreased slightly when compared to control. The pozzolanic reaction produced by the glass powder that replaced 30% of the cement in the mixture densified the concrete matrix, effectively diminishing the decrease in compressive strength. There was a more significant decrease in the compressive strength of U-WGP due to the paper and plastic impurities. Moreover, the presence of aluminium caused expansion that resulted in microcracks. This was caused by the production of hydrogen gas when the aluminium reacted with the alkali in the concrete.
- A decrease in the number of pores in the W-WGP sample led to a denser microstructure whereas in the U-WGP, more pores were evident together with microcracks.
- With regards to alkali-silica reaction (ASR) expansion, both W-WGP and U-WGP did not expand beyond the critical limit of 0.1%. However, this result may not be due to the cleanliness of the glass waste but due to the UHPC's water-to-binder ratio being very low at 0.18.

From these observations, one can conclude that washed waste glass powder gives better results than unwashed waste glass powder. The only benefit of using unwashed waste glass powder is that it has a lower environmental impact since water is not consumed for washing (Zhao et al., 2024).

The reject produced at WasteServ Malta Ltd. contains ceramic inclusions. Studies have been conducted for the possible use of ceramic waste as a possible SCM. Ding et al. investigated ceramic waste derived from households and found that this exhibits pozzolanic reactivity. When ceramic powder with particle size smaller than 40μm is used as an SCM, a

concrete with higher strength is achieved at 28 days when compared to the control with cement only (Ding et al., 2020). However, this type of concrete with ceramic used as an SCM will only exhibit ultimate strengths when allowed to cure sufficiently. At early-curing ages, the rising rate of compressive strength is reduced (Li et al., 2020). Thus, it was concluded that the replacement of cement by ceramic waste gives better properties to the concrete in terms of compressive strength, durability and workability (Jwaida et al., 2024). It seems that a material containing both glass waste and ceramic, similar to the reject from WSML, has not been sufficiently investigated.

3.9 COLOUR

Soda-lime glass is available in different colours, namely clear, green and amber. It seems that there is a slight difference in the chemical composition of the different colours of glass (Hamada et al., 2022). Studies have shown that clear glass contains a higher proportion of iron oxide (Fe_2O_3) than green glass and it might even be absent both in green and amber glass (Değirmenci et al., 2011) (Dhir et al., 2009). Different metal oxides such as Al2O3, MgO, Na2O and K2O might also be present in different proportions in clear and coloured waste glass (Pereira-de-Oliveira et al., 2012). A literature review conducted by Khan et al. revealed that when green waste glass powder replaced 10% of the cement, after 28 days, a 20% increase in compressive strength was observed when compared to a cement mortar whereas, with the same conditions, amber waste glass achieved only a 2% increase in compressive strength (Khan et al., 2020). Moreover, mortar with 25% amber glass exhibited a lower compressive strength of about 34.5% when compared to a mortar with 25% flint glass (a type of clear glass) (Karamberi & Moutsatsou, 2005). Thus, studies claim that different colours of glass show different reactivities when used as SCMs. However, evidence is scarce and the significance of the differences in practical terms is underexplored (Laveglia et al., 2020).

3.10 THERMAL ACTIVATION

Thermal activation is a process where temperature positively influences the behaviour of a material. High temperatures increase the kinetic energy of the particles of the material. This increased energy allows the particles to overcome processes that require increased energy such as new compound formation (Bahr, 2024).

Calcination is a thermal activation process whereby a solid substance is heated at a temperature below its melting point, resulting in the formation of new compounds as well as the removal of substances from the original compound (McGraw-Hill, 2003). For instance, in the calcination of limestone mentioned above, $CaCO_3$ is transformed into CaO and releases CO_2.

Studies have shown that when certain substances used as SCMs in the formation of concrete are calcined, their pozzolanic reactivity improves resulting in concrete with improved properties. Yang et al studied the effects of calcining waste glass residue with drill cuttings and their use as a SCM. It was found that for both calcination at 900^{o}C and 1000^{o}C, a mixture of 80% waste drill cuttings and 20% waste glass residue yielded the highest values for compressive strength. Both outcomes yielded better compressive strength that the control sample that was pure ordinary Portland cement (Yang et al, 2023). Zhang et al also looked at the effects of co-calcining glass waste with another material. It was found that waste glass co-calcined with dolomite sand at 800^{o}C resulted in better mechanical properties for the cemented paste backfill under test (Zhang et al, 2023).

Calcining glass without the introduction of other materials is underexplored. Glass, having amorphous silica is highly reactive when it is finely ground. Calcining glass may have the potential to make it more reactive.

It is important to note that apart from using glass as an SCM, studies have been conducted where glass waste has been used as fine and coarse aggregate, in alkali-activated concrete and in geopolymer concrete. However, these are outside the scope of this dissertation as research has shown that most often the ASR is pronounced when glass is used as an aggregate.

CHAPTER 4 – METHODOLOGY

The methodology used for this study involved both qualitative and quantitative research. The qualitative research yielded qualitative data through semi-structured interviews as described in Chapter 2 and Appendix 1. The quantitative research involved experiments conducted in a laboratory setting at the University of Malta that yielded primary quantitative data that was consequently analysed.

4.1 RAW MATERIALS

During the experiments carried out as part of the quantitative research, the following raw materials were required and acquired:

- Cement of type CEM I 42,5R (*Appendix 2*) which conforms to BS EN 197-1:2011
- Waste glass collected from different entities in Malta (BCRS Ltd. and WSML)
- Dolomite sand

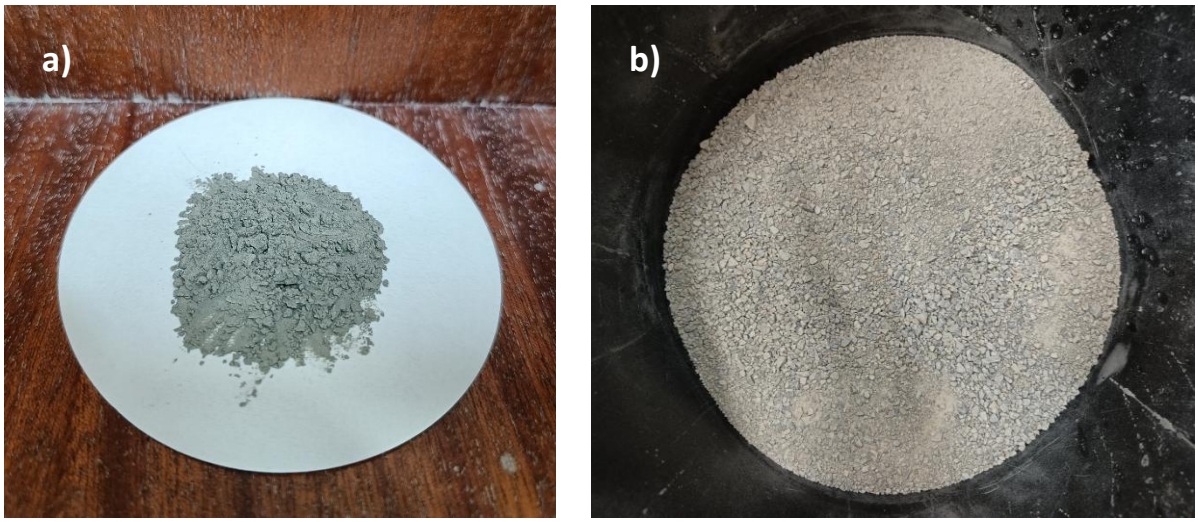

Figure 4.1 - a) Cement CEM I 42,5R & b) Dolomite Sand

Different types of soda-lime waste glass from food and beverage containers were acquired from WasteServ Malta Ltd. and BCRS Ltd.

The following glass waste was collected from WasteServ Malta Ltd.:

- Uncontaminated glass which is cleaned through the processes at their facility
    - Clear glass (Cl)
    - Coloured glass (Co)
    - Mixed clear and coloured glass (Cl + Co W)
- A reject from the glass cleaning and sorting process in their facility that contains glass fines, ceramic and other contaminants (Gl + Ce).

One type of glass waste was collected from BCRS Ltd. This was mixed clear and coloured glass that contains contaminants such as paper, aluminium and plastic (Cl + Co B).

These different types of waste glass gathered can be seen in *Figure 4.2*.

Clear Glass (Cl)

Coloured Glass (Co)

Clear & Coloured Glass (Cl + Co W)

Reject WSML (Gl + Ce)

Clear & Coloured Glass with Contaminants (Cl + Co B)

Figure 4.2 – Different Types of Glass Waste collected from WasteServ Malta Ltd. & BCRS Ltd.

4.2 PREPARATION OF MATERIALS

4.2.1 RINSING, CRUSHING AND MILLING

As discussed in the literature review, Zhao et al. found that the microstructure and the mechanical properties of ultra-high-performance concrete (UHPC) are better when washed glass waste is used as an SCM in comparison to unwashed waste glass powder (Zhao et al., 2024). Zhao et al. showed that washing reduces various solid, organic and metallic contaminants present in unwashed glass powder. This finding was directly implemented into the methodology of this study. Due to the processes at WSML, the glass types Cl, Co and Cl + Co W are uncontaminated and so, the glass waste requires no preparation in terms of cleanliness. Thus, these glass types were not washed. On the other hand, glass waste from the BCRS facility is contaminated. Thus, the glass waste Cl + Co B was rinsed with tap water. Gl + Ce is a reject of the process at WSML and consequently contains contaminants. However, since this glass type consists of fines of size less than 8mm, it could not be washed as it would run off through the sieves. Finer sieves were not used since when attempted this resulted in clogging of the sieve, making washing of Gl + Ce unfeasible.

Glass cullets from all the above-mentioned types of glass waste, excluding Gl + Ce, were initially broken down into smaller pieces by passing them through the jaw crusher. Each glass waste type was further crushed in the Los Angeles machine. Eleven (11) steel balls were used, and each glass type went through 1500 revolutions. The glass fines were then dried by placing them in the oven at 105^{o}C for at least 24 hours. This step was necessary to prepare the samples for grinding in the ball mill.

Jaw Crusher

Los Angeles Machine

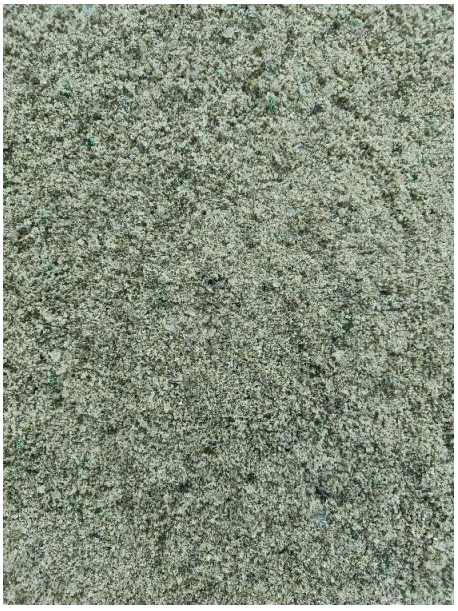

Ground material after crushing with Los Angeles machine

Figure 4.3 – Machinery & Products of Crushing the Glass Waste

Prior to the initiation of grinding, the glass waste was sieved, using a 1.18mm sieve, to exclude the larger shards of glass. This was done to avoid unnecessary stress on and deterioration of the ball mill. At least one (1) kilogram of each type of glass was ground in total, with samples of 220g being ground each time. Thus, each time, 220g of sieved glass waste were placed in the ball mill together with 180g of beads and 7 small steel balls. The glass was ground for 42 minutes at 600 revolutions per minute. This process yielded very fine particles of glass. This was crucial since, from the literature review, it was concluded that smaller particle sizes enhance the pozzolanic reactivity of glass, enhance the durability of concrete in which fine glass is used as an SCM, mitigate ASR and improve the workability of concrete.

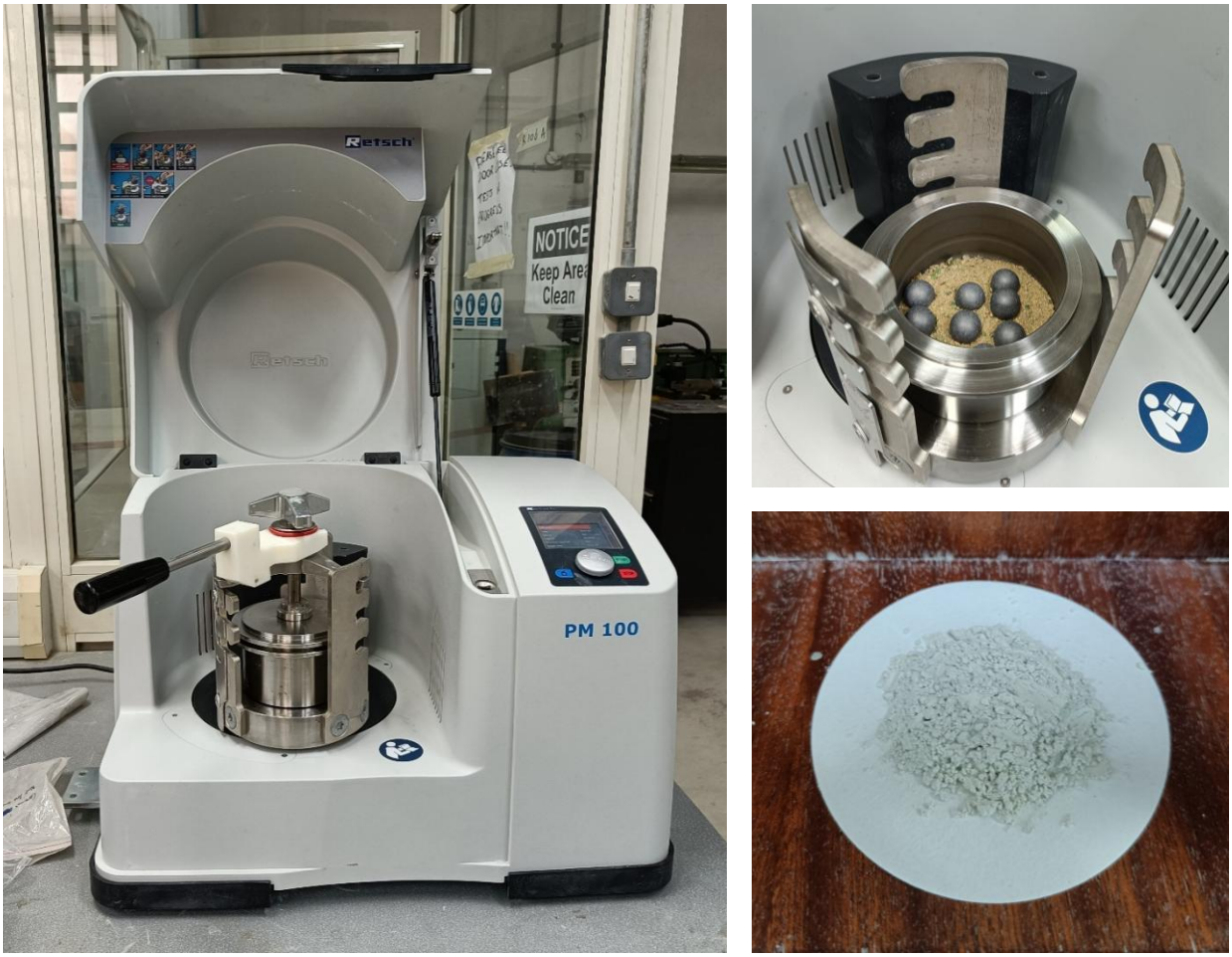

Figure 4.4 – Ball Mill Machine & the Milled Material

After milling, the samples were passed through a sieve. It was found that 94.6% of the glass material had a particle size of below 45µm. According to studies reviewed (*see Chapter 3*), this is a suitable size for glass to be used as an SCM.

4.2.2 THERMAL ACTIVATION

As has been discussed in the literature review (*see Chapter 3*), the effect of heat on waste glass alone is underexplored. Thus, it was decided that this study would investigate the possibility of thermal activation of glass waste alone.

Due to the limitation of time and resources, it was not possible to carry out this investigation on all the types of glass waste available. As mentioned previously, Zhao et al. found that cleaned glass waste yields better results than unwashed glass waste. Thus, a decision was taken whereby one of the uncontaminated glass samples from WSML, namely Cl + Co W, would be investigated for thermal activation. Another reason that directed the choice of Cl + Co W from other types of uncontaminated glass was that Cl + Co W is produced in significantly larger amounts at WSML.

The method described below was followed. After milling of Cl + Co W with the ball mill was completed, the glass powder was heat treated. Since the calcination of glass alone has never been studied before, a starting choice of temperature had to be made. Studies have shown that when glass waste is mixed with another substance and burned, higher temperatures yield better results. In fact, the temperatures used range between 800^{o}C and 1000^{o}C (Yang et al., 2023) (Zhang et al., 2023). Thus, taking into consideration that soda-lime glass melts at a temperature between 1400^{o}C and 1600^{o}C (Soda Lime Glass Melting Point - a Professional Guide for Glassware Industry - DM Glassware, 2024) and so that the lowest energy expenditure possible is used, a starting temperature of 850^{o}C was used. A sample of Cl + Co W was placed into a ceramic crucible and inserted in a furnace. The temperature was allowed to reach 850^{o}C and the sample was heated at this constant temperature for one (1) hour. The furnace was switched off after one (1) hour. The sample was allowed to cool inside the furnace for 24 hours.

At this temperature of 850^{o}C, the glass powder turned into a large white hard material that stuck to the ceramic crucible in which it was burned as seen in *Figure 4.5*.

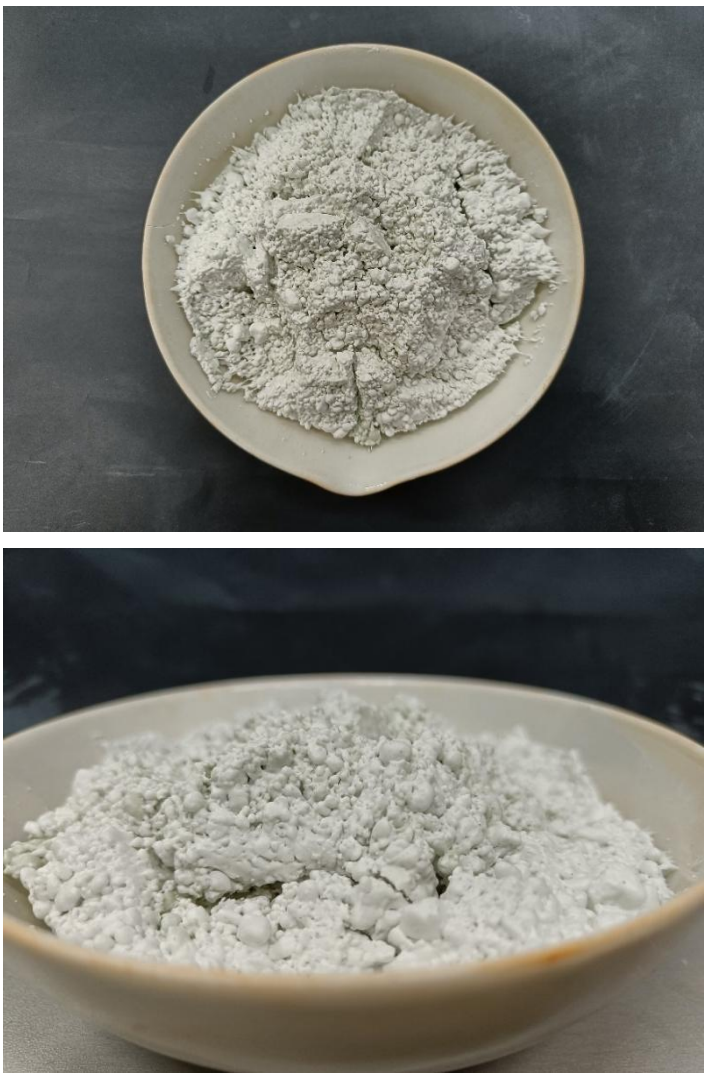

Figure 4.5 – The Cl + Co W sample after heating it at 850^{o}C

After looking into the possibilities of what had occurred, a study by Zaid et al. revealed that, at a temperature of 1300°C for 2 hours, soda-lime glass melted and at a temperature of 800°C for 2 hours, the glass sintered and α-quartz (SiO_2) and a small amount of devitrite ($Ca_3Na_2Si_6O_{16}$) were formed (Zaid et al., 2017). It is possible that this might have happened. Nonetheless, it was decided that the properties of this material, labelled as Cl + Co W Ca 850, would still be investigated for the possibility of being used as an SCM. Samples of 200g each were milled for 15 minutes with 400g of small steel beads to obtain a fine powder once again.

To separate the white hard material from the ceramic container, a chisel and hammer were used. Pieces of the white hard material that remained stuck to the ceramic crucible were discarded. The separated white hard material was then crushed and ground once again for it to be used as an SCM. Since the raw material was limited, small sample amounts were burned at different temperatures as trials to determine the next temperature to be used. The following observations were made for the respective temperatures:

- At 700°C, the same white hard material seemed to be formed.
- At 650°C, the material formed was less hard. However, solid clumps were still present.
- At 600°C, the glass powder remained in powder form.

Figure 4.6 – The different outcomes of heating the same material at different temperatures

Thus, a sample of Cl + Co W was heated at 600^{0}C for one (1) hour. Samples of 200g each of the treated powder, labelled as Cl + Co W Ca 850 was milled for just 2 minutes with 400g of small steel beads.

Figure 4.7 – Cl + Co W Ca 600 powder heated in a crucible

In summary, the following table the different types of glass waste being tested:

SCM Code	Type of SCM
Cem Con	Cement control. No supplementary cementitious material (SCM).
Cl	Clear glass acquired from WSML. This is uncontaminated due to the glass cleaning and sorting process in their facility.
Co	Coloured glass acquired from WSML. This is uncontaminated due to the glass cleaning and sorting process in their facility.
Cl + Co W	Clear and coloured glass acquired from WSML. This is uncontaminated due to the glass cleaning and sorting process in their facility.
Cl + Co B	Clear and coloured glass acquired from BCRS Ltd. This is contaminated due to the glass cleaning and sorting process in their facility. This has been lightly washed with tap water to remove some of the contaminants.
Gl + Ce	A reject from the glass cleaning and sorting process in the WSML facility that contains glass fines that include ceramic and other contaminants.
Cl + Co W Ca 600	Clear and coloured uncontaminated glass acquired from WSML which is then calcined at 600°C in the laboratory at the University of Malta.
Cl + Co W Ca 850	Clear and coloured uncontaminated glass acquired from WSML which is then calcined at 850°C in the laboratory at the University of Malta.

Table 4.1 – Different types of samples under test with code name and description

4.3 CHARACTERISATION TESTS

Characterisation tests were conducted on all the glass waste powders. This is an important step to relate the properties of the powders to the eventual performance indicators for the cement-based composite materials. The characterisation tests conducted directly inform the next phase of the experimental programme in defining the mixes and assessing the performance of the fresh and hardened properties. Characterisation is even more critical when considering the fact that the materials under test refer to a waste material where its properties need to be defined for it to be used as a product.

4.3.1 DENSITY BOTTLE TEST

The density bottle test was conducted on all the raw and treated glass powders to obtain values of their density. The density of materials is a fundamental physical property that characterises the material. It helps guide the mix design parameters as density directly influences the workability of fresh concrete. Since the waste glass powder has a different unit weight than that of cement, the density of the SCM also influences the properties of the hardened concrete (Siddika et al, 2021).

The densities of the powders that were used as an SCM were found following the procedure outlined in BS EN 196-6 :2010. A summary of the method is described below.

1. Five (5) density bottles, also known as pyknometers, were used. Each pyknometer was washed, cleaned with acetone, dried and labelled carefully prior to every use.
2. The mass of the empty pyknometers and their stoppers was found using a scale with precision of ± 0.0005g.
3. All 5 pyknometers were filled with room temperature de-aerated distilled water up to the top of the stopper. It was ensured that no air bubbles were present in the liquid.
4. The pyknometers were placed in a water bath at a temperature of 28^0C. The level of the water only reached the top of the neck of the density bottle. The pyknometers were left in the water bath for 30 minutes.

5. The density bottles were then removed from the water and dried off using a paper towel. A filter paper was used to wipe off any liquid at the top of the neck of the density bottle.
6. The density bottles were allowed to cool.
7. The pyknometers were then weighed after ensuring that the capillary bore within the stopper is topped up and void of air bubbles.
8. Steps 4 to 7 were repeated twice to obtain a total of three (3) mass readings for the pyknometer filled with de-aerated distilled water.
9. The mean of these mass values was calculated. The mass of the empty pyknometer and stopper was subtracted from this value to obtain the mass of the water used to fill the density bottle, W_1.
10. Steps 1 to 8 were repeated. Redistilled kerosine was used as a displacement liquid instead of water.
11. The mean of the mass values obtained, W_3, was calculated. The mass of the empty pyknometer and stopper was subtracted from this value to obtain the mass of the redistilled kerosine used to fill the density bottle, W_2.
12. The density of the redistilled kerosine, P_L, was calculated using the equation below:

$$P_L = \frac{W_2}{W_1} \times P_W$$

where P_W is the density of pure water at the selected temperature

13. Steps 1 and 2 were repeated once again.
14. 8 to 10g of the powder under test were weighed and placed in each pyknometer ensuring that no powder touches the neck of the pycnometer.
15. The pyknometer filled with the powder and stopper were weighed.
16. The mass of powder in the pyknometer, W_4, was obtained by subtracting the mass of the empty pyknometer from the mass of the pyknometer filled with the powder under test.
17. Each pyknometer was then half filled with redistilled kerosine to cover the powder present. The pyknometer was swirled to ensure that the powder is thoroughly wetted.
18. The 5 pyknometers and some beakers filled with redistilled kerosine were placed in a desiccator under vacuum until no more air bubbles are seen being formed.

19. The pyknometers were removed from the desiccator and topped up with the vacuumed redistilled kerosine in the beakers.
20. Steps 4 to 7 were repeated to obtain a total of 3 mass readings for the pyknometer fully filled with the vacuumed redistilled kerosine and the powder under test.
21. The mean of these mass values, W_5, was calculated.
22. The density of the powder under test, P, was calculated using the equation below:

$$P = \frac{W_4 \times P_L}{W_3 + W_4 - W_5}$$

23. Steps 13 to 22 were repeated for all the different powders.

The tables of the data collected during this test can be found in *Appendix 3*.

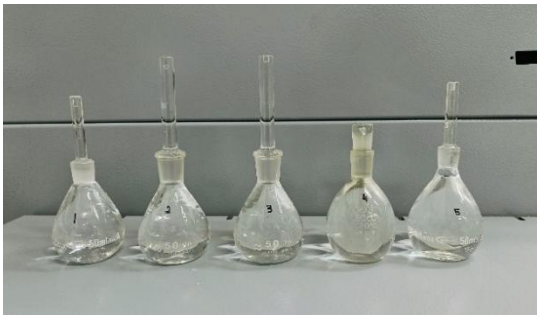

Step 3

Step 4

Step 9

Step 10

Step 14

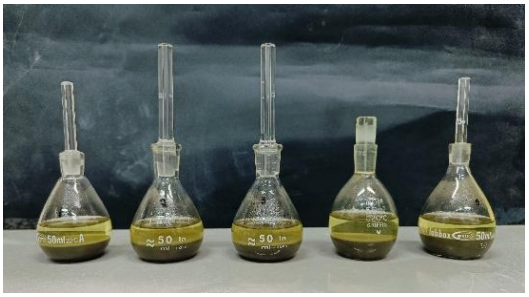

Step 17

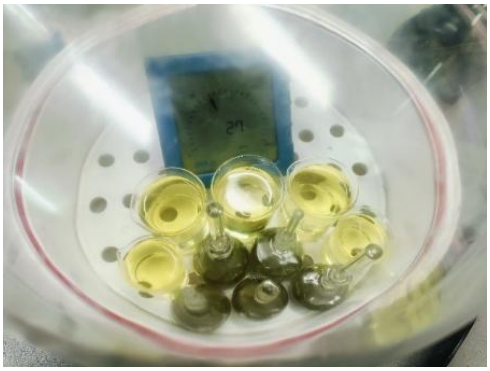

Step 18

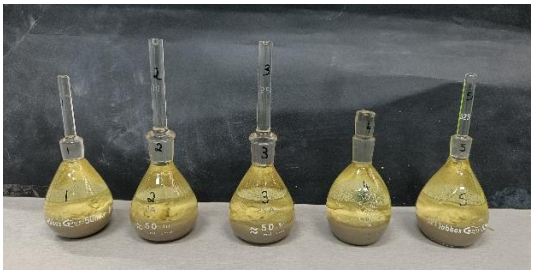

Step 19

Figure 4.8 - Density Bottle Test

4.3.2 X-RAY FLUORESCENCE

The chemical composition of the supplementary cementitious materials (SCMs) under test was analysed by the Bruker ED-XRF X-ray fluorescence spectrometer S2 Ranger. This was crucial to establish whether the impurities present, and heat treatment applied have any effects on the chemical composition of the SCMs.

Figure 4.9 - Bruker ED-XRF X-Ray Fluorescence Spectrometer S2 Ranger

4.3.3 PARTICLE SIZE DISTRIBUTION

A Malvern Instruments particle size analyser was used to determine the particle size distribution (PSD) by means of laser diffraction. For a given sample, this instrument gives data in graphical and tabular means on the different particle sizes present as well as their relative proportion in the sample. This information can be used to determine if most particles in the sample have a size which, based on the literature review, is small enough to be a pozzolan.

The following was the procedure that was carried out for this analysis:

1. 100 mg of powder was weighed.
2. 100ml of deionized ultra-pure water was poured into a pyknometer.
3. The powder was poured into the pyknometer and the solution was then shaken.
4. The sample suspended in the water was then sonicated for 2 minutes with ultrasound.

5. To prepare the instrument for receiving the suspended sample, the Malvern Instruments Hydro 2000S module of the instrument was flushed and cleaned with water twice before measuring the background. This module of the instrument is responsible for washing, sampling and placing the sample inside the Malvern Instruments Mastersizer.
6. The suspended sample was then poured into the sample cell of the Hydro 2000S module. It was ensured that the light obscuration was between 10 to 20%.
7. To stir the sample, the rotation was set to 3000 revolutions per minute (rpm). The ultrasound power was set to 70%. This ensured that the particles within the powder would not be dispersed or agglomerated (also referred to as flocculated) to be able to assess the true particle size and distribution of the powder.
8. The sample is then analysed by the Malvern Instruments Mastersizer by means of laser diffraction to determine the particle size distribution. The parameters for the Malvern Instruments Mastersizer were as follows:
    - Sample measurement time: 5 seconds
    - Background measurement time: 20 seconds
    - Sample measurement snaps: 5000
    - Background measurement snaps: 20,000
    - Number of measurement cycles: 30
    - Delay between measurements: 0 seconds
9. The instrument was set to create the average result for each sample.
10. The entire procedure was then repeated for all the different types of SCMs.

The tables and graphs of the data collected during this test can be found in *Appendix 4*.

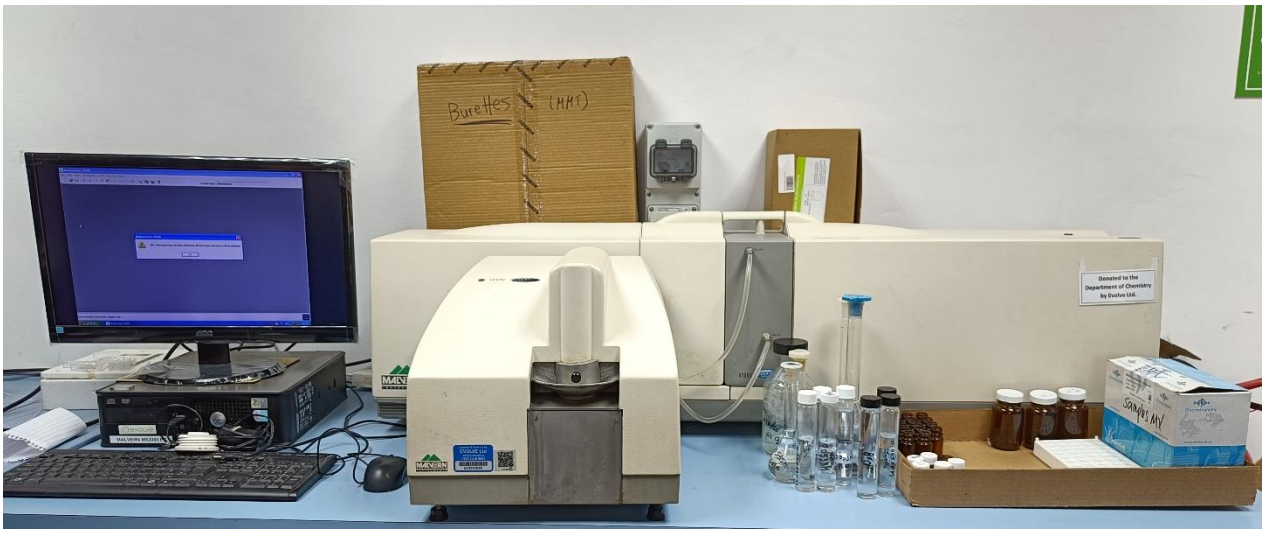

Figure 4.10 - Malvern Instruments Particle Size Analyser

4.3.4 SCANNING ELECTRON MICROSCOPY AND ENERGY DISPERSIVE X-RAY SPECTROSCOPY

Scanning electron microscopy (SEM) and energy dispersive x-ray spectroscopy (EDS) were carried out on the powders used as SCMs for a multitude of reasons. Through SEM, the particle sizes could be observed. These could then be compared to the results of the particle size distribution. The shape of the particles could also be seen. Pereira-de-Oliveira et al. noted that particle shape of ground glass powder was plate-like and elongated (Pereira-de-Oliveira et al., 2012). Hassani et al. also noted that many studies observed that the texture of glass powder appeared to be smooth and slippery having sharp corners and steep slopes even though the particle size is small (Hassani et al., 2023). Different studies have arrived at different conclusions with regards to how the shape of the particles influences workability, if at all (Mohajerani et al., 2017). EDS was performed to determine the prominent elements within the sample as well as their relative proportions.

The SCM powder samples were placed on a metal stub using carbon tape. To improve visibility for SEM, these were then carbon coated. This was also done to mitigate surface charge that could result in damages to the SEM. Unfortunately, the carbon coating affects the percentage of carbon present in the sample and so the value obtained through EDS cannot be fully attributed to the sample itself.

The SEM used for the analysis was a Carl Zeiss Field Emission Scanning Electron Microscope (FESEM) with a Gemini II Column and using SmartSEM software. The EDS detector was an Elect Plus EDS Detector from EDAX Ametek using APEX Suite software.

The parameters and operating conditions used for SEM-EDS were as follows:

- 230V
- 50-60Hz
- Extra High Tension (EHT): 15KV (When doing EDS)
- Iprobe: 1nA (When doing EDS)
- DOM: 2019, 03, 04
- Active Area: 30mm^2

Figure 4.11 - Carl Zeiss Field Emission Scanning Electron Microscope (FESEM) with a Gemini II Column & using SmartSEM software

4.3.5 X-RAY DIFFRACTION (XRD)

X-ray diffraction (XRD) was carried out on all the glass powders that were used as SCMs. XRD is a fundamental analytical technique that aids in the chemical and structural characterisation of the materials. Through the XRD patterns, it can be established whether the materials are amorphous or crystalline. Typically, when an amorphous material such as glass is analysed, broad humps are present rather than sharp peaks (Xiao et al., 2020). This test aims to yet again confirm that the glass waste that was used has an amorphous structure which makes it a suitable SCM.

The instrument used for the analysis was STOE PXRD. A STOE Stadi MP diffractometer equipped with a curved germanium (111) monochromator and a Mythen 1K detector. The samples were scanned using the following measuring parameters:

- Scanning Range (2θ range): 2^{o} – 90.215^{o}
- Step size: 0.015^{o}
- Scanning Speed/Duration/Time per Step: 840.0 sec/step

The equipment settings were set as follows:

- Radiation source: Cu Kα1 radiation (l = 1.54060 Å)
- Voltage: 40 kV
- Current: 40 mA

Figure 4.12 - STOE Stadi MP diffractometer equipped with a curved germanium (111) monochromator and a Mythen 1K detector

4.4 PASTE PREPARATION AND TESTING

4.4.1 PASTE MIX DESIGN

Parameters were chosen for the design mix of the paste samples (*Table 4.2*). The percentage SCM used in the mix was guided by the literature review where it was found that:

- When particle size of the waste glass powder was below 600µm, peak performance was achieved when 20% of the cement was replaced with waste glass powder (Baikerikar et al., 2023).
- When particle size of the waste glass powder was 38µm, peak performance was achieved when 30% of the cement was replaced with waste glass powder (Shao et al., 2000) (Mohajerani et al., 2017).

The particle sizes of the different sample groups under study in this dissertation were determined prior to the paste mix design. The range of particle size in the samples varied from less than 38 µm and did not exceed 600 µm. Thus, a decision was taken to carry out testing with 25% replacement of cement.

Numerous trial mixes were prepared in a structured mixed design programme to establish the optimum water-to-binder ratio and percentage of superplasticizer for the defined performance criteria. As mentioned previously, the cement used for this study was CEM I 42,5R (*see Appendix 2*). The superplasticizer MasterGlenium SKY 698 was used in the mix.

SCM Code	Type of SCM	Percentage Replacement	Water to Binder Ratio (Binder = Cement + SCM)	Superplasticizer Percentage
Cem Con	Cement Control (NO SCM)	0%	0.27	0.6%
Cl	Clear Clean Glass from WSML	25%	0.27	0.6%
Co	Colour Clean Glass from WSML	25%	0.27	0.6%
Cl + Co W	Clear & Colour Clean Glass from WSML	25%	0.27	0.6%
Cl + Co B	Clear & Colour Contaminated Glass from BCRS Ltd.	25%	0.27	0.6%
Gl + Ce	Reject from WSML that contains glass fines that include ceramic and other contaminants	25%	0.27	0.6%
Cl + Co W Ca 600	Clear and Coloured Cleaned Glass from WSML which has been calcined at 600^{o}C	25%	0.27	0.6%
Cl + Co W Ca 850	Clear and Coloured Cleaned Glass from WSML which has been calcined at 850^{o}C	25%	0.27	0.6%

Table 4.2 – Parameters for the Paste Mix Design

The table below shows the mix design amounts with respect to the different mix components.

SCM Code	Cement (kg/m^3)	Glass Powder (kg/m^3)	Water (kg/m^3)	Superplasticizer (kg/m^3)
Cem Con	2,083.33	0.00	562.50	12.50
Cl	1,562.50	520.83	562.50	12.50
Co	1,562.50	520.83	562.50	12.50
Cl + Co W	1,562.50	520.83	562.50	12.50
Cl + Co B	1,562.50	520.83	562.50	12.50
Gl + Ce	1,562.50	520.83	562.50	12.50
Cl + Co W Ca 600	1,562.50	520.83	562.50	12.50
Cl + Co W Ca 850	1,562.50	520.83	562.50	12.50

Table 4.3 – The Amounts of the Different Mix Components

4.4.2 FRESH PROPERTY TESTING ON THE PASTE MIX

4.4.2.1 MINI CONE FLOW TABLE TEST

One of the fresh property tests conducted on the paste mix was the mini cone flow table test. The aim of this test was to evaluate the workability of the fresh paste mixture. This is important since the workability of concrete determines the ease of handling of the concrete mixture. The greater the amount of energy required to complete the compaction of concrete, the less workable the concrete mixture is (Baikerikar et al., 2023). It is important the mixture is neither too stiff nor too flowing. The shape, texture and surface area of the glass particles will affect the workability of the mix. When the particles are small, the workability of concrete decreases due to the filler effect in the microstructure of concrete (Hassani et al., 2023).

The test was conducted following the procedure outlined in BS EN 1015-3:1999. The procedure was carried out as follows:

1. The disc of the flow table and the inside of the mini cone was wiped with a clean damp cloth. The mini cone was used instead of the truncated conical mould since, the mix being for paste, less material was required to be poured into the sample moulds.
2. The disc of the flow table was then wiped dry.
3. The mould was placed at the centre of the disc, and the paste mixture was poured into the mould until it was filled to the brim.
4. Any excess mixture was scrapped off the mould using a palette knife.
5. The mould was slowly raised allowing the mixture to spread.
6. The flow table was then consistently jolted 15 times to spread the mixture even further.
7. The diameter of the mixture was then measured in two orthogonal directions using a vernier calliper.

Figure 4.13 – Flow Table with Paste Mix & Vernier Calliper

4.4.3 ISOTHERMAL CALORIMETRY

Using the Calmetrix I-CAL HPC, isothermal calorimetry was conducted on Cl + Co B, Cl + Co W and Cl + Co W Ca 600. This was done to study their hydration kinetics and the total heat of hydration. This test works by measuring the heat flow as well as the cumulative heat of the paste mixtures as both are released during the hydration process. ASTM C 1679-14 and ASTM C 1702 – 15b were used as guidelines. For this test to be conducted, the proportions of the paste mixture mentioned previously were once again used as the mix design for this test.

The mixture was prepared in a plastic container using a plastic spatula which was then left inside the container. The samples were then placed in the isothermal calorimeter for 4 days and readings were read thereafter.

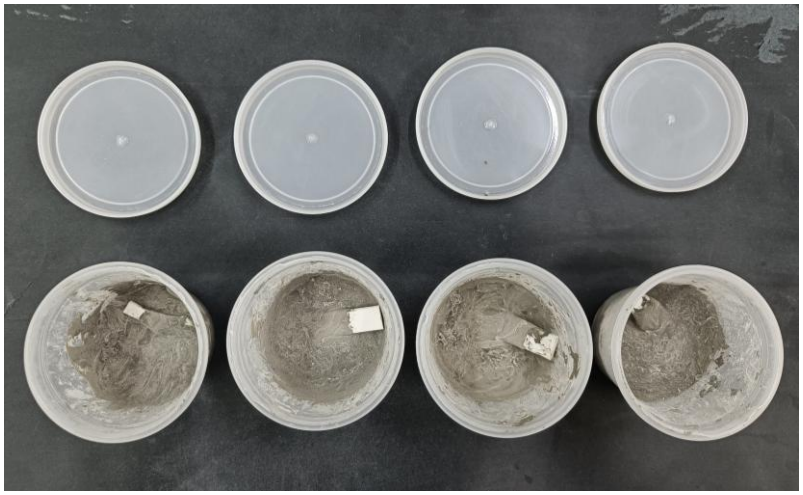

Figure 4.14 - Isothermal Calorimetry Testing on Paste Samples

4.4.4 HARDENED PROPERTIES OF THE PASTE

After the Mini Cone Flow Table test was performed, the mixtures were poured into 20 x 20 x 20mm moulds that were oiled to prevent adherence of the mixture to the moulds. Pouring was done in two stages to ensure that the mix is homogenous. Using a palette knife, the tops of the moulds were scraped and cleaned, ensuring that the mixtures were level with the tops of the moulds. A vibrating table was then used to remove the air bubbles trapped within the mixture. However, it was ensured that the vibration was not excessive to avoid segregation and bleeding. The filled moulds were left to set for 24 hours.

Once the 24 hours elapsed, the cube specimens were demoulded and placed in a curing tank filled with tap water, ensuring that the specimens were fully submerged. A shelve made of chicken wire was placed at the bottom of the curing tank to act as a support for the specimens while allowing the bottom surface of the cubes to be exposed to the water.

With regards to the hardened properties of the paste, two curing dates were considered for this research – 7 days and 21 days. A total of eighteen (18) cubes for each material were cast. For each curing date, nine (9) cubes were allotted – three (3) for compression testing, three (3) for sorptivity testing and three (3) for vacuum saturation porosity testing. Even though raw material was scarce, this could be done since only a small amount of 75 g of each material was required. Once the appropriate curing ages were reached, the cubes were removed from the curing tank and testing was conducted.

4.4.4.1 HARDENED DENSITY TEST

The density of the paste cubes is an important parameter to be measured as it provides insight on the microstructure and in turn, the overall performance of the paste cubes. The density correlates to the packing and filler effect of the SCM as well as the density of the SCM itself.

The density of the pastes' cubes with the different types of SCMs was determined by calculating the mean density of three cubes in each category. Each individual density was calculated by dividing the cube's mass, which was obtained by weighing the cube, by the cube's volume, which was found by multiplying its dimensions. These dimensions were measured using a vernier calliper.

4.4.4.2 VACUUM SATURATION POROSITY TEST

The Vacuum Saturation Porosity Test was carried out to measure the permeable porosity of the paste. The amount and size of pores present in the paste determines the compactness of the material as well as its ease of absorption of water into it (Zhang et al., 2020). Permeable porosity needs to be investigated as it gives light on the durability of concrete as well as on its transport properties which are responsible for deterioration of concrete. Moreover, increased porosity leads to a decreased compressive strength of the concrete (Moon et al., 2016). The method used followed that described by Safiuddin & Hearn (Safiuddin & Hearn, 2005). The procedure is as follows:

1. After reaching the required curing age, the paste cubes were removed from the curing tank and dried in an oven at 105^0C for 48 hours.
2. After the 48 hours elapsed, the samples were removed from the oven and allowed to cool at room temperature.
3. The specimens were then weighed to determine their oven-dry mass (W_d).
4. The apparatus was setup as depicted in the figure below. The two desiccators were connected to the vacuum pump through a water trap. Cool tap water was poured into one of the desiccators.

Figure 4.15 – The Setup of the Apparatus for the Vacuum Saturation Porosity Test

5. The samples were then put in the empty vacuum desiccator. They were placed on shelving made of chicken wire to expose all the surfaces of the cubes. It was ensured that the vacuum desiccator was properly sealed by using petroleum jelly, putty and jubilee clips where required.
6. The vacuum pump was started and run for 3 hours.

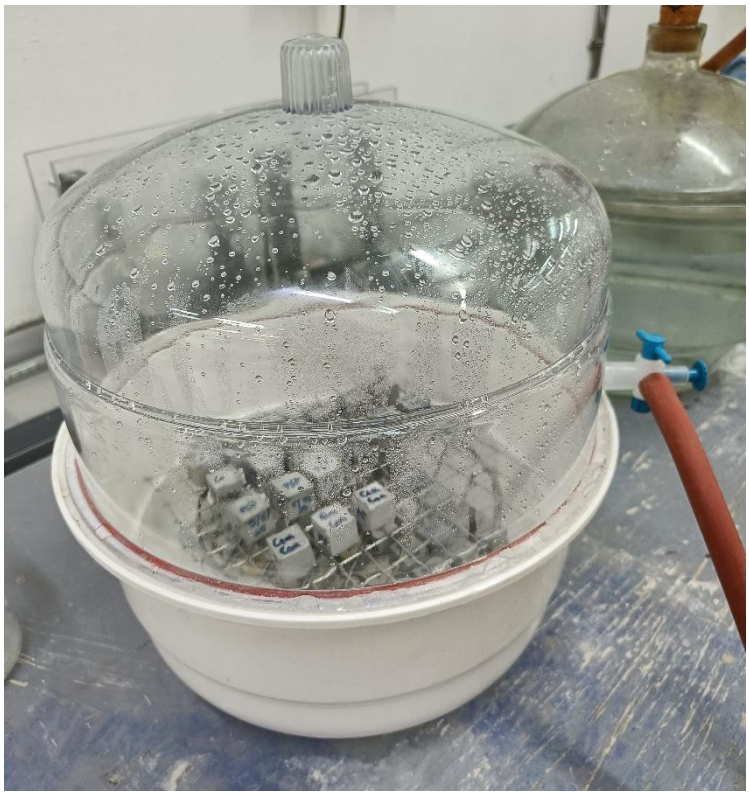

Figure 4.16 – Vacuum Desiccator

7. While leaving the pump still running, the valves were then turned to allow water to enter into the desiccator holding the samples. Water was allowed to enter until the cubes were fully submerged. The water line was then closed. The specimens remained under vacuum for another hour.
8. The pump was then switched off and the samples were left submerged for an additional 20 hours.

9. The buoyant mass (W_b) of the samples was then found using the apparatus depicted in the figure below.

Figure 4.17 – Obtaining the Buoyant Mass of the Samples

10. The specimens were then wiped and patted dry using paper towels to find the saturated surface-dry mass (W_s).
11. The following equation was then used to determine the permeable porosity of all the cubes under test. The average of the values obtained for all the 3 cubes of the same typology was then calculated.

$$Permeable\ Porosity = \frac{W_s - W_d}{W_s - W_b} \times 100\%$$

4.4.4.3 SORPTIVITY TEST

Sorptivity is the rate of absorption of water into concrete by capillary movement. The sorptivity test gives information on the material's microstructure and the capability of the material to take water in it. Thus, a material with higher sorptivity would have a higher porosity and a lower density (Dong et al., 2021). At later curing stages, concrete becomes denser due to the formation of more C-S-H gel leading to decreased voids within the microstructure, resulting in decreased rate of absorption of water.

The sorptivity test measures the increase in mass of a material when water is absorbed into it. Only one surface of the material is exposed to water during the test, allowing only uniaxial penetration of water (Bhardwaj & Kumar, 2019). The following method was followed for this test as per ASTM C 1585-04:

1. In preparation for the test, the specimens were numbered and placed in an oven at 50^{o}C for 3 days. This was done to obtain an unsaturated concrete where the water present within the microstructure of concrete is removed.
2. The specimens were removed from the oven and placed in an airtight container for at least 24 hours.
3. After 24 hours, all the faces of the cubes were sealed with aluminium tape except for one face per cube. It was ensured that the tape was properly aligned with the edge of the exposed face to ensure sealing of the adjacent faces.
4. The area of the exposed face of each cube was measured using a Vernier calliper.
5. This procedure was conducted in a room in the laboratory ensuring that the ambient temperature was kept constant.
6. A container with some distilled water at the bottom was prepared. A level mesh was placed at the bottom the container. It was ensured that the water reached a level of about 1 to 3mm above the mesh and that this level was maintained throughout the duration of the test.
7. The specimens were placed on the mesh and the container was loosely covered with a plastic sheet.
8. During the first day of the test, the specimens were removed from the water one by one at specific intervals as guided by the standard ASTM C 1585-04. Each specimen was

blotted dry using a paper towel and then weighed. The new value of mass obtained was recorded. After this, on the following days, this procedure was done once every day.

9. The original values of the mass of the specimen were deducted from the new values of mass obtained.
10. The following equation was used to determines absorption:

$$I = \frac{m_t}{a \times d}$$

where I = absorption

m_t = change in specimen mass in grams at time, t

a = exposed area of the specimen in mm^2

d = density of water in g/mm^3

11. The outliers for each sample type were excluded.
12. An average of these parameters was then taken for each sample type and used to plot the absorption (I) against the square root of time.
13. The data was then split into two sets, which correspond to data collected up to the 6-hour mark and data collected after the 24-hour mark respectively. The least-squares method was then used to fit the best straight line for the split datasets respectively. This resulted in two distinct gradients that do not intersect one another and with a gap between them.
14. These regression lines were then plotted on the same graph to illustrate the difference between the initial rate of absorption and the secondary rate of absorption.

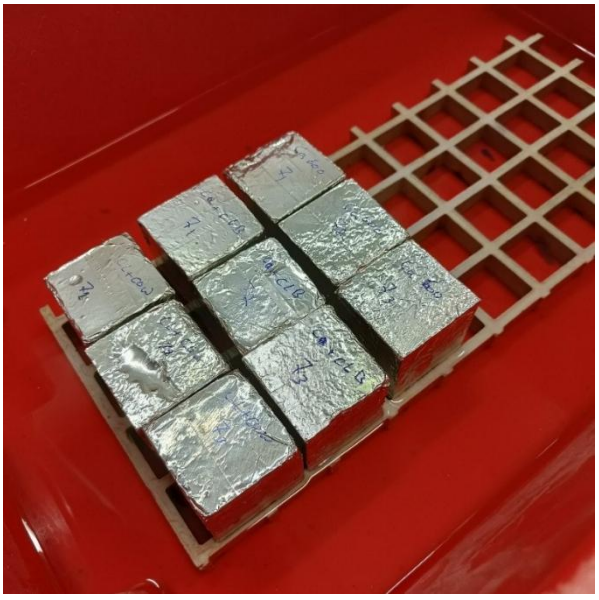

Figure 4.18 – Specimens covered with aluminium tape on all sides except one side which lies on a level mesh immersed in water

4.4.4.4 COMPRESSIVE STRENGTH

The compressive strength of a material is a vital mechanical property. In fact, compressive strength is used as a parameter to test other properties of materials such as pozzolanic reactivity. The performance of a material under an applied load indicates and correlates to the material's microstructure and the formation of C-S-H gel, density and quality.

The test for compressive strength was conducted following BS EN 196-1:2005. After the samples were left in the curing tank for the appropriate curing age, the samples were patted dry. Their volume was measured, and their mass was obtained. The values for each cube were then inputted in the compression machine. Before commencing the test, the surfaces where the cubes would be placed were cleaned from any particles. The load was applied to the smooth surfaces of the cubes. The load rate was set to 2.400MPas and the sensitivity was set to 90.00kN. The strength, in MPa and the applied load, in kN for each cube were then noted. Inconsistent values were discarded.

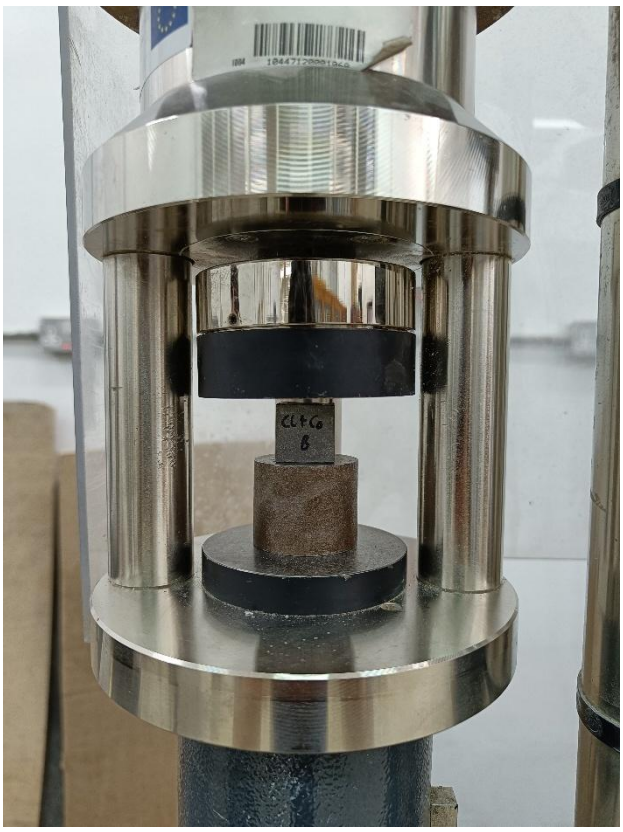

Figure 4.19 – Compression Machine used to measure Compressive Strength

4.4.4.5 SCANNING ELECTRON MICROSCOPY AND ENERGY DISPERSIVE X-RAY SPECTROSCOPY (SEM-EDS)

SEM-EDS was not only carried out on the powder used as SCM. It was also carried out on paste samples that had cured for 7 days. The scope of this analysis was to once again identify the elemental composition in the paste samples and to also observe any changes in morphology when the SCMs were included. This analysis was also crucial to determine both visually and through EDS whether the SCMs did, in fact, act as pozzolans by perceiving additional C-S-H gel.

Powder collected from the samples that were crushed in the compression machine was used for this analysis. The rest of the procedure and parameters were the same as described in the characterisation testing section of the methodology.

4.4.4.6 X-RAY DIFFRACTION (XRD)

As was done on the powders that were used as SCMs, X-Ray diffraction was carried out on the pastes that were cured for 7 days. After compression was carried out, the pieces of the paste cubes were crushed into a powder using a mortar and pestle. The powder was then sieved through a 75-µm sieve in preparation for this test. The procedure and parameters were the same as described in the characterisation testing section of the methodology.

It is essential to conduct XRD analysis on the paste samples to be able to identify the chemical reactions that result in the hydration products that occur as the material hardens such as the formation of C-S-H, N-A-S-H and C-A-S-H gel (Chen et al, 2022) (Zafar et al, 2024). Therefore, through this analysis, the reactivity can be better understood, thus aiding in performance prediction.

4.4.4.7 FOURIER TRANSFORM INFRARED (FTIR) SPECTROSCOPY USING POTASSIUM BROMIDE (KBr)

Fourier Transform Infrared (FTIR) spectroscopy using potassium bromide (KBr) was another technique that was used to analyse the chemical constituents and the evolution of the reaction products of a sample. The infrared absorption spectrum is utilised to carry out this analysis. The instrument used for the FTIR analysis was the Shimadzu IRAffinity–1 with

software Shimadzu IRsolution 1.50. The FTIR was conducted on all the paste samples that cured for 7 days. Fragments from the cubes that had undergone compression were collected, ground into powder using mortar and pestle and then sieved through a 75µm sieve. The method used was as follows:

1. A bolt was screwed into the bottom of a nut.
2. KBr, which was stored in an oven at 105^0C before use, was mixed with the powder sample.
3. The mixture was then placed into the bolt and nut making sure that it fully covers the flat head of the screw.
4. Another bolt was screwed into the other side of the nut. This was done to create pressure for the KBr crystal to form.
5. The crystal was allowed to form for a few seconds before unscrewing the bolts. It was ensured that the crystal had no cracks and was fully formed until the edges of the nut.
6. The nut with the crystal was placed inside of the FTIR machine for the analysis to be carried out. Twenty (20) scans were run for each material.

Figure 4.20 – Apparatus used for FTIR Spectroscopy

4.5 MORTAR PREPARATION AND TESTING

4.5.1 MORTAR MIX DESIGN

Three (3) waste glass types and a control sample were considered for testing mortar – Cem Con, Cl + Co W, Cl + Co B and Cl + Co W Ca 600. These were chosen to study the impact of impurities and the effects of calcination. The choice was based on predictions of likely best performance that were made at an earlier stage of the research process.

The parameters were chosen for the design mix for the mortar samples after trial mixes were conducted (*see Table 4.4*). The cement and superplasticizer used for the mix was the same as those for the paste mix design. The same procedure used for the paste samples was repeated for the mortar samples.

SCM Code	Type of SCM	Percentage Replacement	Water to Binder Ratio (Binder = Cement + SCM)	Cement to Sand Ratio	Superplasticizer Percentage
Cem Con	Cement Control (NO SCM)	0%	0.4	1:2.75	1.5%
Cl + Co W	Clear & Colour Clean Glass (WSML)	25%	0.4	1:2.75	1.5%
Cl + Co B	Clear & Colour Contaminated Glass (BCRS)	25%	0.4	1:2.75	1.5%
Cl + Co W Ca 600	Clear and Coloured Cleaned Glass from WSML which has been calcined at 600^{o}C	25%	0.4	1:2.75	1.5%

Table 4.4 – Parameter for the Design Mix of the Mortar Samples

The amount of material in kg/m^3 used is depicted in *Table 4.5* below.

SCM Code	Cement (kg/m^3)	Glass Powder (kg/m^3)	Sand (kg/m^3)	Water (kg/m^3)	Superplasticizer (kg/m^3)
Cem Con	666.67	0.00	1,833.33	266.67	10.00
Cl + Co W	500.00	166.67	1,833.33	266.67	10.00
Cl + Co B	500.00	166.67	1,833.33	266.67	10.00
Cl + Co W Ca 600	500.00	166.67	1,833.33	266.67	10.00

Table 4.5 – Amounts of Material Used in the Mortar Mix

4.5.2 FRESH PROPERTY TESTING ON THE MORTAR MIX

4.5.2.1 FLOW TABLE TEST

The flow table test was also carried out for the mortar mixtures. The procedure was identical to that used for the paste mixtures. However, for mortars, the standard truncated conical mould was utilised instead of the mini cone.

4.5.3 HARDENED PROPERTIES OF MORTAR

Once again, two curing ages were considered for testing. It was decided that tests would commence on the samples in a specified order after 7 days of curing and again after 21 days of curing. The mixtures were poured into moulds to form 50 x 50 x 50mm cubes, this time. These were oiled to prevent adherence of the mixture to the moulds. The mixture was poured into the mould in two stages to ensure that the mix is homogenous. Using a palette knife, the tops of the moulds were scraped and cleaned, ensuring that the mixtures were level with the tops of the moulds. The vibrating table was used to remove air bubbles from the mixture. It was ensured that the vibration was not excessive that it would lead to segregation and bleeding. The filled moulds were left to set for 24 hours before demoulding.

Once the cubes were demoulded, they were then placed in a curing tank until the appropriate curing ages were reached. Since the mortar moulds require a larger volume and the supply of waste glass powder was limited, a total of 6 cubes were cast for each material under test. Three (3) cubes of each material were used to carry out the following tests at 7-day curing age:

- Density Test
- Vacuum saturation porosity Test
- Sorptivity Test
- UPV
- Compression Test where the load rate was 2400N/s and sensitivity was 90.00kN. This test was carried out on the cubes fourteen (14) days after being removed from the curing tank.

The tests were conducted in the above-mentioned order, leaving the destructive test at the end. The same procedure was repeated after 21 days of curing with the other three (3) cubes.

The procedures for the above-mentioned tests were the same as those carried out on the paste samples.

4.5.3.1 ULTRASONIC PULSE VELOCITY TEST

The Ultrasonic Pulse Velocity (UPV) test on hardened concrete evaluates the quality of concrete and its integrity. This non-destructive test determines the velocity of the propagation of ultrasonic longitudinal and/or transverse waves through concrete. This, in turn, can detect internal flaws. Results can also be used to determine the compressive strength of the concrete and validate these results. Lin et al. found that, with increasing curing age, the UPV in concrete increases and so does its compressive strength, verifying that a measured UPV value is a good prediction of the strength of hardened concrete (Lin et al., 2007). The method used for this test followed BS EN 12504-4:2021 as outlined below:

1. The smoothest opposite surfaces of the cube were chosen.
2. The path length was measured using vernier callipers.

3. Petroleum jelly was placed on the concrete specimen where the transducers would be placed. This was done to ensure a sufficiently smooth finish for adequate acoustical coupling between the transducers and the concrete.
4. A transducer was pressed on a side of the specimen. The same was done to the opposite face.
5. The transit time was determined using the ultrasonic test equipment.
6. The pulse velocity was calculated using the following formula:

$$V = \frac{L}{T}$$

where V = pulse velocity

L = path length in mm

T = transit time in µs

Figure 4.21 – Apparatus used in UPV Test

4.5.3.2 THE ACCELERATED MORTAR BAR TEST (AMBT) FOR ASR

The extent of the alkali-silica reaction (ASR) is an important and critical parameter to be tested when exploiting glass in cement-based materials. The Accelerated Mortar Bar Test (AMBT) was only conducted on mortar since this reaction takes place when aggregate is part of the design mix. As explained in the literature review, the ASR is a deleterious reaction and so, it is vital to test its extent.

The same design mix as that of the 50 x 50 x 50 mortar cubes was used for the specimens of the ASR test. Eleven (11) different moulds, conforming to those in in ASTM C490/C490M – 11, were used to measure the effects of the ASR. These were 285mm long and had a square area of 25 x25 mm. For the expansion of the specimen to be tested, gauge studs were inserted into the edges of the moulds. These were used as a reference point to ensure that the repeated readings were taken from the same point.

The moulds were oiled before pouring the mixture. This ensured easier demoulding. The mixture was poured and vibrated in stages to remove the air bubbles within the mixture while avoiding segregation and bleeding. The specimens were allowed to set for 24 hours before demoulding.

ASTM C1260 – 23 outlines the Accelerated Mortar Bar Test (AMBT). This test exposes the specimens to harsh conditions to evaluate the potential ASR in a fast manner. After demoulding, the bars were labelled and placed inside a water bath at 80^0C for 24 hours. This was done to prepare the specimen to establish the zero reading. The length of the mortar bar from one tip of the gauge stud to the other was measured using vernier callipers. The length was also determined using a length comparator. The specimens were tapped dry before the readings were taken.

Once the zero readings were taken, the specimens were placed in an appropriate container containing a 1N sodium hydroxide (NaOH) solution which was heated to 80^oC in the oven. The containers containing the specimens were then placed in the oven which was set to 80^oC. Readings using the vernier calliper as well as the comparator were taken at 7, 14 and 21 days.

The following calculation was then made for the readings taken using the vernier calliper:

$$Change\ in\ Length = \frac{Reading\ at\ age\ x\ in\ NaOH\ solution - Zero\ Reading}{Zero\ Reading} \times 100\%$$

This was done to determine the change in length in the linear dimension of the test specimen. If the percentage of change in length is 0.1% or lower, the ASR would not negatively impact the specimens.

Figure 4.22 – Process of Accelerated Mortar Bar Test

CHAPTER 5 – RESULTS AND ANALYSIS

The results obtained from the tests described in the Methodology chapter are being presented in this chapter. The first crucial step in the analysis of the data obtained was detecting outliers. These were excluded from the data sets before any analysis was carried out. This was done to ensure that the analysis is not influenced by erroneous data brought about by experimental errors.

5.1 CHARACTERISATION TESTS RESULTS

5.1.1 DENSITY BOTTLE TEST RESULTS

Values for the density of the different types of waste glass powder were obtained by this test *(see Appendix 3*). Any irregular values that were obtained were discarded. The average density for each type of glass powder was found. *Table 5.1* below compares the densities of all the types of waste glass powder under test.

	POWDER SAMPLES							
	Cem Con	**Cl**	**Co**	**Cl + Co W**	**Cl + Co B**	**Gl + Ce**	**Cl + Co W Ca 600**	**Cl + Co W Ca 850**
Average Density (g/cm^3)	3.1174	2.4824	2.4925	2.4992	2.4883	2.4852	2.4646	2.4879
Average Density (kg/m^3)	3117.4	2482.4	2492.5	2499.2	2488.3	2485.2	2464.6	2487.9

Table 5.1 – Average Densities of the Waste Glass Powder under test

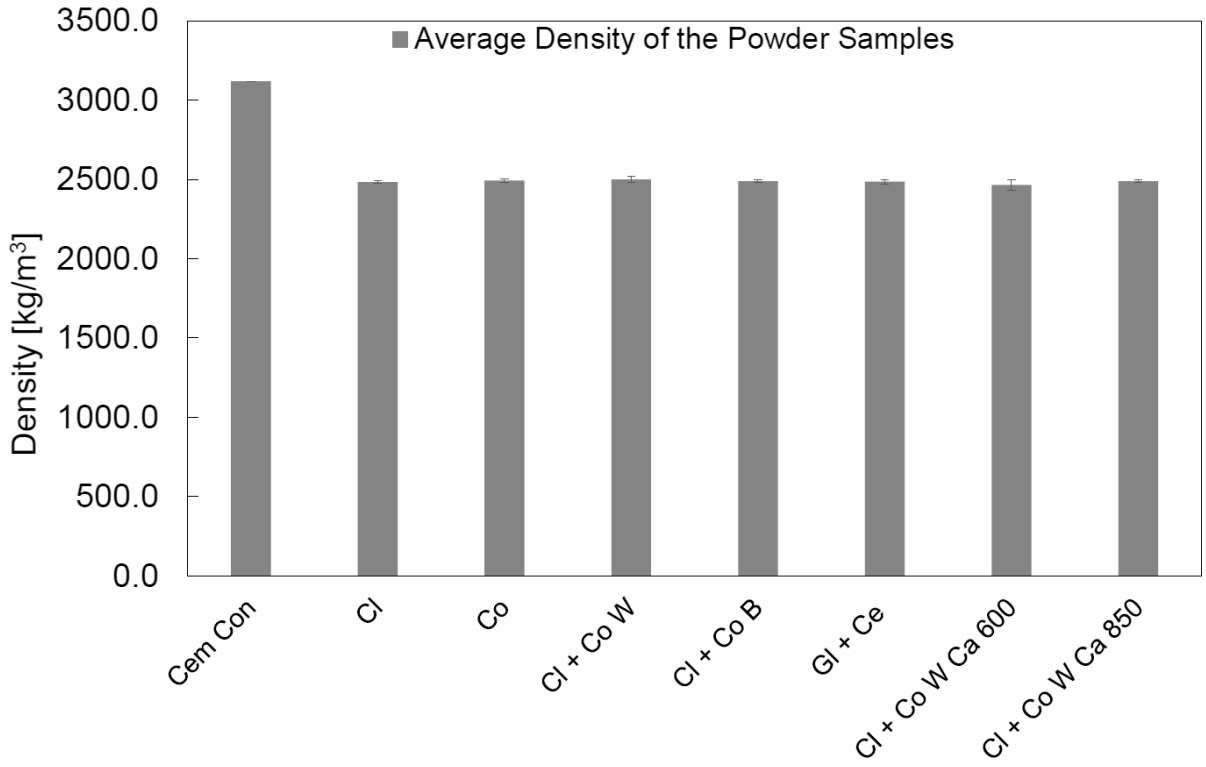

Figure 5.1 – Bar Graph showing the Average Densities of the Powder Samples

The density of soda-lime glass is 2.45 g/cm^3 (Son et al., 2024). The densities of the glass powders obtained are relatively very similar to one another. Results are comparable with the density of soda-lime glass, confirming that the specimens are soda-lime glass. It can also be noted that the densities of the glass powders are lower than that of cement. This result is comparable to data found in literature.

5.1.2 X-RAY FLUORESCENCE (XRF) RESULTS

The table below gives the readings obtained from the XRF spectrometer.

		POWDER SAMPLES							
		Cem Con	Cl	Co	Cl + Co W	Cl + Co B	Gl + Ce	Cl + Co W Ca 600	Cl + Co W Ca 850
CHEMICAL COMPOSITION (wt%)	SiO_2	14.1	66.3	63.4	66.1	63.6	66.0	65	64.4
	Al_2O_3	3.17	1.94	2.36	2.15	1.95	2.05	2.15	2.16
	CaO	62.8	14.5	12.6	12.9	13.1	12.4	13.2	13.6
	Fe_2O_3	2.98	0.408	0.813	0.525	0.607	0.739	0.630	0.854
	P_2O_5	0.470	0.706	0.733	0.617	0.668	0.562	0.721	0.776
	Na_2O	6.76	13.7	17.6	13.2	17.7	14.3	13.4	15.7
	K_2O	1.19	0.860	0.943	0.967	0.815	0.794	0.917	0.888
	MgO	2.29	-	-	1.91	-	1.91	2.41	-
	SO_3	5.48	0.695	0.482	0.579	0.633	0.555	0.610	0.625
	TiO_2	0.209	0.0963	0.113	0.0975	0.0819	-	0.115	0.103
	MnO	0.0640	0.0204	0.0386	0.0306	0.0401	0.0270	0.0299	0.0324
	Cl	0.244	0.467	0.431	0.437	0.471	0.412	0.448	0.480
	Cr_2O_3	0.0157	0.0276	0.165	0.0815	0.134	0.117	0.109	0.104
	V_2O_5	0.0108	0.0087	0.0175	0.0138	-	-	0.0208	0.0100
	CoO	0.0168	0.0033	0.055	0.0056	-	-	0.0042	0.0049
	NiO	0.0086	-	0.0030	-	0.0023	-	-	0.0031
	CuO	0.0217	0.0068	0.0121	0.0079	0.0082	0.0058	0.0097	0.0108
	ZnO	0.0185	0.0179	0.0133	0.0172	0.0221	0.0151	0.0159	0.0187
	Ga_2O_3	0.0030	0.0021	0.0018	0.0028	0.0020	-	0.0019	0.0021
	As_2O_3	0.0038	-	-	-	-	-	-	-
	SeO_2	0.0024	0.0034	0.0029	0.0034	-	0.0024	0.0030	0.0030
	Br	0.0015	0.0022	0.0021	0.0021	0.0019	0.0018	0.0020	0.0022
	Rb_2O	0.0045	0.0074	0.0062	0.0062	0.0051	0.0059	0.0064	0.0070
	SrO	-	0.0218	0.0229	0.0204	-	0.0228	0.0218	0.0229
	Y_2O_3	-	-	-	-	0.0013	-	-	-
	GeO_2	-	-	-	-	-	0.0012	-	0.0018
	ZrO_2	-	0.0286	0.0303	-	0.0320	0.0269	0.0287	-
	CdO	-	0.0022	-	-	-	0.0023		-

Table 5.2 – XRF Spectrometer Results

These values were analysed. There is no considerable difference in chemical composition between the different types of glass waste, not even with the samples that were heat treated. This was expected since heat would only change the structural composition of the material and not the chemical composition.

5.1.2.1 COMPARING THE CHEMICAL COMPOSITION OF THE POWDER SAMPLES TO STANDARDS

The values were also compared to standards as shown below to determine if the glass waste under test satisfies the criteria of a pozzolan, based on its chemical composition.

The following standards were considered:

- ASTM C618 – 12a - Standard Specification for Coal Fly Ash and Raw or Calcined Natural Pozzolan for Use in Concrete
- BS EN 450-1:2005 -Fly ash for concrete – Part 1: Definition, specifications and conformity criteria
- BS EN 197-1:2011 - Cement Part 1: Composition, specifications and conformity criteria for common cements
- NBR 12653 - Pozzolanic Materials – Requirements

The following tables show how the percentages of the chemical compounds for each type of waste glass powder under test compare to the requirements for pozzolanic materials established in each standard.

CODE	CONDITIONS	RESULTS (%)	INFERENCE
		Co	
ASTM C618 − 12a	• SiO_2+Fe_2O_3+ Al_2O_3, minimum% 50-70% • Loss on ignition, maximum 10%	66.573 N/A	Satisfied N/A
BS EN 450-1:2005	• SiO_2+Fe_2O_3+ Al_2O_3, minimum% 70% • Na_2O shall not exceed 5.0 % • MgO shall not be greater than 4.0 % by mass.	66.573 17.6	Not Satisfied Not Satisfied -
BS EN 197-1:2011	• SiO_2 shall be not less than 25.0 % by mass • CaO+SiO_2, minimum 50 % by mass	63.4 76	Satisfied Satisfied
NBR 12653	• SiO_2+Fe_2O_3+Al_2O_3, minimum% 50-70% • Na_2O, % maximum,1.5 %	66.573 17.6	Satisfied Not Satisfied

Table 5.3 – Comparison of the Chemical Composition of the Co Sample to Standards

CODE	CONDITIONS	RESULTS (%)	INFERENCE
		Cl + Co W	
ASTM C618 − 12a	• SiO_2+Fe_2O_3+ Al_2O_3, minimum% 50-70% • Loss on ignition, maximum 10%	68.775 N/A	Satisfied N/A
BS EN 450-1:2005	• SiO_2+Fe_2O_3+ Al_2O_3, minimum% 70% • Na_2O shall not exceed 5.0 % • MgO shall not be greater than 4.0 % by mass.	68.775 13.2 1.91	Not Satisfied Not Satisfied Satisfied
BS EN 197-1:2011	• SiO_2 shall be not less than 25.0 % by mass • CaO+SiO_2, minimum 50 % by mass	66.1 79	Satisfied Satisfied
NBR 12653	• SiO_2+Fe_2O_3+Al_2O_3, minimum% 50-70% • Na_2O, maximum 1.5 %	68.775 13.2	Satisfied Not Satisfied

Table 5.4 - Comparison of the Chemical Composition of the Cl + Co W Sample to Standards

CODE	CONDITIONS	RESULTS (%)	INFERENCE
		Cl	
ASTM C618 − 12a	• SiO_2+Fe_2O_3+ Al_2O_3, minimum% 50-70% • Loss on ignition, maximum 10%	68.648 N/A	Satisfied N/A
BS EN 450-1:2005	• SiO_2+Fe_2O_3+ Al_2O_3, minimum% 70% • Na_2O shall not exceed 5.0 % • MgO shall not be greater than 4.0 % by mass.	68.648 13.7 -	Not Satisfied Not Satisfied -
BS EN 197-1:2011	• SiO_2 shall be not less than 25.0 % by mass • CaO+SiO_2, minimum 50 % by mass	66.3 80.8	Satisfied Satisfied
NBR 12653	• SiO_2+Fe_2O_3+Al_2O_3, minimum% 50-70% • Na_2O, maximum 1.5 %	68.648 13.7	Satisfied Not Satisfied

Table 5.5 - Comparison of the Chemical Composition of the Cl Sample to Standards

CODE	CONDITIONS	RESULTS (%)	INFERENCE
		Cl + Co B	
ASTM C618 – 12a	• SiO_2+Fe_2O_3+ Al_2O_3, minimum% 50-70% • Loss on ignition, maximum 10%	66.157 N/A	Satisfied N/A
BS EN 450-1:2005	• SiO_2+Fe_2O_3+ Al_2O_3, minimum% 70% • Na_2O shall not exceed 5.0 % • MgO shall not be greater than 4.0 % by mass.	66.157 17.7 -	Not Satisfied Not Satisfied -
BS EN 197-1:2011	• SiO_2 shall be not less than 25.0 % by mass • CaO+SiO_2, minimum 50 % by mass	63.6 76.7	Satisfied Satisfied
NBR 12653	• SiO_2+Fe_2O_3+Al_2O_3, minimum% 50-70% • Na_2O, maximum 1.5 %	66.157 17.7	Satisfied Not Satisfied

Table 5.6 - Comparison of the Chemical Composition of the Cl + Co B Sample to Standards

CODE	CONDITIONS	RESULTS (%)	INFERENCE
		Gl + Ce	
ASTM C618 – 12a	• SiO_2+Fe_2O_3+ Al_2O_3, minimum% 50-70% • Loss on ignition, maximum 10%	68.789 N/A	Satisfied N/A
BS EN 450-1:2005	• SiO_2+Fe_2O_3+ Al_2O_3, minimum% 70% • Na_2O shall not exceed 5.0 % • MgO shall not be greater than 4.0 % by mass.	68.789 14.3 1.91	Not Satisfied Not Satisfied Satisfied
BS EN 197-1:2011	• SiO_2 shall be not less than 25.0 % by mass • CaO+SiO_2, minimum 50 % by mass	66.0 78.4	Satisfied Satisfied
NBR 12653	• SiO_2+Fe_2O_3+Al_2O_3, minimum% 50-70% • Na_2O, maximum 1.5 %	68.789 14.3	Satisfied Not Satisfied

Table 5.7 - Comparison of the Chemical Composition of the Gl + Ce Sample to Standards

CODE	CONDITIONS	RESULTS (%)	INFERENCE
		Cl + Co W Ca 600	
ASTM C618 − 12a	• SiO_2+Fe_2O_3+ Al_2O_3, minimum% 50-70% • Loss on ignition, maximum 10%	67.780 N/A	Satisfied N/A
BS EN 450-1:2005	• SiO_2+Fe_2O_3+ Al_2O_3, minimum% 70% • Na_2O shall not exceed 5.0 % • MgO shall not be greater than 4.0 % by mass.	67.780 13.4 2.41	Not Satisfied Not Satisfied Satisfied
BS EN 197-1:2011	• SiO_2 shall be not less than 25.0 % by mass • CaO+SiO_2, minimum 50 % by mass	65.0 78.2	Satisfied Satisfied
NBR 12653	• SiO_2+Fe_2O_3+Al_2O_3, minimum% 50-70% • Na_2O, maximum 1.5 %	67.780 13.4	Satisfied Not Satisfied

Table 5.8 - Comparison of the Chemical Composition of the Cl + Co W Ca 600 Sample to Standards

CODE	CONDITIONS	RESULTS (%)	INFERENCE
		Cl + Co W Ca 850	
ASTM C618 − 12a	• SiO_2+Fe_2O_3+ Al_2O_3, minimum% 50-70% • Loss on ignition, maximum 10%	67.414 N/A	Satisfied N/A
BS EN 450-1:2005	• SiO_2+Fe_2O_3+ Al_2O_3, minimum% 70% • Na_2O shall not exceed 5.0 % • MgO shall not be greater than 4.0 % by mass.	67.414 15.7 -	Not Satisfied Not Satisfied -
BS EN 197-1:2011	• SiO_2 shall be not less than 25.0 % by mass • CaO+SiO_2, minimum 50 % by mass	64.4 78	Satisfied Satisfied
NBR 12653	• SiO_2+Fe_2O_3+Al_2O_3, minimum% 50-70% • Na_2O, maximum 1.5 %	67.414 15.7	Satisfied Not Satisfied

Table 5.9 - Comparison of the Chemical Composition of the Cl + Co W Ca 850 Sample to Standards

5.1.2.2 ANALYSIS OF RESULTS OF XRF OF THE POWDER SAMPLES RESULTS

The most abundant compound in the glass powders is SiO_2 as it exhibits the highest percentage. Thus, due to the high amount of SiO_2 present, these glass powder samples are able to react with the calcium hydroxide ($Ca(OH)_2$) that forms during the hydration of cement.

As expected, these materials used as SCMs also contained notable amounts of calcium oxide (CaO) and sodium oxide (Na_2O). As seen in the above tables, the percentage composition of Na_2O in the different samples varies between 13.2 and 17.7%.

As per BS EN 450-1:2005 and NBR 12653, this does not satisfy the requirements for a pozzolanic material since the amount of Na_2O present is greater than the maximum allowable percentage. This amount of Na_2O would react with the SiO_2 in the aggregate, causing the deleterious ASR. As discussed in the literature review, this can be overcome by reducing the particle size of the material for it to act as an SCM and not as an aggregate. In this way, the small particle sizes ensure that glass is reactive and is acting as a pozzolan. The pozzolanic reaction of the amorphous silica in glass reacting with $Ca(OH)_2$ will occur before the ASR is initiated as very few OH^- ions would be left for the ASR to take place.

According to BS EN 450-1:2005, the minimum percentage of SiO_2, Fe_2O_3 and Al_2O_3 present should be at least 70%. The percentage of these compounds present in the materials tested is very close to the stipulated minimum percentage for that standard. ASTM C618 − 12a and NBR 12653 set the percentages of the same compounds to a range of 50% to 70%. Therefore, the requirement that is marginally not satisfied in BS EN 450-1:2005 is not a cause for concern.

5.1.3 PARTICLE SIZE DISTRIBUTION (PSD) RESULTS

Particle size is of paramount importance in determining whether a material has the capacity to act as a pozzolanic material. Since it was established that the soda-lime glass under test has a high percentage proportion of Na_2O compared to BS EN 450-1:2005, the investigation of the particle size of the powder is of utmost importance. Reducing the particle size, reduces the effects of the deleterious ASR. The results for the particle size distribution of each glass type under test, together with that of cement as a control, are shown below. (*see also Appendix 4).*

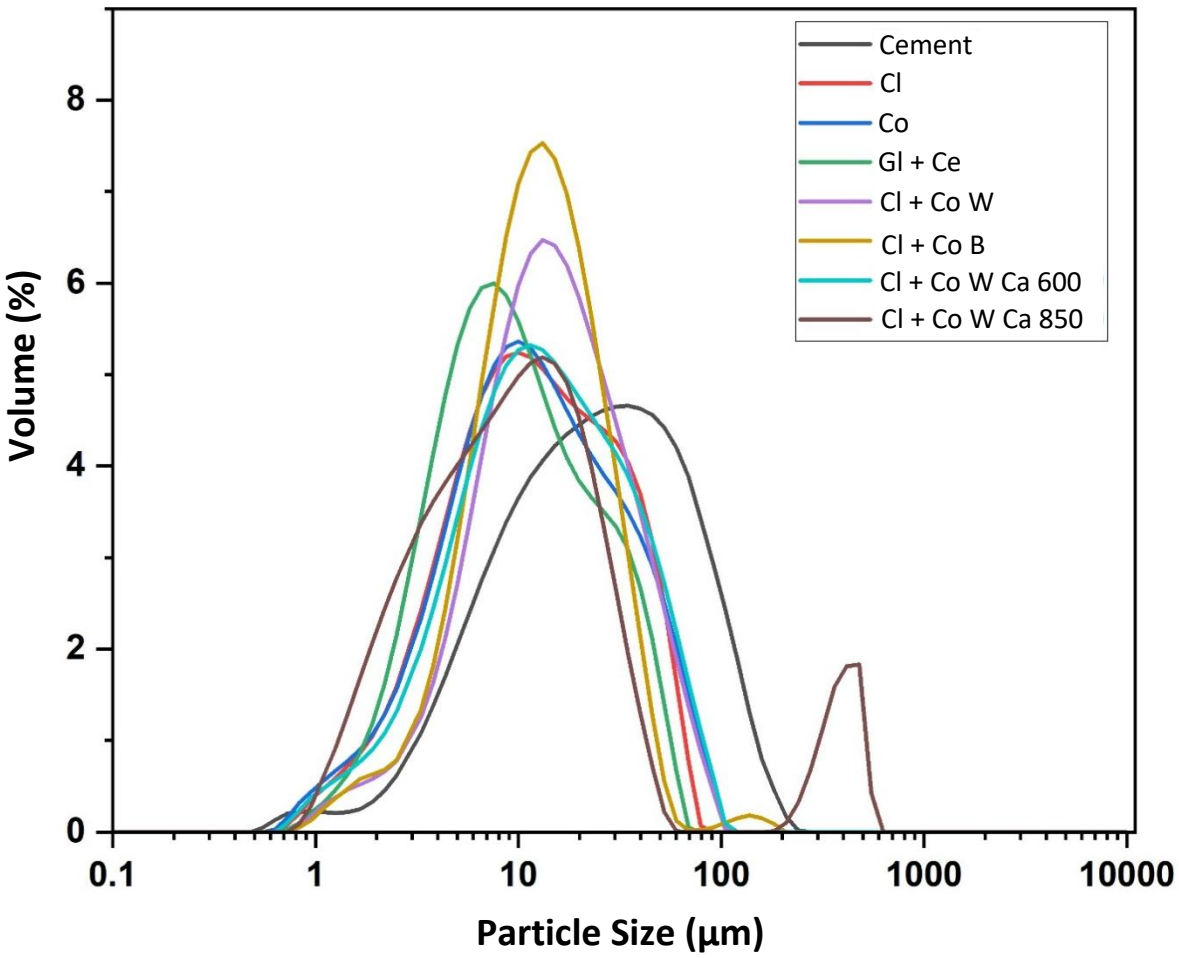

Figure 5.2 – Graph showing Particle Size Distribution of all samples

MATERIAL	D (10) (µm)	D (50) (µm)	D (90) (µm)
Cem Con	4.959	22.257	79.515
Cl	3.024	10.987	37.049
Co	2.945	10.855	40.623
Cl + Co W	3.821	11.681	34.712
Cl + Co B	3.858	11.652	28.252
Gl + Ce	2.837	8.390	30.168
Cl + Co W Ca 600	3.284	12.152	42.497
Cl + Co W Ca 850	2.258	9.199	35.068

Table 5.10 – Table showing D (10), D (50) & D (90) for Particle Size

D (10), D (50) and D (90) represent the diameter of the particles when 10%, 50% and 90% respectively of the particles in the sample have a diameter which is less than that value. From the results in the table, it can be deduced that for all glass waste samples, 90% of the particles are much smaller than those in the cement control and moreover less than 45µm.

As can be seen from the above graphs, particle size distribution analysis by means of laser diffraction show that all the glass waste types, excluding Cl + Co W Ca 850, have particle sizes which are smaller than that of cement. As stated in a literature review by Hassani et al, when the particle sizes of the glass powder are smaller than those of cement, the glass powder creates a denser material as it fills in the pores causing blockages in the interior pores network (Hassani et al., 2023). This insinuates that glass acts as a pozzolan in such cases. This theory can be directly applied to this scenario implying that for all of the SCMs, excluding Cl + Co W Ca 850, the glass powder will probably act as a pozzolan. This would have to be confirmed when testing the hardened properties.

In the case of Cl + Co W Ca 850, a notable number of particles have sizes which are larger than those of cement. This might be attributed to the temperature at which the heat treatment was applied. After calcining the powder at 850^{o}C, the material turned into a solid mass. This had to be crushed and ground once again since the small size of particles in the powder was lost. However, grinding was just done for just 15 minutes. Therefore, most likely, the considerable percentage of large particle sizes has resulted from an insufficient time to grind the material back to the original size. Due to this, it is likely that the particle sizes that range from 181µm to 549µm shall act as an aggregate and not as an SCM. The magnitude of the effects of the large particle sizes will be evaluated at a later stage.

The highest percentage of particle size in the Gl + Ce sample is smaller than in the other types of glass since the initial starting size of the glass waste was the smallest of the different types.

In the Cl + Co B sample obtained from BCRS Ltd., it was found that there is a very small number of particles which are larger than the majority. The crushing and grinding processes to produce the glass powders was the same for all the different types of glass. However, the Cl + Co B sample that was exposed to these processes had pieces of glass that were larger than the samples obtained from WSML. This is because, at WSML, sieving cycles are continued until the cullets are of size between 8mm and 60mm, producing a consistent smaller range of glass cullets. Thus, this resulted in powder with larger particle size in Cl + Co B.

5.1.4 SCANNING ELECTRON MICROSCOPY (SEM) AND ENERGY DISPERSIVE X-RAY SPECTROSCOPY (EDS) RESULTS

Figure 5.3 shows images that resulted from the SEM of the Cl + Co W, Cl + Co B and Cl + Co W Ca 600 samples. There is no significant visual distinction between the different images obtained from different samples.

All samples of glass particles have very fine particle sizes. The particles can be characterized as having:

- a smooth surface
- a glassy slippery texture
- sharp edges
- irregular shapes
- a plate shape due to their flatness
- microcracks in some of the larger particles

This correlates with observations found in literature (Pereira-de-Oliviera et al, 2012) (Lu & Poon, 2018).

In the Cl + Co B sample, there are some particles which seem to be larger than particles in the other two samples. This correlates to the particle size distribution analysis as outlined above. The impurities from the Cl + Co B batch cannot be seen distinctly using the SEM.

The EDS analysis showed that all the three (3) types of glass powder under study contain the presence of elements such as carbon (C), aluminium (Al), silicon (Si), calcium (Ca), oxygen (O), sodium (Na), magnesium (Mg), and potassium (K). In all of the samples, the two most prevalent elements are silicon and oxygen. This correlates with the XRF analysis where it was found that the most abundant compound in the glass waste is SiO_2. As previously mentioned, the prevalence of SiO_2 in the material makes the glass waste under study a good pozzolan. Moreover, once again through this test, it has been shown that there is a presence of Na_2O that needs to be given consideration by having a small particle size to mitigate ASR.

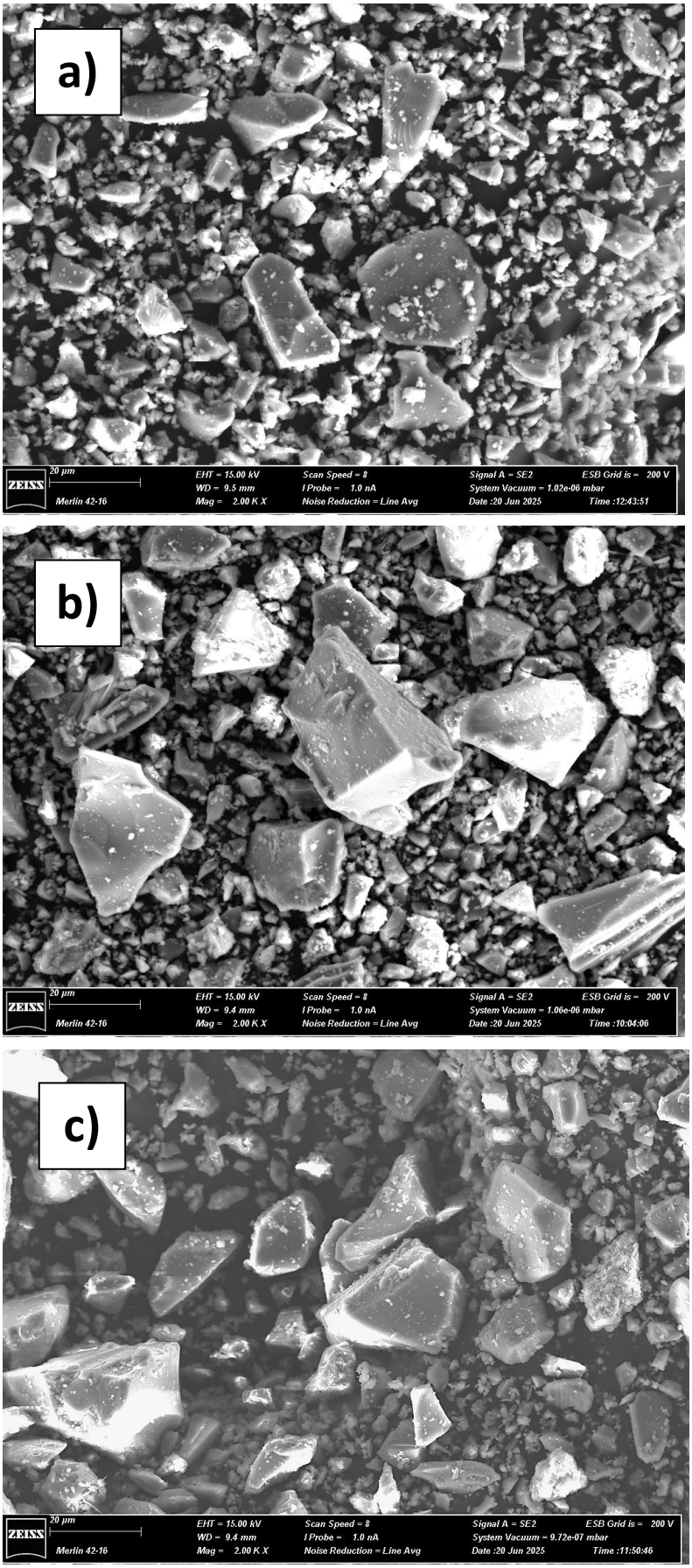

Figure 5.3 – a) SEM Image for Cl + Co W b) SEM Image for Cl + Co B c) SEM Image for Cl + Co W Ca 600

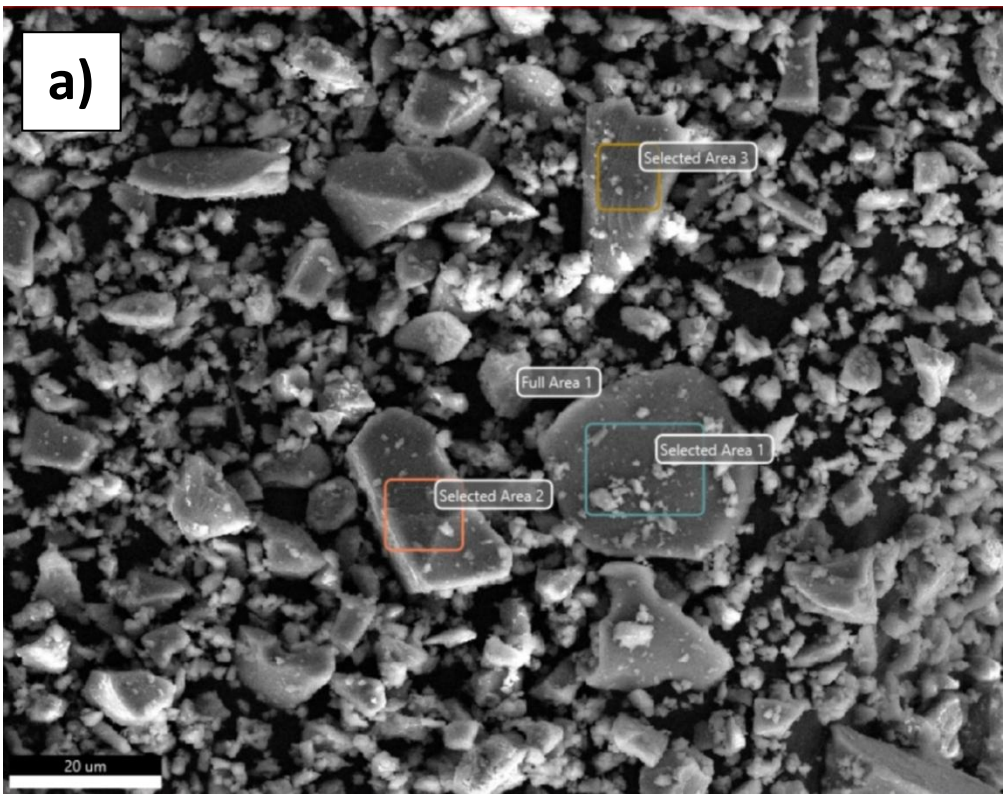

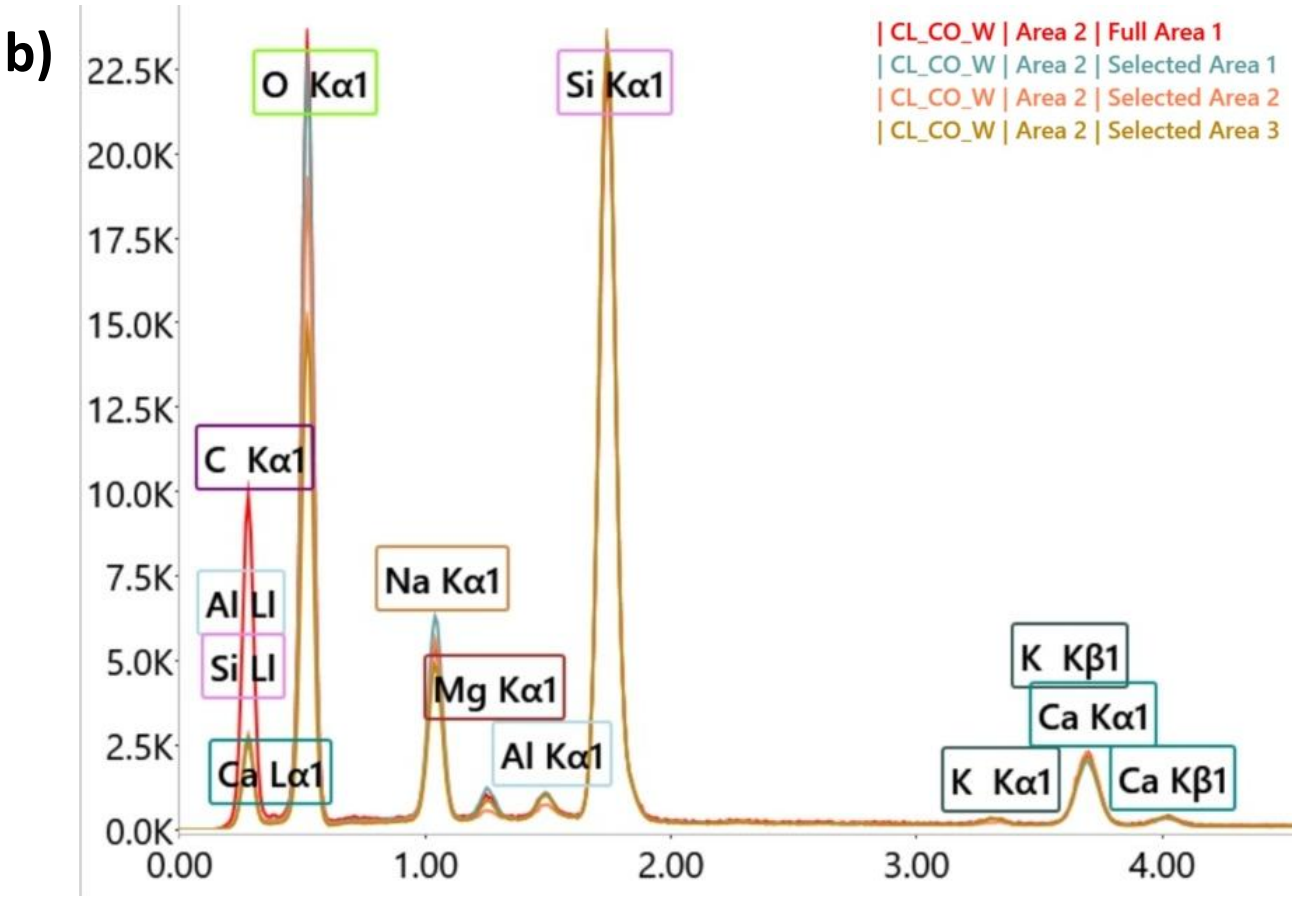

Figure 5.4 – a) SEM Image for Cl + Co W Sample b) Graph showing EDS Analysis of Cl + Co W sample

ELEMENT	WEIGHT %	MDL	ATOMIC %	ERROR %
	Cl + Co W – FULL AREA 1			
C K	22.18	0.10	33.78	8.47
O K	33.37	0.09	38.16	6.49
Na K	4.69	0.07	3.74	4.34
Mg K	0.59	0.06	0.44	6.00
Al K	0.96	0.06	0.65	5.41
Si K	29.67	0.06	19.32	2.36
K K	0.63	0.10	0.29	12.34
Ca K	7.92	0.10	3.62	2.89
	Cl + Co W – SELECTED AREA 1			
C K	7.00	0.09	12.05	9.28
O K	36.45	0.07	47.11	6.06
Na K	6.86	0.06	6.17	4.11
Mg K	1.10	0.05	0.94	4.57
Al K	1.27	0.05	0.97	4.37
Si K	37.84	0.05	27.86	2.36
K K	0.77	0.08	0.41	9.60
Ca K	8.71	0.09	4.49	2.73
	Cl + Co W – SELECTED AREA 2			
C K	8.67	0.11	15.02	9.28
O K	33.43	0.08	43.45	6.30
Na K	6.17	0.07	5.58	4.20
Mg K	0.22	0.06	0.20	10.52
Al K	0.75	0.05	0.58	5.63
Si K	39.98	0.06	29.59	2.32
K K	0.36	0.09	0.19	13.83
Ca K	10.41	0.10	5.40	2.67
	Cl + Co W – SELECTED AREA 3			
C K	9.49	0.13	16.76	9.39
O K	28.80	0.09	38.17	6.49
Na K	5.68	0.07	5.24	4.17
Mg K	0.70	0.06	0.61	5.75
Al K	1.32	0.06	1.04	4.71
Si K	42.48	0.06	32.07	2.31
K K	0.95	0.09	0.51	10.08
Ca K	10.59	0.10	5.60	2.77

Table 5.11 – EDS Results for Cl + Co W Powder Sample

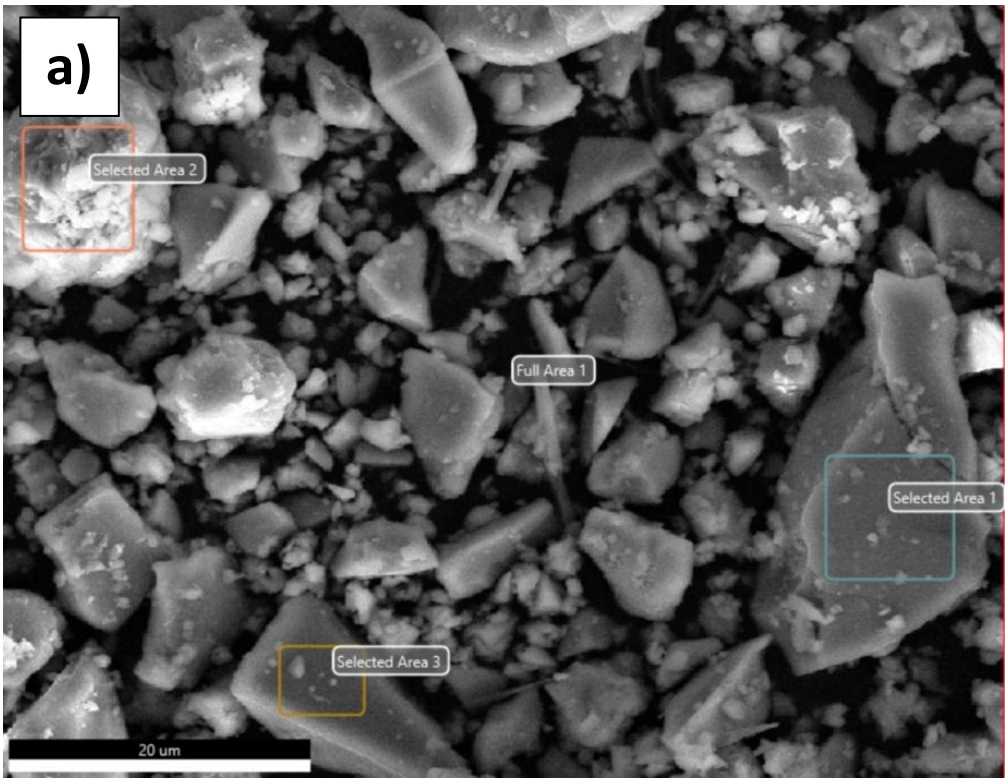

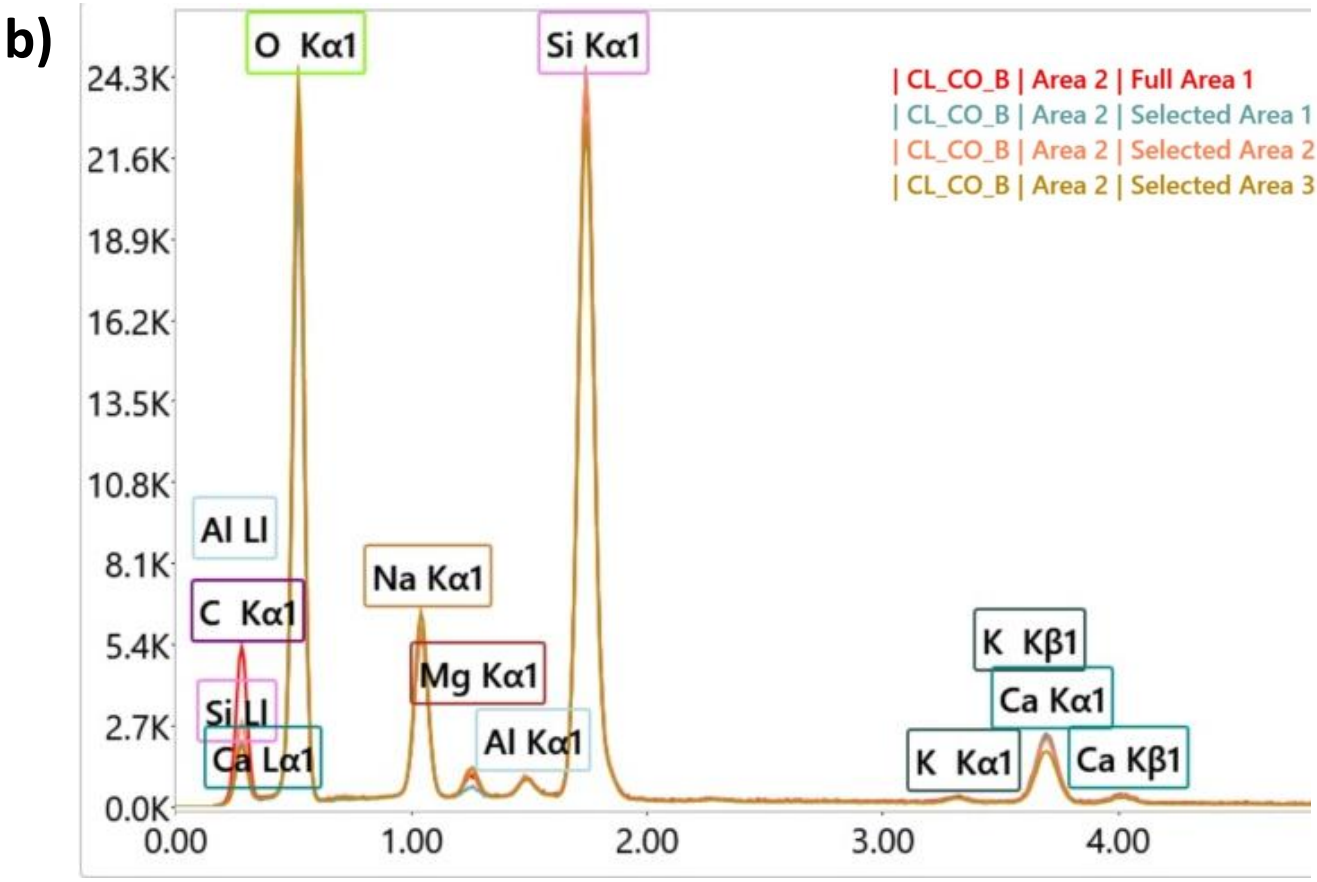

Figure 5.5 - a) SEM Image for Cl + Co B Sample b) Graph showing EDS Analysis of Cl + Co B sample

ELEMENT	WEIGHT %	MDL	ATOMIC %	ERROR %
	Cl + Co B – FULL AREA 1			
O K	38.42	0.11	53.07	6.08
Na K	6.46	0.09	6.21	4.38
Mg K	0.79	0.08	0.72	6.11
Al K	1.08	0.07	0.88	6.05
Si K	41.34	0.07	32.53	2.43
K K	0.85	0.11	0.48	11.25
Ca K	11.06	0.12	6.10	2.92
	Cl + Co B – SELECTED AREA 1			
C K	6.26	0.11	11.03	9.41
O K	34.75	0.08	45.96	6.24
Na K	6.41	0.07	5.90	4.22
Mg K	0.38	0.06	0.33	8.17
Al K	1.05	0.06	0.82	4.92
Si K	39.70	0.06	29.91	2.34
K K	0.74	0.09	0.40	10.30
Ca K	10.71	0.10	5.66	2.68
	Cl + Co B – SELECTED AREA 2			
C K	7.56	0.10	13.01	9.28
O K	36.28	0.07	46.82	6.15
Na K	6.04	0.07	5.42	4.21
Mg K	0.91	0.06	0.77	5.10
Al K	1.07	0.05	0.82	4.78
Si K	38.01	0.05	27.94	2.35
K K	0.58	0.09	0.31	11.10
Ca K	9.54	0.09	4.91	2.73
	Cl + Co B – SELECTED AREA 3			
O K	40.52	0.07	54.81	5.77
Na K	7.69	0.07	7.24	4.14
Mg K	1.36	0.06	1.21	4.53
Al K	1.13	0.05	0.91	4.49
Si K	39.91	0.05	30.75	2.38
K K	0.65	0.26	0.36	10.83
Ca K	8.74	0.09	4.72	2.74

Table 5.12 - EDS Results for Cl + Co B Powder Sample

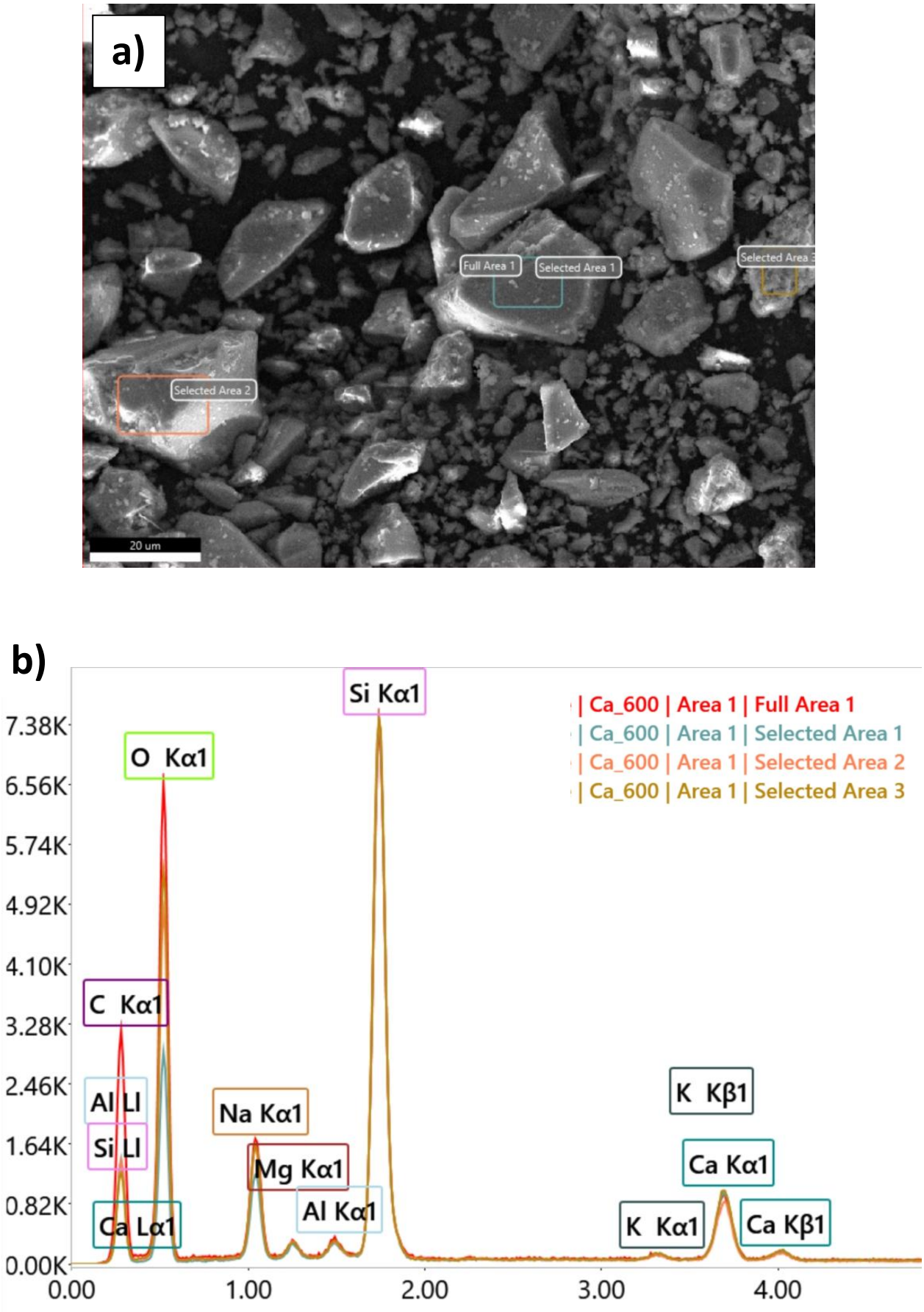

Figure 5.6 - a) SEM Image for Cl + Co W Ca 600 Sample b) Graph showing EDS Analysis of Cl + Co W Ca 600 sample

ELEMENT	WEIGHT %	MDL	ATOMIC %	ERROR %
	Cl + Co W Ca 600 – FULL AREA 1			
C K	22.02	0.19	34.27	8.96
O K	30.46	0.17	35.59	6.93
Na K	4.62	0.13	3.76	4.93
Mg K	0.49	0.14	0.38	9.51
Al K	0.91	0.17	0.63	7.60
Si K	30.22	0.11	20.11	2.55
K K	0.82	0.23	0.39	17.20
Ca K	10.46	0.17	4.88	3.58
	Cl + Co W Ca 600 – SELECTED AREA 1			
C K	16.40	0.26	28.92	9.48
O K	19.06	0.22	25.24	7.44
Na K	4.24	0.12	3.91	4.67
Mg K	0.56	0.12	0.49	8.80
Al K	0.98	0.11	0.77	6.81
Si K	42.50	0.09	32.06	2.39
K K	1.21	0.14	0.66	13.59
Ca K	15.06	0.14	7.96	3.01
	Cl + Co W Ca 600 – SELECTED AREA 2			
O K	30.97	0.14	45.12	6.51
Na K	6.24	0.20	6.33	4.38
Mg K	0.87	0.31	0.84	6.13
Al K	1.21	0.06	1.05	5.92
Si K	45.69	0.04	37.92	2.42
K K	1.08	2.49	0.64	11.21
Ca K	13.95	0.07	8.11	2.90
	Cl + Co W Ca 600 – SELECTED AREA 3			
C K	11.40	0.49	19.78	9.62
O K	29.79	0.11	38.79	6.86
Na K	5.27	0.08	4.77	4.65
Mg K	0.68	0.11	0.58	8.79
Al K	1.09	1.08	0.84	7.29
Si K	37.38	0.07	27.73	2.51
K K	1.06	0.57	0.57	14.48
Ca K	13.32	0.15	6.93	3.20

Table 5.13 - EDS Results for Cl + Co W Ca 600 Powder Sample

5.1.5 X-RAY DIFFRACTION (XRD) RESULTS

The graphs shown below were obtained through XRD. They give information on the structure of the glass powders under test.

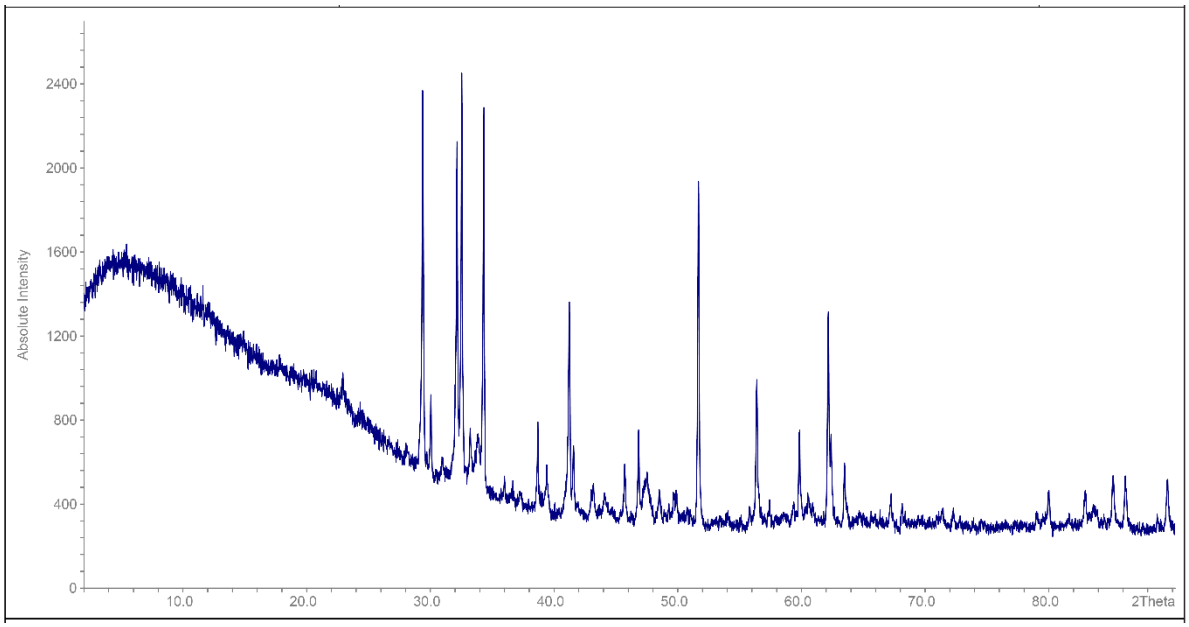

Figure 5.7 – XRD Result of Cement Control

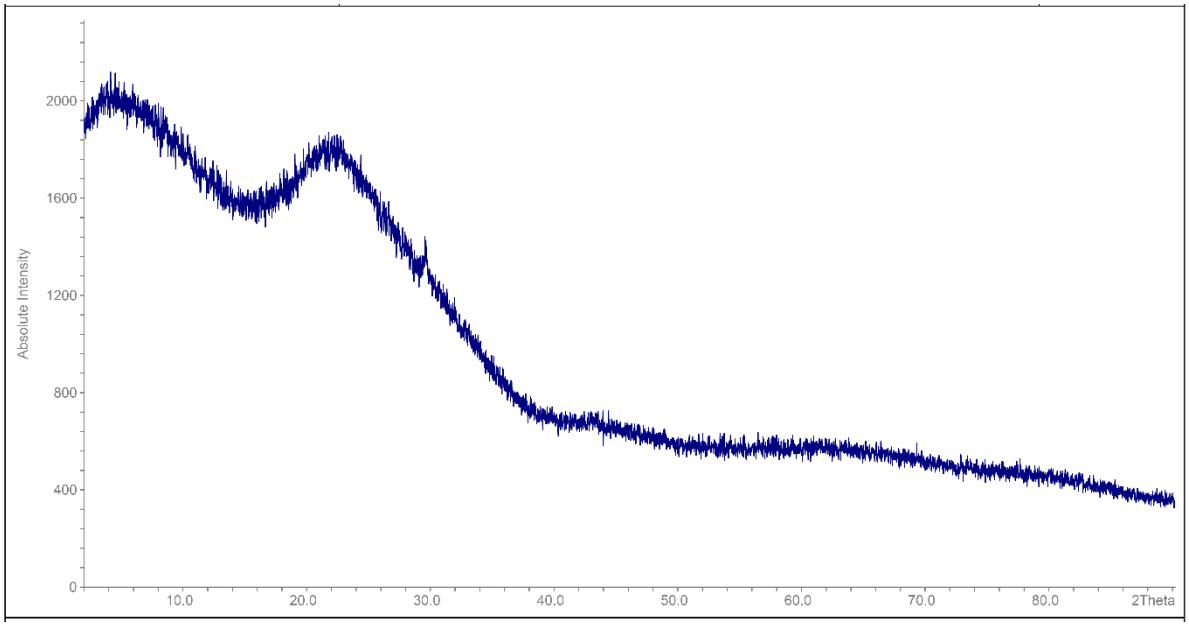

Figure 5.8 – XRD Result of Cl Sample

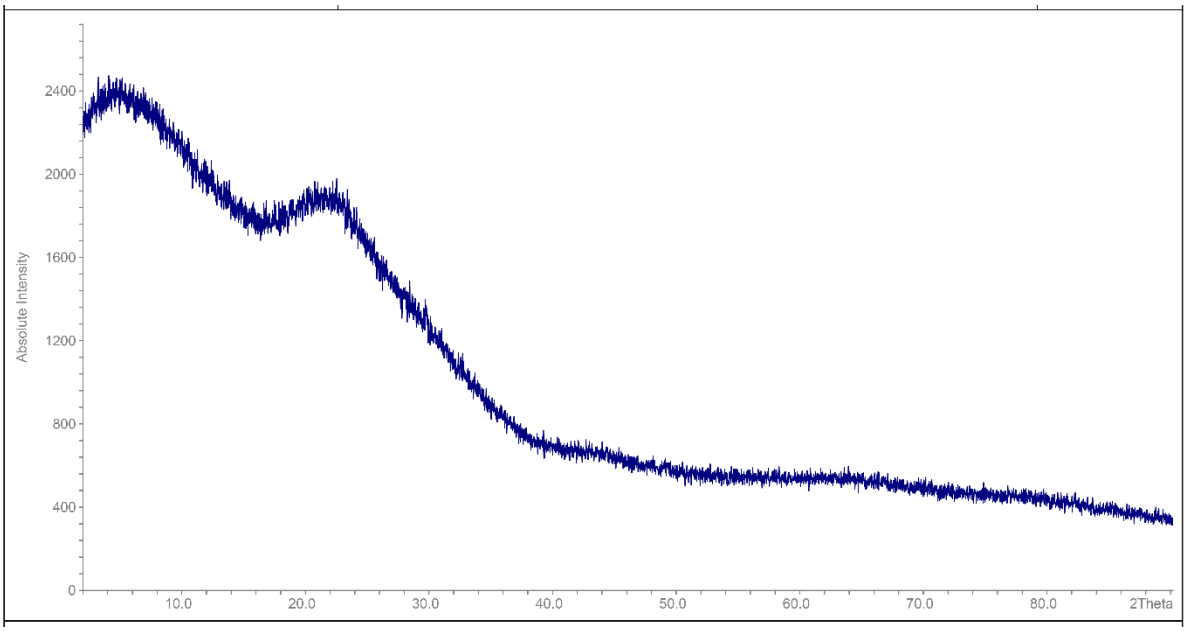

Figure 5.9 - XRD Result for Co Sample

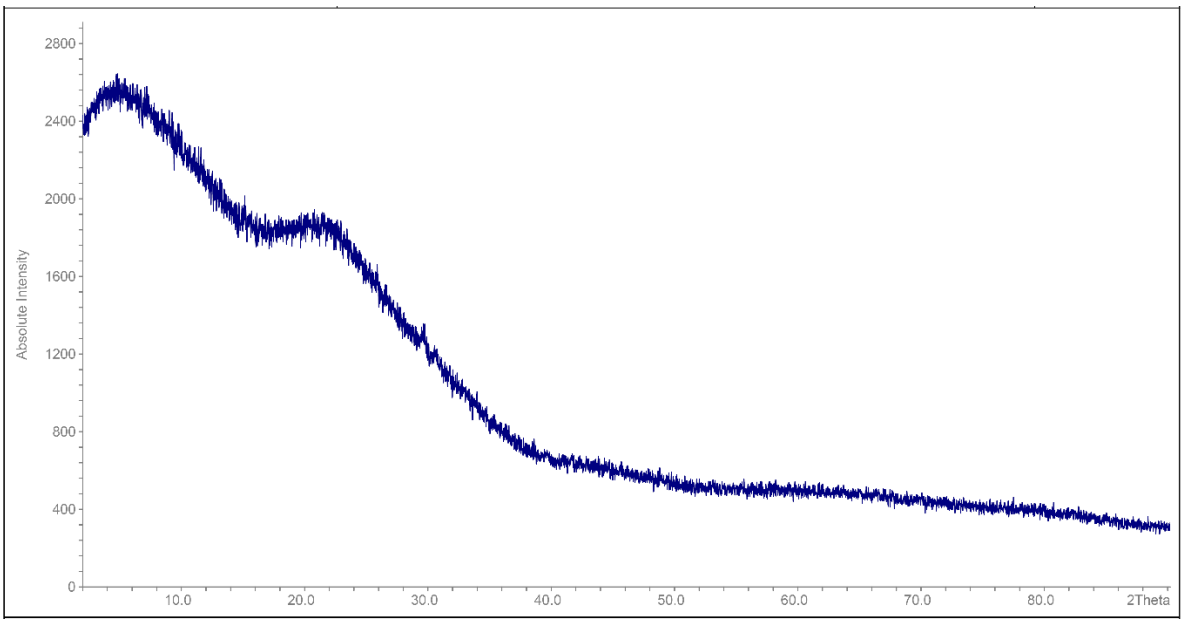

Figure 5.10 – XRD Result for Cl + Co W Sample

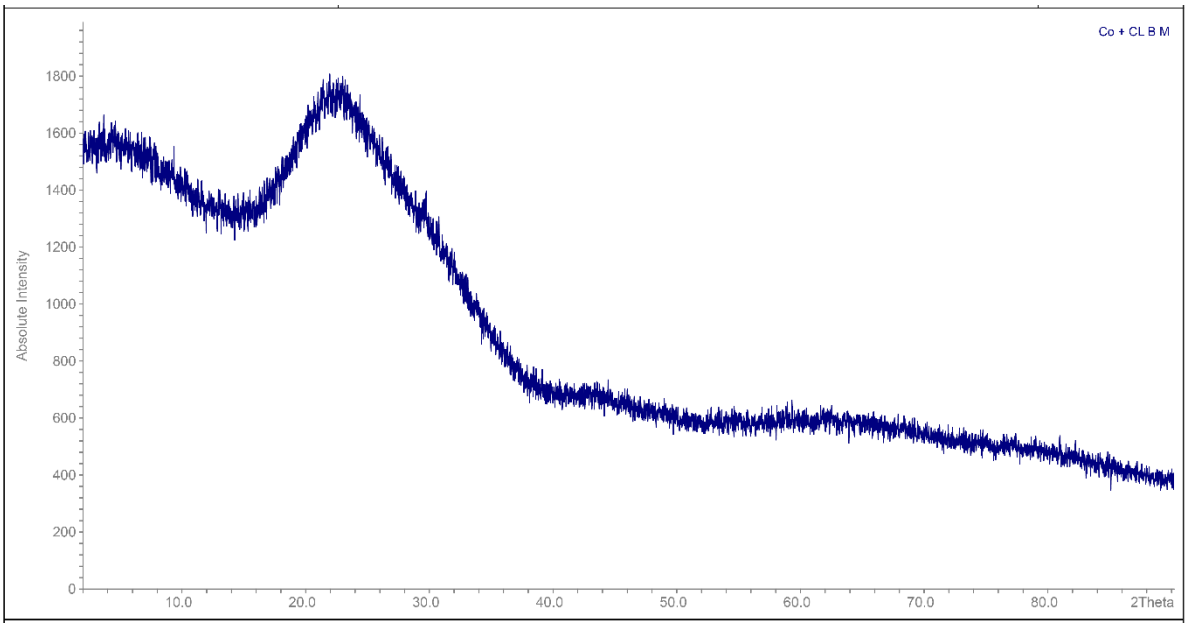

Figure 5.11 – XRD Result for Cl + Co B Sample

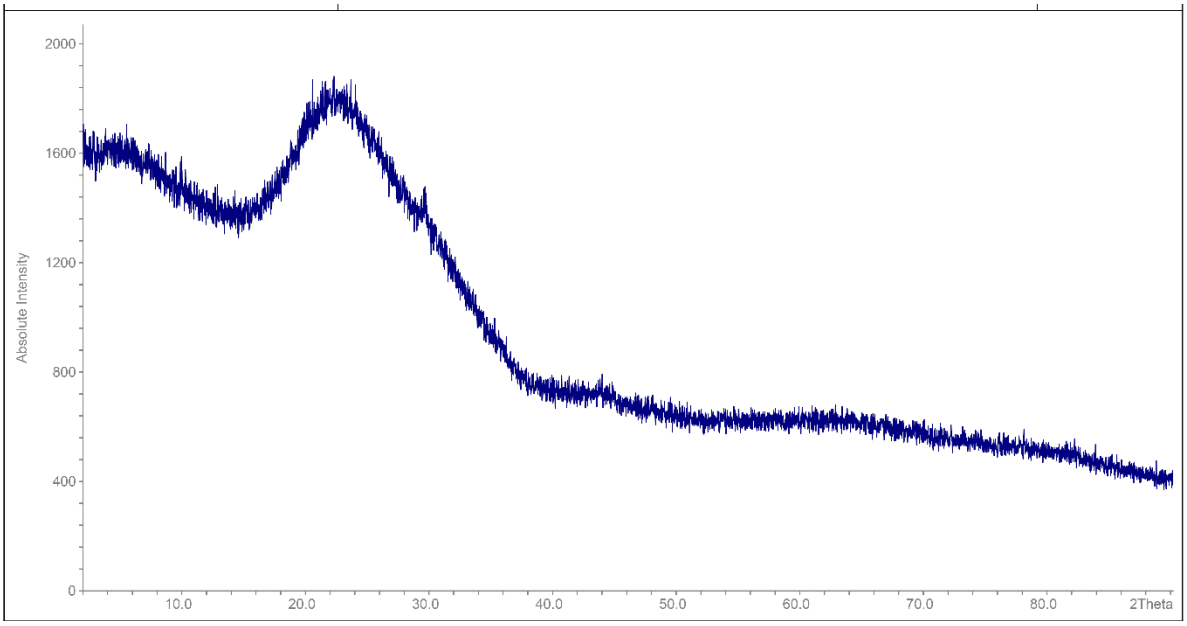

Figure 5.12 - XRD Result of Gl + Ce Sample

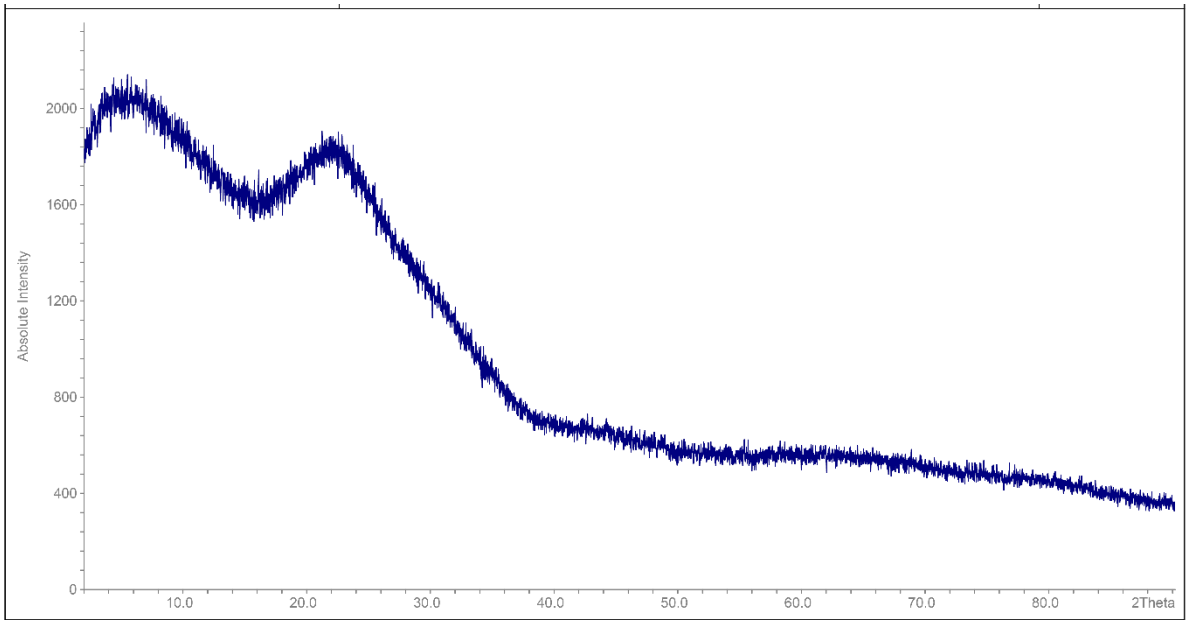

Figure 5.13 - XRD Result of Cl + Co W Ca 600 Sample

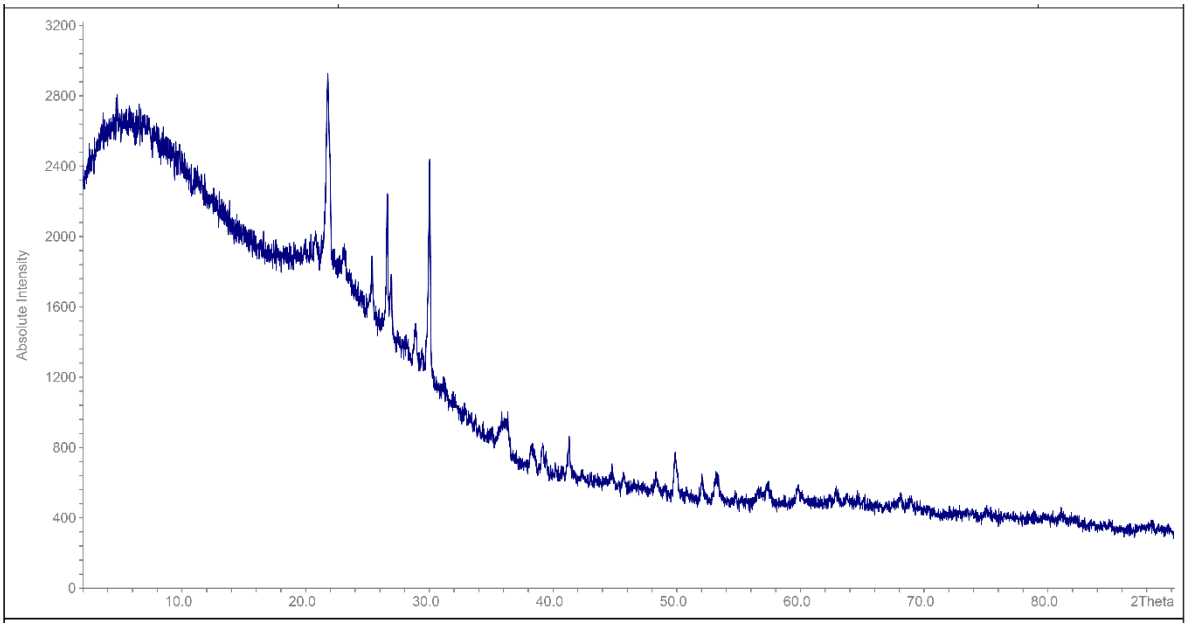

Figure 5.14 - XRD Result of Cl + Co W Ca 850 Sample

For all the glass powder samples, except for Cl + Co W Ca 850 and the control Cem Con which is CEM I 42,5 R, broad humps were visible in the XRD graphs. These were present from 15^{o} to 30^{o}, and this indicates the amorphous quality of glass that stems from the amorphous silica (Huang et al., 2024).

Sharp diffraction patterns can be seen when analysing the CEM I 42,5R. These sharp peaks correspond to the crystalline structure which is typical for CEM I and ordinary Portland cement. The cement contains the crystalline mineral compounds mentioned in the literature review, namely, C_3A, C_4AF, C_{2S} and C_3S. (Huang et al., 2024).

With regards to Cl + Co W Ca 850, broad humps and sharp diffraction patterns were seen. This correlates to a partly amorphous and partly crystalline structure which corresponds to the structure of sintered glass (Zaid et al., 2017).

5.2 PASTE TESTING RESULTS

5.2.1 FRESH PROPERTY TESTING RESULTS ON THE PASTE MIX

5.2.1.1 MINI CONE FLOW TABLE TEST RESULTS

The results of the mini cone flow table test are as follows:

PASTE SAMPLES					
	Diameter 1 (mm)	**Diameter 2 (mm)**	**Mean Diameter (mm)**	**Deviation from Mean Diameter 1 (%)**	**Deviation from Mean Diameter 2 (%)**
Cem Con	120.63	114.77	117.70	-2.49	2.49
Cl	122.92	121.7	122.31	-0.50	0.50
Co	137.35	132.06	134.71	-1.96	1.96
Cl + Co W	129.02	135.04	132.03	2.28	-2.28
Cl + Co B	127.34	124.47	125.91	-1.14	1.14
Gl + Ce	127.53	126.38	126.96	-0.45	0.45
Cl + Co W Ca 600	138.08	129.57	133.83	-3.18	3.18
Cl + Co W Ca 850	127.05	124.89	125.97	-0.86	0.86

Table 5.14 – Results of Mini Cone Tabel Test for Paste Samples

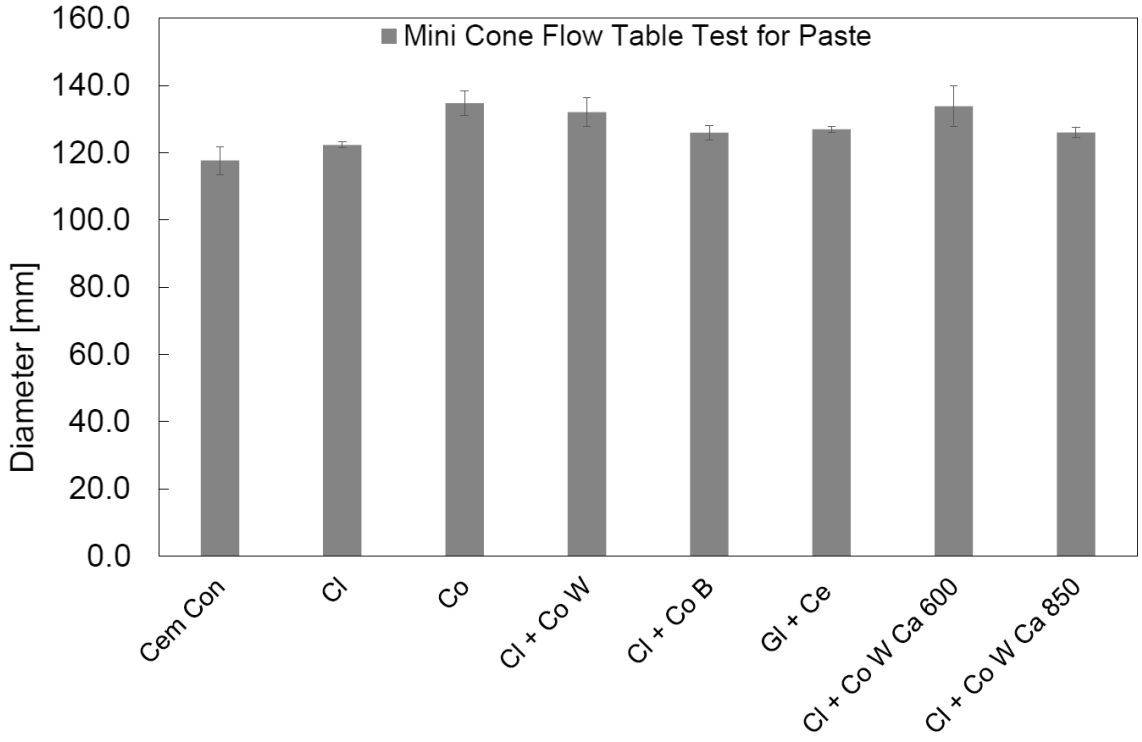

Figure 5.15 – Bar Graph comparing the Diameters of the Paste Samples

The Mini Cone Flow Table test gives information of the workability of the paste. Cl, Cl + Co B, Gl + Ce and Cl + Co W Ca 850 showed no significant difference when compared to Cem Con. On the other hand, an increase in workability was seen in Co, Cl + Co W, Cl + Co W Ca 600.

The results lead to the following interpretations:

- Cem Con has the lowest value for workability. This mixture does not contain any glass particles but has compounds within the mixture that absorb more water. Since cement absorbs more water from the mixture, its workability is decreased.
- Cl + Co B and Gl + Ce contain impurities like paper, plastic, ceramic and aluminium that absorb water from the mixture (Zhao et al, 2024). This leads to a reduction in the flowability, making it comparable the cement control.
- Co and Cl + Co W have an increased workability when compared to cement. This is due to the smooth surface of glass that gives it a slippery texture, enhancing flowability. Glass does not absorb water and so more water is left in the mix, thus increasing the workability of the mix. Moreover, no impurities that absorb water are present in these two samples (Hassani et al., 2023).
- The workability properties of Cl + Co W Ca 600 were similar to those of the original Cl + Co W mix. This means that the heat treatment did not affect the flowability of the mixture Cl + Co W Ca 600.
- It is possible that the decrease in workability of Cl + Co W Ca 850, when compared to the original Cl + Co W, was most likely to be due to a larger particle size of the sintered glass. The PSD results showed that some particles in Cl + Co W Ca 850 were large as the heat product was not ground enough. Literature states that waste glass as a fine aggregate can lead to sharp and angular particle shapes which increase internal friction and, in turn, reduce flowability. Thus, the small percentage of particles in Cl + Co W Ca 850, that are larger than the particle sizes of cement, are likely to be acting as fine aggregate and so the workability decreased (Metwally, 2007).
- The Co sample showed a higher workability than the Cl sample. This difference can be attributed to the presence of a higher concentration of metal oxides, such as Fe_2O_3 and Cr_2O_3, present in coloured glass. During the melting and cooling parts of the manufacturing process, the metal oxides improve the smoothness of the surface of coloured glass and this in turn, enhances the workability.

5.2.1.2 ISOTHERMAL CALORIMETRY RESULTS

The calorimetry results offer valuable insight into the heat transfer patterns of the cement hydration reaction as described in the literature review, together with the pozzolanic reactivity of the glass-blended pastes. The following were the results obtained:

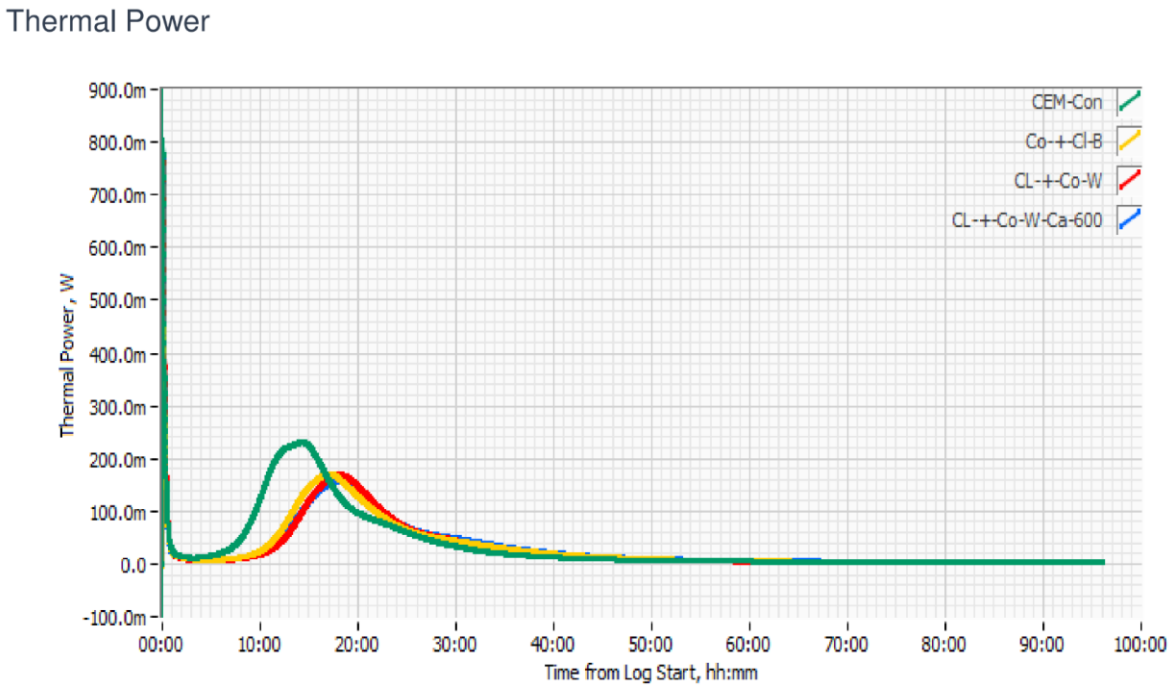

Figure 5.16 – Graph of Thermal Power

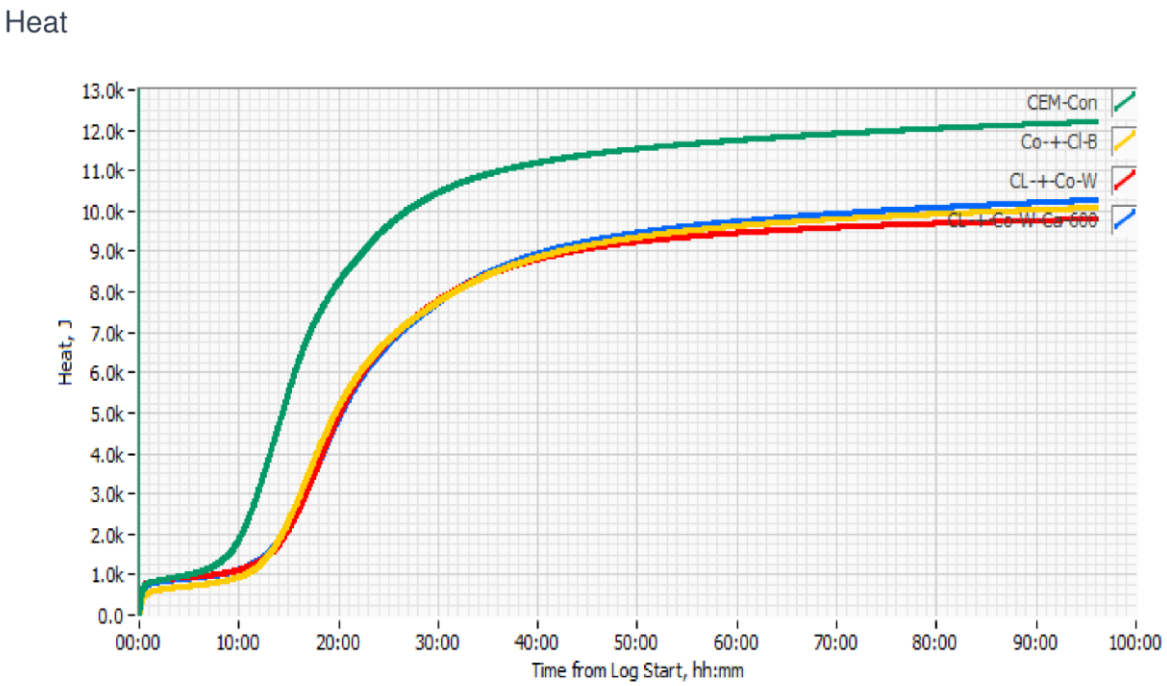

Figure 5.17 – Graph of Heat

The following is the analysis of the results obtained:

PASTE SAMPLES				
	End of Induction Period	**Acceleration Peak Range (hrs)**	**Peak Shape/Shift**	**Total Heat (Qualitative)**
Cem Con	Normal (~4–6 hrs)	10:00–18:00 (broad peak)	Standard hydration peak	Control (highest)
Cl + Co W	Extended (~6–8 hrs)	13:00–23:00 (broad peak)	Delayed, broadened	Slightly lower than control
Cl + Co B	Extended (~6–8 hrs)	13:00–23:00	Similar to Cl + Co W	Slightly lower than control
Cl + Co W Ca 600	Extended (~6–8 hrs)	13:00–23:00	Broadened, reactive	Slightly lower than control

Table 5.15 – Interpretation of the Isothermal Calorimetry Results for Paste Samples

For the cement control, where the hydration reaction is dominated by the C_2S and C_3S hydration, the results correlate well with literature.

For the waste glass paste samples, there was a shift in acceleration peak from 10:00-to-18:00 to 13:00-to–23:00. This indicates a delay in the start of the main alite (C_3S) hydration resulting from the presence of glass. Glass reduces the amount of cement present to react and causes the start of the pozzolanic reaction to take longer to start. The broadening of the peak observed suggests that there is an overlap of the hydration and the pozzolanic reactions. In the Cl + Co B sample, the delay in the start of the acceleration peak may be due to a decreased amount of water available in the mixture to react with the cement since water would have been absorbed by the impurities present. For Cl + Co W Ca 600, there is a sign of sustained reactivity from both glass and hydration products. This means that even more additional C-S-H gels have been formed.

5.2.2 HARDENED PROPERTY TESTING RESULTS ON THE PASTE MIX

5.2.2.1 HARDENED DENSITY OF CUBES RESULTS

Density was calculated by weighing the cubes and finding the volume after measuring the sides of the cube with a vernier calliper. The following tables show the results obtained for the density of the paste cubes measured after 7 days and 21 days of curing.

	DENSITY OF PASTE CUBES AT 7 DAYS							
	Cem Con	**Cl**	**Co**	**Cl + Co W**	**Cl + Co B**	**Gl + Ce**	**Cl + Co W Ca 600**	**Cl + Co W Ca 850**
Average Density (kg/m^3)	2145.06	2087.84	2107.29	2117.97	2114.28	2138.53	2039.67	2133.83
Difference in Density when compared to control (%)		-2.67	-1.76	-1.26	-1.43	-0.30	-4.91	-0.52

Table 5.16 – Densities of the Paste Cubes after 7-day Curing

	DENSITY OF PASTE CUBES AT 21 DAYS							
	Cem Con	**Cl**	**Co**	**Cl + Co W**	**Cl + Co B**	**Gl + Ce**	**Cl + Co W Ca 600**	**Cl + Co W Ca 850**
Average Density (kg/m^3)	2214.54	2103.89	2117.84	2115.43	2118.41	2098.23	2140.02	2109.25
Difference in Density when compared to control (%)		-4.50	-4.37	-4.48	-4.34	-5.25	-3.37	-4.75

Table 5.17 – Densities of the Paste Cubes after 21-day Curing

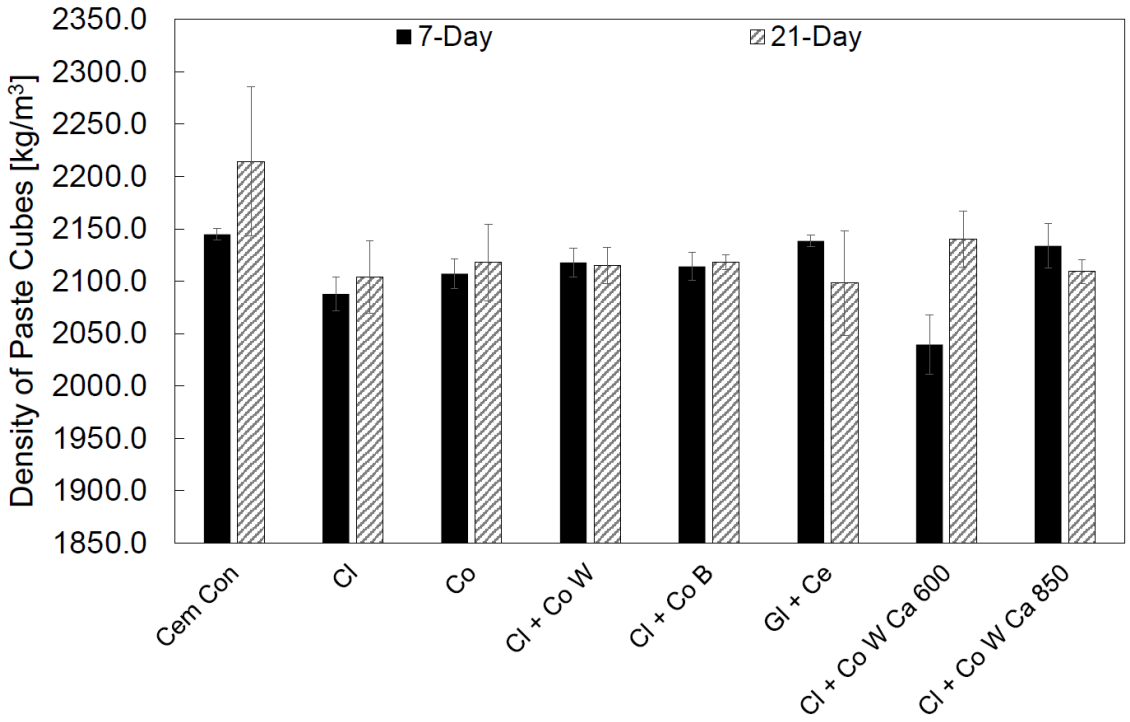

Figure 5.18 – Bar Graph comparing the Densities of the Paste Cubes at 7-day & 21-day Curing

An evident lower density could be observed between the glass waste samples and the control samples both at 7 days and 21 days. Taking into consideration that pozzolanic reactions produce increased density of the concrete microstructure with increasing time, at 21 days, the Cl + Co W Ca 600 was the sample which had a density that deviated least from that of the cement control. Since the density of soda-lime glass is less than that of cement (Son et al.), the decrease in the value of the density is probably due to this difference and not because the microstructure has not densified.

5.2.2.2 POROSITY OF PASTE CUBES RESULTS

The table and graph below show the results obtained that shed light on the porosity of the samples under test. Cement was used as a control.

AVERAGE PERMEABLE POROSITY OF PASTE CUBES			
	Average Permeable Porosity at 7 Days (%)	**Average Permeable Porosity at 21 Days (%)**	**Change in Average Permeable Porosity from 7 to 21 Days (%)**
Cem Con	28.92	28.02	- 0.9
Cl	30.1	28.09	- 2.1
Co	28.68	27.18	- 1.5
Cl + Co W	28.89	27.00	- 1.89
Cl + Co B	29.57	28.35	- 1.22
Gl + Ce	28.49	27.81	- 0.68
Cl + Co W Ca 600	28.62	27.23	- 1.39
Cl + Co W Ca 850	29.12	28.35	- 0.77

Table 5.18 – Average Permeable Porosity Results for the Paste Cubes at 7-day & 21-day Curing

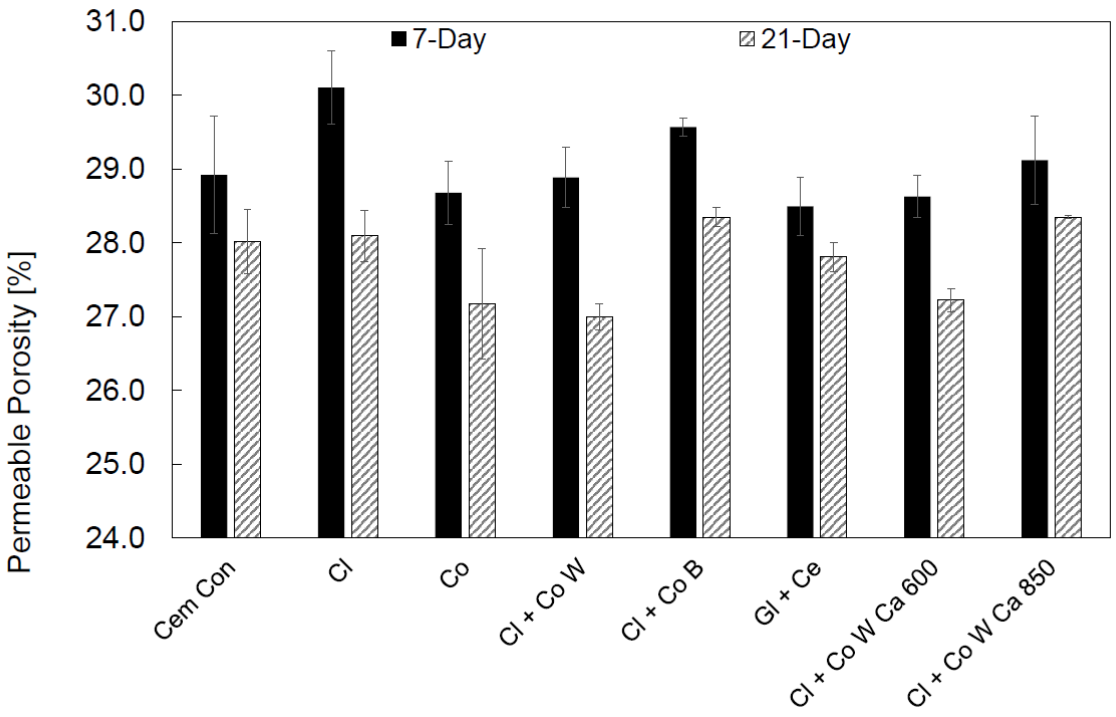

Figure 5.19 – Bar Graph comparing Permeable Porosity of the Paste Samples at 7-day & 21-day Curing

All samples showed a decrease in permeable porosity when comparing values at 7 days to those at 21 days. This is consistent with the hydration reaction which continues to produce C-S-H gel as time passes. In the presence of pozzolans, at an early stage, the pozzolanic reaction would have only been slightly initiated and so its effects are not significant. It is only later, as seen at 21 days, that the reaction becomes significant. This is consistent with the theory that states that as more time passes, the concrete matrix becomes denser due to the formation of additional C-S-H gel.

Gl + Ce and Cl + Co W Ca 850 showed a smaller change in porosity between 7 and 21-day results when compared to the control sample. Gl + Ce contains a significant amount of impurities. These impurities might have led to more water absorption from the mix, thus affecting the hydration of cement and consequent less formation of C-S-H gels. Moreover, since due to the presence of impurities less glass is present in the mixture, a lesser amount of pozzolan is available, leading to less C-S-H gel formation. To further emphasize this, the Cl + Co B, which also has impurities, is the only mix that exhibited a smaller change in porosity when compared to the cleaner glass samples. This might lead to the conclusion that the impurities are causing this change. Despite this, the result of Cl + Co B still shows a decrease in porosity and so a denser microstructure when compared to the control.

XRD of the Cl + Co W Ca 850 has shown that the material in the sample has both an amorphous and crystalline structure. The crystalline nature of the material has decreased the pozzolanic reactivity of this sample when compared to the original Cl + Co W leading to less gel formation. Although C-S-H gel is still formed by the cement hydration reaction, there is decreased gel formation when compared to the superior glass types. Over time, the cement matrix did not become as dense as some of the other samples, making it comparatively more porous.

Clear and coloured glass exhibit a substantial difference between them. From the XRF analysis, coloured glass from WSML has more metal oxides than the clear glass from the same facility. There is a higher percentage of the following metal oxides in coloured glass namely Al_2O_3, Fe_2O_3, Na_2O, K_2O, TiO_2, MnO, Cr_2O_3, CoO, NiO and CuO. These metal oxides react with the $Ca(OH)_2$ and decrease its availability for pozzolanic reactions resulting in less C-S-H gel production. Comparatively, there is a decrease in the densification of the matrix and a decreased change in porosity.

At 21 days, when comparing the porosity of the samples to the porosity of the cement control, Co, Cl + Co W, Gl + Ce and Cl + Co W Ca 600 had a lower porosity than the control. The porosity of the clear glass is comparable to that of the control. The porosities of Cl + Co B and Cl + Co W Ca 850 are higher than that of the control. However, since the change in porosity over time is larger than that of the control, the Cl + Co B has more potential of decreasing its porosity over time. This cannot be said for Cl + Co W Ca 850 since it possesses less pozzolanic potential. At 21 days, Cl + Co W was the sample that exhibited the lowest and most ideal porosity.

5.2.2.3 SORPTIVITY OF PASTE CUBES RESULTS

The rate of absorption of water into the paste cubes by capillary action was measured to gain insight on the sorptivity of the samples. Graphs of absorption (I) against the square root of time were plotted for 7 and 21 day-samples as shown below.

The paste cubes that were cured for 7 days yielded the following results:

- At approximately 150 $sec^{1/2}$, which correlates to the 6^{th} hour of the test, the initial absorption took place.
- At the initial stage of absorption, the cement control had the steepest gradient meaning that it has a high sorptivity. The Cl + Co B sample exhibited the lowest sorptivity. The gradients of the other WGP samples vary within the upper and lower limits showing different rates of absorption.
- The start of the secondary rate of absorption, as per ASTM C 1585 – 04, commences at approximately 300 $sec^{1/2}$, which correlates to 24 hours after the start of the test.
- On visual inspection of the graphs, it is evident that the rate of absorption is significantly reduced in the secondary absorption as evidenced by the flattening of the gradients.
- In the secondary stage of absorption, the rates of absorption, i.e. sorptivity, of all the samples including the control are similar to each other.

To analyse the results of the paste cubes that were cured for 21 days, the same time intervals for the initial and secondary absorption were considered. The test yielded the following results:

- The initial sorptivity is highest for Cl + Co W Ca 600 and lowest for Co. The control sample has the second steepest gradient out of all the samples.
- Once again, the gradients of the secondary absorption are less steep than the gradients of the initial absorption. The sample that had the highest rate of absorption initially, Cl + Co W Ca 600, had the flattest gradient in the second stage of absorption. Conversely, Co which had the flattest gradient in the initial stage, had the steepest gradient in the second phase of absorption. The gradient of the cement control is noticeably steeper than that of Cl + Co W Ca 600. Therefore, since the rate of absorption of the cement control is higher than that of Cl + Co W Ca 600, Cl + Co W Ca 600 is performing better than the control and all the other samples. It can also be seen that Cl + Co B, Gl + Ce and Cl + Co W Ca 850 also have a lower rate of absorption than cement which is beneficial. This is due to the densification of the microstructure brought about by WGP of particle sizes smaller than that of cement and good pozzolanic reactivity.

SECONDARY RATE OF ABSORPTION OF PASTE CUBES		
	Rate of Absorption after 7-Day Curing ($mm/sec^{1/2}$)	**Rate of Absorption after 21-Day Curing ($mm/sec^{1/2}$)**
Cem Con	0.0007	0.0012
Cl	0.0009	0.0016
Co	0.0007	0.0018
Cl + Co W	0.0011	0.0015
Cl + Co B	0.0014	0.0011
Gl + Ce	0.0007	0.0006
Cl + Co W Ca 600	0.0007	0.0005
Cl + Co W Ca 850	0.0013	0.0010

Table 5.19 – Secondary Rate of Absorption of Paste Cubes after 7-day and 21-day curing

Thus, it can be concluded that Cl + Co W Ca 600 exhibits the least sorptivity over time followed by Gl + Ce. This means that these two types of paste mixes are expected to be the most durable.

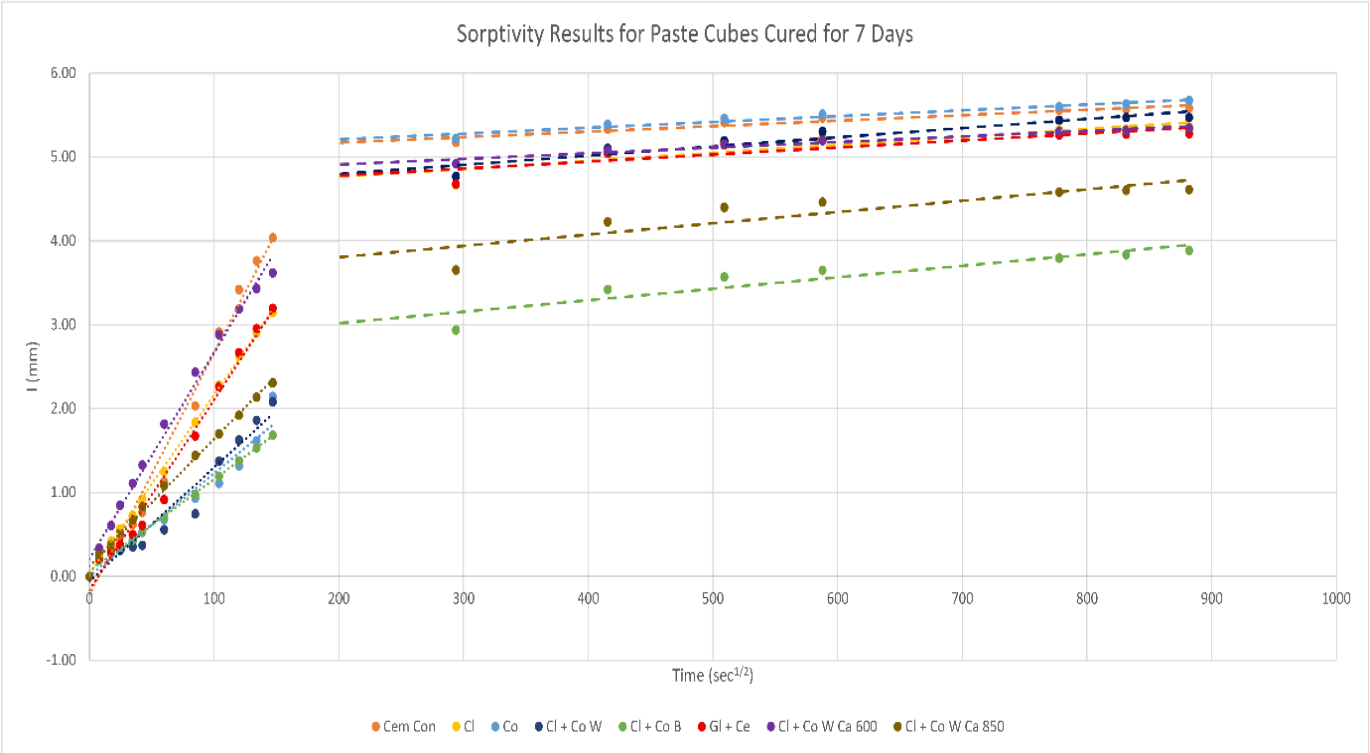

Figure 5.20 - Sorptivity Results for Paste Cubes Cured for 7 days

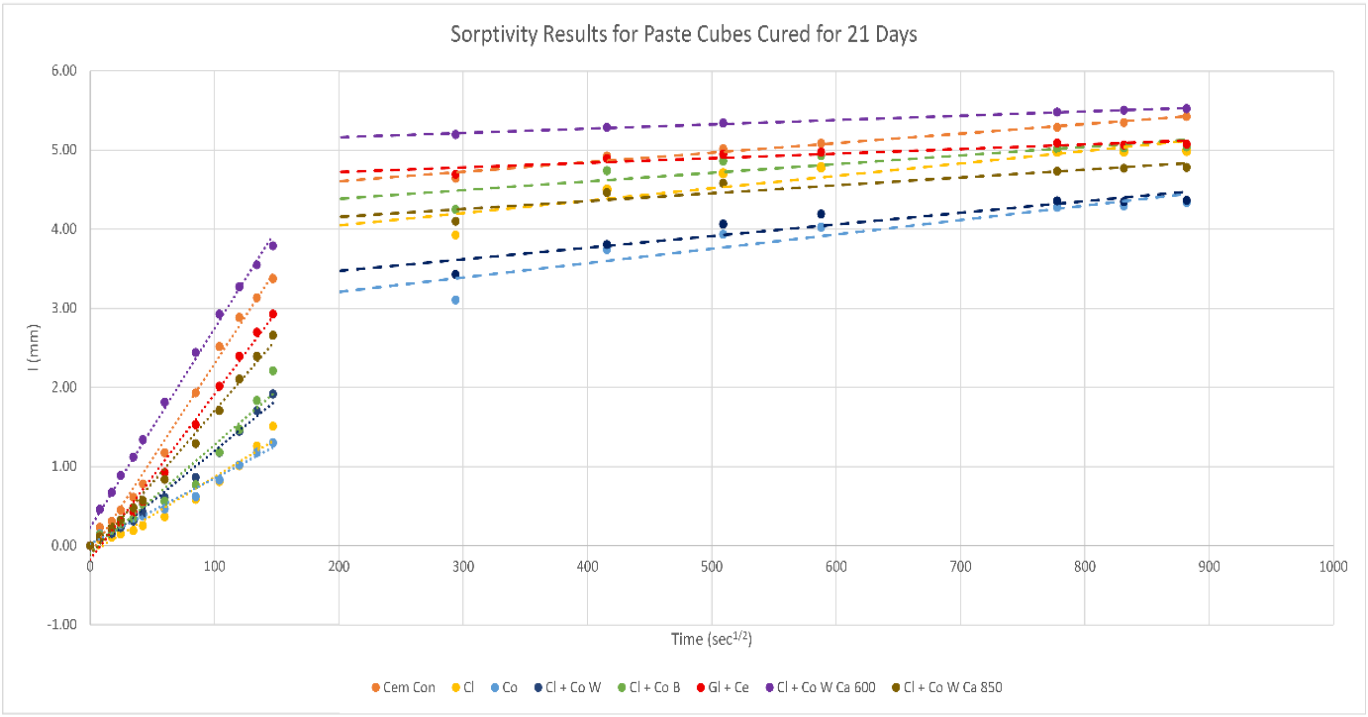

Figure 5.21 – Sorptivity Results for Paste Cubes for 21 days

5.2.2.4 COMPRESSIVE STRENGTH OF PASTE CUBES RESULTS

The values obtained for the compressive strengths of the paste cubes after curing for 7 days and after 21 days are shown below.

AVERAGE COMPRESSIVE STRENGTH OF PASTE CUBES				
	Average Compressive Strength at 7 Days (MPa)	**Standard Deviation from Mean for Compressive Strengths at 7 Days**	**Average Compressive Strength at 21 Days (MPa)**	**Standard Deviation from Mean for Compressive Strengths at 21 Days**
Cem Con	68.93	2.15	91.51	7.21
Cl	84.05	1.71	86.42	9.72
Co	80.62	0.53	85.58	14.23
Cl + Co W	76.79	5.22	93.20	8.95
Cl + Co B	72.00	2.13	96.63	8.72
Gl + Ce	51.03	5.34	98.06	0.25
Cl + Co W Ca 600	74.42	4.99	108.08	6.33
Cl + Co W Ca 850	80.08	6.16	101.04	3.58

Table 5.20 – Average Compressive Strength Values for the Paste Cubes at 7-day & 21-day Curing

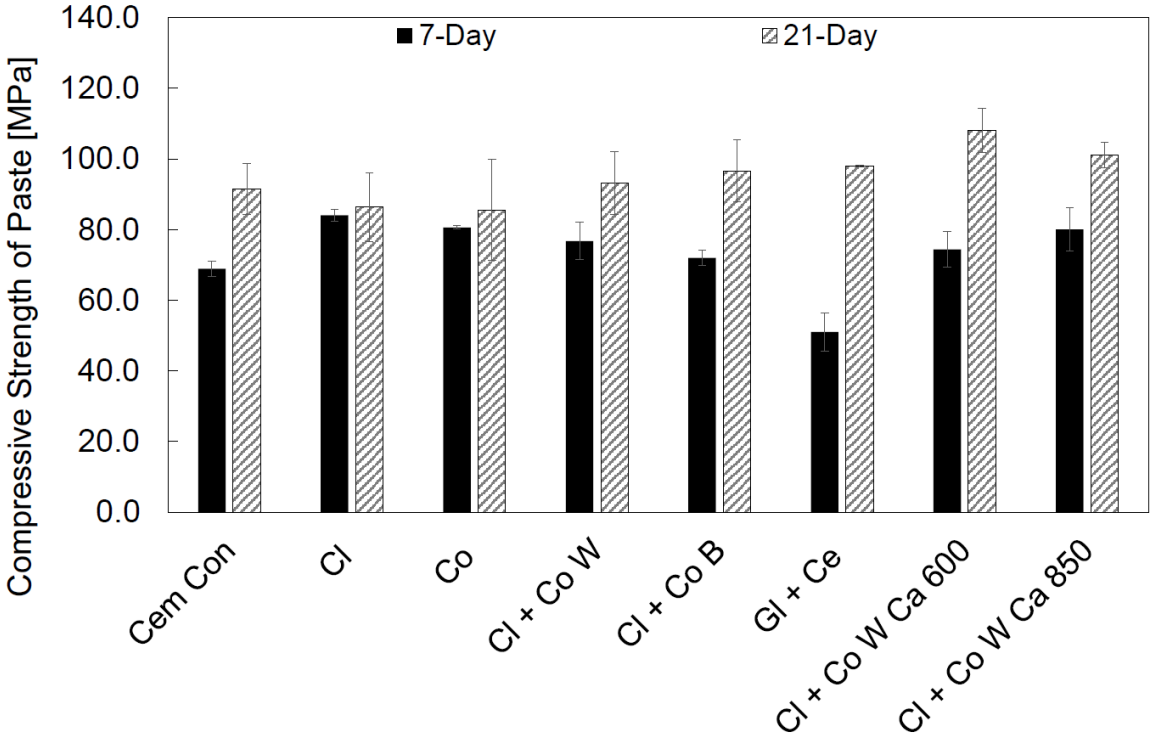

Figure 5.22 – Bar Graph comparing Compressive Strength for Samples cured for 7 days & 21 days

From the graph, it can be concluded that, at 21 days, Cl + Co W Ca 600 is exhibiting the maximum compressive strength which even exceeds the compressive strength of the cement control. This might be due to the effects of thermal activation.

It can also be noted that Cl + Co B and Gl + Ce are exhibiting higher compressive strength than the control at 21 days. This could possibly be due to the impurities present in the samples. Their interaction in the mix might be leading to a superior microstructure.

In the context of this study, other tests like isothermal calorimetry and XRD analysis are needed together with these values of compressive strength to understand fully the events of the process. This is discussed in section 5.2.2.8.

5.2.2.5 SEM-EDS RESULTS OF PASTE SAMPLES

Paste samples Cem Con, Cl + Co W, Cl + Co B and Cl + Co W Ca 600 that had cured for 7 days were analysed with SEM-EDS.

Through SEM analysis, it was determined that the samples that contained glass waste as an SCM, contained more C-S-H gel which typically visually appears as fine light grey pieces which are clumped together (Samarakoon et al., 2021) (Chen et al., 2022). The presence of additional C-S-H gel indicates that the glass waste is working as a pozzolan. In fact, the EDS analysis shows a clear distinction between the silica peak found in the control sample and those present in the different waste glass samples which were higher.

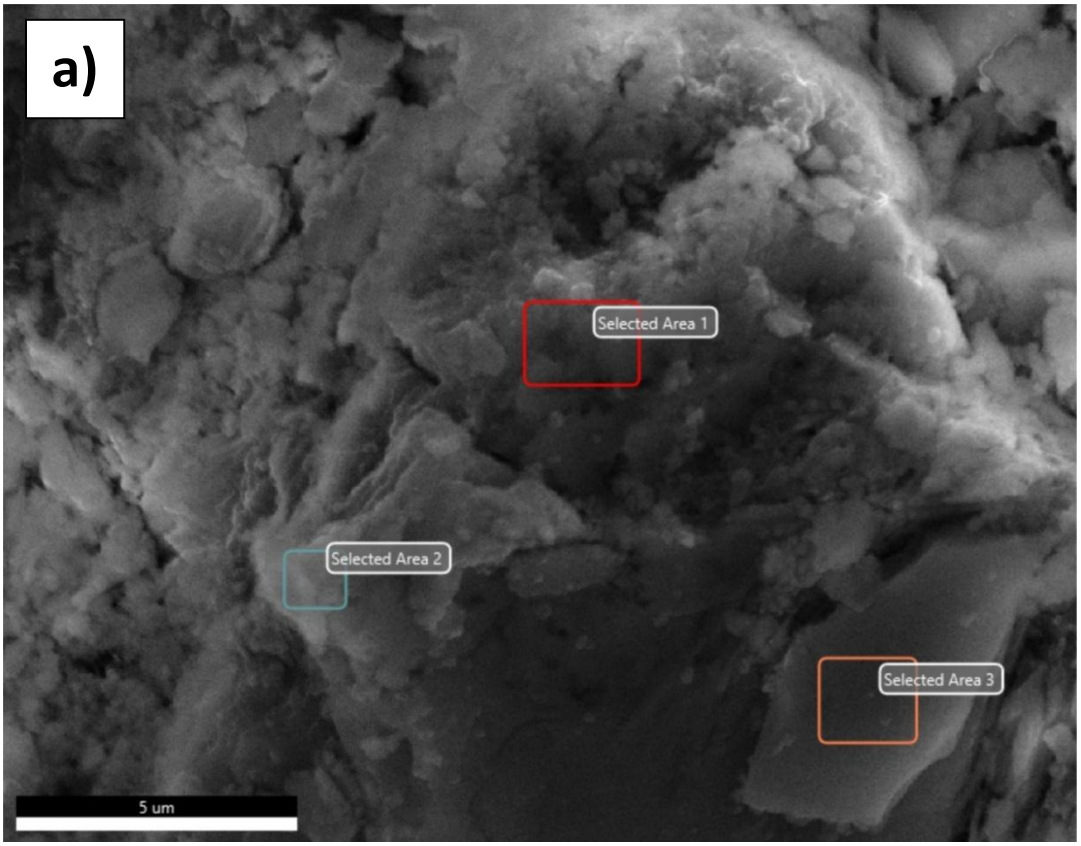

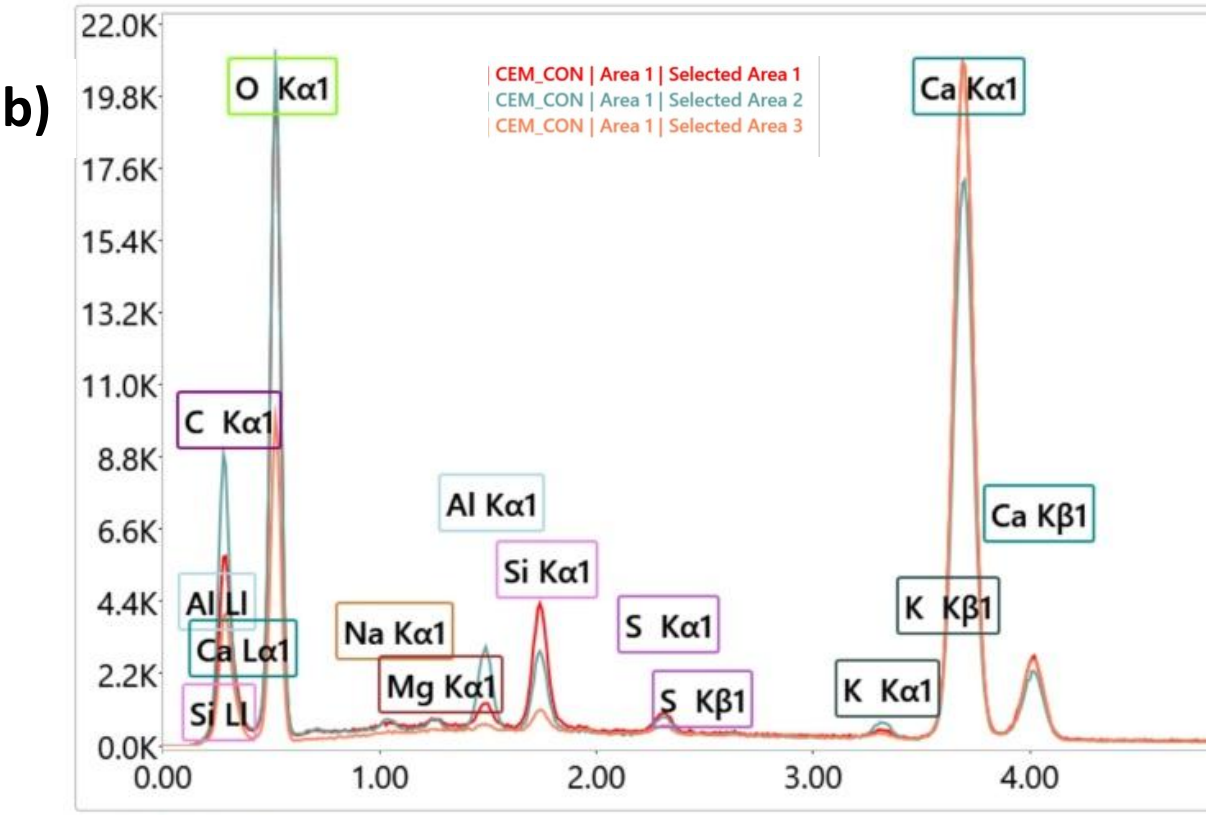

Figure 5.23 – a) SEM of the Cement Control Paste Sample after 7 days of Curing b) Graph showing the EDS Analysis of the Cement Control after 7 days of Curing

ELEMENT	WEIGHT %	MDL	ATOMIC %	ERROR %
	Cem Con Paste 7 Days – SELECTED AREA 1			
C K	4.48	1.22	9.39	7.30
O K	30.57	0.09	48.16	8.10
Mg K	0.21	0.07	0.22	13.04
Al K	0.82	0.05	0.77	6.01
Si K	3.95	0.05	3.55	3.19
S K	1.20	0.50	0.94	4.01
K K	0.59	1.78	0.38	11.83
Ca K	58.19	0.06	36.60	1.98
	Cem Con Paste 7 Days – SELECTED AREA 2			
C K	8.68	0.34	16.88	6.91
O K	32.12	0.06	46.86	7.95
Na K	0.19	0.06	0.19	12.87
Mg K	0.27	0.10	0.26	8.87
Al K	2.68	0.05	2.32	3.81
Si K	2.66	0.12	2.21	3.45
S K	1.10	0.59	0.80	4.07
K K	1.18	1.52	0.71	6.57
Ca K	51.10	0.06	29.76	2.01
	Cem Con Paste 7 Days – SELECTED AREA 3			
C K	3.30	0.16	7.89	7.03
O K	20.81	0.10	37.32	8.71
Al K	0.16	0.07	0.17	19.21
Si K	0.83	0.09	0.85	4.90
S K	0.75	0.11	0.67	6.56
K K	0.52	0.10	0.38	16.10
Ca K	73.63	0.13	52.72	1.96

Table 5.21 - EDS Results for Cement Control Paste Sample

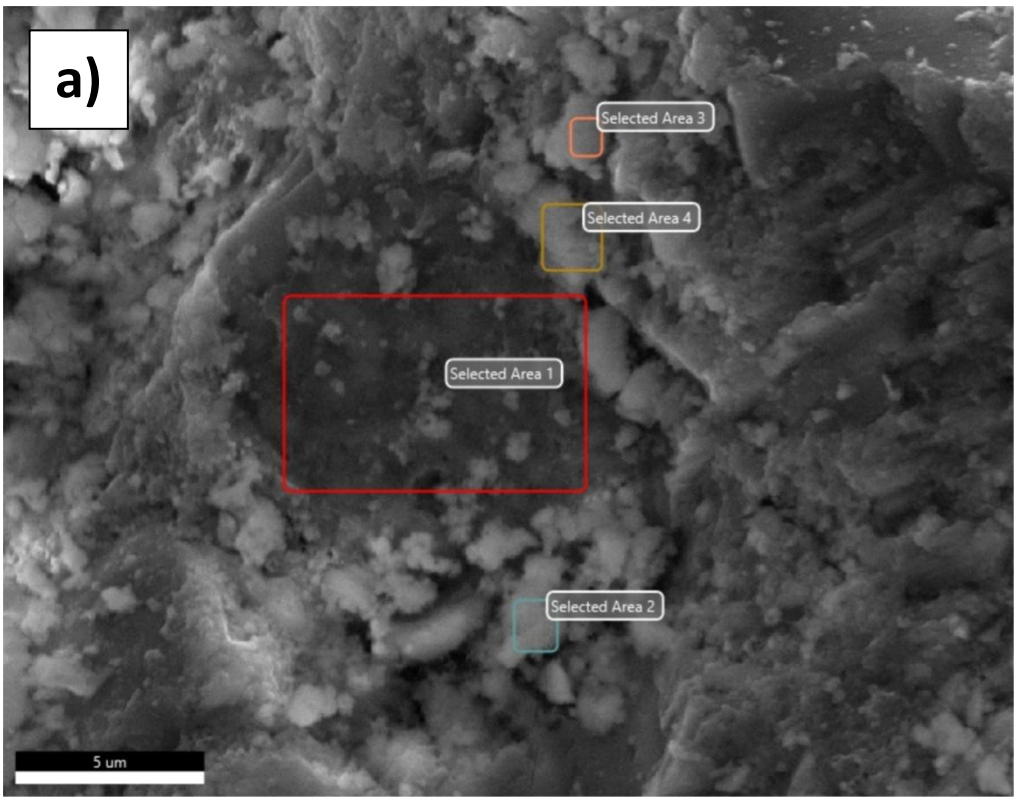

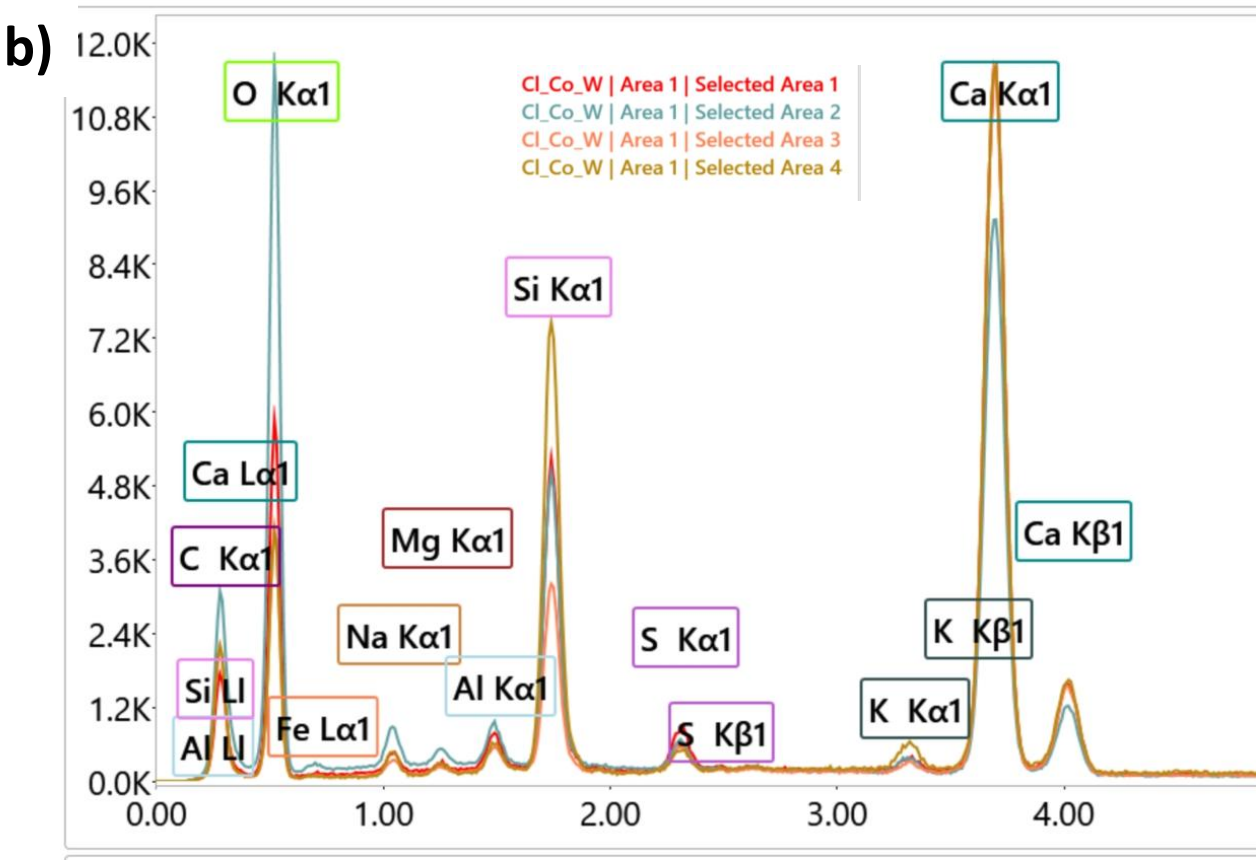

Figure 5.24 - a) SEM of the Cl + Co W Paste Sample after 7 days of Curing b) Graph showing the EDS Analysis of the Cl + Co W after 7 days of Curing

ELEMENT	WEIGHT %	MDL	ATOMIC %	ERROR %
	Cl + Co W Paste 7 Days – SELECTED AREA 1			
C K	3.30	0.17	7.97	8.54
O K	17.55	0.16	31.77	8.75
Al K	0.58	0.11	0.62	8.13
Si K	9.38	0.11	9.67	3.07
S K	1.79	0.12	1.61	6.62
K K	1.01	0.15	0.75	11.92
Ca K	64.59	0.18	46.68	2.11
Fe K	1.80	0.46	0.93	17.88
	Cl + Co W Paste 7 Days – SELECTED AREA 2			
C K	5.50	0.13	11.09	7.80
O K	31.44	0.08	47.60	7.88
Na K	0.70	0.09	0.74	7.27
Mg K	0.28	0.08	0.28	9.01
Al K	1.14	0.12	1.03	4.82
Si K	9.05	0.07	7.80	2.87
S K	1.40	0.33	1.06	4.02
K K	1.12	0.14	0.70	7.04
Ca K	48.55	0.12	29.35	2.07
Fe K	0.82	0.33	0.36	18.54
	Cl + Co W Paste 7 Days – SELECTED AREA 3			
C K	4.85	0.19	11.96	7.55
O K	13.99	0.30	25.92	8.98
Al K	0.31	0.31	0.34	12.03
Si K	6.35	0.06	6.70	3.38
S K	1.01	0.25	0.93	7.30
K K	0.67	1.40	0.51	16.04
Ca K	71.69	0.12	53.03	2.06
Fe K	1.13	0.68	0.60	21.38
	Cl + Co W Paste 7 Days – SELECTED AREA 4			
C K	4.63	0.16	11.56	8.70
O K	11.38	0.25	21.35	9.16
Si K	13.98	0.14	14.94	2.99
S K	0.47	0.19	0.44	15.71
K K	1.76	0.19	1.35	9.42
Ca K	65.71	0.26	49.23	2.18
Fe K	2.07	0.54	1.11	16.78

Table 5.22 - EDS Results for Cl + Co W Paste Sample

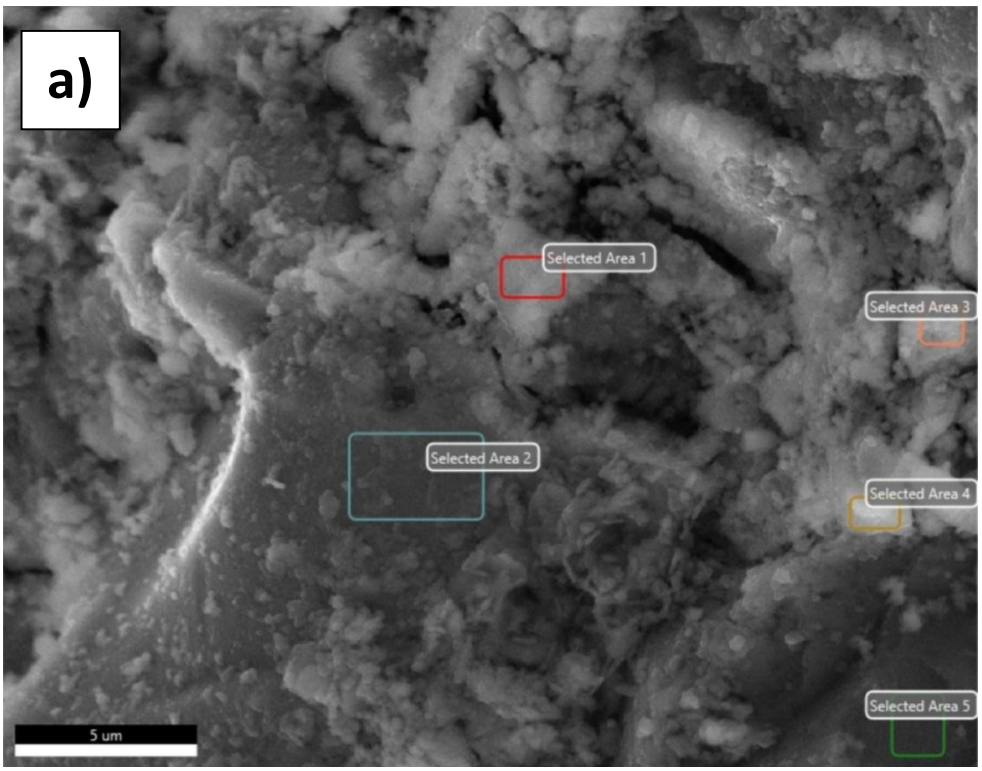

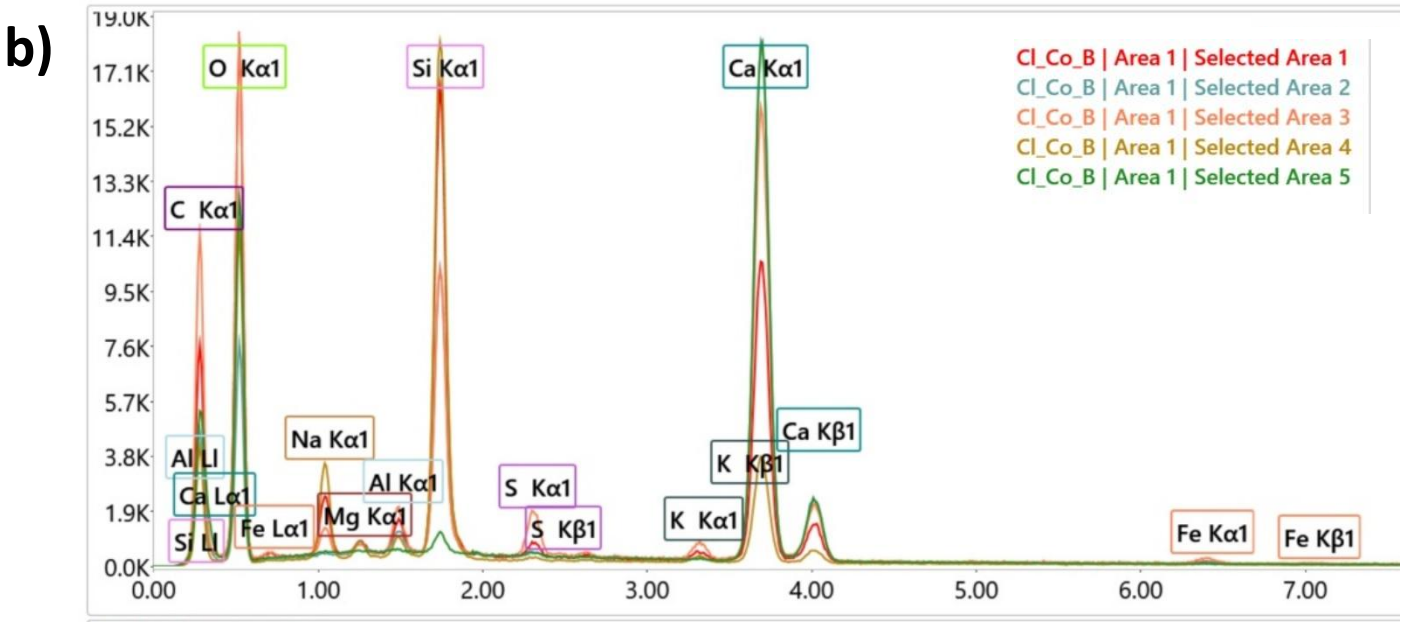

Figure 5.25 - a) SEM of the Cl + Co B Paste Sample after 7 days of Curing b) Graph showing the EDS Analysis of the Cl + Co B after 7 days of Curing

ELEMENT	WEIGHT %	MDL	ATOMIC %	ERROR %
	Cl + Co B Paste 7 Days – SELECTED AREA 1			
C K	12.43	0.11	22.88	8.05
O K	27.91	0.07	38.56	7.59
Na K	1.61	0.05	1.54	5.48
Mg K	0.32	0.13	0.29	8.55
Al K	1.33	0.16	1.09	4.60
Si K	19.05	0.07	14.99	2.56
S K	1.03	0.46	0.71	5.39
K K	0.87	1.74	0.49	9.88
Ca K	34.66	0.05	19.12	2.15
Fe K	0.80	0.28	0.32	20.30
	Cl + Co B Paste 7 Days – SELECTED AREA 2			
C K	6.62	0.23	15.41	7.70
O K	14.65	0.16	25.60	8.66
Mg K	0.23	0.38	0.26	12.81
Al K	0.87	0.07	0.90	5.94
Si K	12.45	0.03	12.40	2.74
S K	0.37	4.38	0.33	11.07
Ca K	64.16	0.04	44.77	2.00
Fe K	0.65	5.04	0.33	24.68
	Cl + Co B Paste 7 Days – SELECTED AREA 3			
C K	14.04	0.15	26.51	7.49
O K	25.65	0.08	36.34	7.98
Na K	0.42	0.15	0.41	8.81
Al K	1.34	0.05	1.12	4.95
Si K	9.79	0.05	7.90	2.82
S K	2.41	0.42	1.70	3.51
K K	1.30	0.85	0.75	7.02
Ca K	43.66	0.07	24.70	2.11
Fe K	1.39	2.10	0.56	13.41

Table continued on next page

ELEMENT	WEIGHT %	MDL	ATOMIC %	ERROR %
	Cl + Co B Paste 7 Days – SELECTED AREA 4			
C K	12.98	0.18	23.11	8.96
O K	25.45	0.09	34.00	7.11
Na K	4.11	0.03	3.82	4.44
Mg K	0.60	0.12	0.52	6.06
Al K	1.13	0.44	0.90	5.72
Si K	34.76	0.03	26.45	2.39
K K	0.83	1.55	0.45	10.06
Ca K	20.14	0.17	23.11	2.43
	Cl + Co B – SELECTED AREA 5			
C K	5.50	0.35	11.97	6.74
O K	26.47	0.13	43.21	8.36
Al K	0.27	0.53	0.26	11.99
Si K	1.10	0.09	1.03	4.31
S K	0.61	1.00	0.50	6.87
Ca K	66.04	0.06	43.03	1.95

Table 5.23 - EDS Results for Cl + Co B Paste Sample

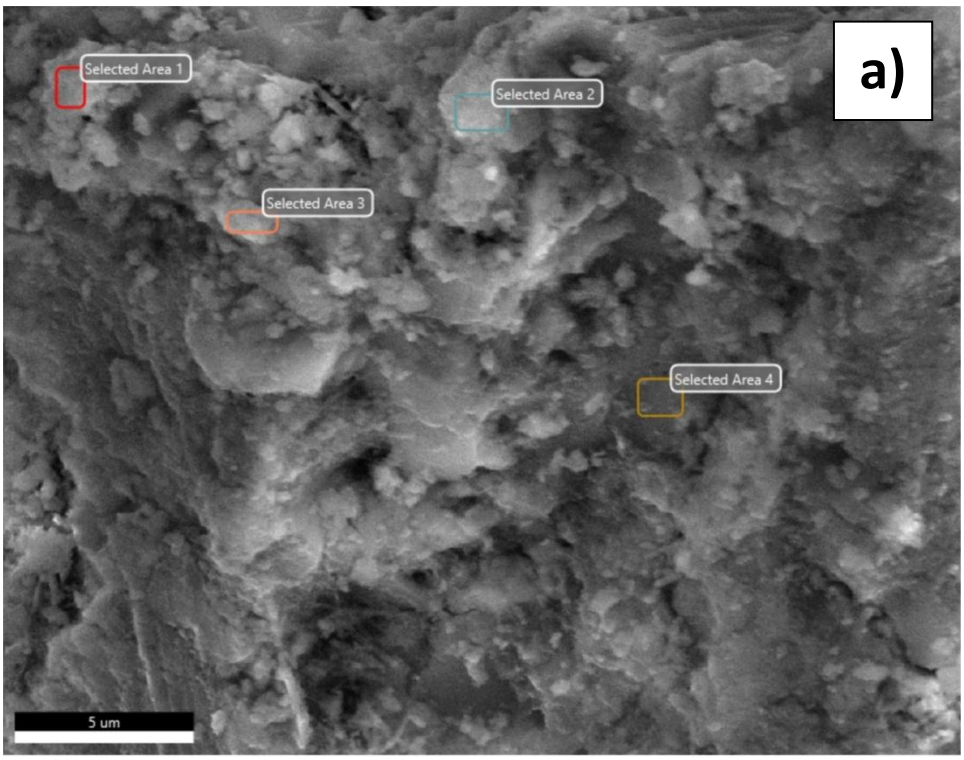

b)

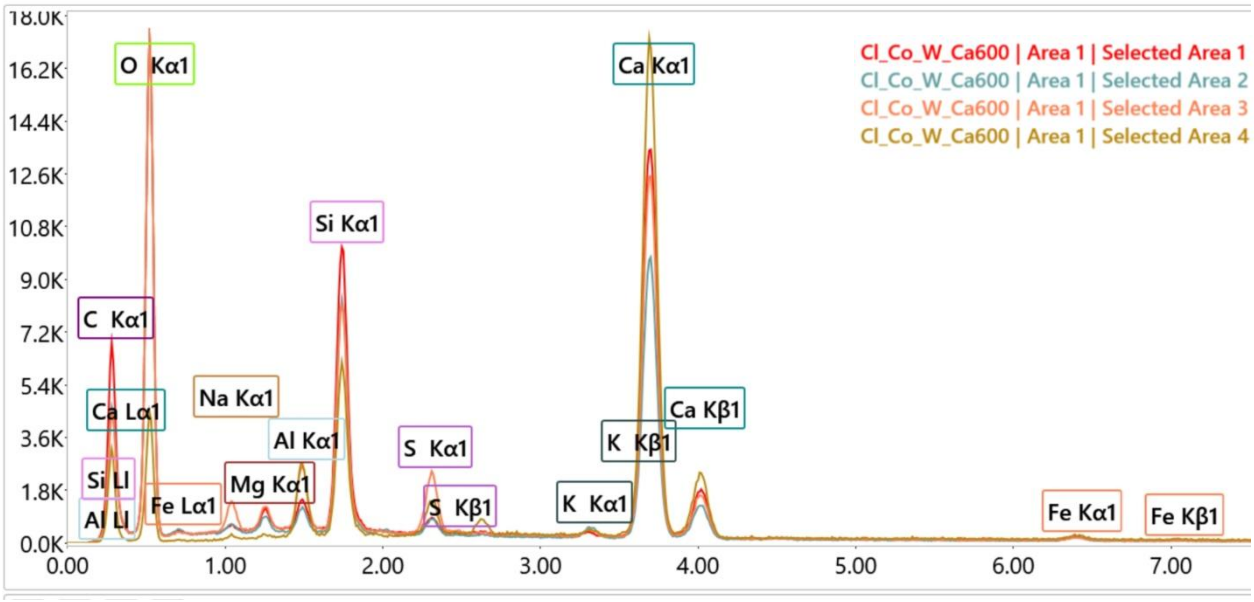

Figure 5.26 - a) SEM of the Cl + Co W Ca 600 Paste Sample after 7 days of Curing b) Graph showing the EDS Analysis of the Cl + Co W Ca 600 after 7 days of Curing

ELEMENT	WEIGHT %	MDL	ATOMIC %	ERROR %
	Cl + Co W Ca 600 Paste 7 Days – SELECTED AREA 1			
C K	9.26	0.08	18.02	7.70
O K	29.31	0.07	42.79	7.87
Mg K	0.47	0.15	0.45	8.40
Al K	1.09	0.17	0.94	5.34
Si K	11.77	0.04	9.79	2.78
S K	0.98	0.23	0.71	6.89
K K	0.37	4.69	0.22	16.09
Ca K	45.65	0.06	26.61	2.09
Fe K	1.09	4.47	0.45	13.96
	Cl + Co W Ca 600 Paste 7 Days – SELECTED AREA 2			
C K	7.34	0.12	13.94	7.87
O K	34.88	0.07	49.74	7.60
Na K	0.11	0.42	0.11	24.29
Mg K	0.46	0.24	0.43	8.39
Al K	1.08	0.29	0.91	5.08
Si K	12.05	0.04	9.79	2.76
S K	1.22	0.79	0.87	6.86
K K	1.04	1.47	0.61	9.84
Ca K	40.58	0.09	23.10	2.10
Fe K	1.24	0.30	0.51	13.06
	Cl + Co W Ca 600 Paste 7 Days – SELECTED AREA 3			
C K	5.81	0.15	11.67	8.27
O K	30.07	0.08	45.33	7.78
Na K	0.75	0.07	0.79	7.08
Mg K	0.73	0.12	0.72	6.04
Al K	2.62	0.10	2.34	3.97
Si K	9.99	0.05	8.58	2.85
S K	4.15	0.17	3.12	3.21
K K	0.73	1.21	0.45	12.68
Ca K	44.19	0.09	26.59	2.11
Fe K	0.96	0.34	0.41	18.80

Table continued on next page

ELEMENT	WEIGHT %	MDL	ATOMIC %	ERROR %
	Cl + Co W Ca 600 Paste 7 Days – SELECTED AREA 4			
C K	4.70	0.62	12.12	8.43
O K	9.17	0.73	17.73	9.28
Al K	2.70	0.07	3.10	4.49
Si K	7.92	0.05	8.72	3.41
S K	2.22	0.25	2.14	4.27
K K	0.68	1.57	0.54	17.49
Ca K	70.74	0.07	54.61	2.12
Fe K	1.86	1.90	1.03	14.83

Table 5.24 - EDS Results for Cl + Co W Ca 600 Paste Sample

5.2.2.6 XRD RESULTS OF PASTE SAMPLES

The graphs obtained from the XRD analysis of all the paste cubes have been superimposed on each other to facilitate the comparison of the data obtained from the different samples as shown below.

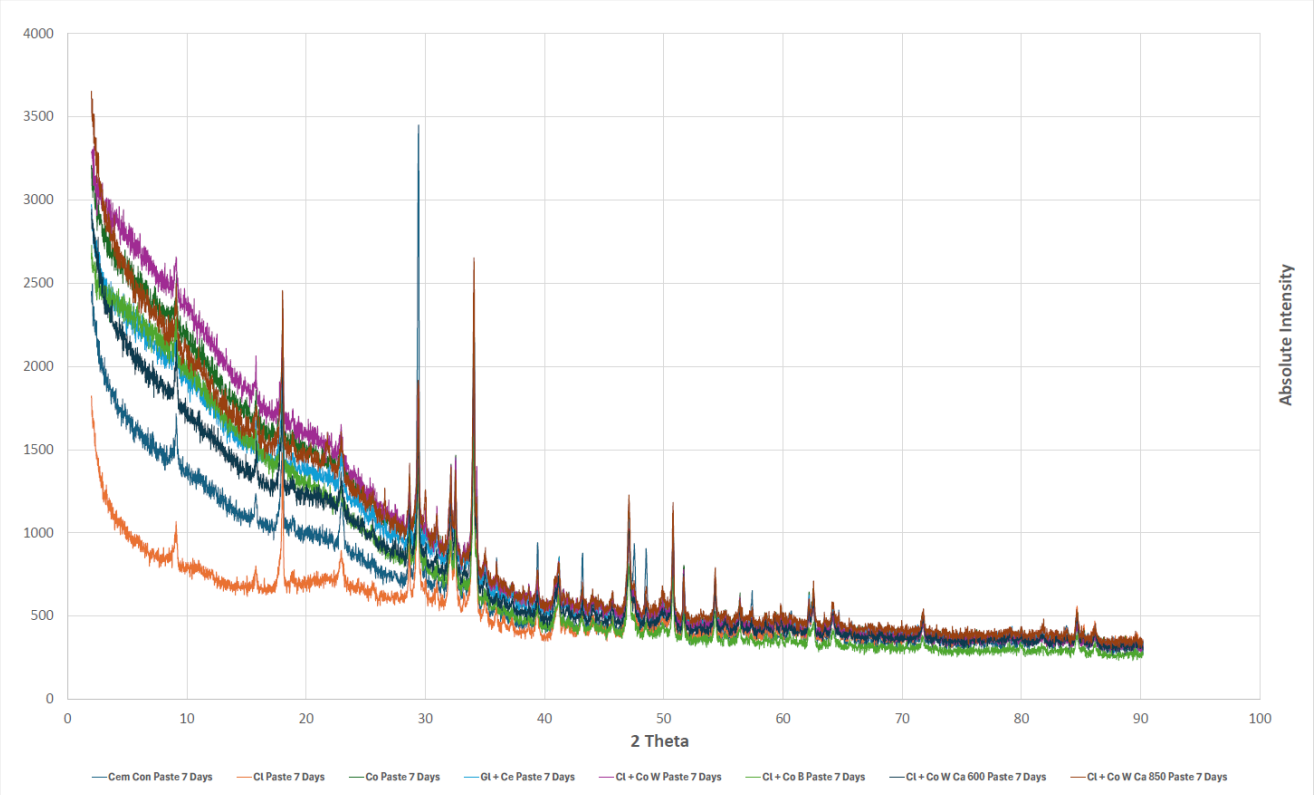

Figure 5.27 – Superimposition of the XRD Results of all the paste samples at 7 days Curing

For better legibility, the individual graphs obtained from XRD analysis of the paste cubes are shown below.

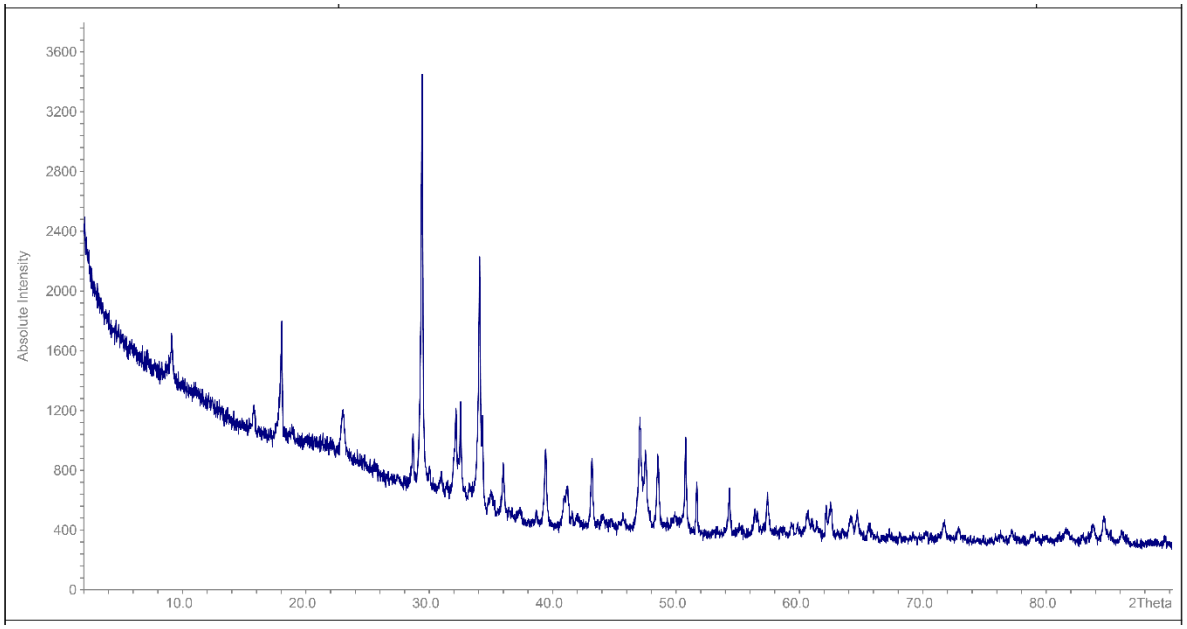

Figure 5.28 – XRD Result of the Cement Paste Control at 7 days Curing

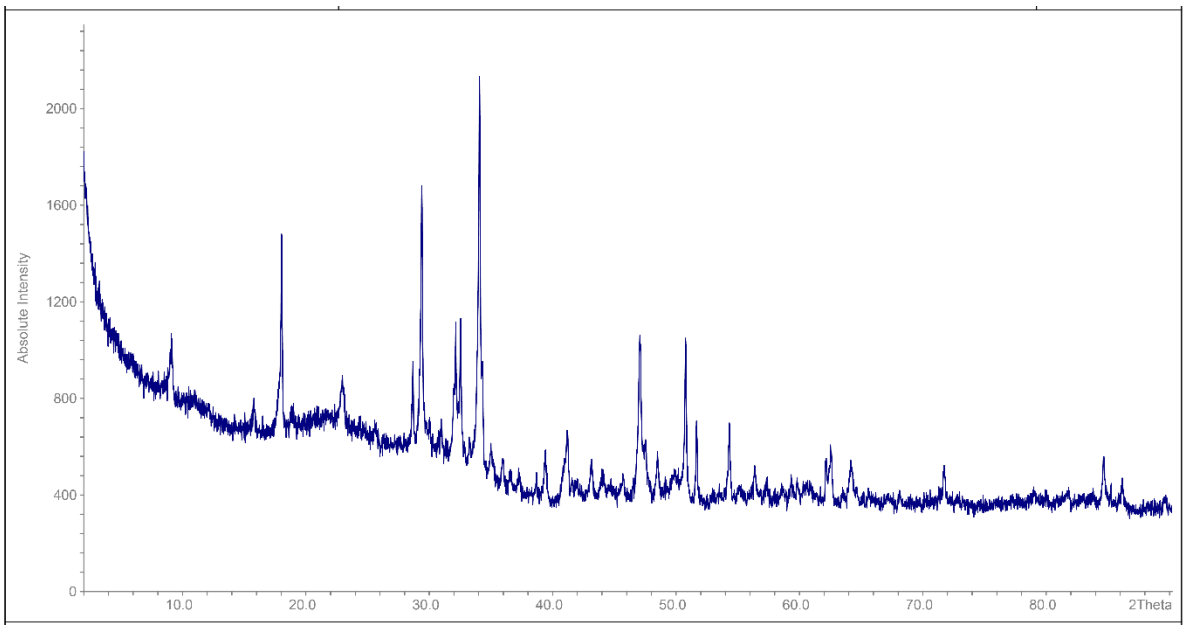

Figure 5.29 - XRD Result of Cl Paste Sample at 7 days Curing

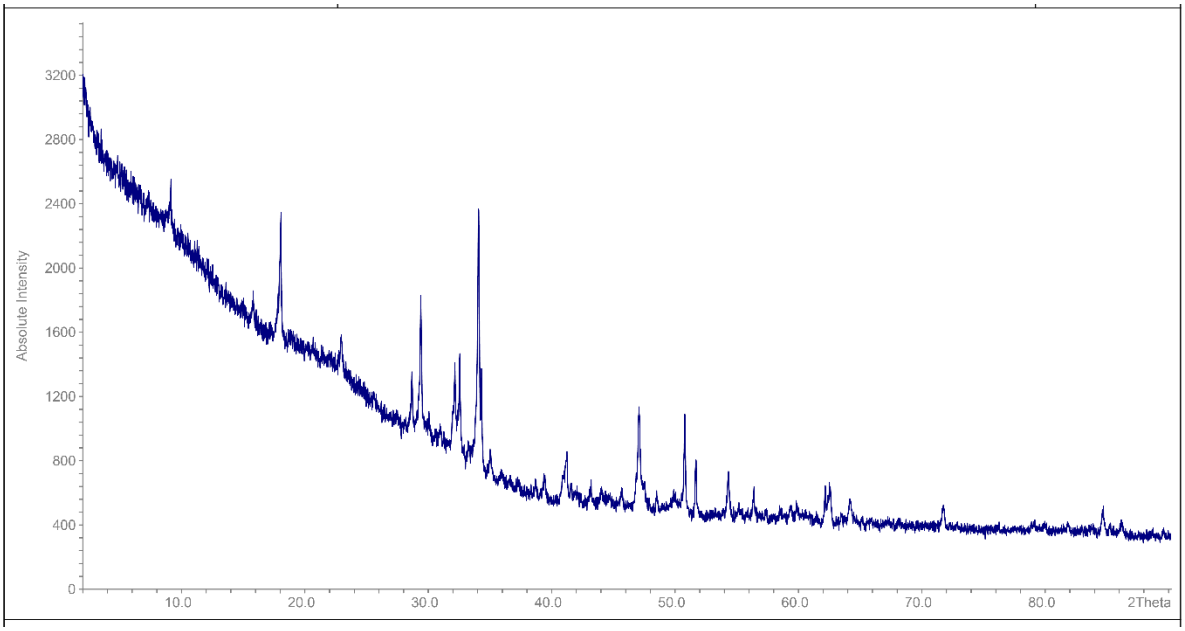

Figure 5.30 – XRD Result of the Co Paste Sample at 7 days Curing

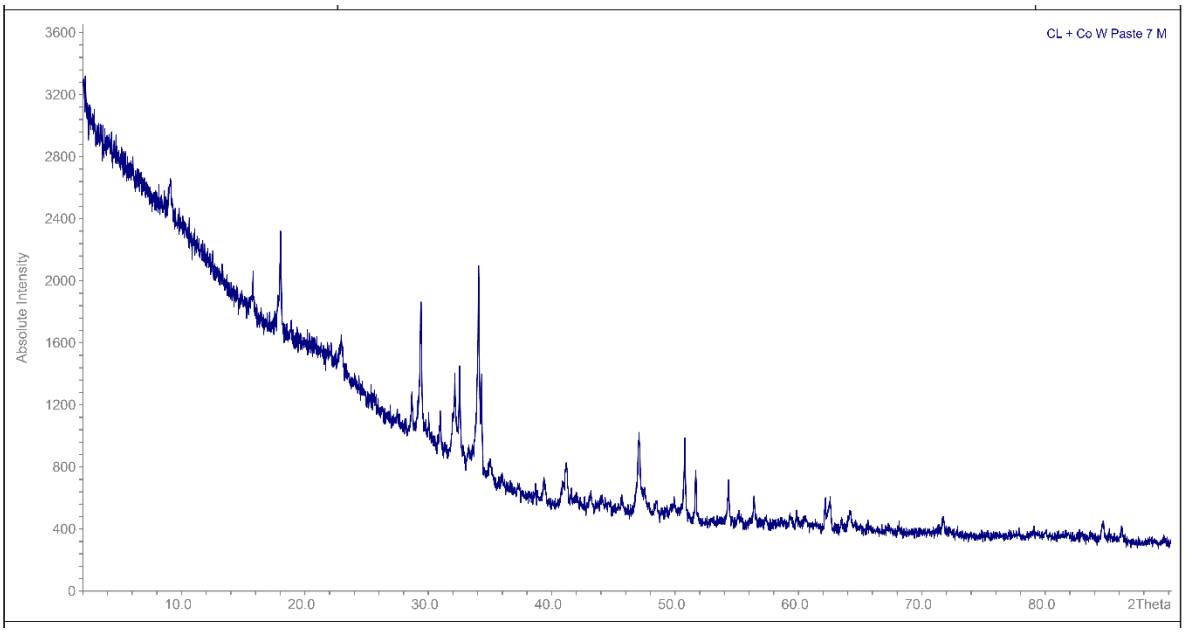

Figure 5.31 – XRD Result of the Cl + Co W Paste Sample at 7 Days Curing

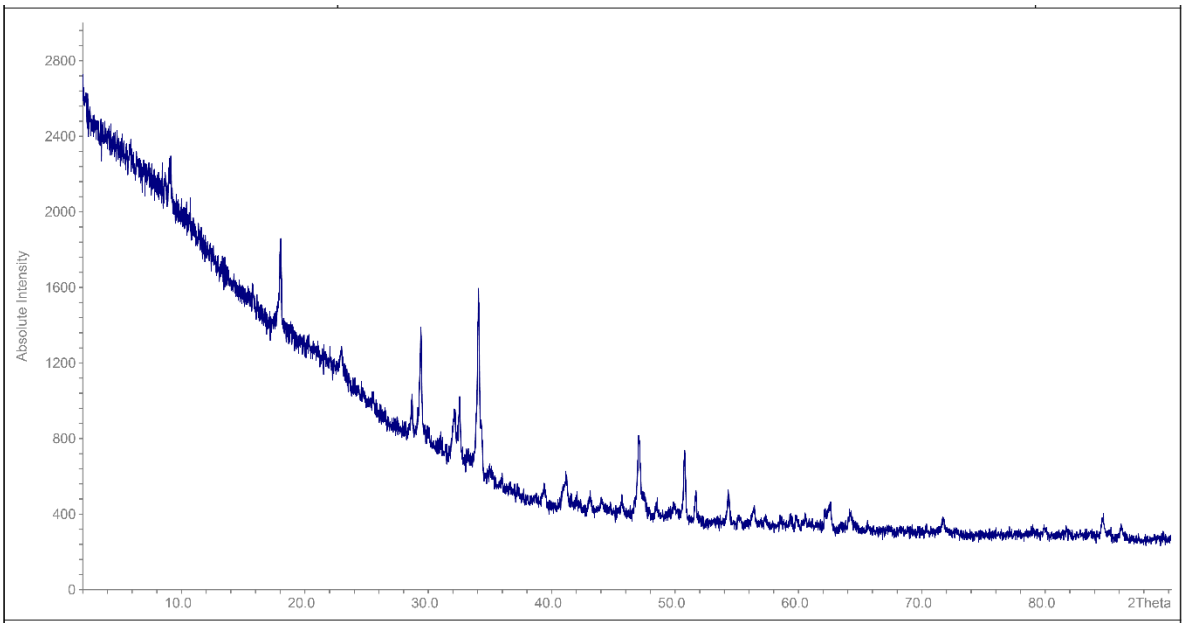

Figure 5.31 – XRD Result of the Cl + Co B Paste Sample at 7 Days Curing

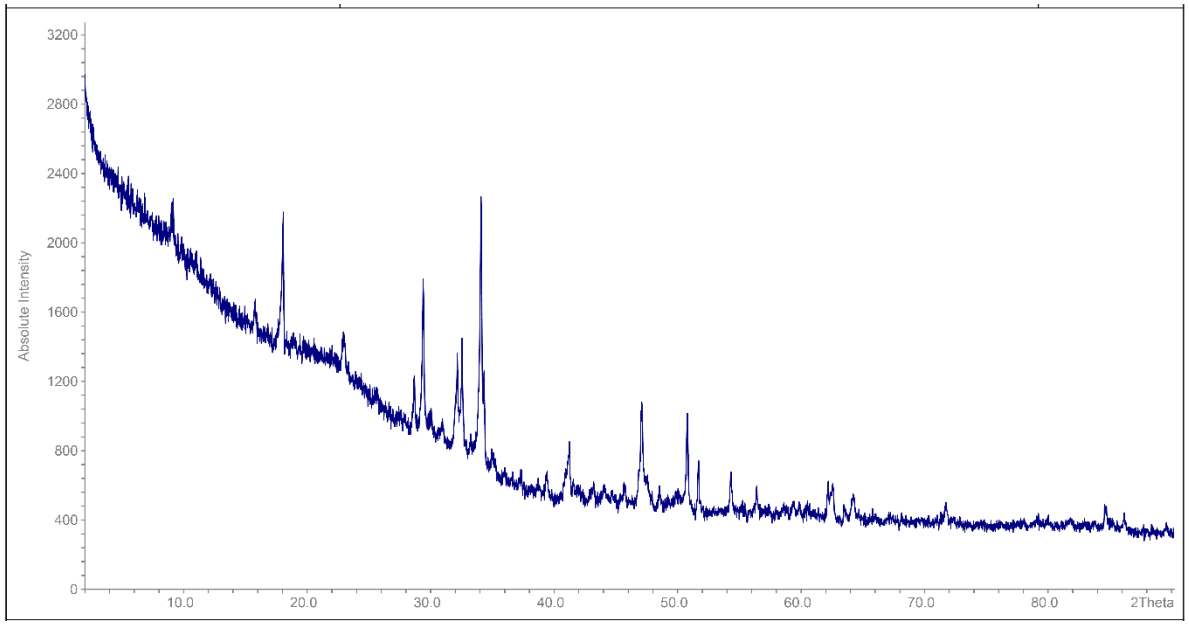

Figure 5.33 - XRD Result of Gl +Ce Paste Sample at 7 Days Curing

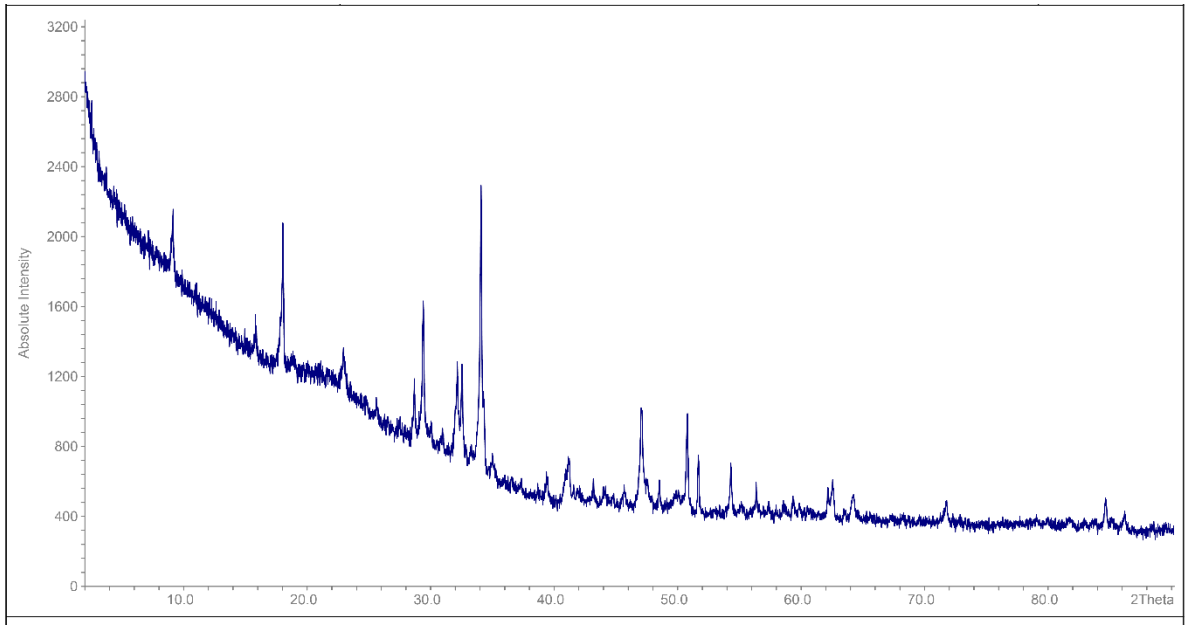

Figure 5.34 – XRD Result of Cl + Co W Ca 600 Paste Sample at 7 Days Curing

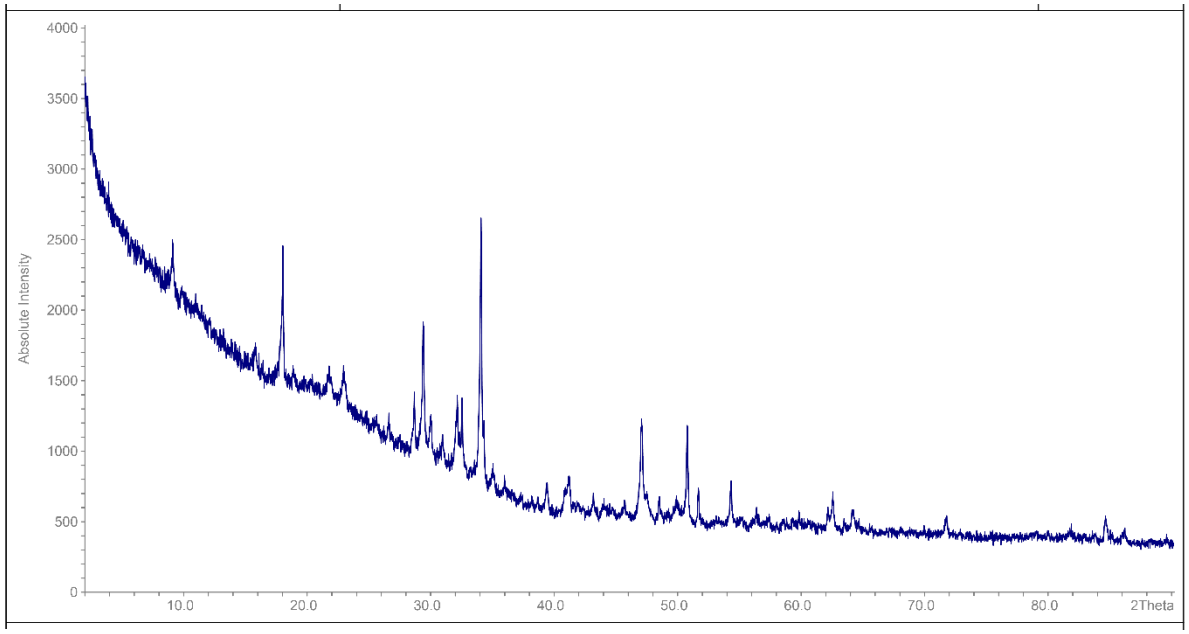

Figure 5.35 – XRD Result of Cl + Co W Ca 850 Paste sample at 7 Days Curing

The following important observations could be deduced from the analysis of the peaks of the graphs:

1. Cem Con (Control)
    - When cement is hydrated, $Ca(OH)_2$ (portlandite) is formed. The presence of portlandite is deduced by peaks at 18°, 34°, 47–48.5° and 50.8° implying that hydration has occurred.
    - Ettringite, a hydration product, is indicated at approx. 9°, proving that hydration has occurred.
2. Cl, Co & Cl + Co W Samples
    - When the pozzolanic reaction takes place, less portlandite would be present. In the graph, a noticeable reduction in the portlandite peaks at 18°, 34°, 47–48.5° when compared to those for Cem Con. This shows that since portlandite has decreased, the pozzolanic reaction is occurring even at 7 days.
3. Cl + Co B Sample
    - This sample is exhibiting more peaks at 39.5° and 54.1° when compared to other samples. This might be due to the presence of albite also known as feldspar ($NaAlSi_3O_8$) and mullite that arise from the contaminants.
    - In this sample, the portlandite peaks are more intense at 18° and 47°, indicating the presence of more portlandite. This suggests slower pozzolanic consumption.
4. Gl + Ce Sample
    - The portlandite peaks in this sample are weaker than that of the control at 18°, 34°, 47–48.5°.
    - This sample is exhibiting an intense peak at 34° peak suggesting C-S-H gel formation from late-reacting glass.
5. Cl + Co W Ca 850 Sample
    - The peaks present at 26.5°, 34° and 39.5° indicate the presence of portlandite. The 850°C calcination may have reduced reactivity by forming stable crystalline compounds as a result of the possible devitrification of the glass in the sample.
6. Cl + Co W Ca 600 Sample
    - When compared to Cl + Co W Ca 850, this sample contains less portlandite, indicating that the SCM used in this sample is a better pozzolan.
    - This shows the presence of new C-S-H gel.

In summary, pozzolanic reactivity is evident since the presence of portlandite is reduced when the glass waste is acting as a good pozzolan. Moreover, Cl + Co W Ca 600 appears to be the sample with the optimal pozzolan since it has exhibited a balance between portlandite consumption and new C-S-H gel formation. This is due to the calcination process at 600^{o}C that was applied to the glass waste. Moreover, this sample showed retained pozzolanic activity. The temperature of heating also played a major role in this since an increase in the heating temperature of the glass waste to 850^{o}C led to increased presence of portlandite cement, implying that less reaction has taken place. The heat applied caused a change in the physical structure of the glass from amorphous to crystalline decreasing its reactivity. Long-term analysis as well as energy-performance trade-off must be considered for heat treatment especially if the processes were to be scaled to industrial levels.

5.2.2.7 FTIR SPECTROSCOPY RESULTS OF PASTE SAMPLES

In FTIR spectroscopy, the events occurring in the formation of concrete are looked into. When cement undergoes the hydration reaction, it produces portlandite ($Ca(OH)_2$) and C-S-H gel. There are also unreacted cement phases especially since the samples under test have only been cured for 7 days. The following graphs were obtained as results for FTIR of the paste samples that cured for 7 days. Different peaks can be observed:

- Portlandite – A band is present at 3600 - 3650 cm^{-1}. This region is characterised by OH stretching of the portlandite because of cement hydration. This band indicates the extent of cement hydration with the water present, and the available CaO present for pozzolanic reactions.
- C-S-H gel formation – A band is present at 1000 – 1080 cm^{-1}. This region represents Si-O stretching where vibrations stretch the Si-O bonds asymmetrically. This shift indicates the formation of C-S-H gel. Unreacted cement phases are also present at the lower values of this range.
- Carbonation Reaction – A band is present at 1400 – 1500 cm^{-1}. This region represents C-O stretching where calcite (CO_3^{2-}) vibrates, indicating carbonation by the atmospheric CO_2.

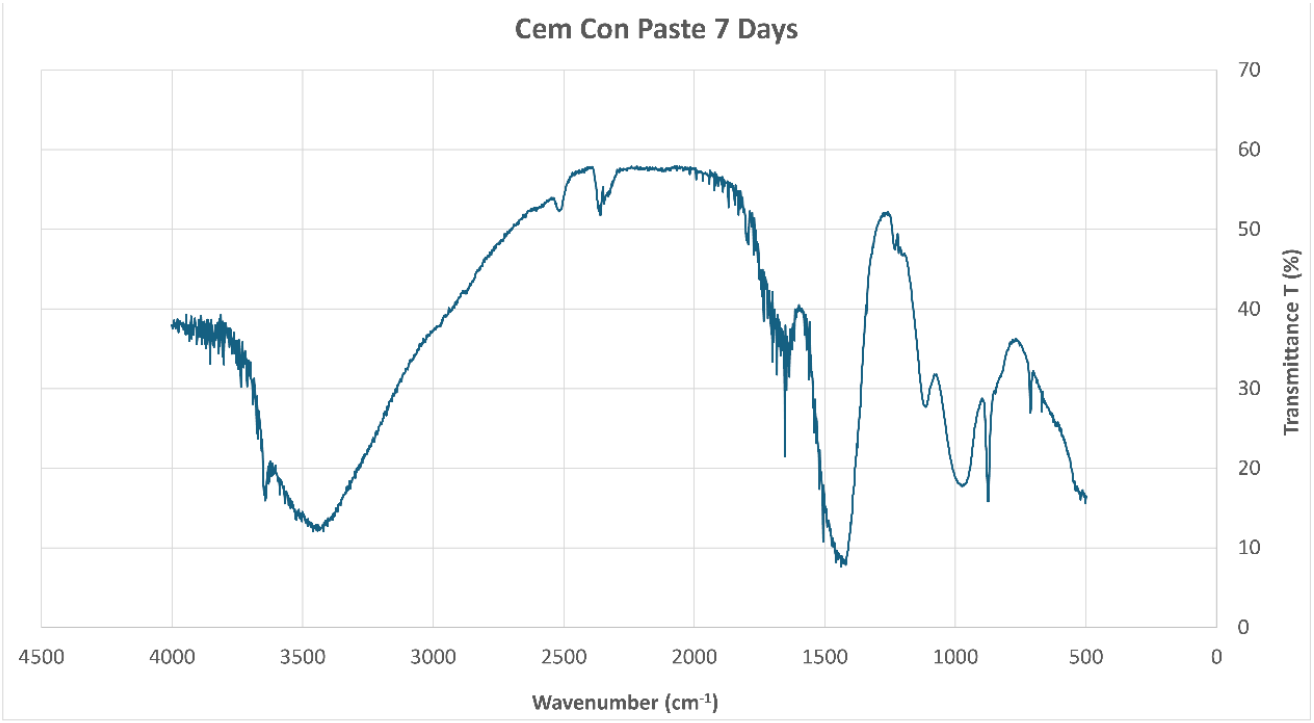

Figure 5.36 – FTIR Spectroscopy Result for the Cement Control Sample after 7 Days Curing

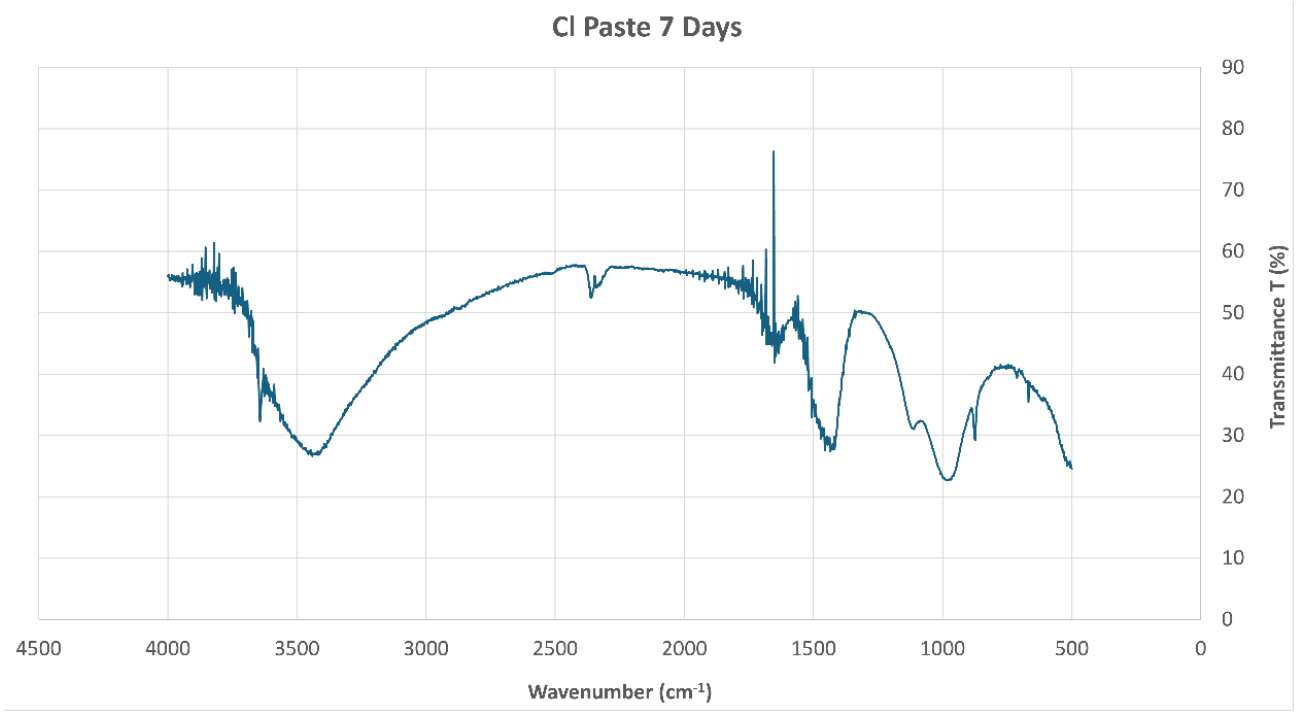

Figure 5.37 - FTIR Spectroscopy Result for the Cl Paste Sample after 7 Days Curing

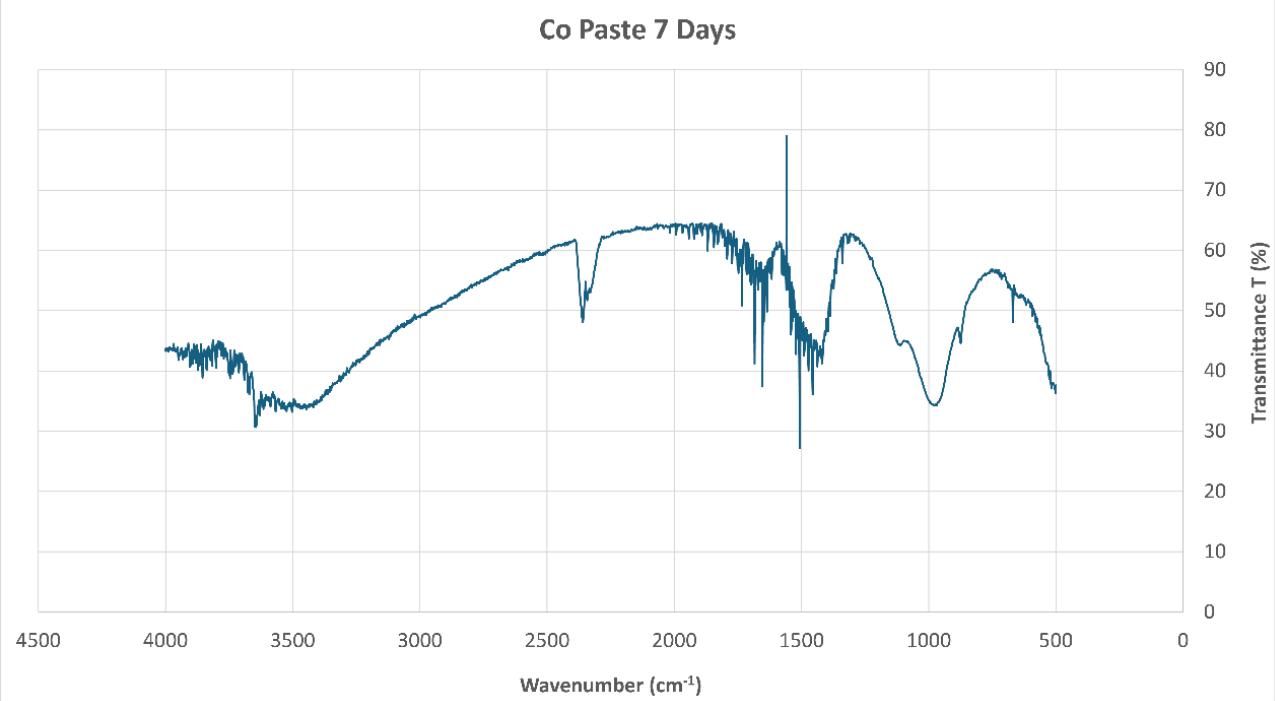

Figure 5.38 - FTIR Spectroscopy Result for the Co Paste Sample after 7 Days Curing

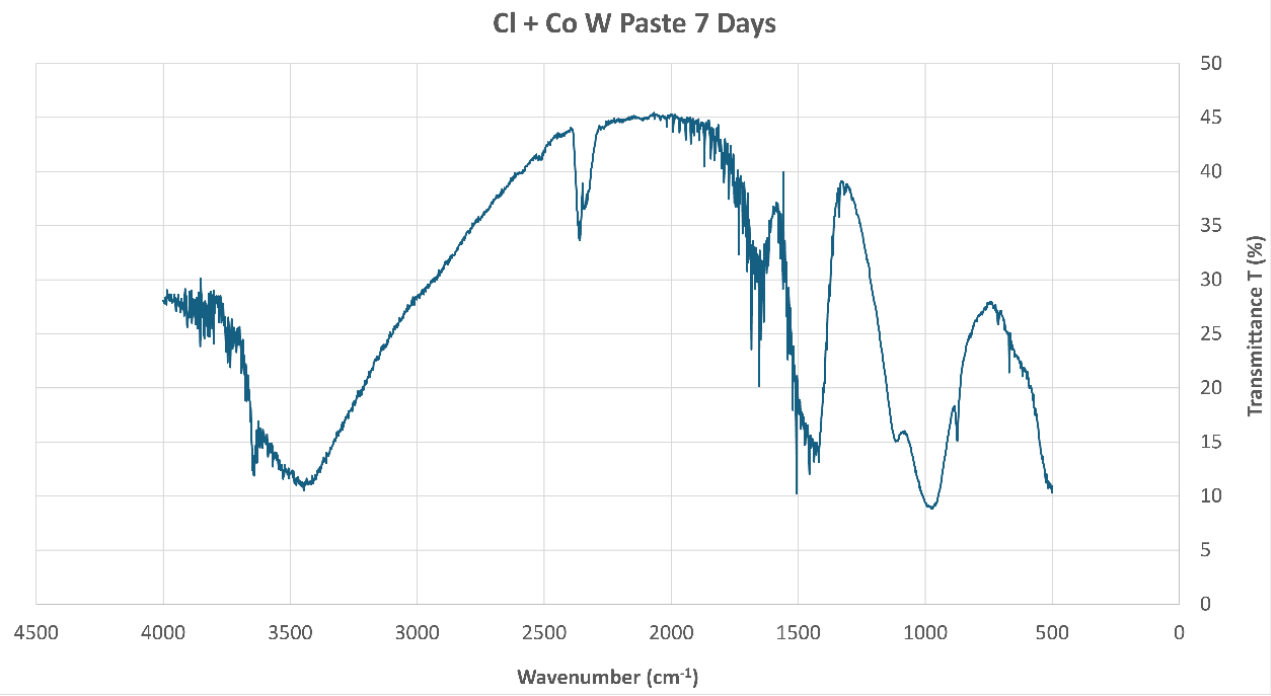

Figure 5.39 - FTIR Spectroscopy Result for the Cl + Co W Paste Sample after 7 Days Curing

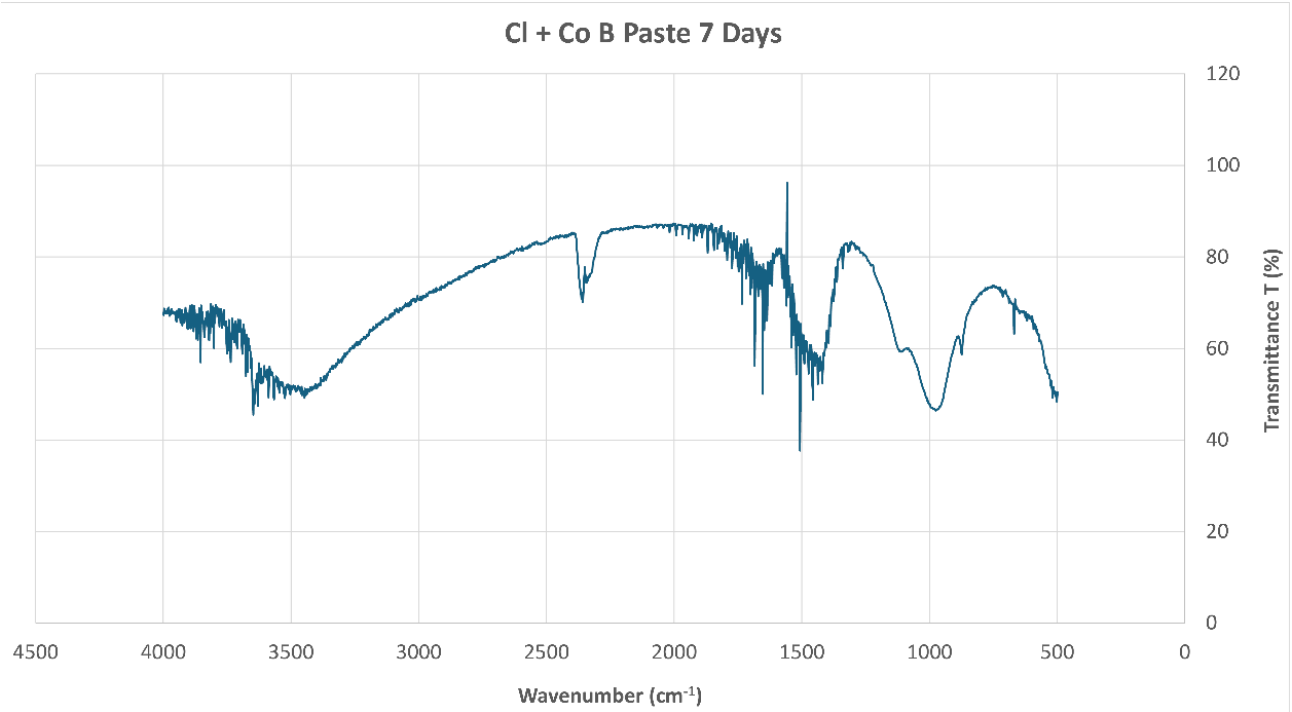

Figure 5.40 - FTIR Spectroscopy Result for the Cl + Co B Paste Sample after 7 Days Curing

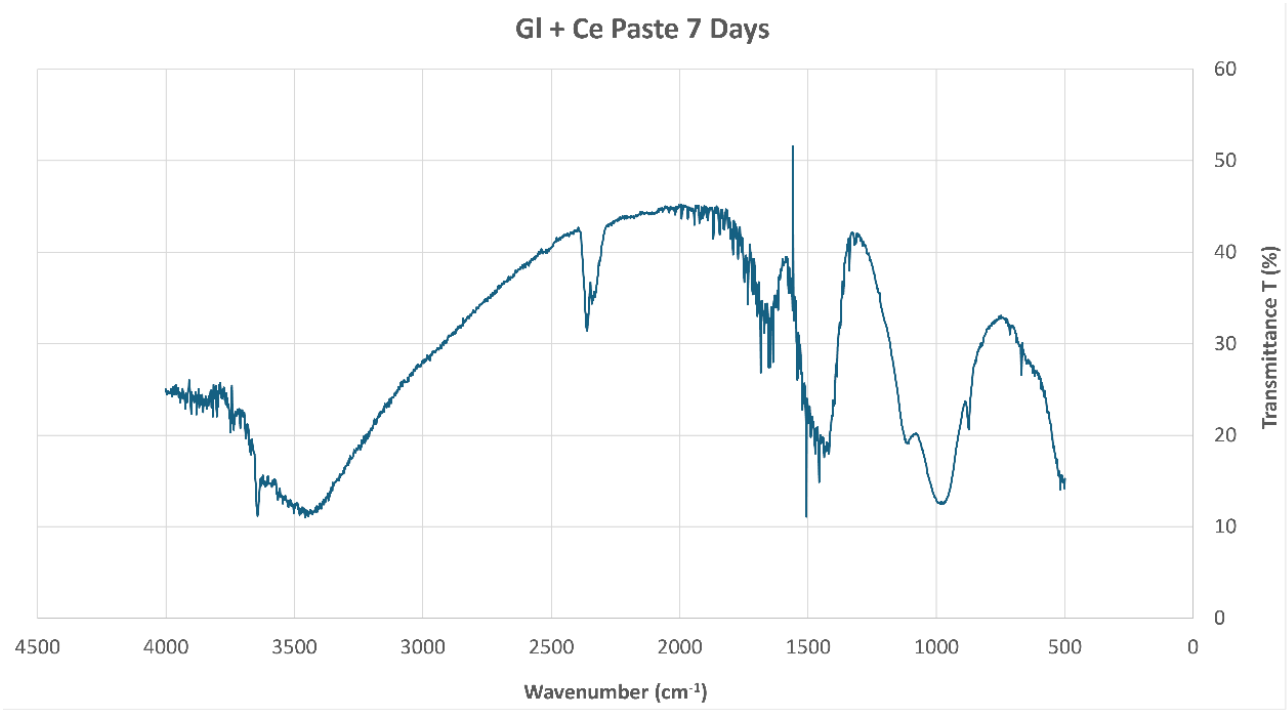

Figure 5.41 - FTIR Spectroscopy Result for the Gl + Ce Paste Sample after 7 Days Curing

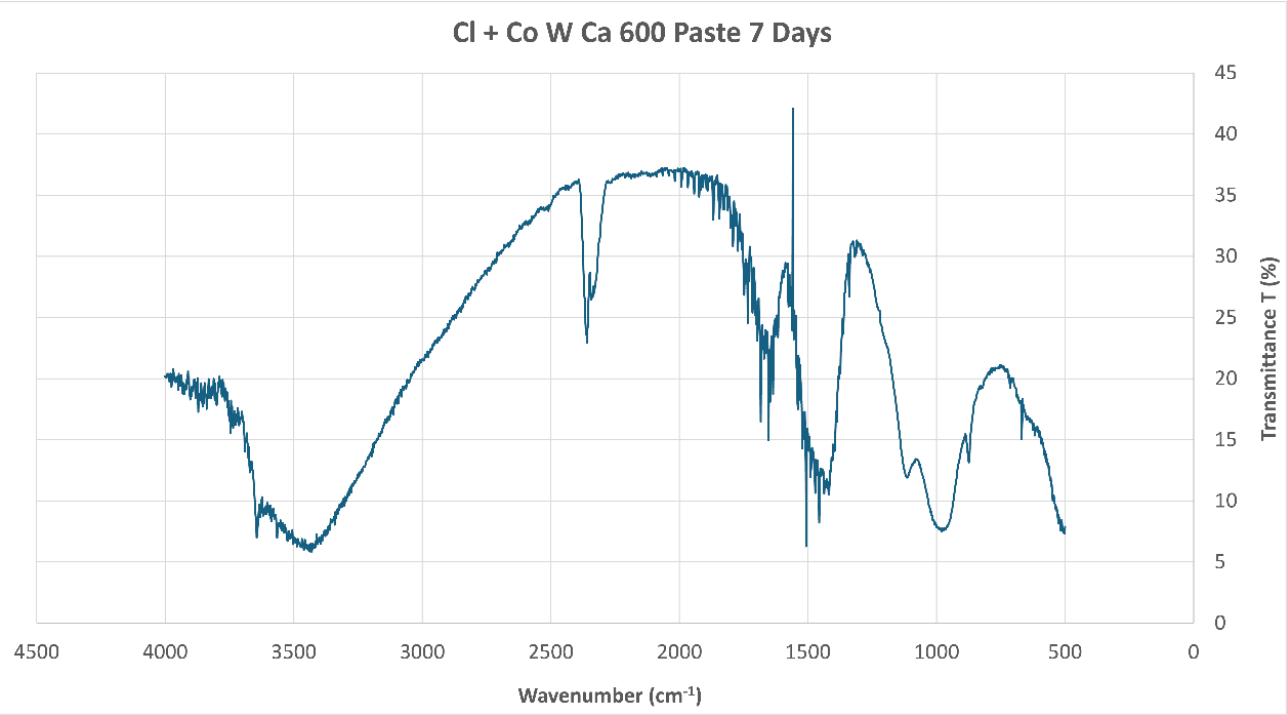

Figure 5.42 - FTIR Spectroscopy Result for the Cl + Co W Ca 600 paste Sample after 7 Days Curing

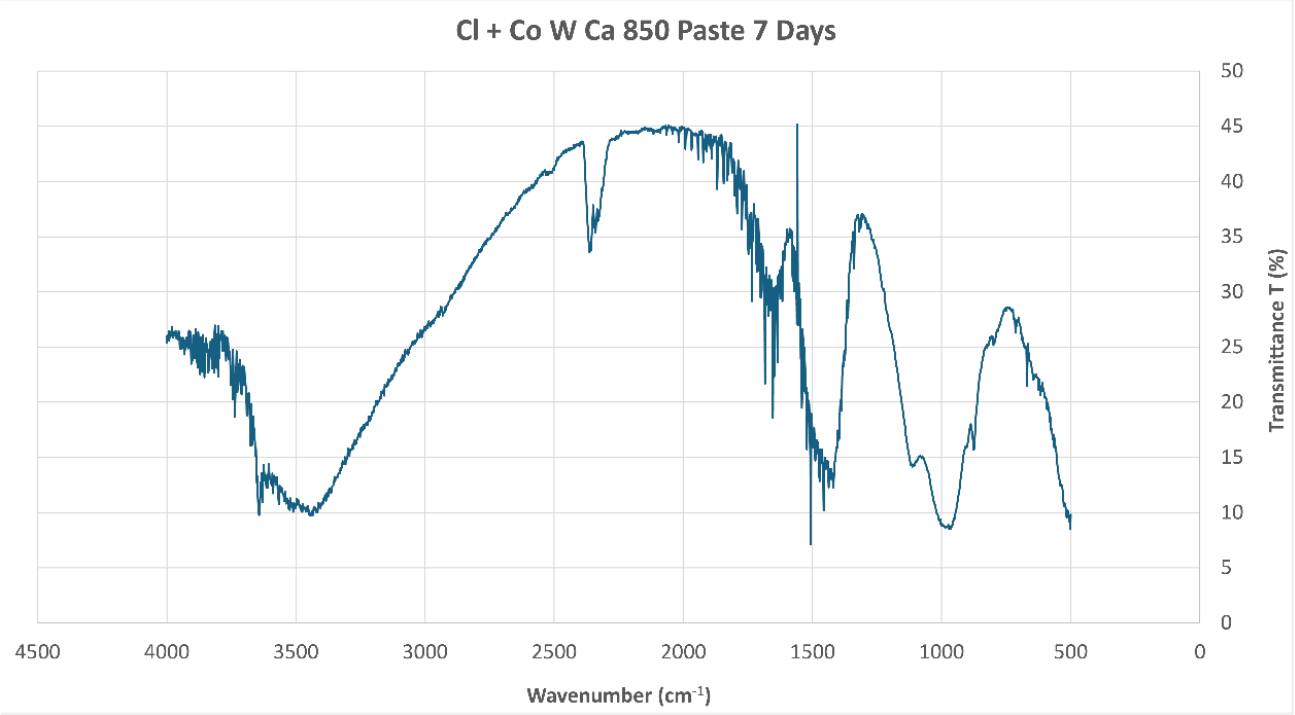

Figure 5.43 - FTIR Spectroscopy Result for the Cl + Co W Ca 850 Sample after 7 Days Curing

Wavenumber in sample (cm^{-1})			
	$Ca(OH)_2$ Region	**C–S–H Gel Region**	**Carbonation Region**
	3600 – 3650 cm^{-1}	**950 – 1350 cm^{-1}**	**1400 – 1500 cm^{-1}**
Cem Con	3622 (peak) 3643 (drop)	974 (drop) 1072 (peak)	1437 (drop)
Cl	3630 (peak) 3644 (drop)	977 (drop) 1082 (peak) 1117 (drop)	1418 (drop)
Co	3624 (peak) 3645 (drop)	968 (drop) 1111 (drop)	1456 (drop)
Cl + Co W	3626 (peak) 3642 (drop)	972 (drop) 1078 (peak) 1107 (drop)	1419 (drop)
Cl + Co B	3446 (drop) 3626 (peak) 3647 (drop)	975 (drop) 1116 (drop) 1305 (peak)	1419 (drop)
Gl + Ce	3605 (peak) 3644 (drop)	979 (drop) 1072 (peak) 1107 (drop)	1456 (drop)
Cl + Co W Ca 600	3624 (peak) 3643 (drop)	979 (drop) 1070 (peak) 1115 (drop)	1417 (drop)
Cl + Co W Ca 850	3641 (drop)	964 (drop) 1306 (peak)	1419 (drop)

Table 5.25 – Wavenumbers in FTIR Graphs for Paste Samples

The presence of a high amount of portlandite indicates that mild pozzolanic activity is occurring since the portlandite is not being consumed by the pozzolanic reaction. The intensity of the C-S-H gel also yields information regarding pozzolanic activity - the stronger the gel presence, the larger the pozzolanic reactivity. Moreover, FTIR gives information on the carbonation reaction that occurs between atmospheric CO_2 and the paste samples.

The following table compares FTIR interpretations of the different samples relative to the cement control paste at 7 days.

	$Ca(OH)_2$ Region	C–S–H Gel Region	Carbonation Region	Interpretation of Reactivity
Cem Con	Moderate Presence	Gel Present	Moderate Carbonation	**Baseline – moderate typical hydration**
Cl	Low Presence	Strong gel	Lower carbonation	**High reactivity – strong pozzolanic reaction**
Co	High Presence	Weaker gel	High carbonation	**Low reactivity – limited $Ca(OH)_2$ use** **The characteristics of Cl & Co are distinct - presence of the colourants Fe_2O_3 and Cr_2O_3**
Cl + Co B	High Presence	Moderate gel	High carbonation	**Low reactivity – limited $Ca(OH)_2$ use** **Presence of organic impurities interfering with the pozzolanic reaction**
Gl + Ce	Low Presence	Strong Gel	Moderate Carbonation	**High reactivity – strong pozzolanic reaction**
Cl + Co W Ca 600	Very Low Presence	Strong Gel	Moderate Carbonation	**High reactivity due to calcination – strong pozzolanic reaction** **More reactive silica due to calcination that did NOT cause significant structural changes**
Cl + Co W Ca 850	Very Low Presence	Strong Gel	Moderate Carbonation	**High reactivity at the 7-day mark – most complete $Ca(OH)_2$ use** **Due to the devitrification, the long-term outcomes might vary.**

Table 5.26 - FTIR interpretations of the different samples relative to the cement control paste at 7 days

5.2.2.8 COMPARING RESULTS FROM DIFFERENT TESTS

The calorimetry results can be linked to the XRD results and offer insight on strength. The results and interpretations are shown below in *Table 5.27*:

PASTE SAMPLES				
	Delayed Heat Peak	**CH Consumption (XRD)**	**21-Day Strength (MPa)**	**Interpretation**
Cem Con	No	High CH (baseline)	91.51	Strong early and late hydration
Cl + Co W	Yes (~13–23h)	Moderate CH reduction	93.20	Effective SCM behaviour, slower early kinetics
Cl + Co B	Yes (~13–23h)	Moderate CH reduction + crystalline phase	**96.63**	Excellent long-term strength
Cl + Co W Ca 600	Yes (~13–23h)	Low CH, strong C-S-H	**108.08**	Best performance; delayed but intense long-term hydration

Table 5.27 – Comparing Isothermal Calorimetry Results with XRD Results for Paste Samples

In summary, all three glass waste paste mixes delay early hydration, but show strong secondary reactions that are consistent with pozzolanic glass reactivity. However, Cl + Co W Ca 600 exhibits the most favourable delayed broad peak indicating a highly beneficial pozzolanic profile. Despite slightly lower heat evolution, all the SCM paste mixes produce equal or better 21-day strength, validating their latent hydraulic or pozzolanic nature. Yet again, long-term analysis as well as energy-performance trade-off must be considered for heat treatment especially if the processes were to be scaled to industrial levels.

More comparisons can be made from results obtained from XRD and compressive strength testing. These are shown in *Table 5.28* below.

STRENGTH VS. XRD-BASED REACTIVITY						
	CH Peak Intensity based on XRD	**C-S-H Presence from XRD**	**7-Day Strength (MPa)**	**21-Day Strength (MPa)**	**Strength Change (MPa)**	**Interpretation**
Cem Con	High CH (Baseline)	Moderate (Baseline)	68.93	91.51	+22.58	Full cement hydration (Baseline)
Cl	Reduced CH	High	84.05	86.42	+2.37	Fast early pozzolanic reaction that slows down with time
Co	Reduced CH	High	80.62	85.58	+4.96	Fast early pozzolanic reaction that slows down with time
Cl + Co W	Moderate CH	High	76.79	93.20	+16.41	Balanced pozzolanic activity. Clean glass helps hydration.
Cl + Co B	Moderate CH	High	72.00	96.63	+24.63	Contaminants are seen in XRD. High late strength potentially from filler effect
Gl + Ce	Low CH	Higher	51.03	98.06	+47.03	Delayed but significant pozzolanic reaction yielding high 21-day strength
Cl + Co W Ca 600	Medium - Low CH	Higher	74.42	108.08	+34.38	Most reactive overall – calcination at 600^{o}C seems to optimise reactivity. Excellent strength at 7 & 21 days
Cl + Co W Ca 850	Moderate CH	High	80.08	101.04	+20.96	High early strength with a slight drop in reactivity likely due to the devitrification that occurred when heating at 850^{o}C

Table 5.28 – Comparing Compressive Strength and XRD Results for Paste Samples

It can be concluded that Cl + Co W Ca 600 is the optimal sample in terms of reactivity and strength as it shows the best long-term strength and portlandite consumption. This is due to optimised pozzolanic reactivity.

As previously mentioned, the pozzolanic reaction decreases the amount of portlandite (CH) present and, in turn, increases the presence of C-S-H. Cl, Co and Gl + Ce showed the best CH reduction.

The higher C-S-H peaks in Gl + Ce and Cl + Co W Ca 600 correspond to the largest positive strength development with an increase of 47.03 MPa and 34.38 MPA respectively.

The compressive strength of Cl + Co B and Cl + Co W Ca 850 are most likely due to a filler and packing effect caused by the presence of contaminants and quartz from devitrification respectively.

5.3 MORTAR TESTING RESULTS

5.3.1 FRESH PROPERTY TESTING RESULTS ON MORTAR MIX

5.3.1.1 FLOW TABLE TEST RESULTS

The results obtained from the Flow Table Test that give information on the workability of the mortar mix are shown below.

MORTAR SAMPLES					
	Diameter 1 (mm)	**Diameter 2 (mm)**	**Mean Diameter (mm)**	**Deviation from Mean Diameter 1 (%)**	**Deviation from Mean Diameter 2 (%)**
Cem Con	195.79	196.97	196.38	0.30	-0.30
Cl + Co W	206.97	204.23	205.60	-0.67	0.67
Cl + Co B	199.06	195.84	197.45	-0.82	0.82
Cl + Co W Ca 600	211.11	213.80	212.45	0.63	-0.63

Table 5.29 – Densities of Mortar Samples obtained from Flow Table Test

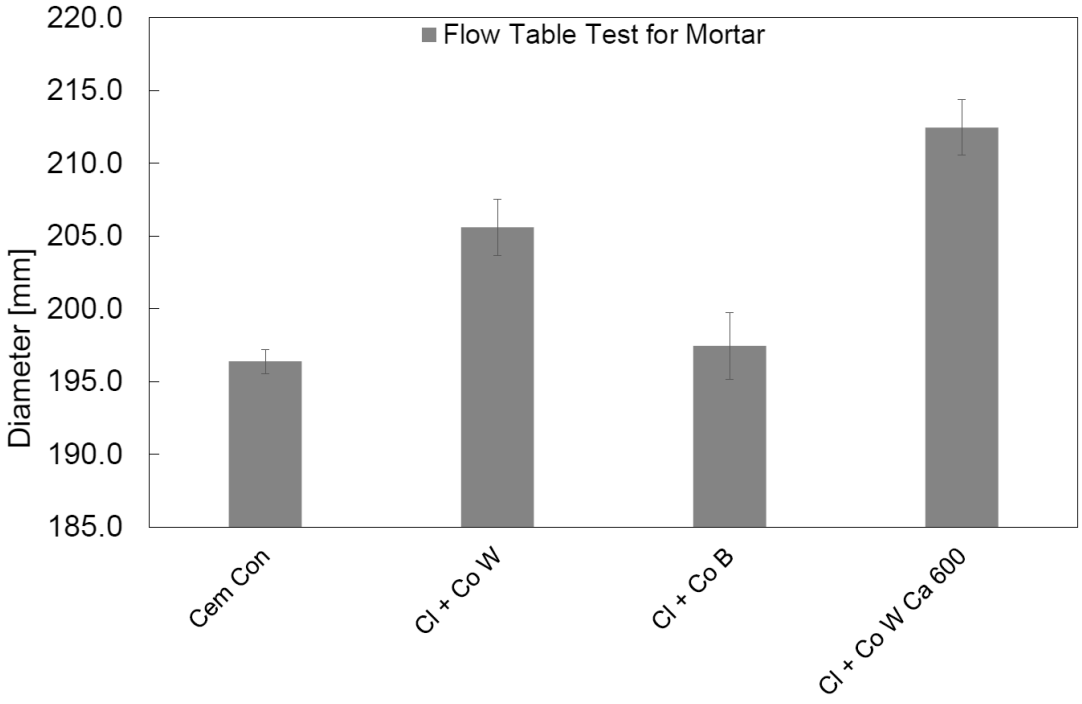

Figure 5.44 – Bar Graph comparing the Diameters of the Mortar Samples from the Flow Table Test

Cem Con has the lowest value for workability. Cl + Co B showed no significant difference when compared to Cem Con. On the other hand, an increase in workability was seen in Cl + Co W and Cl + Co W Ca 600. These results together with the plausible explanation are comparable with the mini cone flow table test results for the paste mixtures which were previously discussed in Section 5.2.1.1.

5.3.2 HARDENED PROPERTY TESTING RESULTS OF THE MORTAR MIX

5.3.2.1 DENSITY TEST RESULTS FOR MORTAR SAMPLES

The values for the density of the mortar cubes obtained at 7 days and at 21 days *(see Appendix 8)* are represented in the bar graph below.

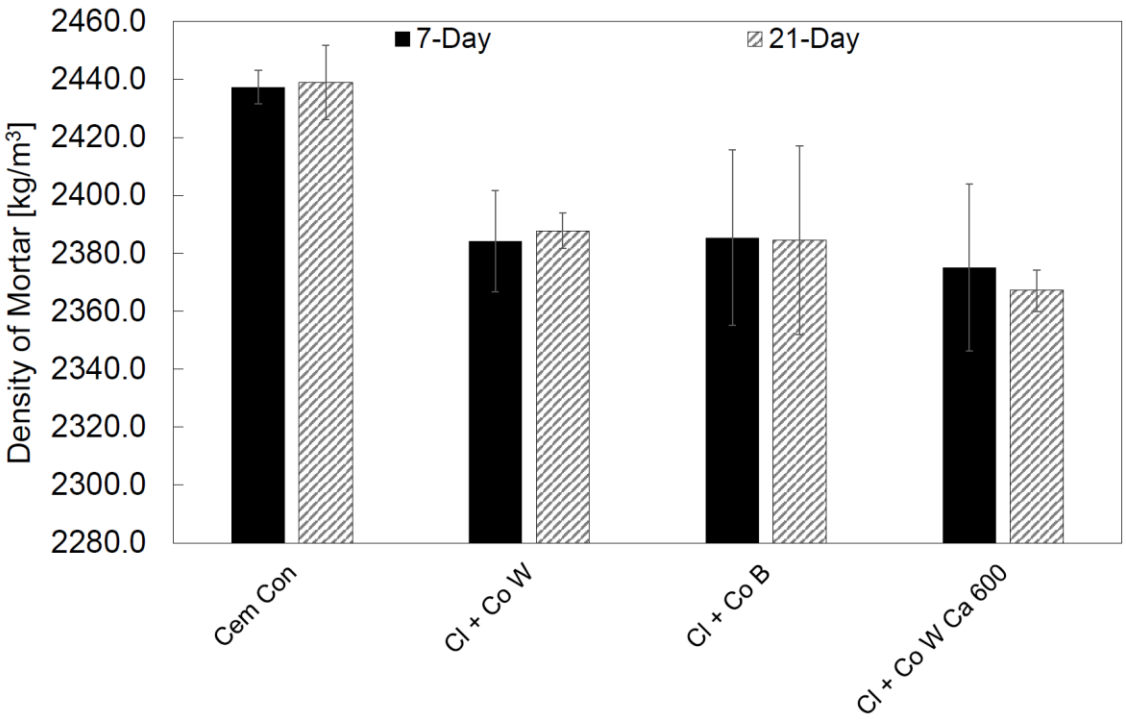

Figure 5.45– Bar Graph comparing the densities of Mortar samples after 7-Day & 21-Day Curing

As seen with the paste samples, the density of the mortar cubes containing WGP have a lower density than that of cement. As previously explained, this cannot be extrapolated onto the density of the microstructure of the material. In the case of mortar, at 21 days, the Cl + Co W sample exhibited the lowest difference from the cement control.

When comparing the density of the paste and mortar, the density of the mortar cubes is larger than that of the paste for the same sample. This is due to the presence of dolomite sand.

5.3.2.2 VACUUM SATURATION POROSITY TEST RESULTS FOR MORTAR SAMPLES

The values in *Table 5.30* below show the porosity of the samples with time.

MORTAR SAMPLES			
	Average Permeable Porosity that cured for 7 days in a curing tank (%)	**Average Permeable Porosity that cured for 21 days in a curing tank (%)**	**Change in Average Permeable Porosity from 7 to 21 days (%)**
Cem Con	14.93	14.38	- 0.55
Cl + Co W	15.44	15.30	- 0.14
Cl + Co B	15.82	14.96	- 0.86
Cl + Co W Ca 600	16.55	16.01	- 0.54

Table 5.30 – Average Permeability Porosity Results for Mortar Samples

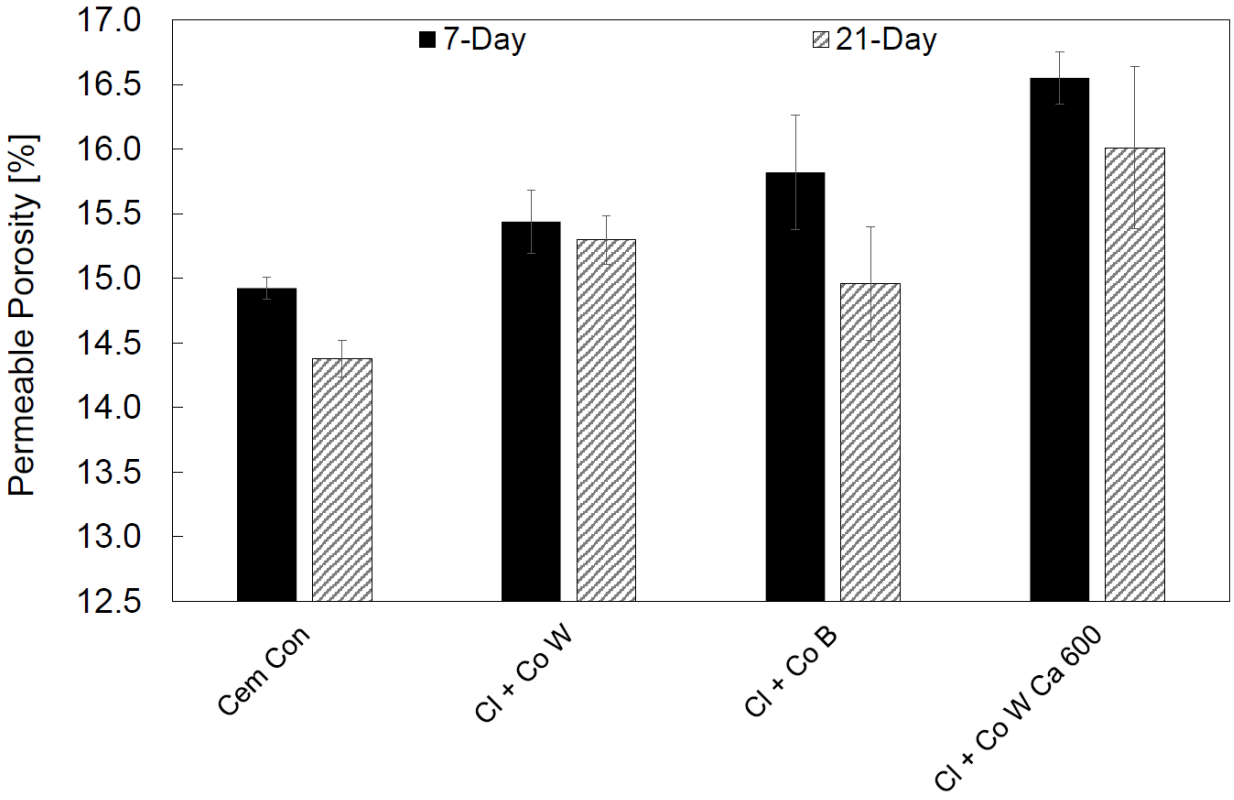

Figure 5.46 – Bar Graph comparing the Permeable Porosity of the different Mortar samples after 7-Day & 21-Day Curing

The porosity values for paste and mortar are different. The paste samples exhibited a larger porosity value than the mortar samples. This is because mortar contains added dolomite sand, the most predominant constituent in the mortar, that changes the porosity properties of the mortar samples. Mortar cubes are also denser due to increased packing.

Out of all the mortar samples containing WGP, Cl + Co B was the least porous. However, the cement control was the least porous out of all samples. This contrasts with the results obtained for the paste samples where Cl + Co W was the least porous out of all the samples including the cement control. The decreased porosity of Cl + Co B is probably due to the presence of contaminants. The microparticles of contaminants could have acted as microfiller in the mortar which resulted in better gradation of the material within the mortar. Organic material present in the WGP also most likely created strong bonds during the hydration reaction leading to a decrease in porosity.

5.3.2.3 SORPTIVITY TEST RESULTS FOR MORTAR SAMPLES

The sorptivity of the samples was measured as for the paste cubes. Graphs of absorption (I) against the square root of time were plotted for 7 and 21 day-samples as shown below.

The mortar cubes that were cured for 7 days yielded the following results:

- At the initial stage of absorption, the cement control had the lowest gradient meaning that it has the lowest sorptivity. The Cl + Co W Ca 600 sample exhibited the highest sorptivity. The sorptivity of the other two samples are almost identical and lie their values lie between the aforementioned samples.
- In the secondary absorption phase, the gradient of the cement control was by far the steepest, meaning that it has the highest sorptivity. All of the samples that contain WGP as an SCM outperformed the control at 7 days. The best result was obtained by Cl + Co W Ca 600.

The mortar cubes that were cured for 21 days, yielded the following results:

- The initial sorptivity is highest for Cl + Co W and lowest for Cl + Co B, performing comparably with the control sample.
- In the secondary phase of absorption, all of the samples, excluding Cl + Co W, performed in the same way. Cl + Co W exhibited superior performance, thus having a lower rate of absorption.

SECONDARY RATE OF ABSORPTION OF MORTAR CUBES		
	Rate of Absorption after 7-Day Curing ($mm/sec^{1/2}$)	**Rate of Absorption after 21-Day Curing ($mm/sec^{1/2}$)**
Cem Con	0.0031	0.0230
Cl + Co W	0.0020	0.0010
Cl + Co B	0.0018	0.0021
Cl + Co W Ca 600	0.0013	0.0022

Table 5.31 – Secondary rates of Absorption of Mortar Cubes after 7-day and 21-day curing

At early ages, Cl + Co W Ca 600 performs better. However, the results differ between 7-day and 21-day curing. Further investigation is warranted for long-term performance of the samples.

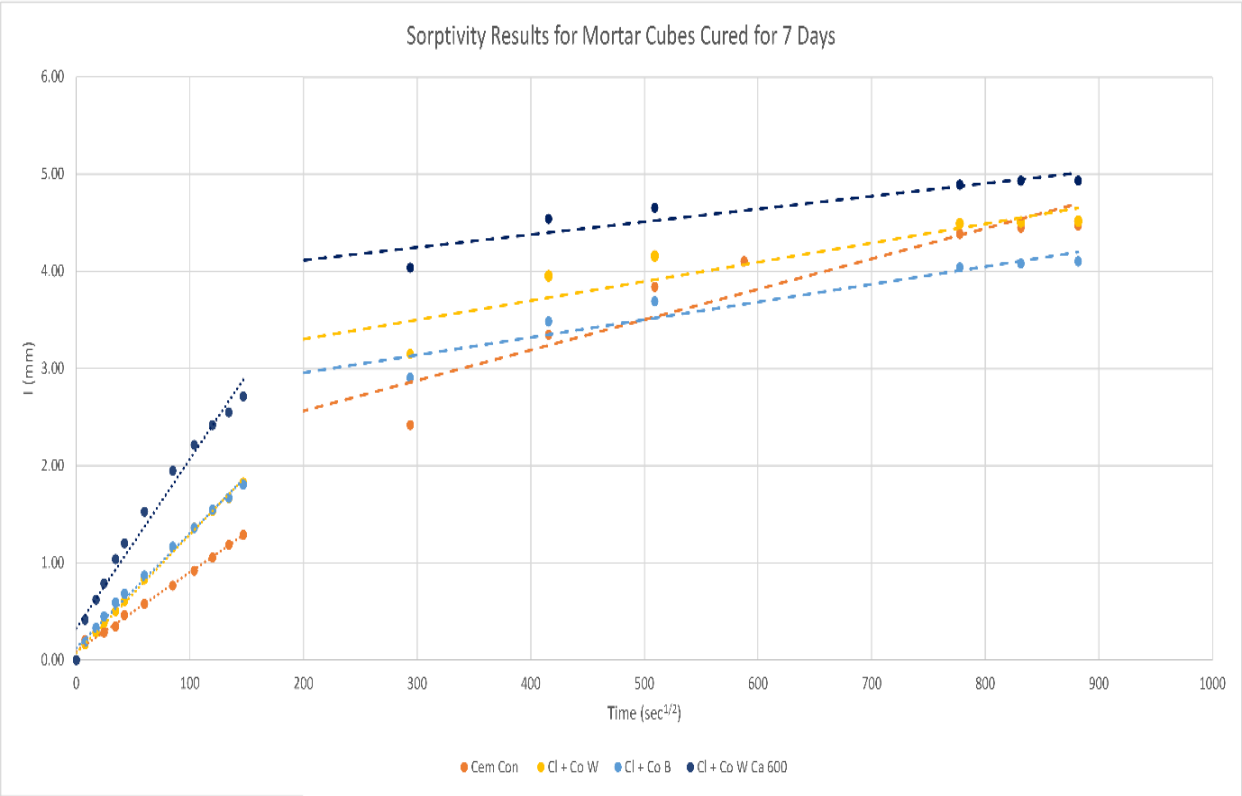

Figure 5.47 – Sorptivity Results for Mortar Cubes cured for 7 days

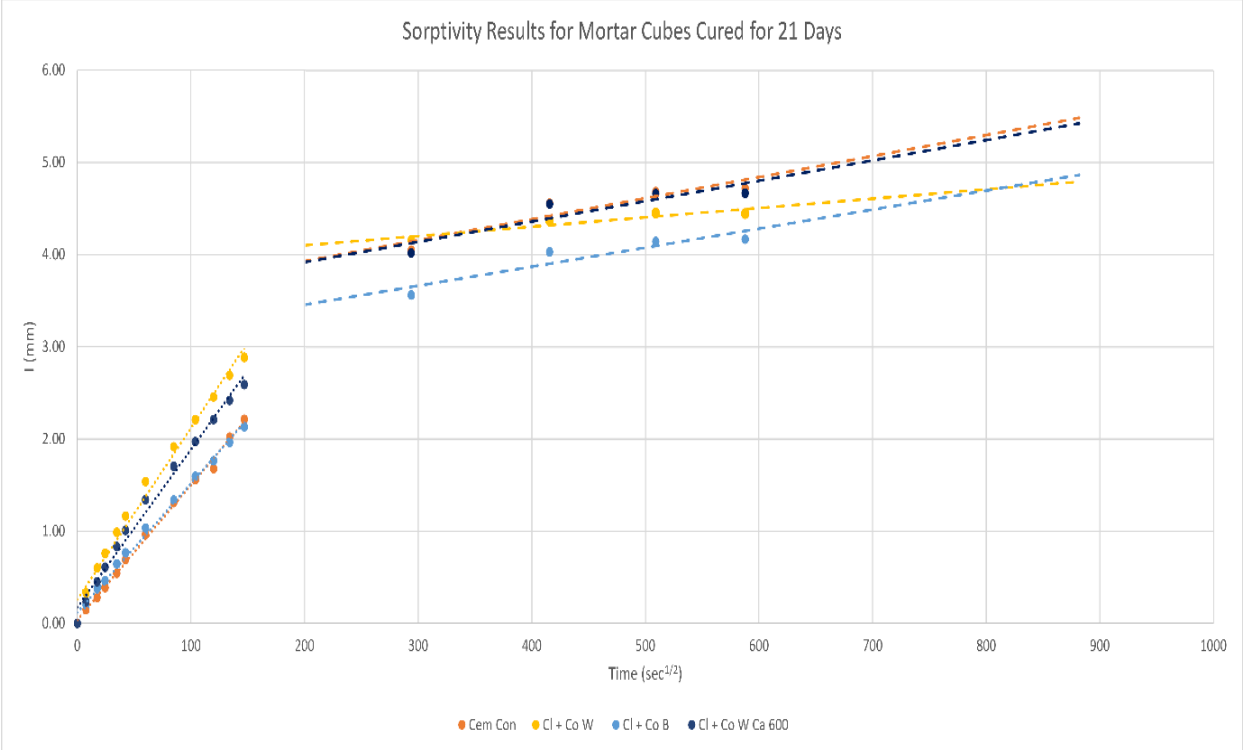

Figure 5.48 – Sorptivity Results for Mortar Cubes cured for 21 days

5.3.2.4 ULTRASONIC PULSE VELOCITY (UPV) RESULTS

Table 5.32 depicts the results obtained:

MORTAR SAMPLES		
	Average Pulse Velocity of Mortar Cubes that have cured for 7 Days (km/s)	**Average Pulse Velocity of Mortar Cubes that have cured for 14 Days (km/s)**
Cem Con	4.44	3.97
Cl + Co W	4.37	4.59
Cl + Co B	4.45	4.15
Cl + Co W Ca 600	4.57	4.33

Table 5.32– UPV Results for Mortar Cubes

As per BS EN 12504-4:2021, ASTM C597-2016 and BIS 13311 – 1:1992, the values for the pulse velocity obtained are mostly between 3.5 and 4.5 km/s, meaning that the concrete has a good quality grading. Two values are above 4.5 km/s which indicate that the concrete has an excellent quality grading.

5.3.2.5 COMPRESSIVE STRENGTH TEST RESULTS

The values obtained from compressive strength testing on the mortar cubes are shown in the table below.

MORTAR SAMPLES				
	Average Compressive Strength at 7 Days (MPa)	**Standard Deviation of Compressive Strengths at 7 Days**	**Average Compressive Strength at 21 Days (MPa)**	**Standard Deviation of Compressive Strengths at 21 Days**
Cem Con	73.11	1.80	74.48	1.44
Cl + Co W	56.56	6.16	65.23	4.77
Cl + Co B	57.01	3.99	72.53	4.69
Cl + Co W Ca 600	57.30	5.59	70.94	3.43

Table 5.33 – Average Compressive Strength Results for Mortar Cubes

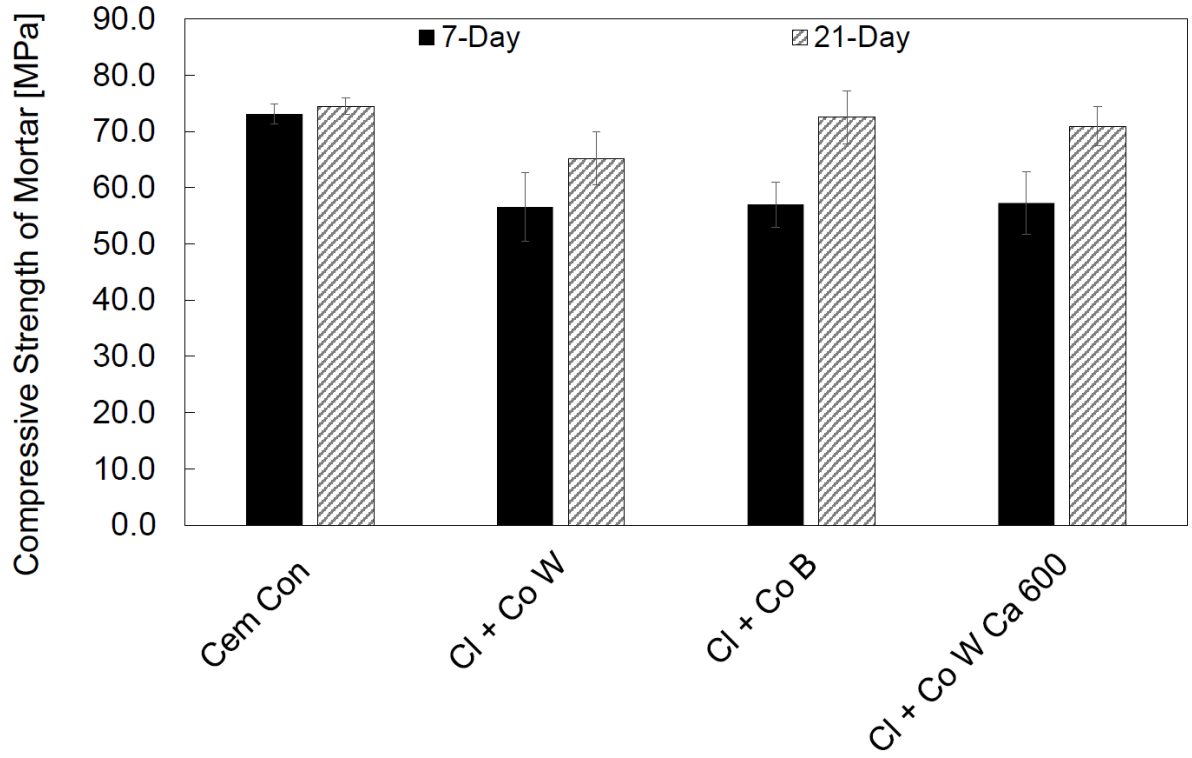

Figure 5.49 – Bar Graph comparing the Compressive Strengths of Mortar Cubes after 7-day & 21-day curing

At 21 days, the compressive strength of Cl + Co B and Cl + Co W Ca 600 are comparable to the control sample of cement. In the case of Cl + Co W Ca 600, this is probably due to the calcination of the material under test. As previously discussed, with regards to Cl + Co B, it is possible that is strength is gained from the filler and packing effect.

In all samples containing WGP, there is a significant increase in compressive strength at 21 days when compared to the 7-day values. This is not seen in the cement control. This is possibly due to the late onset pozzolanic reaction that occurs in the presence of the WGP.

For both the paste and mortar samples, the cement control is showing a small increase in strength but its values at 7 and 21 days are still comparable. On the other hand, the other three (3) samples showed a large improvement in compressive strength from the 7-day mark to the 21-day mark. Thus, it can be concluded that there is a trend of rapid recovery in strength between the 7-day and 21-day strength for paste and mortar samples when compared to the control.

5.3.2.6 ACCELERATED MORTAR BAR TEST FOR ASR RESULTS

The alkali-silica reaction (ASR) is detrimental to the structure of concrete. Thus, it is important that the extent of this reaction is measured. The following are the results for the accelerated mortar bar test used to measure the extent of ASR.

MORTAR SAMPLES			
	Average Length Change after 7 Days in NaOH (%)	**Average Length Change after 14 Days in NaOH (%)**	**Average Length Change after 21 Days in NaOH (%)**
Cem Con	0.0034	0.0051	0.0068
Cl + Co W	0.0136	0.0407	0.0509
Cl + Co B	0.0407	0.0441	0.0475
Cl + Co W Ca 600	0.0170	0.0222	0.0222

Table 5.31 – Accelerated Mortar Bar Test Results for Mortar Samples

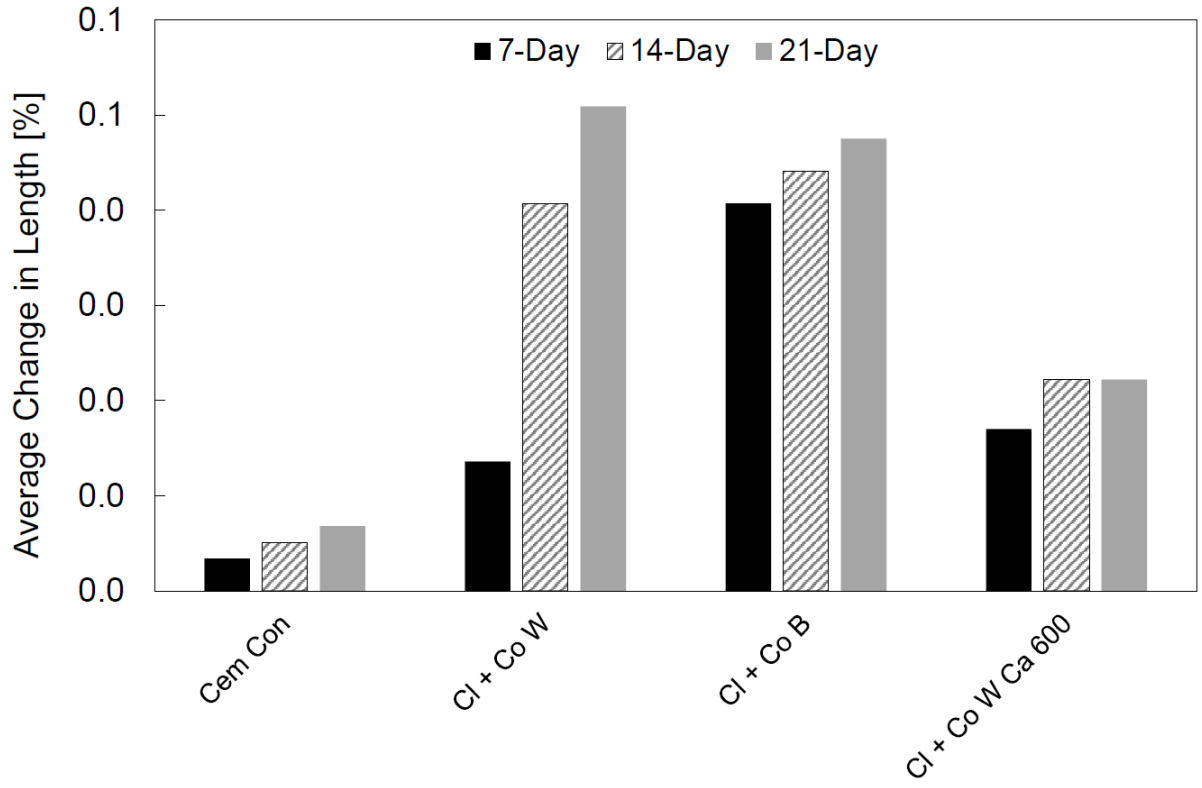

Figure 5.40

According to ASTM C 1260, if the change in length of the bars due to ASR is less than 0.1%, these results are satisfactory, meaning that ASR is not problematic. All values obtained are below 0.1% and so the glass waste powders under test are acting as SCMs. This is due to their sufficiently small particle size which allows the glass to act as an SCM and not as an aggregate.

It is important to note that although all of the values are below the critical limit, the samples that have glass as an SCM have a larger percentage change than the cement control.

5.4 CONCLUDING REMARKS

The trends show that, in both paste and mortar, the different types of glass waste have great potential for long-term use. Since great attention was given during the characterisation tests to establish the ideal parameters of the materials to be used for further experimentation, a good basis for study was set. Different results were observed for paste and mortar samples. This is most likely due to the presence of dolomite sand in mortar that dilutes the effects of contaminants and variations between the glass types. Nonetheless, the trends show promising results in using different types of waste glass as cementitious materials.

CHAPTER 6 – CONCLUSION

The aim of this dissertation was to gain further knowledge on glass waste powder used as an effective supplementary cementitious material in the production of low carbon cement-based materials. The motivation for this research emerged from a need for effective glass waste management and a goal of working towards more sustainable practices in the construction industry. This continued to evolve as gaps in literature were identified. The contributions of this study encompass the understanding of practices in the glass waste cleaning and sorting industry in Malta, the scientific results obtained and their applicability to industry.

This study addresses some sustainable development goals (SDGs) namely goals 8, 9, 12 and 13. The use of glass waste as a binder in industry targets climate action by reducing the carbon footprint of glass waste itself as well as that of the construction industry. This also ensures sustainable and effective use of glass waste instead of recycling it which still poses some negative environmental impacts. Simultaneously, this would be beneficial in building resilient infrastructure in a sustainable manner.

This dissertation sheds light on the global and local impacts that arise when glass waste cannot be tackled at source. When exportation of glass for recycling is required to avoid the dumping of waste glass in landfills for countries which share the same struggles as Malta, glass a liability rather than an asset. Thus, solutions presented that reduce financial losses are welcomed as they simultaneously contribute to a more effective waste management strategy which lessens the carbon footprint.

Valuable information about the glass waste at source has been obtained – its cleanliness, size, amounts, differences and types. In the laboratory research setting, under-researched areas of the research topic have been explored. The aim was to predominantly gain knowledge on the effects of contaminants to the properties of cement-based materials, as well as the effects of heat treatment of the glass itself. Throughout this dissertation, further contributions to other areas of study have been made, such as the outcomes of coloured glass compared to those of clear glass when they are used as binder in cement-based material.

From the laboratory investigations conducted the following conclusions can be drawn:

- For paste samples, the workability of Co, Cl + Co W and Cl + Co W Ca 600 was higher than the control sample. The workability of Cl, Cl + Co B, Gl + Ce and Cl + Co W Ca 850 was similar to that of the control. For mortar samples, the workability the results obtained were comparable to those of the paste.
    - The increase in workability could be attributed to the texture and inherent non-absorbent nature of the waste glass powder.
    - The presence of impurities in absorb water from the mix counteracting these effects.
    - Larger particle sizes than that of cement might have acted more like a fine aggregate causing friction and in turn reducing workability.

- The pozzolanic reactivity as determined by isothermal calorimetry varied slightly for the glass types under test. Cl + Co W Ca 600 exhibited sustained reactivity when compared to the others under test.

- The porosity of paste samples is higher and that of the mortar samples. This may be attributed to the filler effect contributed by the dolomite sand.
    - When compared to the control, a reduction in porosity of the majority of the paste samples containing WGP was seen at 21 days. Cl + Co W had the lowest porosity out of all the paste samples.
    - With regards to mortar, Cl + Co B exhibited the lowest porosity out of all the WGP samples at 21 days but its porosity was still higher than that of the control sample.
    - Further investigation is warranted considering later curing dates to establish a better understanding of long-term results.

- For paste samples, it could be seen that Cl + Co W Ca 600 and Gl + Ce had the lowest rates of absorption at later stages. They outperformed the cement control due to the glass acting as an effective pozzolan. With regards to the mortar samples, the 7-day results for the secondary rate of absorption showed Cl + Co W Ca 600 to be superior to the rest with the other WGP mortars still outperforming the control sample. At later stages, the WGP samples still exhibited decreased sorptivity when compared to the control. It can also be said the calcining of the glass has good potential in the long term.

- The vast majority of the paste samples yielded better compressive strength when compared to the control at 21 days. The highest compressive strength was achieved by Cl + Co W Ca 600. The data suggests that thermal activation at suitable temperatures improves the compressive strength and the overall performance of the material. Less radical discrepancies could be seen between the WGP mortar samples. The results show the positive effect of the pozzolanic reaction with time. The majority of the mortar samples had comparable compressive strengths at 21 days. The variation in results for paste and mortar are likely attributed to the addition of dolomite sand.

- The accelerated mortar bar test proved that the alkali-silica reaction is not deleterious for the WGP samples due to the size of the waste glass particles.

- When analysing the XRD results with the compressive strength, it can be concluded that Cl, Co and Cl + Co W Ca 850 exhibit early strength developments but are not as reactive over time. On the other hand, Cl + Co W Ca 600 and Gl + Ce have greater potential in the long term. Contamination of the glass waste can prove to be a viable option in the construction industry especially when the effect of contamination is reduced when aggregate is introduced. Overall, Cl + Co W Ca 600 so far is deemed to be optimal choice with regards to its properties. Long term results would also need to be considered to determine whether the benefits of the improved properties of calcination outweigh the disadvantages of the carbon footprint of the thermal treatment.

Results from the study showed a consistent trend where all the different variations of the waste glass collected from the BCRS Ltd. and WasterServ Malta Ltd., when used as a binder, show promising pozzolanic activity. The long-term outcomes need to be studied further for definitive conclusions. However, the trends already show that partial cement replacement with waste glass are likely to produce cement-based materials that maintain the strength and durability of traditional materials with cement clinker and may even have the potential to exceed it as observed with the paste samples. Cl, Co and Cl + Co W Ca 850 have exhibited superior early strength development. The strength of Cl + Co B indicates that this material can be a viable alternative in blended systems. The reject Gl + Ce and the heat-activated Cl + Co W Ca 600 show excellent long-term performance and durability within the time-frame of testing.

Future studies might target the following aspects:

- The degree and type of contamination can be quantified experimentally to further characterise the glass waste. This would improve the technical depth and industrial relevance of the study.
- Even though emphasis on very small particle size has been made throughout the dissertation, studies with different durations of the grinding process could be carried out to assess whether prolonged grinding provides a significant improvement in pozzolanic activity or whether comparable effectiveness can be attained through shorter grinding times. An energy-time-performance analysis can be produced to determine optimal grinding durations.
- Late-stage behaviour of the samples under test could be further studied to determine long-term effects.
- The experimentation that was carried out in this study can also be carried out on concrete samples to further mimic the construction industry.
- From the analysis of the results obtained in this study, the waste glass heat-treated at 600^{o}C showed superior performance in certain categories. Thus, with regards to heat treatment of Cl + Co W Ca 600, an energy-performance trade-off can be carried out to thoroughly assess whether this process is advantageous when energy consumption is compared with concrete performance of the material. Moreover, this would help assess the feasibility of scaling the process to industrial levels.
- To further investigate the effects of thermal activation of waste glass powder, it would be beneficial to conduct tests on the chosen material utilising different temperatures other than the ones used in this study. Moreover, heat treatment of glass waste with contaminant can also be explored.
- A life cycle analysis, comparing traditional building materials to that of the low carbon concrete produced using waste glass powder, could be conducted to have a more in-depth environmental impact assessment.

References & Bibliography

Aliabdo, A. A., Abd Elmoaty, A. E. M., & Aboshama, A. Y. (2016). Utilization of waste glass powder in the production of cement and concrete. Construction and Building Materials, 124, 866–877. https://doi.org/10.1016/j.conbuildmat.2016.08.016

ASTM C 597-2016 Standard Test Method for Pulse Velocity through Concrete

ASTM C 1585-04 Standard Test Method for Measurement of Rate of Absorption of Water by Hydraulic-Cement Concretes

ASTM C 1679-14 Standard Practice for Measuring Hydration Kinetics of Hydraulic Cementitious Mixtures Using Isothermal Calorimetry

ASTM C 1702 – 15b Standard Test Method for Measurement of Heat of Hydration of Hydraulic Cementitious Materials Using Isothermal Conduction Calorimetry

ASTM C1260 – 23 Standard Test Method for Potential Alkali Reactivity of Aggregates (Mortar-Bar Method)

ASTM C490/C490M – 11 Standard Practice for Use of Apparatus for the Determination of Length Change of Hardened Cement Paste, Mortar, and Concrete

ASTM C618 – 12a - Standard Specification for Coal Fly Ash and Raw or Calcined Natural Pozzolan for Use in Concrete

Automated Glass Sorting Line | WasteServ Malta. (2020). Wsm.com.mt. https://www.wsm.com.mt/en/san-antnin-plant#gsc.tab=0

Bahr, B. (2024). Thermal Activation - (Organic Chemistry). https://library.fiveable.me/key-terms/organic-chem/thermal-activation

Baikerikar, A., Mudalgi, S., & Ram, V. V. (2023). Utilization of waste glass powder and waste glass sand in the production of Eco-Friendly concrete. Construction and Building Materials, 377, 131078. https://doi.org/10.1016/j.conbuildmat.2023.131078

BCRS Malta Ltd. (2021, June 16). BCRS Malta Ltd. https://bcrsmalta.mt/about-us/

BCRS Malta Ltd. (2024, October 17). BCRS Malta Ltd. https://bcrsmalta.mt/faqs/#el-f5667cb5

Bhardwaj, B., & Kumar, P. (2019). Comparative study of geopolymer and alkali activated slag concrete comprising waste foundry sand. Construction and Building Materials, 209, 555–565. https://doi.org/10.1016/j.conbuildmat.2019.03.107

BIS 13311 – 1:1992 Non-Destructive Testing of Concrete – Methods of Test Part 1 Ultrasonic Pulse Velocity

Bouchikhi, A., Mamindy-Pajany, Y., Maherzi, W., Albert-Mercier, C., El- Moueden, H. et al. (2023). Use of residual waste glass in an alkali-activated binder – Structural characterization, environmental leaching behaviour and comparison of reactivity. https://hal.science/hal-03360292

BS EN 1015-3:1999 Methods of test for mortar for masonry - Determination of consistence of fresh mortar (by flow table)

BS EN 12504-4:2021 Testing Concrete in Structures Part 4: Determination of Ultrasonic Pulse Velocity

BS EN 196-1:2005 Methods of testing cement – Part 1: Determination of strength

BS EN 196-6 :2010 Methods of testing cement - Determination of fineness

BS EN 197-1:2011 Cement Part 1: Composition, specifications and conformity criteria for common cements

BS EN 450-1:2005 -Fly ash for concrete – Part 1: Definition, specifications and conformity criteria

CE Malta. (2025, June 19). CE Malta. https://www.cemalta.gov.mt/about/

Chen, X., Zhang, D., Cheng, S., Xu, X., Zhao, C., Wang, X., Wu, Q., & Bai, X. (2022). Sustainable reuse of ceramic waste powder as a supplementary cementitious material in recycled aggregate concrete: Mechanical properties, durability and microstructure assessment. Journal of Building Engineering, 52, 104418. https://doi.org/10.1016/j.jobe.2022.104418

CTP Consulting Engineers (2025, June 9). Ras Ħanzir Cargo Facility Project, Malta. CTP Website. https://ctp-llp.com/portfolio-items/ras-hanzir-cargo-facility-project-malta/

Değirmenci, N., Yılmaz, A., & Çakır, Ö.A. (2011). Utilization of waste glass as sand replacement in cement mortar. Balikesir.edu.tr; Natl Inst Science Communication-Niscair. https://acikerisim.balikesir.edu.tr/items/18f00ff7-e3a6-428d-bfeb-62cc66457cc1

Demolition Waste Recycling, 339–354. https://doi.org/10.1016/b978-0-12-819055-5.00017-6

Dhir, R. K., Dyer, T. D., & Tang, M. C. (2009). Alkali-silica reaction in concrete containing glass. Materials and Structures, 42(10), 1451–1462. https://doi.org/10.1617/s11527-008-9465-8

Ding, Y., Dong, H., Cao, M., Pacheco-Torgal, F., & Azevedo, C. (2020). Recycled household ceramic waste in eco-efficient cement: A case study. Advances in Construction and

Directive - 94/62 - EN - EUR-Lex. (2018). Europa.eu. https://eur-lex.europa.eu/eli/dir/1994/62/oj/eng

Dong, W., Li, W., & Tao, Z. (2021). A comprehensive review on performance of cementitious and geopolymeric concretes with recycled waste glass as powder, sand or cullet. Resources, Conservation and Recycling, 172, 105664. https://doi.org/10.1016/j.resconrec.2021.105664

Dyer, T. D., & Dhir, R. K. (2001). Chemical Reactions of Glass Cullet Used as Cement Component. Journal of Materials in Civil Engineering, 13(6), 412–417. https://doi.org/10.1061/(asce)0899-1561(2001)13:6(412)

Gartner, E., & Sui, T. (2018). Alternative cement clinkers. Cement and Concrete Research, 114, 27–39. https://doi.org/10.1016/j.cemconres.2017.02.002

Global Status Report for Buildings and Construction - https://www.unep.org/resources/report/global-status-report-buildings-and-construction

Hamada, H., Alattar, A., Tayeh, B., Yahaya, F., & Thomas, B. (2022). Effect of recycled waste glass on the properties of high-performance concrete: A critical review. Case Studies in Construction Materials. https://doi.org/10.1016/j.cscm.2022.e01149

Hassani, M. S., Matos, J. C., Zhang, Y., & Teixeira, E. R. (2023). Green Concrete with Glass Powder—A Literature Review. Sustainability, 15(20), 14864. https://doi.org/10.3390/su152014864

Ħġieġ Nadif Ħġieġ Riċiklabbli | WasteServ Malta. (2021). Wsm.com.mt. https://www.wsm.com.mt/en/glass-collection#gsc.tab=0

Huang, Y., Bian, Z., Ji, W., Yio, M., Chen, Z., Lu, J.-X., Cheeseman, C., & Poon, C. S. (2024). Production of glass-ceramic aggregates from solid wastes for high-strength and low-shrinkage lightweight mortars. Construction and Building Materials, 416, 135244. https://doi.org/10.1016/j.conbuildmat.2024.135244

Idir, R., Cyr, M., & Tagnit-Hamou, A. (2010). Use of fine glass as ASR inhibitor in glass aggregate mortars. Construction and Building Materials, 24(7), 1309–1312. https://doi.org/10.1016/j.conbuildmat.2009.12.030

Jackson, N., & Dhir, R. K. (1996). Civil Engineering Materials (Fifth Edition). Palgrave. Jochem, L. F., Casagrande, C. A., Onghero, L., Venâncio, C., & Gleize, P. J. P. (2021). Effect of partial replacement of the cement by glass waste on cementitious pastes. Construction and Building Materials, 273, 121704. https://doi.org/10.1016/j.conbuildmat.2020.121704

Jwaida, Z., Dulaimi, A., & Bernardo, L.F.A. (2024). The Use of Waste Ceramic in Concrete: A Review. CivilEng 2024, 5(2), 482–500. https://doi.org/10.3390/civileng5020024

Karamberi, A., & Moutsatsou, A. (2005). Participation of coloured glass cullet in cementitious materials. Cement and Concrete Composites, 27(2), 319–327. https://doi.org/10.1016/j.cemconcomp.2004.02.021

Khaiyum, M. Z., Sarker, S., & Kabir, G. (2023). Evaluation of Carbon Emission Factors in the Cement Industry: An Emerging Economy Context. https://doi.org/10.3390/su152115407

Khan, Md. N. N., Saha, A. K., & Sarker, P. K. (2020). Reuse of waste glass as a supplementary binder and aggregate for sustainable cement-based construction materials: A review. Journal of Building Engineering, 28, 101052. https://doi.org/10.1016/j.jobe.2019.101052

Khmiri, A., Chaabouni, M., & Samet, B. (2013). Chemical behaviour of ground waste glass when used as partial cement replacement in mortars. Construction and Building Materials, 44, 74–80. https://doi.org/10.1016/j.conbuildmat.2013.02.040

Kopp Glass, Inc. (2015). 3 Common Glass Types: Properties and Applications. https://www.koppglass.com/blog/3-common-glass-types-properties-and-applications

Kumari, S., Agarwal, S., & Khan, S. (2022). Micro/nano glass pollution as an emerging pollutant in near future. Journal of Hazardous Materials Advances, 6, 100063. https://doi.org/10.1016/j.hazadv.2022.100063

Laveglia, A., Trezza, M. A., & Rahhal, V. F. (2020). Does the colour of the waste glass affect their efficiency as supplementary cementitious material? International Journal of Construction Management, 22(7), 1–11. https://doi.org/10.1080/15623599.2020.1842959,

Li, L., Liu, W., You, Q., Chen, M., & Zeng, Q. (2020). Waste ceramic powder as a pozzolanic supplementary filler of cement for developing sustainable building materials. Journal of Cleaner Production, 259, 120853. https://doi.org/10.1016/j.jclepro.2020.120853

Lin, Y., Kuo, S. F., Hsiao, C., & Lai, C. P. (2007). Investigation of Pulse Velocity-Strength Relationship of Hardened Concrete. ACI Materials Journal, 104(4), 334–350. https://doi.org/10.14359/18823

Lu, J.-X., & Poon, C. S. (2018). Use of waste glass in alkali activated cement mortar. Construction and Building Materials, 160, 399–407. https://doi.org/10.1016/j.conbuildmat.2017.11.080

McGraw-Hill. (2003). Dictionary of Scientific and Technical Terms, 6th Edition. McGraw Hill Professional.

Metwally, I. M. (2007). Investigations on the Performance of Concrete Made with Blended Finely Milled Waste Glass. Advances in Structural Engineering, 10(1), 47–53. https://doi.org/10.1260/136943307780150823

Mohajerani, A., Vajna, J., Cheung, T. H. H., Kurmus, H., Arulrajah, A., & Horpibulsuk, S. (2017). Practical recycling applications of crushed waste glass in construction materials: A review. Construction and Building Materials. https://doi.org/10.1016/j.conbuildmat.2017.09.005

Moon, G. D., Oh, S., & Choi, Y. C. (2016). Effects of the physicochemical properties of fly ash on the compressive strength of high-volume fly ash mortar. Construction and Building Materials, 124, 1072–1080. https://doi.org/10.1016/j.conbuildmat.2016.08.148

Nasir, M., Mahmood, A. H., & Bahraq, A. A. (2024). History, recent progress, and future challenges of alkali-activated binders – An overview. Construction and Building Materials. https://doi.org/10.1016/j.conbuildmat.2024.136141

NBR 12653 - Pozzolanic Materials – Requirements

Nehdi, M. L., & Yassine, A. (2020). Mitigating Portland Cement CO2 Emissions Using Alkali-Activated Materials: System Dynamics Model. Materials, 13(20), 4685. https://doi.org/10.3390/ma13204685

Neville, A. M. (2011). Properties of Concrete (Fifth Edition). Pearson Education Limited.

Neville, A. M., & Brooks, J. J. (1987). Concrete Technology (Second Edition). Longman Scientific and Technical.

Pavoine, A., Harbec, D., Chaussadent, T., Tagnit-Hamou, A, & Divet, L. (2014). Impact of Alternative Cementitious Material on Mechanical and Transfer Properties of Concrete. ACI Materials Journal, 111(3), 251–262. https://doi.org/10.14359/51686828

Pereira-de-Oliveira, L. A., Castro-Gomes, J. P., & Santos, P. M. S. (2012). The potential pozzolanic activity of glass and red-clay ceramic waste as cement mortars components. Construction and Building Materials, 31, 197–203. https://doi.org/10.1016/j.conbuildmat.2011.12.110

Poudel, S., Bhetuwal, U., Kharel, P., Khatiwada, S., Diwakar, K.C., Dhital, S., Lamichhane, B., Yadav, S. K., & Suman, S. (2025). Waste Glass as Partial Cement Replacement in Sustainable Concrete: Mechanical and Fresh Properties Review. Buildings, 15(6), 857–857. https://doi.org/10.3390/buildings15060857

Purton, M. (2024, September 13). Cement Is a Big Problem for the environment. Here's How to Make It More Sustainable. World Economic Forum. https://www.weforum.org/stories/2024/09/cement-production-sustainable-concrete-co2-emissions/

Rajabipour, F., Maraghechi, H., & Fischer, G. (2010). Investigating the Alkali-Silica Reaction of Recycled Glass Aggregates in Concrete Materials. Journal of Materials in Civil Engineering, 22(12), 1201–1208. https://doi.org/10.1061/(asce)mt.1943-5533.0000126

Regulation - EU - 2025/40 - EN - EUR-Lex. (2025). Europa.eu. https://eur-lex.europa.eu/legal-content/EN/TXT/?uri=OJ:L_202500040&pk_campaign=todays_OJ&pk_source=EUR-Lex&pk_medium=X&pk_content=Environment&pk_keyword=Regulation

Safiuddin, Md., & Hearn, N. (2005). Comparison of ASTM saturation techniques for measuring the permeable porosity of concrete. Cement and Concrete Research, 35(5), 1008–1013. https://doi.org/10.1016/j.cemconres.2004.09.017

Sales | WasteServ Malta. (2025). Wsm.com.mt. https://www.wsm.com.mt/en/sales#gsc.tab=0

Samarakoon, M. H., Ranjith, P. G., Hui Duan, W., Haque, A., & Chen, B. K. (2021). Extensive use of waste glass in one-part alkali-activated materials: Towards sustainable construction practices. Waste Management, 130, 1–11. https://doi.org/10.1016/j.wasman.2021.04.060

Saud, R. (2024). Exploring the Chemical Composition, Production, and Uses of Glass across Industries. Print) International Journal of Life Sciences Research, 12, 11–18. https://doi.org/10.5281/zenodo.13986382

Shao, Y., Lefort, T., Moras, S., & Rodriguez, D. (2000). Studies on concrete containing ground waste glass. Cement and Concrete Research, 30(1), 91–100. https://doi.org/10.1016/s0008-8846(99)00213-6

Sharifi, Y., Afshoon, I., Firoozjaei, Z., & Momeni, A. (2016). Utilization of Waste Glass Micro-particles in Producing Self-Consolidating Concrete Mixtures. International Journal of Concrete Structures and Materials, 10(3), 337–353. https://doi.org/10.1007/s40069-016-0141-z

Shore-to-Ship. (2024, March). Infastructure Malta. https://www.infrastructuremalta.com/projects/shore-ship

Siddika, A., Hajimohammadi, A., Ferdous, W., & Sahajwalla, V. (2021). Roles of Waste Glass and the Effect of Process Parameters on the Properties of Sustainable Cement and Geopolymer Concrete—A State-of-the-Art Review. Polymers, 13(22), 3935. https://doi.org/10.3390/polym13223935

Siddique, R., & Paulo Cachim. (2018). Waste and supplementary cementitious materials in concrete : characterisation, properties and applications. Woodhead Publishing, An Imprint Of Elsevier. https://www.sciencedirect.com/science/article/abs/pii/B9780081021569000018

Singh, A. (2023). Waste Glass a Supplementary Cementitious Material in Cement Production. International Journal of Technical Research & Science, 8(12), 1–4. https://doi.org/10.30780/ijtrs.v08.i12.001

Soda Lime Glass Melting Point - A Professional Guide for Glassware Industry - DM Glassware. (2024, July 31). Glass Tableware, Glassware Manufacturing Factory in China. https://dmglassware.com/soda-lime-glass-melting-point/

Son, M., Kim, G., Lee, S., Kim, H., & Nam, J. (2024). Investigation of Conditions for Using Mass-Produced Waste Glass as Sustainable Fine Aggregate for Mortar. International Journal of Concrete Structures and Materials, 18(1). https://doi.org/10.1186/s40069-024-00697-6

Sumra, Y., Payam, S., & Zainah, I. (2020). The pH of Cement-based Materials: A Review. Journal of Wuhan University of Technology-Mater. Sci. Ed., 35(5), 908–924. https://doi.org/10.1007/s11595-020-2337-y

Taha, B., & Nounu, G. (2008). Properties of concrete contains mixed colour waste recycled glass as sand and cement replacement. Construction and Building Materials, 22(5), 713–720. https://doi.org/10.1016/j.conbuildmat.2007.01.019

Times of Malta (2024, August 9). Buġibba breakwater project is 70% complete. Times of Malta. https://timesofmalta.com/article/bugibba-breakwater-project-70-complete.1096551

UN Environment Programme (2025). Global Status Report for Buildings and Construction 2024/2025. UNEP - UN Environment Programme. https://www.unep.org/resources/report/global-status-report-buildings-and-construction-20242025

Wang, B., Yan, L., Fu, Q., & Kasal, B. (2021). A Comprehensive Review on Recycled Aggregate and Recycled Aggregate Concrete. Resources, Conservation and Recycling, 171, 105565. https://doi.org/10.1016/j.resconrec.2021.105565

Waste Collection | Wasteserv Malta. (2017). Wsm.com.mt. https://www.wsm.com.mt/statistics/waste_collection.aspx#gsc.tab=0

What we Do | Wasteserv Malta. (2025). Www.wsm.com.mt. https://www.wsm.com.mt/en/about-us

Xiao, R., Ma, Y., Jiang, X., Zhang, M., Zhang, Y., Wang, Y., Huang, B., & He, Q. (2020). Strength, microstructure, efflorescence behavior and environmental impacts of waste glass geopolymers cured at ambient temperature. Journal of Cleaner Production, 252, 119610. https://doi.org/10.1016/j.jclepro.2019.119610

Yang, J., Chen, M., Wang, Z., Yan, X., Xie, G., & Liu, Y. (2023). A novel supplementary cementitious material based on calcined drill cuttings with waste glass to accelerate cement hydration. Materials Chemistry and Physics, 301, 127679. https://doi.org/10.1016/j.matchemphys.2023.127679

Zafar, M.J., Elsayed, H., & Bernardo, E. (2024). Waste Glass Upcycling Supported by Alkali Activation: An Overview. Materials, 17(9), 2169–2169. https://doi.org/10.3390/ma17092169

Zaid, M., Matori, K., Ab, A., Wahab, Z., & Rashid, S. (2017). Effect of sintering on crystallization and structural properties of soda lime silica glass. Science of Sintering, 49(4), 409–417. https://doi.org/10.2298/sos1704409z

Zhang, P., Wang, K., Li, Q., Wang, J., & Ling, Y. (2020). Fabrication and engineering properties of concretes based on geopolymers/alkali-activated binders - A review. Journal of Cleaner Production, 258, 120896. https://doi.org/10.1016/j.jclepro.2020.120896

Zhang, S., Wang, K., Zhang, X., & Jiang, Y. (2023). Preparing new supplementary cementitious materials with co-calcined waste glass-dolomite and environmental assessment. Construction and Building Materials, 389, 131770. https://doi.org/10.1016/j.conbuildmat.2023.131770

Zhao, X., Lu, J.-X., Lv, X., Tian, W., Cyr, M., Tagnit-Hamou, A., & Poon, C. S. (2024). Recycling of contaminated waste glass in ultra-high-performance concrete: Impurities impact. Construction and Building Materials, 437, 136971. https://doi.org/10.1016/j.conbuildmat.2024.136971

APPENDIX 1 – INTERVIEWS CONDUCTED

Consent was given by the interviewees that included the use of and publication thereof of the information given.

APPENDIX 1.1 – INTERVIEW WITH CEO OF CE MALTA

- **Which government entities deal with glass waste?**

WasteServ Malta Ltd. is a government entity that primarily deals with glass waste. Glass is also collected through the **Beverage Container Refund Scheme (BCRS)**, a private non-profit company created through the collaboration of the Malta Beverage Producers Association, the Malta Beverage Importers Association and the Malta Beverage Retailers Association. **Circular Economy (CE) Malta** is the regulator of this BCRS scheme.

- **Are there any Maltese private companies that deal with glass waste or is it solely the government that deal with glass waste?**

BCRS Ltd is a private company that has its own private contractor that handles the glass collected. There are other private companies that collect glass. These deposit the collected glass at WasteServ that then deals with the glass waste.

- **How many tonnes of glass are collected as a whole through all the government entities?**

In 2023, 5000 tonnes of glass waste are collected in Malta.

- **How does Malta compare to foreign countries with regards to glass waste collection as a whole?**

I can give you information regarding the BCRS. The targets set for BCRS have been superseded. Mata is very comparable with foreign countries. The target for BCRS for glass waste collection in 2023 was 75% of the glass containers sold. 80% was collected which was that the target was superseded. This year, 2024, glass collection was 81% in June, and we are expecting that 84% of the glass containers sold will be collected by the end of the year.

- **I know that 100% collection is impossible, but do you think that Malta can even collect more glass waste even though a considerable amount is already being collected?**

Yes, 100% collection is very difficult. However, the BCRS excludes wine, spirit and juice bottles. There might be a scope that these are collected as well in the scheme. This does not mean that this glass is not being collected by WasteServ.

- **In your opinion, are there any other ways or incentives that can increase the amount of glass that is currently being collected?**

    - One way of increasing glass collection is what has been mentioned before – collecting glass beverage bottles that are not included in the BCRS today.
    - The deposit on the glass bottles can differ from one beverage to another because for example a 10c deposit on a beer bottle is a greater incentive than on a whisky bottle which is relatively minimal compared to its price.

- My wish is to reduce glass usage. We need to collect more but need to reduce the use of glass for beverages because the environmental impact created by a glass beverage bottle is big when one considers the very short time it is utilised when drinking a drink.

- **How many tonnes of the collected glass waste can potentially be given to be used in the construction industry?**

This depends on whether all the types of glass waste can be utilised. Since glass is being exported at a cost and so financially it is not feasible (excluding the argument if this is environmentally feasible that the glass waste is being transported to another country to be reused.) If it is proved that all types of gas can be used in the construction industry, there shouldn't be any problem in giving the collected glass to the construction industry. In this way, it can almost be completely reutilised.

- **Where is glass waste stored currently?**

1. **BCRS** have their own plant in Hal Far. Glass is either broken in the collecting machines themselves and it is packed into containers without being cleaned or else glass bottles which are usually collected manually from restaurants are broken in the plant itself and packed in the same way.
2. **WasteServ** has a similar facility. However, they process glass more by breaking it down into smaller pieces than BCRS.

- **What is the cost of glass storage before exportation?**

BCRS ship glass when they have filled up a 2-foot container with broken glass. So, they do not have a large storage capacity. WasteServ have a bigger place where to store the glass waste and they store both glass as it is received as well as processed glass. From experience, one can say that **the biggest cost of glass waste** lies in the **transportation of glass** from the place it is disposed of (RVMs) to the central site using several vehicles going around the country. There is another **cost of transportation overseas**.

- **Is all of the glass waste collected exported overseas?**

All glass waste is transported overseas. To be reused, glass must be melted down - process which is very energy intensive. We do not know of any small private companies in Malta who are doing this except for glass factories like Mdina Glass, Valletta Glass who are processing glass.

- **Is it feasible to dedicate part of the storage facilities for glass waste to its storage for eventual use in the construction industry if my dissertation proposal is adapted to the local climate?**

The probability is that if the glass waste is going to be used in the construction industry, BCRS would want to hand over the glass waste to the construction industry and not store it itself. Thus, a symbiosis needs to be created so that the output of one process becomes the input of another process. If in your experimentation, you would find that lass can replace cement in the manufacture of concrete and this is implemented locally, such a project would only replace a small fraction of the cement demand of the country. In this way, if such a product is created which is commercially a more viable product than cement, the demand for it would increase as it would mean that this would be a cheaper option. If commercially viable, this concrete option would eliminate the storage problem as all collected glass will be utilised almost immediately without the need of storage. A storage facility would come at an additional cost which in my opinion should be avoided.

- Due to SL 549.61, as from 2028 developments of 16 units or more shall be required to reuse, recycle and/or recover construction and demolition waste (CDW) as well as use recycled or reused material. Glass is a component of CDW since buildings have apertures or glass facades. **Are there any envisaged expectations with regards to how many tonnes of glass waste shall be collected from CDW?**

  So far, I do not have any information about this. However, this consideration of yours is very valid.

- **What is the plan of action for glass waste from CDW?**

This can complement the present schemes of glass waste collection. This can also give way to the collection of glass leftovers and cutouts from glass factories. This is a very good concept where all national glass waste is incorporated.

The following are sets of questions directed towards BCRS. Do you mind if I ask you these questions as well so that if you are in a position to answer them, it will be helpful for me?

- **Plastic, metal and glass beverage containers are collected as part BCRS. How many tonnes of glass beverage containers are collected through the BCRS scheme?**
  5000 tonnes

- **What percentage of glass beverages bought are returned through the BCRS scheme**?
  Around 85%

- **What would be the reason why certain containers, that seem to adhere to the scope of the scheme, are not accepted? Reason being the more we collect the better. For example Moscato D'Asti glass bottle of wine (even though it has a 5% alcohol content, has a capacity between 0.1 litres and 3 litres and is non-refillable)**

The probability is that it is classified as wine. Wines and spirits are automatically excluded. But, I will do some research into this.

- **Why are the following not considered in the BCRS scheme? Such as the following:**
  - **Alcoholic beverages exceeding 5% alcohol content (Wines and Spirits)**
  - **Foreign alcoholic beverages that do not exceed 5% alcohol content**
  - **Glass bottles that carry sauces, sundried tomatoes etc**

There are a variety of reasons.

- First of all, one must note that the Maltese Deposit Refund Scheme (DRS) is very similar to DRSs in foreign countries. By the beginning of 2029, the DRS is going to be mandatory in all European countries. Malta has been the 13th country in Europe to introduce the DRS. When it was introduced, the Maltese scheme was modelled on other European schemes and adapted to the Maltese scenario. The DRS requirements for those countries who have not yet introduced the scheme do not include any obligation for the collection of glass waste. This means that Malta is way ahead than other European countries. Having said that this does not mean that these countries have no other obligations for glass waste.

- Wine and spirits glass containers are excluded from DRS in all European countries. This is due to the different sizes and weights of the glass bottles. The machines seem to be designed to handle smaller bottles. Smaller bottles that are not beverage bottles like sauce bottles are more likely to contain contaminants especially if they are not washed by the consumer. The remnants of a beverage in a beverage glass container is very minimal.

This does not exclude the possibility of national targets being extended to such glass bottles.

- **Online, I found the following information:**
  "Used beverage containers collected by Reverse Vending Machines .... arrive at the purposely built BCRS Clearing Centre in Hal Far where they will be sorted according to material type using specialized equipment and packed efficiently to be exported for recycling."

  Are the glass beverage containers cleaned after they are collected or is the waste simply sorted and exported?

  I am asking this question because certain cleaning agents, both mechanical and chemical, they might alter the properties of the concrete.

No, BCRS Ltd does not clean the containers. Glass bottles are not even separated by colour. Green, brown and transparent glass is all mixed together.

WasteServ separates the glass by colour.

- **What is the cost of exportation of the collected glass containers**?

Not answered

- **Is there any other information that can be provided that you think could be useful in aiding my research?**

I think you have covered all aspects. One thing that I encourage you in is – Let's take this to market!

APPENDIX 1.2 – INTERVIEW WITH COO OF BCRS LTD.

Before glass waste from BCRS Ltd was exported to Italy. Nowadays, it is **exported to Turkey**. This company executes the **Deposit Return Scheme (DRS)** which is obligatory for every country in the European Union under EU regulation. A country is exempted from having its DRS only if it demonstrates that it is reaching a 90% collection target. **Malta** is the **first country in the Mediterranean** which has adopted this DRS. The collection and recycling targets have always been exceeded till now, making this scheme adoption a success. At the moment, the company is targeting **to improve user experience and reduce complaints**. This requires more investment but like any business this escalates step by step.

In Malta, from BCRS data, it is estimated that around **300 million glass and plastic bottles and cans** are utilized every year for the consumption of water, energy drinks, beer, squashes, soft drinks. **Only 9% of that 300 million is glass**, which means **27 million glass bottles**. **By weight**, this is equivalent to **50% of the exported tonnage**. This scheme excludes wine and spirit bottles. Glass is a loss from the start, the moment it enters the Reverse Vending Machine (RVM). Collection, transportation to BCRS and the actual exportation of glass are all paid for by BCRS, making glass a liability from the start. Currently, BCRS is making a loss of 1Euro per tonne on shipping excluding management fees. This might not seem like a lot but despite the whole operation, a loss is still being made. This still needs to be done because the product still needs to be recycled. The other materials still compensate for it since from the other materials there is a good saving according to the market.

Within the BCRS scheme, glass is crushed as soon as it is deposited in the reverse vending machines (RVMs). This is done for 2 reasons:

- **Financial** – The glass bottles are compacted at source. When a glass bottle is accepted by the RVM and the deposit on the bottle is refunded, crushing the bottle ensures that no other deposit can be claimed on that bottle. Even though such RVMs are more expensive, this option is more viable.
- Breaking the glass yields **more storage capacity** in the RVM. If this had not been done, the current problem with full RVMs would have been greater.

BCRS Ltd has 2 glass waste streams – RVMs and door-to-door pickup from bars and restaurants.

- In RVMs, glass waste is never mixed with plastic or metal since glass bottles can only be deposited in an RVM that accepts glass only. RVMs contribute to 90% of the glass waste collected by BCRS which consists of single-use glass containers which would otherwise be thrown away in the Maghtab landfill. This is mixed crushed glass and collected by vehicles dedicated solely to glass. Each vehicle is weighed, and the glass waste is deposited in a designated garage near the Hal Far facility. Glass does not enter into the Hal Far facility. Glass doesn't give BCRS any economic value as is. Since glass would greatly damage "mal-linja", processing the glass and separating would increase the maintenance costs. Till date, BCRS Ltd hasn't considered the separation of glass waste to be economically viable. The glass waste produced by BCRS is **mixed glass of different colours mixed with contaminants coming from labels and caps**. This is probably the reason for the lower income acquired from it. A study was conducted a few years back where it was found that it would not be economically viable to invest in a separation process and then sell the separated glass.
- Door-to-door pickup takes place from bars, restaurants and small grocer shops. **80% of the waste** collected via this route is **glass waste**. This type of collection is quite innovative for Malta. Bags and tags are given to these places. The waste is placed inside the bags so the

owners might also include wine and spirit bottles that do not fall under the BCRS. The bag is closed via a label that contains a barcode number that identifies the shop, restaurant or bar from where the waste originated. Through an app, a booking for collection can be made. The bags are transported to the Hal Far facility. A machine scans the label barcode, and all bottles deposited in the machine at that time would be refunded to the specific bar, restaurant or shop.

The rejects are recycled by BCRS. However, this is still an added cost for BCRS because the rejects were still collected in the first place. This is a considerable and significant cost. In 2023, BCRS had about 30 containers filled with rejects. Even though this is significant, no other option is feasible since it is not going to be deposited at Magħtab and no operation created to transfer it to WasteServ is economically viable. These rejects are simply recycled with the rest of the glass and the foreign recyclers have found no objection in receiving mixed glass waste.

Even though the mixed glass waste is transported here as a whole, every glass bottle deposited in the RVM is logged and through the barcode on the bottle, data is gathered on the clear and coloured glass. (In Malta, most of the glass used is clear or green in colour. Brown glass bottles are not collected since they are refillable. Brown bottles accidentally arrive at BCRS through the door-to-door waste stream. Via the bar-code reading, no brown bottles will be accepted by the RVMs. These brown bottles are handed over to the producer to be refilled since this process is even better – reuse instead of recycle. This is confidential data and can be provided for the purpose of this dissertation if needed.

- **Plastic, metal and glass beverage containers are collected as part BCRS. How many tonnes of glass beverage containers are collected through the BCRS scheme?**

Tonnage collected sent by emailing.

The crushing of glass yields to cutlets.

20-foot containers for shipment

- **What percentage of glass beverages bought are returned through the BCRS scheme?**

78% return. A sheet for 2024 was given. Malta compares very well with other countres. Considering that this scheme started 2 years ago, the return is very good. BCRS is projecting that at the end of 2024, **82%** of glass beverage bottles will be returned. In 2024, BCRS is obliged to collect 80% by law and this will be surpassed. In 2025, the obligation will rise to 85% and from 2026 and the following 5 years, obligatory collection will rise to 90%.

- **Are there any other incentives that you think would increase the percentage return?**

The way that collection has been made so far has satisfied the need to reach targets. However, this would not be sustainable enough to reach the increased expected targets. In the RVMs, glass is collected in two bins, each of which takes 250 glass bottles which weighs 50kg. Collection of these two full bins depends on trucks that come on site to unload these bins. In Malta, traffic affects downtime. To mitigate this and ensure that the higher targets are reached, spare bins are being added to the back of the RVMs.

Plastic and metal cans are emptied by people on motorcycles who go round all the time emptying machines and store the bags at the back of the hub. Early in the morning, trucks go round to collect the bags and empty the hub. This is both efficient and environmentally friendly. It is planned that whilst doing this, the full glass bins are rolled out of the machines on wheels and

replaced with 2 empty glass bins by the truck personnel. The designated glass truck will still go for pickup once but will collect 4 bins instead of 2. This should increase collection because once you increase the RVM uptime, the RVM is more available to the public and so collection increases.

25 bags free collection per month are offered for door-to-door pickup. Each bag has the capacity for 55 bottles since these are intact and not broken bottles. This is not enough for bars, restaurants and small grocer shops. Any extra filled bags are collected at a cost for the retailers. Most often, the extra bottles are taken to the RVMs. The bags cannot be bigger as the threshold of carrying by a worker would be exceeded due to health and safety regulations. Negotiations are ongoing to give these retailers unlimited free collection as an incentive to increase collection. Since this would decrease the income for BCRS from extra bags however the targets need to be reached. Discussions on finance will remain ongoing.

This gives BCRS two big advantages – Collecting from restaurants directly, especially if not completely funded by BCRS, has a positive financial impact. To deter the retailers from using the RVMs and leave them more available for the general public, it is more worthwhile collecting all bottles directly from the retail outlets. This will increase the collection of glass.

Thus, increasing the redundancy by increasing the number of bins behind the RVMs and increasing manual collection would lead to the targets being achieved.

- **With regards to the collection trucks, what type of engines do they have – petrol, diesal electric?**

BCRS has **9 trucks** that collect glass – **5 of them are electric** and **4** of them are fueled by **unleaded petrol**. At the beginning of the scheme, it wasn't expected that manual collection would pick up so quickly. Thus, the contractor was obliged to buy 4 electric trucks, and 5 electric trucks were bought. The pickup was so fast that 4 other vans were needed urgently, and electric ones were not available and so unleaded trucks were bought due to urgency. If this had not happened, the process of collection would have been completely by electric vehicles.

- **How many vehicle trips take place to collect glass?**

3 trucks that can easily maneuver underground carparks and narrow streets collect from RVMs all around Malta, 7 days a week. A big truck (trakk tal-gebel) goes over to Gozo once a month.

A reconciliation process is carried out between what is collected in the RVMs and what has arrived at the Hal Far facility. For exportation, the truck is weighed on a weigh bridge. The glass is emptied in a garage. The containers are brought over and tilted at 45^0 and they are filled with glass by means of a bucket excavator. Each container weighs a maximum of 25 tonnes. 12 containers are shipped every 2 weeks to Turkey in bulk.

The trucks that transport the containers and the ships are diesel-operated.

- **What would be the reason why certain containers, that seem to adhere to the scope of the scheme, are not accepted? Reason being the more we collect the better. For example, Moscato D'Asti glass bottle of wine (even though it has a 5% alcohol content, has a capacity between 0.1 litres and 3 litres and is non-refillable)**

BCRS has a government license to operate the DRS. Operation has to abide by the BCRS regulations which are law. Parliament decided what is to be included in the BCRS. Wines are not

included and so even if the company wants to collect these bottles, it cannot as it would be breaking the law.

- **Why are the following not considered in the BCRS scheme?**
    - **Alcoholic beverages exceeding 5% alcohol content (Wines and Spirits)**
    - **Foreign alcoholic beverages that do not exceed 5% alcohol content**
    - **Glass bottles that carry sauces, sundried tomatoes etc**

  I found the following answer to this question online. Could the reason behind not including comore containers be clarified further please?
  "Beverage Containers are more likely to be consumed on the go, hence are more likely to be littered or thrown away in mixed waste. Beverages tend to be consumed quickly and soon after they are purchased, thus making up a big portion of single-use waste."

For the same reason stated above – laws and regulations

- **Online, I found the following information:**
  "Used beverage containers collected by Reverse Vending Machines .... arrive at the purposely built BCRS Clearing Centre in Hal Far where they will be sorted according to material type using specialised equipment and packed efficiently to be exported for recycling.
  Are the glass beverage containers cleaned after they are collected or is the waste simply sorted and exported?

Glass bottles are not cleaned.

- **What is the cost of exportation of the collected glass containers?**

Not answered

- **Are the bottles crushed before exportation? If yes, to what size?**

The glass is crushed in the RVMs. The glass collected by manual collection will arrive intact at the Hal Far Facility. It will be transported to the garage where crushed glass is stored, and a crusher is present there to ensure that no glass bottle is refunded more than once.

- **Is there any other information that can be provided that you think could be useful in aiding my research?**

Glass waste collection comes at a loss. We really look forward to the results of your dissertation as this would mean that a use is found for glass in Malta and exportation is avoided. This not only reduces expenses but also avoids the useless transactions of exportation whilst glass would be reused in Malta, resulting in circular economy.

BCRS is a data driven company where every operation is driven by data.

APPENDIX 1.3 – INTERVIEW WITH BUSINESS DEVELOPMENT MANAGER MSTREAM LTD.

By using glass waste in the construction industry, the volume of waste currently being disposed of in existing landfills is reduced, benefitting both the environment and maximising spatial use. Since glass waste is NOT recycled locally but rather exported to registered waste brokers, using glass waste in the local construction industry will repurpose glass waste locally (potentially reducing carbon emissions but there needs to be a study on exportation vs transportation emissions). I wished to determine the feasibility of using the glass waste collected locally in the construction industry.

- **For which companies/ entities do you collect glass waste?**

We export on behalf of BCRS

- **Are there any restrictions on glass waste transportation? Are there any restrictions on what type of glass waste can be transported?**

There are no restrictions. Mixed glass waste is considered as a non-hazardous product, and therefore no specialpermits (apart from the standard waste broker and waste carrier permits) are required. The glass we export ismixed glass culets that does not undergo any additional treatment (i.e. no washing, removal of labels, caps, etc.)

- **Does MStream Ltd. require a specific process for the preparation of glass waste for transport or specific end product before it is shipped?** *For example, in metal containers of a certain size, fully intact glass bottles, completely filled to avoid glass from shattering?*

As mentioned above, no special requirements are required. The glass is collected by BCRS in their depositingsystem, then they are crushed in the Hal Far Factory, and these are loaded by us into 20ft containers as is (seesome pictures)

- **How much glass waste is collected for transportation?**

Since the beginning of this year, we have exported 4,628 tonnes of crushed glass. We anticipate approximately500-700 more tonnes by the end of the year.

- **How often is the waste collected? Do you always collect the same amount? Is the collection of glass waste consistent throughout the year/s? Is each container filled completely before transportation?**

We collect every week

- **Do you always collect the same amount? Is the collection of glass waste consistent throughout the years?**

Amounts vary considerably depending on the season. In the summer months (July – Sept) the volumes shoot upquite drastically, as can be expected.

- **Is each container fi lled completely before transportation?**

Each 20ft container has an average of 25 tonnes. We cannot fi ll them completely, since otherwise we wouldexceed the weight limit. Also, since the glass is loose, the container cannot be fully packed.

- **What is the journey of the glass waste for which MStream Ltd is involved?**

We used to ship to Italy (Genoa) butsince last week we started shipping to Turkey (Izmir) since Italy is no longer interested in the product.

- **What is/are the starting point/s of the vehicles that go to collect the glass waste from designated sites?**

Qormi or Hal Far

- **From where is the glass waste collected?**

BCRS plant in Hal Far

- **Does the glass waste go straight to the dock for shipment after it is collected?**

Yes, to Freeport

- **Does MStream Ltd's responsibility of the glass waste stop on land or does it involve shipment overseas?**

Although our involvement stops strictly at BCRS facility, we oversee that the containers are delivered to our supplier. However, the shipment happens through our haulers and shipping agents.

- **Is MStream Ltd. involved in the transportation of glass waste to a recycling plant (or any other location) overseas?**

See above

- **How long is the journey in terms of kilometres and timewise?**

According to this, 884 nautical miles to get to port http://ports.com/sea-route/port-of-valletta,malta/port-of-izmir,turkey/. Following that, the container needs to be taken to the facility, which is another approximately 55km according to Google Maps.

- **Which type of vehicles are used to transport waste?** Trucks, ships etc

20ft container which is then loaded onto a ship. I have no information on the vessel type, sorry, but I can get you in contact with our shipping agent

- **Are these vehicles electric or diesel? If diesel, how much diesel is consumed?**

Diesel. I cannot say, unfortunately, but one most consider – diesel for the container to get to Malta, diesel of the JCB, diesel to get the container to destination.

- **How many vehicles are required?**

Depends on how many containers we have to load per week, but the average is 18 per month.

- **If overseas shipment is included, how many ships are typically used?**

All containers are loaded on a single ship for that week, so 1 ship per week.

- **Is there a possibility of more sustainable methods in the near future? Or does this seem out of reach with the current options available as well as advancements in technology?**

Once a week

- **Is there a possibility of more sustainable methods in the near future? Or does this seem out of reach with thecurrent options available as well as advancements in technology?**

Unfortunately for the time being, the only viable option is to ship abroad.

- **What is the cost of the transportation of waste for MStream Ltd. as well as for the companies/entities that use this service?**

Over 1,000 eur per container to ship to Turkey.

- **Is there any other information that can be provided that you think could be useful in aiding my research?**

I will send an email to the UK people to set up a communication channel.

APPENDIX 1.4 – INTERVIEW WITH CEO & CO CIRCULAR ECONOMY WASTESERV MALTA LTD.

- **How many tonnes of glass waste were collected in the years prior to 2023?**

An average of 8,000 - 9,000 tonnes per annum of glass packaging (such as bottles and jars) were being received by WSM prior to 2023. Around 600 tonnes of mixed flat glass were received per year.

Gozo gathers less glass than Malta and this can be attributed to the smaller population in Gozo. The Northern part collects more glass because the number of hotels there is large. To put you in the picture, Birkirkara in Malta uses the same of water supply as all of Gozo.

- **The data of previous years (2012-2022) has glass included within the green/grey bags. Are there statistics which determine the percentage of glass waste in those green/grey bags in that period?**

Regular studies are done. Glass in the grey bag is now minimal, not more than 1%.

- **What percentage of collected glass can actually be cleaned, sorted and prepared for exportation?**

The output of good quality material from sorting is circa 60%. This is heavily dependent on the quality of the input. However, as we are going for a higher quality output, any contaminants are removed.

The plant processes bottled glass as well as flat glass in two separate streams. Glass is broken, sorted into transparent and mixed coloured glass through automated machinery. This makes the glass furnace-ready (all labels and attached materials are removed. Any ceramics are removed as it causes a lot of damage to the furnace.

Different colours of glass can be separated at WasteServ.

20-25% of collected glass is lost due to caps, labels and also since small pieces of glass are lost as they're too small.

- **In which ways can the percentage of glass that cannot be cleaned and sorted be reduced?**

Better separation at source by waste generators. The pieces of glass attached to labels might be retrieved by soaking these pieces to remove the labels and clean glass can be retrieved as an extra source.

- **Is there a way in which incentives can be created to encourage the community to collect more glass waste?**

A lot of glass is being collected especially from restaurants and hotels. Through education campaigns.

- **Apart from separating transparent glass from coloured glass, are the different colours also separated?**

Although the machinery in the plant can separate glass of different colours, currently only two outputs are achieved – Clear Glass and Mixed Coloured Glass.

- **How is the automated glass sorting line at the Sant'Antnin waste treatment plant fuelled?**

In 2020, glass was sorted manually by pickers. Then, a rudimentary sorting line was installed where the glass used to pass on a conveyor belt, and it was sorted manually by workers. Since summer 2024, the new automated glass sorting line was installed. Since summer, 4000 tonnes of glass have been placed on the market for sale.

The automated sorting line is fuelled by an electrical supply. Consumption can be given per hour.

- **When was the new waste sorting line implemented?**

June 2024

- **To what degree is the glass cleaned?**

Glass cullet out is 99.9% pure. CSPs, Labels, Organic content, Corks, Foil are all removed.

- **What are the chemical/mechanical processes for cleaning glass waste?**

All cleaning processes are mechanical. Ceramic and all taps are removed by the plant.

Apart from bottles, flat glass (example window panes) is also processed. This diversifies the range of glass types that can be diverted away from the landfill.

- **What are these different types?**

Laminated and non-laminated glass are received. At the moment, these are accepted together at WSM.

- **Which type of glass is collected the most?**

Most material received is packaging glass (bottles and jars)

- **What does it cost to export? Wages, operating costs, etc?**

This is not determined by WSM but by the brokers that acquire such material.

- **What is the profit margin from exportation?**

This is not determined by WSM but by the brokers that acquire such material. Since the quality of the glass produced has been improved, it is expected that glass will be sold at a profit since the cleaner the glass the more expensive it is.

Glass is deposited at WasteServ at the cost of 30 Euro per tonne and then who is buying the glass has to pay for the shipping. WasteServ is not involved in the transportation of glass or its cost both to and from the plant.

- **How much glass waste is being exported?**

All glass placed on the market by WSM is exported.

- **It can be seen that sometimes, Wasteserv pays to remove glass waste even though sometimes, glass is also sold. Can this be confirmed please?**

Confirmed, this is dependent on the international market prices, quality and also tonnage available

- **Considering the above statistics, is glass waste bought locally in enough occurrence and profit?**

Brokers are private entities which for sure operate at a profit. The profit margins are not known. In order to ensure economies of scale, WSM puts on the market large batches of glass.

- **Is glass waste exported in enough occurrence and profit?**

Brokers are private entities which for sure operate at a profit. The profit margins are not known. In order to ensure economies of scale WSM puts on the market large batches.

All glass is exported overseas to large furnaces that process glass.

APPENDIX 1.5 – INTERVIEW WITH COO INFRASTRUCTURE MALTA

- **Is there an estimate of how much concrete (cubic tonnes or other measure) has been used in previous projects?**
  Since major projects use large amounts of concrete, data will be gathered on how much concrete (in m^3) was used in major projects and what type of cement was used in this concrete in the last 5 years.

- **Is there an estimate of how much concrete (cubic tonnes or other measure) will be used in projects in the near future?**

  Msida Creek data

- **Is any recyclable material currently being used in projects/ proposed projects?**
  Concrete utilising recycled materials is or can be used in maritime works or in land projects where specialised concrete utilising silica fume is used.

- **Would Infrastructure Malta be open to exploring the possibility of incorporating glass waste in the concrete mixture used for projects to reduce the environmental impact caused by cement?**
  Infrastructure Malta is normally very open to innovative types of concrete, and these could be used in pilot projects. However, the concrete would need to have undergone rigorous testing at the University of Malta regarding strength and durability (50-year lifetime) and other properties such as slippery. Case studies have been doen in the past with the University of Malta.

- **Would it be difficult for this idea to be implemented considering that Infrastructure Malta is dependent on contractors to carry out the works?**
  This is more difficult! Usually, contractors would want to stick to systems that they have worked with and are used to. For example, changing from normal concrete which utilises CEM1 cement to concrete that is used in the sea that utilises XS3 cement was a very laborious process as it was difficult for the contractors to align with the requirements of Infrastructure Malta. They resisted the change by not importing that type of cement.

- **Do you think contractors would oppose to this idea's implementation?**
  If it has been done, it can be done but a lot of work has to be put into it.

- **Is there any other information that can be provided that you think could be useful in aiding my research?**
  Be aware that other issues might crop up. For instance, when glass aggregate was being used in asphalt mix and used on roads, it was found that glass was reflecting light into driver's eyes, hindering road vision. Slipperiness is another property that might be looked into if glass is included. Another thing to think about is where can the concrete with glass waste be used according to its properties.

APPENDIX 2 – CERTIFICATE OF CEMENT USED

	SOCIETE DES CIMENTS DE GABES	INNORPI CE
SECIL	Fiche Technique du Produit // Technical Data sheet **CEM I 42,5 R**	ISO 9001 ISO 14001 ISO 45001

Période// Period: Janvier 2025/ January 2025

Désignation // Designation			Valeur // Value	Exigence// Requirement NT 47.01 & EN 197.1
Essais Physiques// Physical Tests				
Début de prise *Initial setting*		(mn)	160	≥ **60**
Expansion *Soundness*		(mm)	0.50	≤ **10**
Surface Spécifique Blaine *Blaine Specific Surface*		m^2/kg	370	----
Essais Mécaniques// Mécanical Tests				
Résistance à la compression à 2j *Compression Strength 2d*		(MPa)	**30.0**	> **20**
Résistance à la Flexion à 2j *Bending Strength 2d*		(MPa)	5.0	----
Résistance à la compression à 28j *Compression Strength 28d*		(MPa)	**58.0**	≥ **42,5 et ≤ 62,5**
Résistance à la Flexion à 28j *Bending Strength 28d*		(MPa)	8.4	----
Analyses Chimiques//Chemical Analysis				
Oxyde de Calcium *Calcium Oxide*	CaO	(%)	63.65	----
Oxyde de Silice *Silica Oxide*	SiO2	(%)	19.50	----
Oxyde d'alumine *Alumina Oxide*	Al2O3	(%)	4.35	----
Oxyde de Fer *Iron Oxide*	Fe2O3	(%)	3.00	----
Oxyde de magnésium *Magnesium Oxide*	MgO	(%)	1.35	----
Oxyde de soufre *Sulfur Oxide*	SO3	(%)	3.60	≤ **4,0**
Oxyde de Sodium *Sodium Oxide*	Na2O	(%)	0.11	----
Oxyde de Potassium *Potassium Oxide*	K2O	(%)	0.60	----
Clorures *Chlorides*	Cl	(%)	0.02	≤ **0,1**
Perte au Feu à 950 °C *Loss of Ignition*		(%)	3.20	≤ **5**
Residue Insoluble *Insoluble Residue*		(%)	1.50	≤ **5**
Equivalent Alcalin *Alcalin Equivalent*		(%)	0.50	----
Taux d'ajout		(%)	3.50	≤ **5**

Note: For chromuim VI, we comply with EN 196-10 requirement, less than 2 ppm.

VISA	APPROBATION// APPROVAL
	Mme YEHMED Imen

SOCIETE DES CIMENTS DE GABES IMP-EXP

APPENDIX 3

DATA OBTAINED FROM DENSITY BOTTLE TEST

MASS OF WATER					
Container No.	**1**	**2**	**3**	**4**	**5**
Mass of Empty Container /g	26.3292	38.3917	38.8893	35.2052	37.7839
Mass of pyknometer Full of Water (M_1) /g	74.6002	88.5744	88.9950	84.9126	88.1414
Mass of pyknometer Full of Water (M_2) /g	74.6071	88.5189	88.9254	84.8825	88.0766
Mass of pyknometer Full of Water (M_3) /g	74.5440	88.4810	88.8935	84.8994	88.0365
Mean of M_1, M_2, M_3 /g	74.5838	88.5248	88.9380	84.8982	88.0848
Mass of Water (W_1) /g	48.2546	50.1331	50.0487	49.6930	50.3009

RESULTS USING 1ST BATCH OF KEROSINE

MASS OF KEROSINE (DISPLACEMENT LIQUID)					
Container No.	**1**	**2**	**3**	**4**	**5**
Mass of Empty Container /g	26.3291	38.3911	38.8891	35.2049	37.7838
Mass of pyknometer Full of Kerosine (M_1) /g	64.8319	78.4378	78.8658	74.7651	78.0172
Mass of pyknometer full of Kerosine (M_2) /g	64.7978	78.4048	78.8549	74.7449	77.9994
Mass of pyknometer full of Kerosine (M_3) /g	64.8187	78.4272	78.8566	74.7625	77.9985
Mean of M_1, M_2, M_3 (**W_3**) /g	64.8161	78.4233	78.8591	74.7575	78.0050
Mass of Kerosine (W_2) /g	38.4870	40.0322	39.9700	39.5526	40.2212

DENSITY OF REDISTILLED KEROSINE (Pl) in g/cm^3 using Table NC.1					
Container No.	**1**	**2**	**3**	**4**	**5**
Density of pure water at 28^{0}C as the selected operating temperature of the water bath (**P_w**) in **g/cm^3**	0.9963	0.9963	0.9963	0.9963	0.9963
P_L = (W_2/W_1) x P_w in **g/cm^3**	0.7946	0.7956	0.7957	0.7930	0.7967
P_L = (W_2/W_1) x P_w in k**g/m^3**	794.6	795.6	795.7	793.0	796.7

DENSITY OF Cement in g/cm^3					
Container No.	**1**	**2**	**3**	**4**	**5**
Mass of Empty Container /g	26.3286	38.3913	38.889	35.2045	37.7836
Mass of Container with Powder /g	36.098	46.9932	48.6221	45.15	47.6359
Mass of Powder (W_4) **/g**	9.7694	8.6019	9.7331	9.9455	9.8523
Mass of Container Full of Powder + Kerosine (M_1) **/g**	72.0814	85.6866	86.1142	82.166	85.2972
Mass of Container Full of Powder + Kerosine (M_2) **/g**	72.123	85.6795	86.1308	82.1439	85.3471
Mass of Container Full of Powder + Kerosine (M_3) **/g**	72.0801	85.6337	86.0803	82.1413	85.3195
Mean of M1, M2, M3 (W_5) **/g**	72.0948	85.6666	86.1084	82.1504	85.3213
Density of Cement = $(W_4 \times P_L) / (W_3 + W_4 - W_5)$ in **g/cm^3**	3.1168	5.0372	3.1180	3.0897	3.0949
Density of Cement = $(W_4 \times P_L) / (W_3 + W_4 - W_5)$ in **kg/m^3**	3116.8	5037.2	3118.0	3089.7	3094.9

DENSITY OF Cl in g/cm^3					
Container No.	**1**	**2**	**3**	**4**	**5**
Mass of Empty Container /g	26.3286	38.3913	38.8890	35.2045	37.7836
Mass of Container with Powder /g	36.2749	48.3204	48.7907	45.1037	47.7702
Mass of Powder (W_4) **/g**	9.9463	9.9291	9.9017	9.8992	9.9866
Mass of Container Full of Powder + Kerosine (M_1) **/g**	71.5921	85.1605	85.5927	81.5608	84.7791
Mass of Container Full of Powder + Kerosine (M_2) **/g**	71.5951	85.1683	85.5882	81.5385	84.7691
Mass of Container Full of Powder + Kerosine (M_3) **/g**	71.5914	85.1811	85.5814	81.5297	84.7682
Mean of M1, M2, M3 (W_5) **/g**	71.5928	85.1700	85.5874	81.5430	84.7721
Density of Cl = $(W_4 \times P_L) / (W_3 + W_4 - W_5)$ in **g/cm^3**	2.4936	2.4822	2.4827	2.5211	2.4711
Density of Cl = $(W_4 \times P_L) / (W_3 + W_4 - W_5)$ in **kg/m^3**	2.4936	2.4822	2.4827	2.5211	2.4711

DENSITY OF Co in g/cm^3					
Container No.	**1**	**2**	**3**	**4**	**5**
Mass of Empty Container /g	26.3286	38.3913	38.889	35.2045	37.7836
Mass of Container with Powder /g	36.3086	48.3679	48.8476	45.1531	47.7689
Mass of Powder (**W_4**) **/g**	9.98	9.9766	9.9586	9.9486	9.9853
Mass of Container Full of Powder + Kerosine (**M_1**) **/g**	71.6389	85.2325	85.642	81.6147	84.7987
Mass of Container Full of Powder + Kerosine (**M_2**) **/g**	71.6177	85.2034	85.6129	81.5938	84.7522
Mass of Container Full of Powder + Kerosine (**M_3**) **/g**	71.6289	85.2344	85.6403	81.5806	84.7995
Mean of M_1, M_2, M_3 (**W_5**) **/g**	71.6285	85.2234	85.6317	81.5964	84.7835
Density of Co = **(W_4 x P_L) / (W_3 + W_4 - W_5)** in **g/cm^3**	2.5036	2.4987	2.4871	2.5369	2.4806
Density of Co = **(W_4 x P_L) / (W_3 + W_4 - W_5)** in **kg/m^3**	2503.6	2498.7	2487.1	2536.9	2480.6

DENSITY OF Cl + Co W in g/cm^3					
Container No.	**1**	**2**	**3**	**4**	**5**
Mass of Empty Container /g	26.3286	38.3913	38.8890	35.2045	37.7836
Mass of Container with Powder /g	36.3169	48.367	48.8757	45.1716	47.7515
Mass of Powder (**W_4**) **/g**	9.9883	9.9757	9.9867	9.9671	9.9679
Mass of Container Full of Powder + Kerosine (**M_1**) **/g**	71.6514	85.2429	85.6815	81.5985	84.7679
Mass of Container Full of Powder + Kerosine (**M_2**) **/g**	71.6883	85.2577	85.6885	81.4689	84.7692
Mass of Container Full of Powder + Kerosine (**M_3**) **/g**	71.6066	85.2049	85.6273	81.4543	84.7546
Mean of M_1, M_2, M_3 (**W_5**) **/g**	71.6488	85.2352	85.6658	81.5072	84.7639
Density of Cl + Co W = **(W_4 x P_L) / (W_3 + W_4 - W_5)** in **g/cm^3**	2.5152	2.5085	2.4987	2.4566	2.4746
Density of Cl + Co W = **(W_4 x P_L) / (W_3 + W_4 - W_5)** in **kg/m^3**	2515.2	2508.5	2498.7	2456.6	2474.6

DENSITY OF Cl + Co B in g/cm^3					
Container No.	**1**	**2**	**3**	**4**	**5**
Mass of Empty Container /g	26.3286	38.3913	38.889	35.2045	37.7836
Mass of Container with Powder /g	36.2764	48.3724	48.8715	45.1687	47.7581
Mass of Powder (**W_4**) **/g**	9.9478	9.9811	9.9825	9.9642	9.9745
Mass of Container Full of Powder + Kerosine (**M_1**) **/g**	71.6122	85.2287	85.6725	81.6121	84.7887
Mass of Container Full of Powder + Kerosine (**M_2**) **/g**	71.5919	85.198	85.6381	81.5921	84.749
Mass of Container Full of Powder + Kerosine (**M_3**) **/g**	71.5964	85.2178	85.647	81.5859	84.7669
Mean of M_1, M_2, M_3 (**W_5**) **/g**	71.6002	85.2148	85.6525	81.5967	84.7682
Density of Cl + Co B = **(W_4 x P_L) / (W_3 + W_4 - W_5)** in **g/cm^3**	2.4986	2.4896	2.4906	2.5285	2.4744
Density of Cl + Co B = **(W_4 x P_L) / (W_3 + W_4 - W_5)** in **kg/m^3**	2498.6	2489.6	2490.6	2528.5	2474.4

RESULTS USING 2ND BATCH OF KEROSINE

MASS OF KEROSINE (DISPLACEMENT LIQUID)					
Container No.	**1**	**2**	**3**	**4**	**5**
Mass of Empty Container /g	26.3279	38.3911	38.8884	35.2051	37.7831
Mass of pyknometer Full of Kerosine (M_1) /g	64.5334	78.1066	78.5776	74.4312	77.6609
Mass of pyknometer full of Kerosine (M_2) /g	64.5599	78.1394	78.57	74.4167	77.6911
Mass of pyknometer full of Kerosine (M_3) /g	64.5034	78.0933	78.5185	74.4168	77.666
Mean of M_1, M_2, M_3 (**W_3**) /g	64.5322	78.1131	78.5554	74.4216	77.6727
Mass of Kerosine (W_2) /g	38.2043	39.7220	39.6670	39.2165	39.8896

DENSITY OF REDISTILLED KEROSINE (Pl) in g/cm^3 using Table NC.1					
Container No.	**1**	**2**	**3**	**4**	**5**
Density of pure water at 28^{0}C as the selected operating temperature of the water bath (**P_w**) in **g/cm^3**	0.9963	0.9963	0.9963	0.9963	0.9963
P_L = (W_2/W_1) x P_w in **g/cm^3**	0.7888	0.7894	0.7896	0.7863	0.7901
P_L = (W_2/W_1) x P_w in **kg/m^3**	788.8	789.4	789.6	786.3	790.1

DENSITY OF Gl + Ce in g/cm^3					
Container No.	**1**	**2**	**3**	**4**	**5**
Mass of Empty Container /g	26.3286	38.3913	38.889	35.2045	37.7836
Mass of Container with Powder /g	36.3092	48.3753	48.8869	45.1777	47.7714
Mass of Powder (W_4) **/g**	9.9806	9.984	9.9979	9.9732	9.9878
Mass of Container Full of Powder + Kerosine (M_1) **/g**	71.278	84.9824	85.4242	81.1343	84.4242
Mass of Container Full of Powder + Kerosine (M_2) **/g**	71.2266	84.9209	85.3484	81.1307	84.4816
Mass of Container Full of Powder + Kerosine (M_3) **/g**	71.3336	84.9228	85.3657	81.1218	84.4921
Mean of M_1, M_2, M_3 (W_5) **/g**	71.2794	84.9420	85.3794	81.1289	84.4660
Density of Gl + Ce = **(W_4 x P_L) / (W_3 + W_4 - W_5)** in **g/cm^3**	2.4348	2.4980	2.4874	2.4011	2.4702
Density of Gl + Ce = **(W_4 x P_L) / (W_3 + W_4 - W_5)** in **kg/m^3**	2434.8	2498.0	2487.4	2401.1	2470.2

DENSITY OF Cl + Co W Ca 600 in g/cm^3					
Container No.	**1**	**2**	**3**	**4**	**5**
Mass of Empty Container /g	26.3286	38.3913	38.889	35.2045	37.7836
Mass of Container with Powder /g	36.3017	48.3671	48.868	45.1831	47.7577
Mass of Powder (W_4) **/g**	9.9731	9.9758	9.979	9.9786	9.9741
Mass of Container Full of Powder + Kerosine (M_1) **/g**	71.2937	84.9133	85.3727	81.0765	84.4015
Mass of Container Full of Powder + Kerosine (M_2) **/g**	71.2732	84.9216	85.3856	81.0746	84.3819
Mass of Container Full of Powder + Kerosine (M_3) **/g**	71.3053	84.9122	85.3852	81.0718	84.4306
Mean of M_1, M_2, M_3 (W_5) **/g**	71.2907	84.9157	85.3812	81.0743	84.4047
Density of Cl + Co W Ca 600 = **(W_4 x P_L) / (W_3 + W_4 - W_5)** in **g/cm^3**	2.4472	2.4817	2.4990	2.3590	2.4306
Density of Cl + Co W Ca 600 = **(W_4 x P_L) / (W_3 + W_4 - W_5)** in **kg/m^3**	2447.2	2481.7	2499.0	2359.0	2430.6

DENSITY OF Cl + Co W Ca 850 in g/cm^3					
Container No.	**1**	**2**	**3**	**4**	**5**
Mass of Empty Container /g	26.3286	38.3913	38.889	35.2045	37.7836
Mass of Container with Powder /g	36.296	48.3758	48.862	45.1788	47.7704
Mass of Powder (**W_4**) **/g**	9.9674	9.9845	9.973	9.9743	9.9868
Mass of Container Full of Powder + Kerosine (**M_1**) **/g**	71.3446	84.9192	85.3502	81.2728	84.5257
Mass of Container Full of Powder + Kerosine (**M_2**) **/g**	71.3291	84.9249	85.3707	81.2739	84.4968
Mass of Container Full of Powder + Kerosine (**M_3**) **/g**	71.3251	84.9057	85.3523	81.2255	84.4735
Mean of M_1, M_2, M_3 (**W_5**) **/g**	71.3329	84.9166	85.3577	81.2574	84.4987
Density of Cl + Co W Ca 850 = (W_4 x P_L) / (W_3 + W_4 - W_5) in **g/cm^3**	2.4828	2.4778	2.4837	2.4988	2.4963
Density of Cl + Co W Ca 850 = (W_4 x P_L) / (W_3 + W_4 - W_5) in **kg/m^3**	2482.8	2477.8	2483.7	2498.8	2496.3

APPENDIX 4 – PARTICLE SIZE DISTRIBUTION

PARTICLE SIZE DISTRIBUTION FOR CEMENT					
Size (µm)	Volume (%)	Size (µm)	Volume (%)	Size (µm)	Volume (%)
0.010	0.00	1.096	0.22	120.226	1.88
0.011	0.00	1.259	0.21	138.038	1.30
0.013	0.00	1.445	0.22	158.489	0.80
0.015	0.00	1.660	0.25	181.970	0.46
0.017	0.00	1.905	0.33	208.930	0.17
0.020	0.00	2.188	0.45	239.883	0.02
0.023	0.00	2.512	0.62	275.423	0.00
0.026	0.00	1.884	0.83	316.228	0.00
0.030	0.00	3.311	1.08	363.078	0.00
0.035	0.00	3.802	1.38	416.869	0.00
0.040	0.00	4.365	1.70	478.630	0.00
0.046	0.00	5.012	2.05	549.541	0.00
0.052	0.00	5.754	2.40	630.957	0.00
0.060	0.00	6.607	2.75	724.436	0.00
0.069	0.00	7.586	3.08	831.764	0.00
0.079	0.00	8.710	3.39	954.993	0.00
0.091	0.00	10.000	3.65	1096.478	0.00
0.105	0.00	11.482	3.88	1258.925	0.00
0.120	0.00	13.183	4.06	1445.440	0.00
0.138	0.00	15.136	4.22	1659.587	0.00
0.158	0.00	17.378	4.35	1905.461	0.00
0.182	0.00	19.953	4.45	2187.762	0.00
0.209	0.00	22.909	4.54	2511.886	0.00
0.240	0.00	26.303	4.61	2884.032	0.00
0.275	0.00	30.200	4.65	3311.311	0.00
0.316	0.00	34.674	4.66	3801.894	0.00
0.363	0.00	39.811	4.63	4365.158	0.00
0.417	0.00	45.709	4.56	5011.872	0.00
0.479	0.00	52.481	4.42	5754.399	0.00
0.550	0.05	60.256	4.20	6606.934	0.00
0.631	0.13	69.183	3.88	7585.776	0.00
0.724	0.20	79.433	3.42	8709.636	0.00
0.832	0.22	91.201	2.95	10000.000	0.00
0.955	0.23	104.713	2.45		

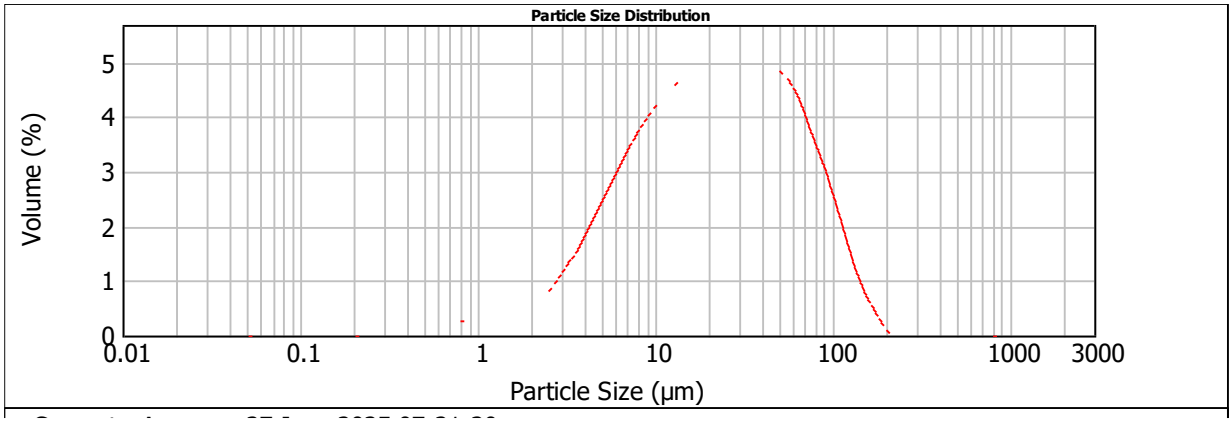

PARTICLE SIZE DISTRIBUTION FOR Cl					
Size (µm)	Volume (%)	Size (µm)	Volume (%)	Size (µm)	Volume (%)
0.010	0.00	1.096	0.47	120.226	0.00
0.011	0.00	1.259	0.59	138.038	0.00
0.013	0.00	1.445	0.72	158.489	0.00
0.015	0.00	1.660	0.86	181.970	0.00
0.017	0.00	1.905	1.05	208.930	0.00
0.020	0.00	2.188	1.29	239.883	0.00
0.023	0.00	2.512	1.60	275.423	0.00
0.026	0.00	1.884	1.98	316.228	0.00
0.030	0.00	3.311	2.42	363.078	0.00
0.035	0.00	3.802	2.90	416.869	0.00
0.040	0.00	4.365	3.40	478.630	0.00
0.046	0.00	5.012	3.91	549.541	0.00
0.052	0.00	5.754	4.37	630.957	0.00
0.060	0.00	6.607	4.76	724.436	0.00
0.069	0.00	7.586	5.04	831.764	0.00
0.079	0.00	8.710	5.20	954.993	0.00
0.091	0.00	10.000	5.24	1096.478	0.00
0.105	0.00	11.482	5.19	1258.925	0.00
0.120	0.00	13.183	5.06	1445.440	0.00
0.138	0.00	15.136	4.90	1659.587	0.00
0.158	0.00	17.378	4.74	1905.461	0.00
0.182	0.00	19.953	4.61	2187.762	0.00
0.209	0.00	22.909	4.50	2511.886	0.00
0.240	0.00	26.303	4.40	2884.032	0.00
0.275	0.00	30.200	4.27	3311.311	0.00
0.316	0.00	34.674	4.05	3801.894	0.00
0.363	0.00	39.811	3.70	4365.158	0.00
0.417	0.00	45.709	3.18	5011.872	0.00
0.479	0.00	52.481	2.48	5754.399	0.00
0.550	0.00	60.256	1.64	6606.934	0.00
0.631	0.00	69.183	0.77	7585.776	0.00
0.724	0.08	79.433	0.07	8709.636	0.00
0.832	0.20	91.201	0.00	10000.000	0.00
0.955	0.36	104.713	0.00		

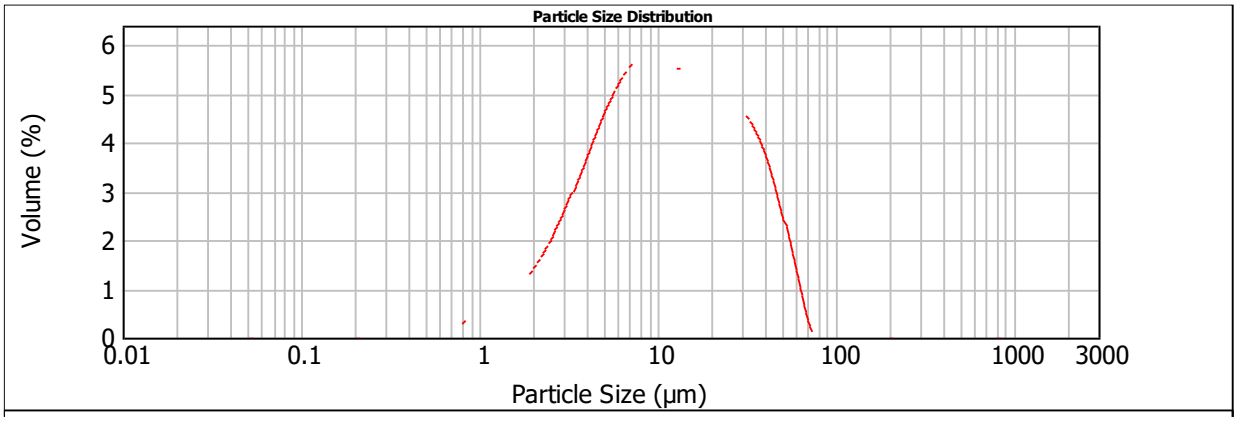

PARTICLE SIZE DISTRIBUTION FOR Co					
Size (µm)	Volume (%)	Size (µm)	Volume (%)	Size (µm)	Volume (%)
0.010	0.00	1.096	0.56	120.226	0.00
0.011	0.00	1.259	0.67	138.038	0.00
0.013	0.00	1.445	0.78	158.489	0.00
0.015	0.00	1.660	0.90	181.970	0.00
0.017	0.00	1.905	1.07	208.930	0.00
0.020	0.00	2.188	1.28	239.883	0.00
0.023	0.00	2.512	1.56	275.423	0.00
0.026	0.00	1.884	1.91	316.228	0.00
0.030	0.00	3.311	2.33	363.078	0.00
0.035	0.00	3.802	2.81	416.869	0.00
0.040	0.00	4.365	3.32	478.630	0.00
0.046	0.00	5.012	3.85	549.541	0.00
0.052	0.00	5.754	4.34	630.957	0.00
0.060	0.00	6.607	4.77	724.436	0.00
0.069	0.00	7.586	5.10	831.764	0.00
0.079	0.00	8.710	5.30	954.993	0.00
0.091	0.00	10.000	5.36	1096.478	0.00
0.105	0.00	11.482	5.29	1258.925	0.00
0.120	0.00	13.183	5.11	1445.440	0.00
0.138	0.00	15.136	4.87	1659.587	0.00
0.158	0.00	17.378	4.61	1905.461	0.00
0.182	0.00	19.953	4.35	2187.762	0.00
0.209	0.00	22.909	4.12	2511.886	0.00
0.240	0.00	26.303	3.91	2884.032	0.00
0.275	0.00	30.200	3.72	3311.311	0.00
0.316	0.00	34.674	3.50	3801.894	0.00
0.363	0.00	39.811	3.24	4365.158	0.00
0.417	0.00	45.709	2.91	5011.872	0.00
0.479	0.00	52.481	2.50	5754.399	0.00
0.550	0.00	60.256	2.01	6606.934	0.00
0.631	0.03	69.183	1.49	7585.776	0.00
0.724	0.15	79.433	0.98	8709.636	0.00
0.832	0.32	91.201	0.47	10000.000	0.00
0.955	0.44	104.713	0.08		

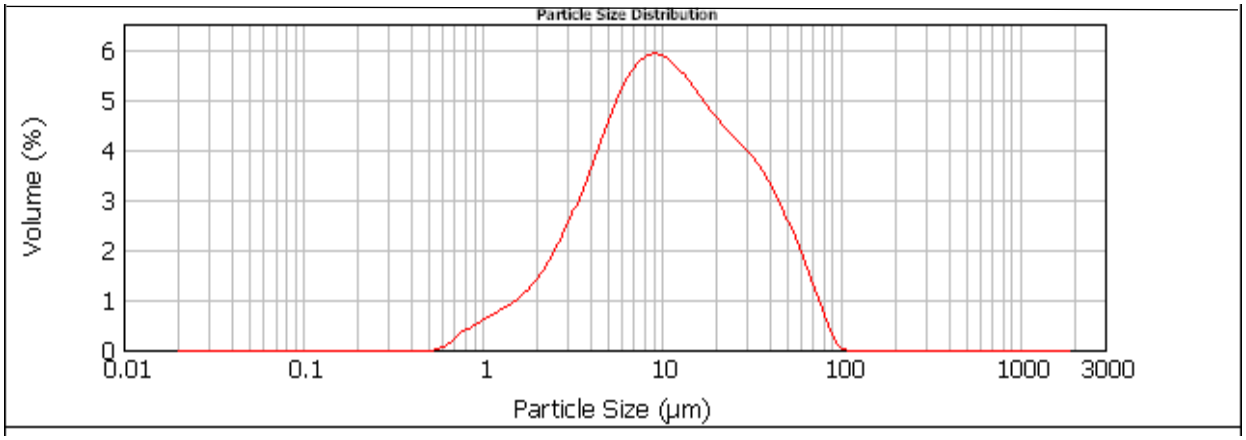

PARTICLE SIZE DISTRIBUTION FOR Cl + Co W					
Size (µm)	Volume (%)	Size (µm)	Volume (%)	Size (µm)	Volume (%)
0.010	0.00	1.096	0.30	120.226	0.00
0.011	0.00	1.259	0.38	138.038	0.00
0.013	0.00	1.445	0.46	158.489	0.00
0.015	0.00	1.660	0.52	181.970	0.00
0.017	0.00	1.905	0.58	208.930	0.00
0.020	0.00	2.188	0.66	239.883	0.00
0.023	0.00	2.512	0.78	275.423	0.00
0.026	0.00	1.884	0.97	316.228	0.00
0.030	0.00	3.311	1.25	363.078	0.00
0.035	0.00	3.802	1.63	416.869	0.00
0.040	0.00	4.365	2.12	478.630	0.00
0.046	0.00	5.012	2.71	549.541	0.00
0.052	0.00	5.754	3.39	630.957	0.00
0.060	0.00	6.607	4.11	724.436	0.00
0.069	0.00	7.586	4.83	831.764	0.00
0.079	0.00	8.710	5.46	954.993	0.00
0.091	0.00	10.000	5.98	1096.478	0.00
0.105	0.00	11.482	6.32	1258.925	0.00
0.120	0.00	13.183	6.47	1445.440	0.00
0.138	0.00	15.136	6.41	1659.587	0.00
0.158	0.00	17.378	6.19	1905.461	0.00
0.182	0.00	19.953	5.84	2187.762	0.00
0.209	0.00	22.909	5.41	2511.886	0.00
0.240	0.00	26.303	4.96	2884.032	0.00
0.275	0.00	30.200	4.48	3311.311	0.00
0.316	0.00	34.674	4.00	3801.894	0.00
0.363	0.00	39.811	3.50	4365.158	0.00
0.417	0.00	45.709	2.97	5011.872	0.00
0.479	0.00	52.481	2.43	5754.399	0.00
0.550	0.00	60.256	1.89	6606.934	0.00
0.631	0.00	69.183	1.37	7585.776	0.00
0.724	0.00	79.433	0.88	8709.636	0.00
0.832	0.07	91.201	0.45	10000.000	0.00
0.955	0.17	104.713	0.04		

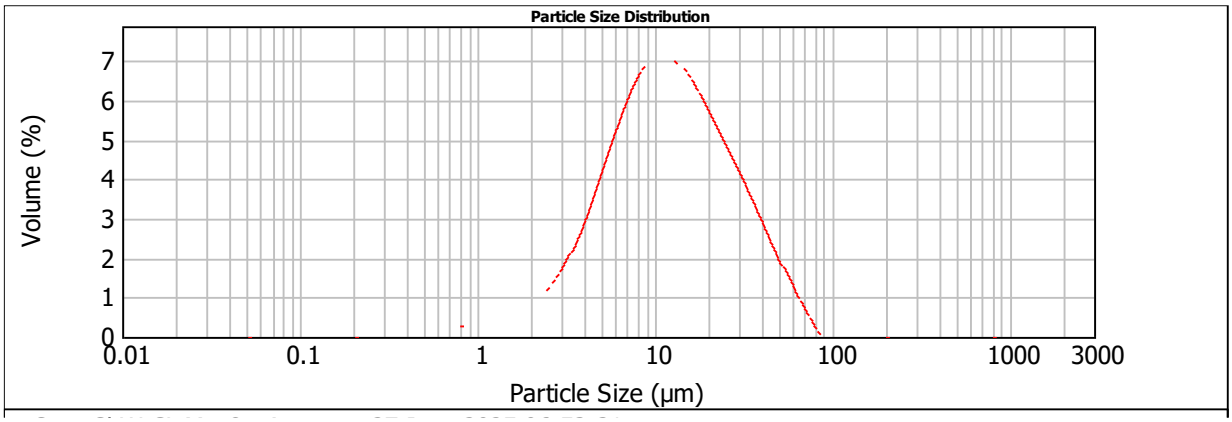

PARTICLE SIZE DISTRIBUTION FOR Cl + Co B					
Size (µm)	Volume (%)	Size (µm)	Volume (%)	Size (µm)	Volume (%)
0.010	0.00	1.096	0.26	120.226	0.15
0.011	0.00	1.259	0.37	138.038	0.18
0.013	0.00	1.445	0.47	158.489	0.15
0.015	0.00	1.660	0.58	181.970	0.09
0.017	0.00	1.905	0.63	208.930	0.00
0.020	0.00	2.188	0.68	239.883	0.00
0.023	0.00	2.512	0.79	275.423	0.00
0.026	0.00	1.884	1.00	316.228	0.00
0.030	0.00	3.311	1.34	363.078	0.00
0.035	0.00	3.802	1.81	416.869	0.00
0.040	0.00	4.365	2.44	478.630	0.00
0.046	0.00	5.012	3.19	549.541	0.00
0.052	0.00	5.754	4.03	630.957	0.00
0.060	0.00	6.607	4.92	724.436	0.00
0.069	0.00	7.586	5.76	831.764	0.00
0.079	0.00	8.710	6.52	954.993	0.00
0.091	0.00	10.000	7.09	1096.478	0.00
0.105	0.00	11.482	7.43	1258.925	0.00
0.120	0.00	13.183	7.53	1445.440	0.00
0.138	0.00	15.136	7.36	1659.587	0.00
0.158	0.00	17.378	6.97	1905.461	0.00
0.182	0.00	19.953	6.38	2187.762	0.00
0.209	0.00	22.909	5.65	2511.886	0.00
0.240	0.00	26.303	4.81	2884.032	0.00
0.275	0.00	30.200	3.94	3311.311	0.00
0.316	0.00	34.674	3.04	3801.894	0.00
0.363	0.00	39.811	2.15	4365.158	0.00
0.417	0.00	45.709	1.28	5011.872	0.00
0.479	0.00	52.481	0.55	5754.399	0.00
0.550	0.00	60.256	0.12	6606.934	0.00
0.631	0.00	69.183	0.02	7585.776	0.00
0.724	0.00	79.433	0.02	8709.636	0.00
0.832	0.05	91.201	0.05	10000.000	0.00
0.955	0.13	104.713	0.10		

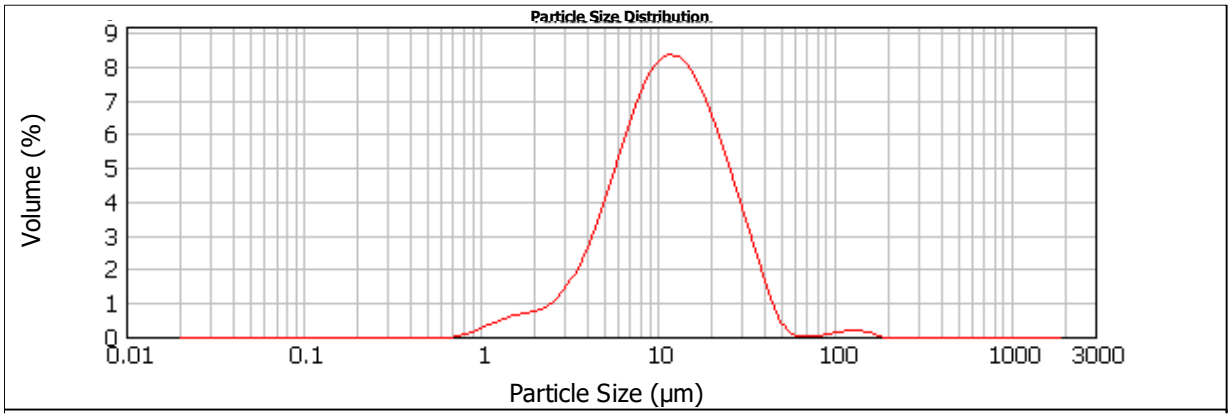

PARTICLE SIZE DISTRIBUTION FOR Gl + Ce					
Size (µm)	Volume (%)	Size (µm)	Volume (%)	Size (µm)	Volume (%)
0.010	0.00	1.096	0.32	120.226	0.00
0.011	0.00	1.259	0.46	138.038	0.00
0.013	0.00	1.445	0.63	158.489	0.00
0.015	0.00	1.660	0.86	181.970	0.00
0.017	0.00	1.905	1.19	208.930	0.00
0.020	0.00	2.188	1.62	239.883	0.00
0.023	0.00	2.512	2.16	275.423	0.00
0.026	0.00	1.884	2.78	316.228	0.00
0.030	0.00	3.311	3.45	363.078	0.00
0.035	0.00	3.802	4.13	416.869	0.00
0.040	0.00	4.365	4.77	478.630	0.00
0.046	0.00	5.012	5.32	549.541	0.00
0.052	0.00	5.754	5.72	630.957	0.00
0.060	0.00	6.607	5.95	724.436	0.00
0.069	0.00	7.586	6.00	831.764	0.00
0.079	0.00	8.710	5.86	954.993	0.00
0.091	0.00	10.000	5.58	1096.478	0.00
0.105	0.00	11.482	5.21	1258.925	0.00
0.120	0.00	13.183	4.81	1445.440	0.00
0.138	0.00	15.136	4.42	1659.587	0.00
0.158	0.00	17.378	4.09	1905.461	0.00
0.182	0.00	19.953	3.84	2187.762	0.00
0.209	0.00	22.909	3.66	2511.886	0.00
0.240	0.00	26.303	3.51	2884.032	0.00
0.275	0.00	30.200	3.34	3311.311	0.00
0.316	0.00	34.674	3.09	3801.894	0.00
0.363	0.00	39.811	2.68	4365.158	0.00
0.417	0.00	45.709	2.11	5011.872	0.00
0.479	0.00	52.481	1.39	5754.399	0.00
0.550	0.00	60.256	0.66	6606.934	0.00
0.631	0.00	69.183	0.05	7585.776	0.00
0.724	0.03	79.433	0.00	8709.636	0.00
0.832	0.10	91.201	0.00	10000.000	0.00
0.955	0.22	104.713	0.00		

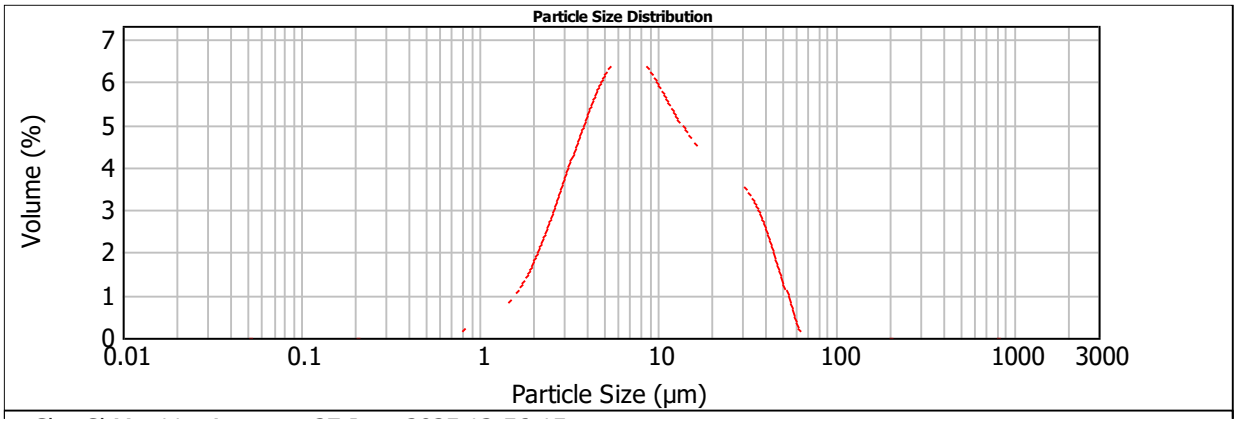

PARTICLE SIZE DISTRIBUTION FOR Cl + Co W Ca 600					
Size (µm)	Volume (%)	Size (µm)	Volume (%)	Size (µm)	Volume (%)
0.010	0.00	1.096	0.48	120.226	0.00
0.011	0.00	1.259	0.57	138.038	0.00
0.013	0.00	1.445	0.66	158.489	0.00
0.015	0.00	1.660	0.77	181.970	0.00
0.017	0.00	1.905	0.90	208.930	0.00
0.020	0.00	2.188	1.08	239.883	0.00
0.023	0.00	2.512	1.32	275.423	0.00
0.026	0.00	1.884	1.63	316.228	0.00
0.030	0.00	3.311	2.00	363.078	0.00
0.035	0.00	3.802	2.44	416.869	0.00
0.040	0.00	4.365	2.92	478.630	0.00
0.046	0.00	5.012	3.44	549.541	0.00
0.052	0.00	5.754	3.95	630.957	0.00
0.060	0.00	6.607	4.42	724.436	0.00
0.069	0.00	7.586	4.81	831.764	0.00
0.079	0.00	8.710	5.10	954.993	0.00
0.091	0.00	10.000	5.27	1096.478	0.00
0.105	0.00	11.482	5.32	1258.925	0.00
0.120	0.00	13.183	5.27	1445.440	0.00
0.138	0.00	15.136	5.13	1659.587	0.00
0.158	0.00	17.378	4.95	1905.461	0.00
0.182	0.00	19.953	4.75	2187.762	0.00
0.209	0.00	22.909	4.55	2511.886	0.00
0.240	0.00	26.303	4.35	2884.032	0.00
0.275	0.00	30.200	4.14	3311.311	0.00
0.316	0.00	34.674	3.89	3801.894	0.00
0.363	0.00	39.811	3.57	4365.158	0.00
0.417	0.00	45.709	3.18	5011.872	0.00
0.479	0.00	52.481	2.72	5754.399	0.00
0.550	0.00	60.256	2.19	6606.934	0.00
0.631	0.00	69.183	1.64	7585.776	0.00
0.724	0.10	79.433	1.11	8709.636	0.00
0.832	0.24	91.201	0.62	10000.000	0.00
0.955	0.38	104.713	0.10		

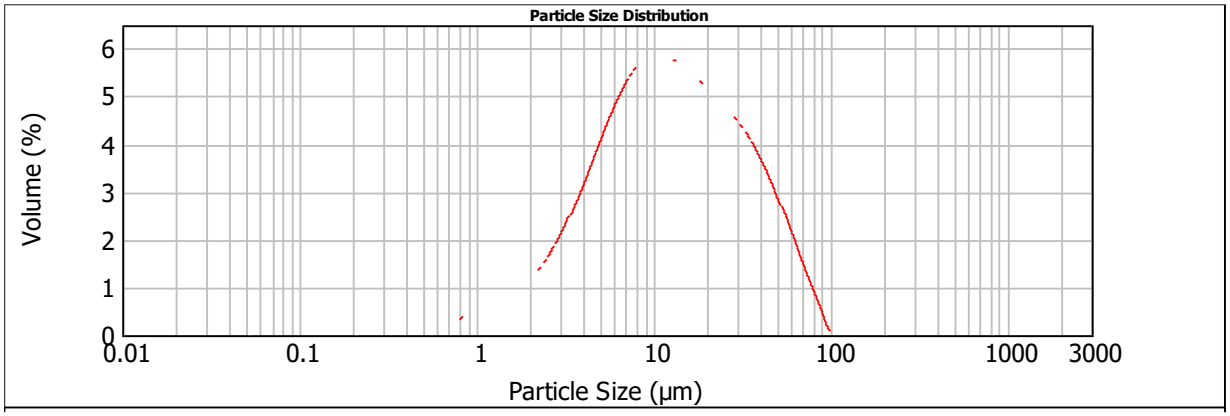

PARTICLE SIZE DISTRIBUTION FOR Cl + Co W Ca 850					
Size (µm)	Volume (%)	Size (µm)	Volume (%)	Size (µm)	Volume (%)
0.010	0.00	1.096	0.61	120.226	0.00
0.011	0.00	1.259	0.92	138.038	0.00
0.013	0.00	1.445	1.29	158.489	0.00
0.015	0.00	1.660	1.68	181.970	0.01
0.017	0.00	1.905	2.07	208.930	0.10
0.020	0.00	2.188	2.44	239.883	0.32
0.023	0.00	2.512	2.78	275.423	0.67
0.026	0.00	1.884	3.10	316.228	1.12
0.030	0.00	3.311	3.37	363.078	1.59
0.035	0.00	3.802	3.61	416.869	1.81
0.040	0.00	4.365	3.82	478.630	1.83
0.046	0.00	5.012	4.01	549.541	0.42
0.052	0.00	5.754	4.20	630.957	0.00
0.060	0.00	6.607	4.39	724.436	0.00
0.069	0.00	7.586	4.59	831.764	0.00
0.079	0.00	8.710	4.79	954.993	0.00
0.091	0.00	10.000	4.98	1096.478	0.00
0.105	0.00	11.482	5.13	1258.925	0.00
0.120	0.00	13.183	5.19	1445.440	0.00
0.138	0.00	15.136	5.12	1659.587	0.00
0.158	0.00	17.378	4.91	1905.461	0.00
0.182	0.00	19.953	4.53	2187.762	0.00
0.209	0.00	22.909	4.00	2511.886	0.00
0.240	0.00	26.303	3.36	2884.032	0.00
0.275	0.00	30.200	2.65	3311.311	0.00
0.316	0.00	34.674	1.95	3801.894	0.00
0.363	0.00	39.811	1.31	4365.158	0.00
0.417	0.00	45.709	0.72	5011.872	0.00
0.479	0.00	52.481	0.22	5754.399	0.00
0.550	0.00	60.256	0.01	6606.934	0.00
0.631	0.00	69.183	0.00	7585.776	0.00
0.724	0.00	79.433	0.00	8709.636	0.00
0.832	0.09	91.201	0.00	10000.000	0.00
0.955	0.29	104.713	0.00		

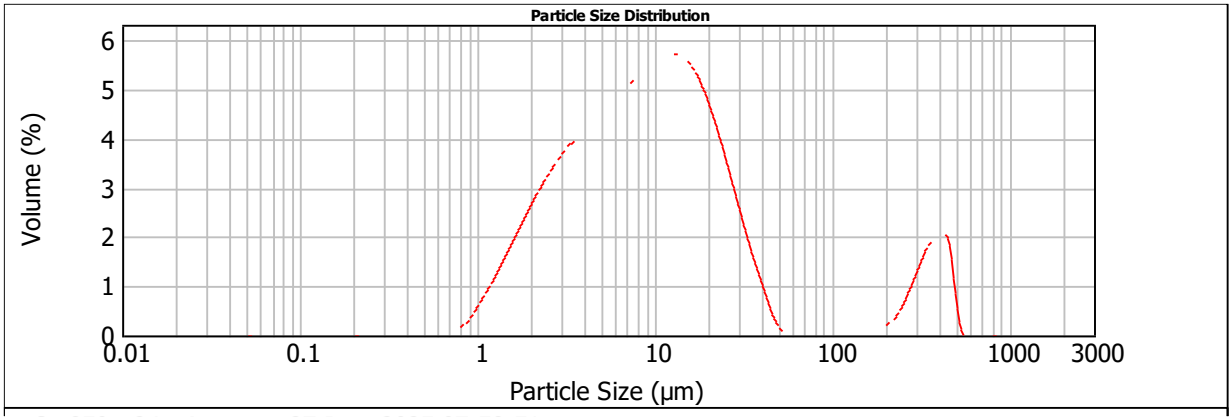

APPENDIX 5 – FLOW TABLE TEST FOR PASTE MIX

PASTE SAMPLES					
	Diameter 1 (mm)	**Diameter 2 (mm)**	**Mean Diameter (mm)**	**Deviation from Mean Diameter 1 (%)**	**Deviation from Mean Diameter 2 (%)**
Cem Con	120.63	114.77	117.70	-2.49	2.49
Cl	122.92	121.7	122.31	-0.50	0.50
Co	137.35	132.06	134.71	-1.96	1.96
Cl + Co W	129.02	135.04	132.03	2.28	-2.28
Cl + Co B	127.34	124.47	125.91	-1.14	1.14
Gl + Ce	127.53	126.38	126.96	-0.45	0.45
Cl + Co W Ca 600	138.08	129.57	133.83	-3.18	3.18
Cl + Co W Ca 850	127.05	124.89	125.97	-0.86	0.86

APPENDIX 6 – DENSITY OF PASTE CUBES

PASTE SAMPLES								
7 DAYS								
		Length (mm)	Breadth (mm)	Height (mm)	Volume (mm^3)	Mass (g)	Density (kg/m^3)	Average Density (kg/m^3)
Cem Con	Cube 1	20.05	19.81	19.89	7900.1190	16.9127	2140.8158	2145.0563
	Cube 2	19.95	19.94	20.17	8023.6865	17.2592	2151.0312	
	Cube 3	19.95	19.99	19.82	7904.2259	16.9413	2143.3218	
Cl	Cube 1	19.91	20.04	19.89	7936.0384	16.4704	2075.3932	2087.8447
	Cube 2	19.91	19.86	19.59	7746.1328	16.3152	2106.2381	
	Cube 3	19.97	20.03	19.86	7943.9821	16.5386	2081.9030	
Co	Cube 1	19.96	19.95	19.7	7844.5794	16.6069	2116.9905	2107.2889
	Cube 2	20.00	19.85	19.81	7864.5700	16.6243	2113.8219	
	Cube 3	20.01	19.94	20.28	8091.7078	16.9202	2091.0542	
Cl + Co W	Cube 1	19.91	19.89	19.79	7837.0359	16.6968	2130.4994	2117.9655
	Cube 2	19.98	20.03	20.02	8011.9920	16.8548	2103.6966	
	Cube 3	19.92	19.83	20.19	7975.3246	16.9053	2119.7006	
Cl + Co B	Cube 1	19.77	19.77	19.63	7672.4424	16.1164	2100.5567	2114.2775
	Cube 2	19.67	19.73	19.65	7625.9508	16.2228	2127.3151	
	Cube 3	19.71	19.57	19.87	7664.3498	16.2098	2114.9609	
Gl + Ce	Cube 1	19.85	19.76	19.85	7785.8846	16.6047	2132.6671	2138.5327
	Cube 2	19.86	19.64	19.86	7746.4009	16.5720	2139.3161	
	Cube 3	19.77	19.69	19.74	7684.2155	16.4720	2143.6151	
Cl + Co W Ca 600	Cube 1	20.34	19.63	20.13	8037.3896	16.4641	2048.4387	2039.6748
	Cube 2	20.14	20.63	19.86	8251.5957	16.5702	2008.1207	
	Cube 3	20.33	19.89	19.92	8054.9249	16.6130	2062.4649	
Cl + Co W Ca 850	Cube 1	19.88	19.79	19.54	7687.5284	16.2726	2116.7532	2133.8328
	Cube 2	19.82	19.61	19.44	7555.7487	16.0713	2127.0295	
	Cube 3	19.65	19.71	19.59	7587.2364	16.3711	2157.7158	

PASTE SAMPLES								
21 DAYS								
		Length (mm)	Breadth (mm)	Height (mm)	Volume (mm^3)	Mass (g)	Density (kg/m^3)	Average Density (kg/m^3)
Cem Con	Cube 1	20.03	19.01	19.87	7565.9059	17.373	2296.2221	2214.5360
	Cube 2	19.98	20.01	19.89	7952.0180	17.3102	2176.8311	
	Cube 3	20.00	19.8	19.77	7828.9200	16.9931	2170.5548	
Cl	Cube 1	20.08	20.07	19.51	7862.6393	16.2902	2071.8488	2103.8851
	Cube 2	19.91	20.00	19.3	7685.2600	16.4531	2140.8645	
	Cube 3	19.88	19.87	19.77	7809.4584	16.3916	2098.9420	
Co	Cube 1	20.00	20.02	19.99	8005.2929	16.6634	2081.5451	2117.8412
	Cube 2	19.89	19.96	19.96	7923.1939	16.7759	2117.3119	
	Cube 3	20.01	19.95	19.88	7939.3407	17.1066	2154.6667	
Cl + Co W	Cube 1	20.03	19.97	19.94	7979.5363	16.7211	2095.4963	2115.4307
	Cube 2	19.93	19.95	20.00	7950.5866	16.9100	2126.8823	
	Cube 3	20.01	19.93	20.01	7981.5519	16.9521	2123.9136	
Cl + Co B	Cube 1	19.91	19.93	20.01	7939.9194	16.8123	2117.4396	2118.4098
	Cube 2	19.89	19.93	20.01	7930.9854	16.748	2111.7174	
	Cube 3	19.95	20.02	20.00	7988.4399	16.984	2126.0722	
Gl + Ce	Cube 1	19.94	20.29	20.24	8188.7518	16.7762	2048.6883	2098.2270
	Cube 2	20.23	19.58	20.05	7941.8732	16.6581	2097.5026	
	Cube 3	19.64	19.9	19.81	7742.4612	16.6346	2148.4900	
Cl + Co W Ca 600	Cube 1	19.98	19.92	19.68	7832.6715	16.5922	2118.3322	2140.0243
	Cube 2	19.79	19.91	19.51	7687.3087	16.6794	2169.7320	
	Cube 3	19.9	20	19.65	7820.7000	16.6738	2132.0086	
Cl + Co W Ca 850	Cube 1	20.03	20.07	19.58	7871.2011	16.7025	2121.9760	2109.2496
	Cube 2	20.05	20.03	19.43	7803.1171	16.3903	2100.4811	
	Cube 3	20.07	20.08	19.67	7927.1202	16.6889	2105.2917	

APPENDIX 7

VACUUM SATURATION POROSITY TEST FOR PASTE CUBES

PASTE SAMPLES						
7 DAYS						
		Oven-Dry Mass, W_d (g)	Buoyant Mass, W_b (g)	Saturated Surface-Dry Mass, W_s (g)	Permeable Porosity = $\frac{W_s - W_d}{W_s - W_b} \times 100\%$	Average Permeable Porosity (%)
Cem Con	Cube 1	15.05	9.56	17.27	28.80	28.92
	Cube 2	14.40	9.08	16.66	29.77	
	Cube 3	14.79	9.40	16.90	28.19	
Cl	Cube 1	14.34	8.98	16.64	29.98	30.10
	Cube 2	14.16	8.82	16.42	29.68	
	Cube 3	14.25	8.85	16.63	30.65	
Co	Cube 1	14.40	9.04	16.52	28.28	28.68
	Cube 2	14.49	9.05	16.72	29.13	
	Cube 3	14.41	8.99	16.58	28.62	
Cl + Co W	Cube 1	14.50	9.05	16.66	28.42	28.89
	Cube 2	14.65	9.15	16.91	29.09	
	Cube 3	14.46	9.03	16.70	29.15	
Cl + Co B	Cube 1	14.50	9.06	16.79	29.62	29.57
	Cube 2	14.71	9.19	17.01	29.43	
	Cube 3	14.44	9.02	16.73	29.66	
Gl + Ce	Cube 1	14.50	9.04	16.72	28.87	28.49
	Cube 2	14.27	8.89	16.41	28.52	
	Cube 3	14.11	8.82	16.18	28.09	
Cl + Co W Ca 600	Cube 1	14.25	8.91	16.42	28.95	28.62
	Cube 2	14.34	8.98	16.48	28.51	
	Cube 3	14.19	8.90	16.29	28.42	
Cl + Co W Ca 850	Cube 1	14.55	8.84	16.85	28.69	29.12
	Cube 2	14.36	8.73	16.64	28.86	
	Cube 3	14.20	8.76	16.51	29.81	

PASTE SAMPLES						
21 DAYS						
		Oven-Dry Mass, W_d (g)	Buoyant Mass, W_b (g)	Saturated Surface-Dry Mass, W_s (g)	Permeable Porosity = $\frac{W_s - W_d}{W_s - W_b} \times 100\%$	Average Permeable Porosity (%)
Cem Con	Cube 1	14.92	9.41	17.03	27.65	28.02
	Cube 2	15.31	9.65	17.50	27.91	
	Cube 3	14.37	9.00	16.51	28.50	
Cl	Cube 1	14.41	8.93	16.54	28.05	28.09
	Cube 2	14.26	8.85	16.41	28.46	
	Cube 3	14.41	8.94	16.52	27.77	
Co	Cube 1	14.32	8.91	16.30	26.84	27.18
	Cube 2	14.57	9.01	16.59	26.66	
	Cube 3	14.42	8.96	16.55	28.03	
Cl + Co W	Cube 1	14.50	8.99	16.52	26.83	27.00
	Cube 2	14.64	9.09	16.69	26.98	
	Cube 3	14.59	9.08	16.64	27.18	
Cl + Co B	Cube 1	14.42	8.97	16.56	28.20	28.35
	Cube 2	14.76	9.22	16.96	28.41	
	Cube 3	14.77	9.19	16.99	28.44	
Gl + Ce	Cube 1	14.34	8.88	16.46	28.03	27.81
	Cube 2	14.57	9.06	16.67	27.66	
	Cube 3	14.51	9.05	16.60	27.73	
Cl + Co W Ca 600	Cube 1	14.38	8.91	16.45	27.39	27.23
	Cube 2	14.40	8.93	16.45	27.21	
	Cube 3	14.40	8.92	16.44	27.08	
Cl + Co W Ca 850	Cube 1	14.22	8.73	16.40	28.37	28.35
	Cube 2	14.61	8.95	16.85	28.33	
	Cube 3	14.26	8.74	16.45	28.34	

APPENDIX 8

DENSITY TEST RESULTS FOR MORTAR SAMPLES

	DENSITY OF MORTAR AT 7 DAYS			
	Cem Con	**Cl + Co W**	**Cl + Co B**	**Cl + Co W Ca 600**
Average Density (kg/m^3)	2437.34	2384.17	2385.35	2375.01
Difference in Density when compared to control (%)		-2.18	-2.13	-2.56

	DENSITY OF MORTAR AT 21 DAYS			
	Cem Con	**Cl + Co W**	**Cl + Co B**	**Cl + Co W Ca 600**
Average Density (kg/m^3)	2438.89	2387.75	2384.50	2367.12
Difference in Density when compared to control (%)		-2.10	-2.23	-2.94

APPENDIX 9 – DENSITY OF MORTAR CUBES

MORTAR SAMPLES								
7 DAYS								
		Length (mm)	Breadth (mm)	Height (mm)	Volume (mm^3)	Mass (g)	Density (kg/m^3)	Average Density (kg/m^3)
Cem Con	Cube 1	50.33	50	50.64	127435.56	311.38	2443.431017	2437.340633
	Cube 2	50.29	50.11	50.51	127286.8113	310.14	2436.544658	
	Cube 3	50.03	50.33	50.76	127814.1825	310.85	2432.046224	
Cl + Co W	Cube 1	50.23	50.43	50.32	127465.5366	306.44	2404.100811	2384.169846
	Cube 2	50.77	50.07	50.28	127814.4701	303.17	2371.953659	
	Cube 3	50.86	50.28	50.28	128578.0674	305.56	2376.455068	
Cl + Co B	Cube 1	50.4	51.14	50.88	131140.9613	311.79	2377.518031	2385.349894
	Cube 2	50.4	49.34	50.66	125978.0458	304.72	2418.834156	
	Cube 3	50.72	50.61	50	128346.96	302.86	2359.697495	
Cl + Co W Ca 600	Cube 1	50.45	49.83	50.83	127782.7315	307.64	2407.524056	2375.013554
	Cube 2	50.17	50.57	50.27	127539.8612	301.62	2364.907702	
	Cube 3	50.7	50.24	50.6	128886.7008	303.22	2352.608905	

MORTAR SAMPLES								
21 DAYS								
		Length (mm)	Breadth (mm)	Height (mm)	Volume (mm^3)	Mass (g)	Density (kg/m^3)	Average Density (kg/m^3)
Cem Con	Cube 1	50.3	50.21	50.11	126555.9619	308.75	2439.632201	2438.889983
	Cube 2	50.01	50.45	50.59	127638.7977	309.61	2425.673116	
	Cube 3	50.14	50.19	50.2	126329.6353	309.68	2451.364632	
Cl + Co W	Cube 1	50.71	50.22	50.64	128962.67	307.2	2382.084677	2387.753864
	Cube 2	50.71	50.26	50.35	128326.2696	306.31	2386.962552	
	Cube 3	50.69	49.87	50.23	126976.9344	304.01	2394.214363	
Cl + Co B	Cube 1	50.5	50.67	50.25	128581.4588	301.84	2347.461313	2384.496161
	Cube 2	50.06	50.43	50.19	126705.9499	305.24	2409.042355	
	Cube 3	50.51	51	50.27	129496.0227	310.4	2396.984815	
Cl + Co W Ca 600	Cube 1	50.12	50.31	50.52	127388.0593	300.53	2359.169309	2367.117494
	Cube 2	50.41	50.46	50.74	129066.7596	305.78	2369.161518	
	Cube 3	50.37	50.45	50.59	128557.6132	305.07	2373.021654	

APPENDIX 10

VACUUM SATURATION POROSITY TEST FOR MORTAR CUBES

MORTAR SAMPLES						
7 DAYS						
		Oven-Dry Mass, W_d (g)	**Buoyant Mass, W_b (g)**	**Saturated Surface-Dry Mass, W_s (g)**	**Permeable Porosity = $\frac{W_s - W_d}{W_s - W_b} \times 100\%$**	**Average Permeable Porosity (%)**
Cem Con	**Cube 1**	291.34	185.36	309.91	14.91	14.93
	Cube 2	289.75	184.20	308.40	15.02	
	Cube 3	290.83	184.92	309.30	14.85	
Cl + Co W	**Cube 1**	285.94	181.16	304.92	15.34	15.44
	Cube 2	282.98	179.85	302.21	15.72	
	Cube 3	285.01	180.8	303.77	15.26	
Cl + Co B	**Cube 1**	291.51	185.06	310.75	15.31	15.82
	Cube 2	283.7	179.92	303.49	16.02	
	Cube 3	280.81	177.66	300.65	16.13	
Cl + Co W Ca 600	**Cube 1**	286.60	182.57	306.92	16.34	16.55
	Cube 2	279.64	177.66	300.14	16.74	
	Cube 3	281.06	178.3	301.49	16.58	

MORTAR SAMPLES						
21 DAYS						
		Oven-Dry Mass, W_d (g)	**Buoyant Mass, W_b (g)**	**Saturated Surface-Dry Mass, W_s (g)**	**Permeable Porosity = $\frac{W_s - W_d}{W_s - W_b} \times 100\%$**	**Average Permeable Porosity (%)**
Cem Con	**Cube 1**	290.25	185.13	307.71	14.24	14.38
	Cube 2	290.73	185.43	308.62	14.52	
	Cube 3	291.12	185.68	308.82	14.37	
Cl + Co W	**Cube 1**	287.03	182.02	305.73	15.12	15.30
	Cube 2	286.02	181.38	304.90	15.28	
	Cube 3	283.66	179.83	302.69	15.49	
Cl + Co B	**Cube 1**	281.85	178.61	300.75	15.47	14.96
	Cube 2	286.15	181.48	304.21	14.72	
	Cube 3	291.07	184.63	309.40	14.69	
Cl + Co W Ca 600	**Cube 1**	278.89	176.96	299.2	16.61	16.01
	Cube 2	284.64	180.37	304.6	16.07	
	Cube 3	284.87	180.65	303.78	15.36	